

# TURKISH JOURNAL OF AGRICULTURAL ENGINEERING RESEARCH

VOLUME: 4  
ISSUE: 1  
YEAR: 2023



# TURKAGER

# 2023



e-ISSN:2717 - 8420

<https://dergipark.org.tr/tr/pub/turkager>



TURKISH JOURNAL OF AGRICULTURAL  
ENGINEERING RESEARCH

TURKAGER



e-ISSN: 2717 - 8420

<https://dergipark.org.tr/tr/pub/turkager>

Volume 4,  
Issue 1,  
Year 2023

Indexing / Abstracting



Source Index



DIRECTORY  
OF OPEN ACCESS  
SCHOLARLY  
RESOURCES



ADVANCED SCIENCE INDEX



BASE

Bielefeld Academic Search Engine



Directory of  
Research Journal  
Indexing



IJIFACTOR  
INDEXING



ASOS  
indeks



ROOTINDEXING  
JOURNAL ABSTRACTING AND INDEXING SERVICE



TOGETHER WE REACH THE GOAL

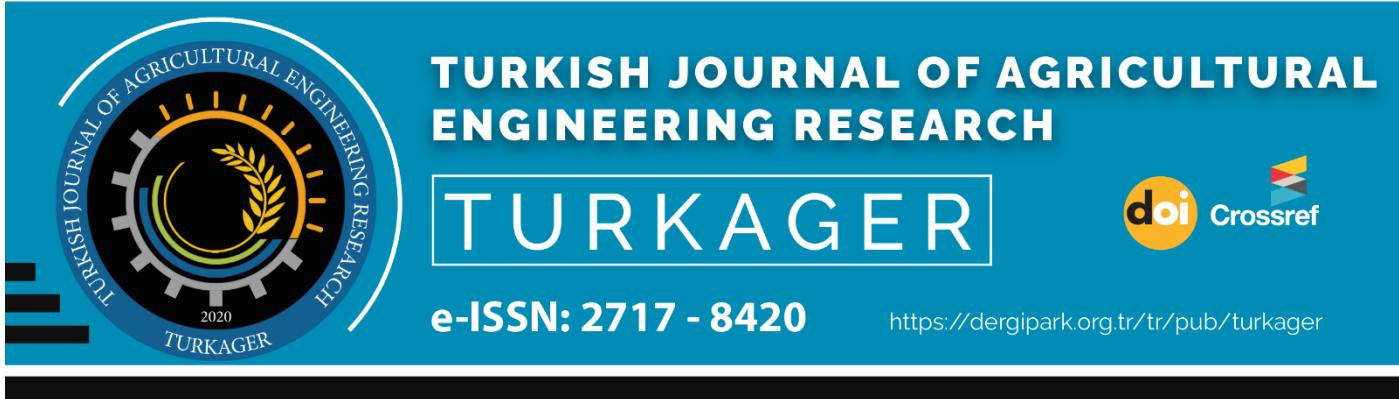


TIB  
LEIBNIZ INFORMATION CENTRE  
FOR SCIENCE AND TECHNOLOGY  
UNIVERSITY LIBRARY



Scientific Indexing Services

Quality Open Access Market



## Turkish Journal of Agricultural Engineering Research

# TURKAGER

### PUBLISHER

Prof. Dr. Ebubekir ALTUNTAŞ

Tokat Gaziosmanpaşa University, TÜRKİYE

### ABOUT

*Turkish Journal of Agricultural Engineering Research is licensed (CC-BY-NC-4.0) under a Creative Commons Attribution 4.0 International License. This license lets others remix, adapt, and build upon your work non-commercially, and although their new works must also acknowledge you and be non-commercial, they don't have to license their derivative works on the same terms.*

*Turkish Journal of Agricultural Engineering Research (Turk J Agr Eng Res, TURKAGER) is an international open-access online, and peer double-blind reviewed journal. TURKAGER publishes the original English and Turkish research articles and a very limited number of review articles. There are no page charges for manuscript publishing in this journal. TURKAGER has an open access system and online journal published twice a year in June and December.*

*Turk J Agr Eng Res (TURKAGER) is a peer double-blind reviewed journal and an interdisciplinary journal concerned with all parts of Agricultural Engineering (Horticulture, Plant Protection, Biosystems Engineering, Field Crops, Agricultural Economics, Soil Science and Plant Nutrition, Aquaculture, Animal Science), Food Science and Technology, Biology, and Environment.*

*Turkish Journal of Agricultural Engineering Research (TURKAGER) is indexed/abstracted in CABI, EBSCO, Information Matrix for the Analysis of Journals (MIAR), CAS Source Index (CASSI), Food Science & Technology Abstracts (FSTA), BASE, Directory Research Journals Indexing (DRJI), ROAD (Directory of Open Access Scholarly Resources), WorldCat, ResearchBible, Beluga-Catalogue of Hamburg Libraries, Advanced Science Index (ASI), Scientific Literature (Scilit), Scholar Article Journal Index (SAJI), IJIFACTOR Indexing, Electronic Journals Library (EZB), SJIF Master Journals List, International Institute of Organized Research (I2OR), Cite Factor, International Services for Impact Factor and Indexing (ISIFI), ASOS INDEX, Cosmos, Technical Information Library (TIB), ROOTINDEXING, Scientific Indexing Services (SIS), Journal Tables of Contents, Quality Open Access Market.*



**TURKISH JOURNAL OF AGRICULTURAL  
ENGINEERING RESEARCH**

**TURKAGER**

**e-ISSN: 2717 - 8420**

<https://dergipark.org.tr/tr/pub/turkager>



## **Turkish Journal of Agricultural Engineering Research TURKAGER**

### **EDITORIAL BOARD TEAM**

#### **EDITOR-in-CHIEF**

**Prof. Dr. Ebubekir ALTUNTAŞ / Tokat Gaziosmanpaşa University, TÜRKİYE**

#### **ASSISTANT EDITORS**

**Prof. Dr. Sedat KARAMAN / Tokat Gaziosmanpaşa University, TÜRKİYE**

**Dr. Bahadır ŞİN / Sakarya University of Applied Sciences, TÜRKİYE**

#### **TECHNICAL EDITOR**

**Dr. Bahadır ŞİN / Sakarya University of Applied Sciences, TÜRKİYE**

#### **LANGUAGE EDITORS**

**Prof. Dr. Fatih YILMAZ / Tokat Gaziosmanpaşa University, TÜRKİYE**

**Assoc. Prof. Dr. Gülay KARAHAN / Çankırı Karatekin University, TÜRKİYE**

**Dr. Manoj Kumar MAHAWAR, ICAR-Central Institute for Res. on Cotton Tech. INDIA**

#### **STATISTICS EDITOR**

**Assoc. Prof. Dr. Yalçın TAHTALI / Tokat Gaziosmanpaşa University, TÜRKİYE**

**Dr. Lütfi BAYYURT, Tokat Gaziosmanpaşa University, TÜRKİYE**

#### **SECRETARIAT (\*)**

**Researcher Ayşe Nida KAYAALP, Muş Alparslan University, TÜRKİYE**

**Researcher Burcu AKSÜT, Tokat Gaziosmanpaşa University, TÜRKİYE**

**Researcher Hamide ERSOY, Tokat Gaziosmanpaşa University, TÜRKİYE**

**Researcher Esra Nur GÜL, Tokat Gaziosmanpaşa University, TÜRKİYE**

(\*): The list is based on the surname of the editors in alphabetical order



**TURKISH JOURNAL OF AGRICULTURAL  
ENGINEERING RESEARCH**

**TURKAGER**



**e-ISSN: 2717 - 8420**

<https://dergipark.org.tr/tr/pub/turkager>

## SECTION EDITORS (\*)

**Prof. Dr. Zümrüt AÇIKGÖZ**, Animal Science, Ege University, [TÜRKİYE](#)

**Prof. Dr. Bilge Hilal ÇADIRCI EFELİ**, Biology, Tokat Gaziosmanpaşa University, [TÜRKİYE](#)

**Assoc. Prof. Dr. Hasan Gökhan DOĞAN**, Agricultural Economics, Kırşehir Ahi Evran University, [TÜRKİYE](#)

**Assoc. Prof. Dr. Gülay KARAHAN**, Land Scape and Architecture, Çankırı Karatekin University, [TÜRKİYE](#)

**Dr. Ayşe ÖLMEZ**, Fisheries Engineering, Tokat Gaziosmanpaşa University, [TÜRKİYE](#)

**Dr. Mahir ÖZKURT**, Field Crops, Muş Alparslan University, [TÜRKİYE](#)

**Assoc. Prof. Dr. Ahmet ÖZTÜRK**, Horticulture, Ondokuz Mayıs University, [TÜRKİYE](#)

**Prof. Dr. Bahadır SAYINCI**, Biosystems Engineering, Bilecik Şeyh Edebali University, [TÜRKİYE](#)

**Prof. Dr. Serkan SELLI**, Food Engineering, Cukurova University, [TÜRKİYE](#)

**Prof. Dr. Osman SÖNMEZ**, Soil Science and Nutrition, Erciyes University, [TÜRKİYE](#)

**Dr. Şerife TOPKAYA**, Plant Protection, Tokat Gaziosmanpaşa University, [TÜRKİYE](#)

(\*): The list is based on the surname of the editors in alphabetical order.



**TURKISH JOURNAL OF AGRICULTURAL  
ENGINEERING RESEARCH**

**TURKAGER**



e-ISSN: 2717 - 8420

<https://dergipark.org.tr/tr/pub/turkager>

## ADVISORY BOARD (\*)

- Prof. Dr. Şenol AKIN, Yozgat Bozok University, TÜRKİYE  
Prof. Dr. Omar Ali AL-KHASHMAN, Al-Hussein Bin Talal University, Ma'an-JORDAN  
Assoc. Prof. Dr. Tewodros AYALEW, Hawassa University, ETHIOPIA  
Dr. İlkey BARITÇI, Dicle University, TÜRKİYE  
Prof. Dr. Zeki BAYRAMOĞLU, Selçuk University, TÜRKİYE  
Assoc. Prof. Dr. Abdullah BEYAZ, Ankara University, TÜRKİYE  
Assoc. Prof. Dr. Hatem BENTAHER, Electromechanical Systems, Sfax University, TUNISIA  
Assoc. Prof. Dr. Özer ÇALIŞ, Akdeniz University, TÜRKİYE  
Prof. Dr. Ahmet ÇELİK, Atatürk University, TÜRKİYE  
Assoc. Prof. Dr. Ashlhan DEMİRDÖVEN, Tokat Gaziosmanpasa University, TÜRKİYE  
Prof. Dr. Alper DURAK, Malatya Turgut Ozal University, TÜRKİYE  
Assoc. Prof. Dr. Ramadan ELGAMAL, Agricultural Engineering, Suez Canal University, EGYPT  
Dr. Hamideh FARIDI, University of Tehran, IRAN  
Prof. Dr. Simon V. IRTWANGE, University of Agriculture, Makurdi, NIGERIA  
Prof. Dr. Ali İSLAM, Ordu University, TÜRKİYE  
Prof. Dr. Tomislav JEMRIC, University of Zagreb, CROATIA  
Dr. Avinash Suresh KAKADE, Univ.of Vasantrao Naik Marathwada Krushi Vidyapeeth, INDIA  
Dr. Zdzisław KALINIEWICZ, Uniwersytet Warmińsko-Mazurski, ul. Olsztyn, POLAND  
Dr. Manal H.G. KANAAN, Middle Technical University, Baghdad, IRAQ  
Dr. Muhammad Wasim Jan KHAN, Institute of Southern Punjab (ISP), Multan, PAKISTAN  
Assist. Prof. Dr. Alltane J KRYEZIU, University of Prishtina, Pristina, REPUBLIC OF KOSOVO  
Dr. Ahmed Moustafa Mohamed Ibrahim MOUSA, Al-Azhar University, Cairo, EGYPT  
Assoc. Prof. Dr. Shahid MUSTAFA, University of Sargodha, Sargodha, PAKISTAN  
Dr. Muhammad Ather NADEEM, University of Sargodha, Sargodha, PAKISTAN  
Assoc. Prof. Dr. Seyed Mehdi NASIRI, Shiraz University, Shiraz, IRAN  
Assoc. Prof. Dr. Chinenye Macmanus NDUKWU, Michael Okpara Univ. of Agriculture, NIGERIA  
Assoc. Prof. Dr. Zhongli PAN, California University, Davis, California, USA  
Assoc. Prof. Dr. Gheorghe Cristian POPESCU, Pitesti University, ROMANIA  
Dr. Monica POPESCU, University of Pitesti, ROMANIA  
Prof. Dr. Y. Aris PURWANTO, IPB University, INDONESIA  
Prof. Dr. Hidayet OĞUZ, Necmettin Erbakan University, TÜRKİYE  
Prof. Dr. Esen ORUÇ, Tokat Gaziosmanpasa University, TÜRKİYE  
Dr. Shafiee SAHAMEH, Tarbiat Modares University, Tehran, IRAN  
Prof. Dr. Mehmet Ali SAKİN, Tokat Gaziosmanpasa University, TÜRKİYE  
Prof. Dr. Şenay SARICA, Tokat Gaziosmanpasa University, TÜRKİYE  
Prof. Dr. Gordana SEBEK, University of Montenegro, Podgorica, MONTENEGRO  
Assoc. Prof. Dr. Marisennayya SENAPATHY, Wolaita Sodo University, Ethiopia, EAST AFRICA  
Dr. Feizollah SHAHBAZI, Lorestan University, Khoram Abad, IRAN  
Assoc. Prof. Dr. İsmail SEZER, Ondokuz Mayıs University, TÜRKİYE  
Prof. Dr. Metin SEZER, Karamanoğlu Mehmetbey University, TÜRKİYE  
Dr. Alaa SUBR, University of Baghdad, IRAQ  
Hilary UGURU, Delta State Polytechnic, Ozoro, Delta State, NIGERIA

(\*): The list is based on the surname of the editors in alphabetical order.



TURKISH JOURNAL OF AGRICULTURAL  
ENGINEERING RESEARCH

TURKAGER



e-ISSN: 2717 - 8420

<https://dergipark.org.tr/tr/pub/turkager>

## Turkish Journal of Agricultural Engineering Research TURKAGER

Volume 4,  
Issue 1,  
June 30, 2023

### REFEREES (\*)

- **Olufemi ADETOLA**, *Federal University of Technology Akure, NIGERIA*
- **Nazan AN**, *Boğaziçi University, TÜRKİYE*
- **Gamze BAYRAM**, *Tokat Gaziosmanpaşa University, TÜRKİYE*
- **Onur Fatih BULUT**, *Turkish Standard Institution, TÜRKİYE*
- **Hüseyin Kürşat ÇELİK**, *Akdeniz University, TÜRKİYE*
- **Ashhan DEMİRDÖVEN**, *Tokat Gaziosmanpaşa University, TÜRKİYE*
- **İlknur DURSUN**, *Ankara University, TÜRKİYE*
- **Mohamed GHONIMY**, *Cairo University, EGYPT*
- **Metin GÜNER**, *Ankara University, TÜRKİYE*
- **Hakan KIR**, *Kırşehir Ahi Evran University, TÜRKİYE*
- **Halil KIRNAK**, *Çukurova University, TÜRKİYE*
- **Hakan KİBAR**, *Bolu Abant İzzet Baysal University, TÜRKİYE*
- **Yasemin KUKUL KURTTAŞ**, *Ege University, TÜRKİYE*
- **Manoj Kumar MAHAWAR**, *Indian Council of Agricultural Research, INDIA*
- **Mehmet Serhat ODABAŞ**, *Ondokuz Mayıs University, TÜRKİYE*
- **Nuri ORHAN**, *Selçuk University, TÜRKİYE*
- **Mustafa Nevzat ÖRNEK**, *Konya Technical University, TÜRKİYE*
- **Harun ÖZER**, *Ondokuz Mayıs University, TÜRKİYE*
- **Hakan POLATCI**, *Tokat Gaziosmanpaşa University, TÜRKİYE*
- **Shiva SADIGHFARD**, *Tokat Gaziosmanpaşa University, TÜRKİYE*
- **Necdettin SAĞLAM**, *Tokat Gaziosmanpaşa University, TÜRKİYE*
- **Üstün ŞAHİN**, *Atatürk University, TÜRKİYE*
- **Burak ŞEN**, *Niğde Ömer Halisdemir University, TÜRKİYE*
- **Hilary UGURU**, *Delta State University of Science And Technology, NIGERIA*
- **Ali ÜNLÜKARA**, *Erciyes University, TÜRKİYE*
- **Onur TAŞKIN**, *Bursa Uludağ University, TÜRKİYE*
- **Muhammed TAŞOVA**, *Tokat Gaziosmanpaşa University, TÜRKİYE*
- **Serkan YAZAREL**, *Tokat Gaziosmanpaşa University, TÜRKİYE*
- **Demet YILDIRIM**, *Black Sea Agricultural Research Institute, TÜRKİYE*
- **Taner YILDIZ**, *Ondokuz Mayıs University, TÜRKİYE*
- **Hasan YUMAK**, *Bolu Abant İzzet Baysal University, TÜRKİYE*

(\*) The list is based on the surname of the editors in alphabetical order.

**Turkish Journal of Agricultural Engineering Research  
TURKAGER**

**Volume 4,  
Issue 1,  
June 30, 2023**



<b>No</b>	<b>Articles</b>	<b>Author/s</b>	<b>Pages</b>
1	Development and Performance Evaluation of a Hand Operated Maize Sheller	<b><u>Muyiwa Abiodun OKUSANYA,</u></b> Francis Ehis AGBONGIABAN	1-14
2	A microcontroller - Based Irrigation Scheduling Using FAO Penman-Monteith Equation	Olugbenga Kayode OGIDAN, <b><u>Samuel Dare OLUWAGBAYIDE,</u></b> Thomas Olabode ALE	15-25
3	AquaCrop Model Validation for Simulating Biomass and Water Productivity Under Climate Change for Potatoes	<b><u>AbdelGawad SAAD,</u></b> Hani Abdelghani MANSOUR, Elsayed ALI, Mostafa Mohamed AZAM	26-45
4	Development of a Cowpea Threshing Machine	<b><u>Mohamed Mansour Shalaby</u></b> <b><u>REFAAY,</u></b> Ahmed Shawky EL-SAYED, Mokhtar Cottb Ahmed AWAD	46-60
5	Influence of N fertilizing on Single-cut Sorghum × Sudangrass Hybrids' Forage Yield and Nutritive Profile	<b><u>Ugur OZKAN,</u></b> Nesim YILDIZ, Celal PEKER	61-72
6	Performance and Cost Comparison of Photovoltaic and Diesel Pumping Systems: In Central Rift Valley of Ethiopia	<b><u>Maney Ayalew DESTA,</u></b> Getachew Shunki TIBA, Mubarek Mohammed ISSA, Wariso HEY	73-90
7	Mathematically Predicting the Performance Rate of Plow-Type Trenchless Machine	<b><u>Mohamed Ibrahim GHONIMY</u></b>	91-103
8	Simulation-Optimization Modelling of Yield and Yield Components of Tomato Crop	<b><u>Nura Jafar SHANONO,</u></b> Lawal AHMAD, Nuraddeen Mukhtar NASIDI, Abdul'aziz Nuhu JIBRIL, Mukhtar Nuhu YAHYA	104-124
9	Design and Development of a Model Smart Storage System	Omokaro IDAMA, <b><u>Ovuakporaye Godwin</u></b> <b><u>EKRUYOTA</u></b>	125-132
10	Development and Performance Evaluation of Hand Operated Screw Juicer for Small Scale Application	Muyiwa Abiodun OKUSANYA, <b><u>Francis Ehis AGBONGIABAN</u></b>	133-150





Research Article

## Development and Performance Evaluation of a Hand Operated Maize Sheller

Muyiwa Abiodun OKUSANYA<sup>a\*</sup>, Francis Ehis AGBONGIABAN<sup>a</sup>

<sup>a</sup>Department of Agricultural and Bio-Environmental Engineering, School of Engineering The Federal Polytechnic, Ilaro, Ogun State, NIGERIA

(\*): Corresponding Author: [muyiwaok2002@yahoo.com](mailto:muyiwaok2002@yahoo.com)

### Article Info

Received: 23.09.2022

Accepted: 22.01.2023

Published: 30.06.2023

## ABSTRACT

Maize is a popular food crop of the world. After harvest, maize is shelled traditionally by small holders of farms. This method has not proved to be effective due to drudgery attached, kernel breakage and poor shelling capacity. Over time, motorized shellers have been introduced to address the challenges faced by processors; they have not gained widely adoption due to unaffordable cost of owning one. There is the need to design a cost effective and eco-friendly solution that will suit the need of subsistence farmers in the industry. This work focuses on development of a hand-operated maize sheller. A major component is the lever arm fitted to a ball bearing to transfer rotational motion to stripping chute. The machine uses the principle of abrasion to shell maize. Model ( $Y=54.92+ 0.248 X1-2.68 X2 \pm 1.187$ ) obtained from evaluation reveals that shelling capacity is a function of two predictors, speed ( $X1$ ) and moisture content ( $X2$ ). For every unit increase in cranking speed at a particular moisture content (23.2%, 18.5% or 14%) shelling capacity increases considerably. When the experiment is run at much lower moisture content (18.5%) shelling capacity increases significantly. The machine reached highest shelling capacity (60 kg h<sup>-1</sup>) at lowest moisture content (14%) and highest speed (120 rpm). The machine was developed at affordable cost of \$61. Shelling efficiency is also a function of speed and moisture content at which it is processed. For this condition, maximum shelling efficiency is achieved at lowest moisture content possible (14%) and terminal speed of 80 rpm. Mechanical damage resulted when the speed and moisture content are inconsiderably high. The machine is suitable for use by small and medium scale processors; it can efficiently replace the manual shelling methods as it is affordable, less stressful and easy to maintain.

**Keywords:** Crank, Stripping chute, Sheller, Multivariate data, Shelling capacity

**To cite:** Okusanya MA and Agbongiaban FE (2023). Development and Performance Evaluation of a Hand Operated Maize Sheller. *Turkish Journal of Agricultural Engineering Research (TURKAGER)*, 4(1), 1-14. <https://doi.org/10.46592/turkager.1178281>



## INTRODUCTION

Maize is one of the most prominent cereal crops of the world. In Nigeria, it is a staple food of choice largely consumed for its nutritional benefits. The grain crop serves as a key input in many manufacturing companies and poultry industry. Empirical facts gathered reveals that 60 percent of Nigeria's maize is used for the production of poultry feeds, 25 percent is used up by the food and beverage industry while the remaining is consumed by households (Okojie, 2022).

Nigeria is mainly susceptible to shocks that affect global agriculture grain supplies (Boluwade and Smith 2022). According to USDA (2022), maize importation into Nigeria doubled from 500,000 metric tonnes to one million metric tonnes between October 2019 and October 2020. This rise made incumbent administration to halt use of foreign exchange for border trade of cereal to boost domestic production of maize and other cereal products. The ripple effect of the policy has made maize to be sold at prohibitively exorbitant price in the recent time. From the forgoing, there is need for stake holders at all levels of maize production to be actively involved to bridge the gap between the increasing demands and production capacity (Okusanya and Oladigbolu, 2020).

Maize shelling involves removal of maize kernel from cob through impact or abrasion. It is one of the most important postharvest operations in maize production line. Report by Amare *et al.* (2017) reveals that maize shelling is difficult at moisture content above 25% as it makes stripping efficiency to be low, thereby causing mechanical damage to the seed. Danilo (2003) further stressed that maize is more efficiently shelled when the moisture content is in the range of 13 to 14%. After harvesting and de-husking, shelling is the next operation in the production line. Maize is shelled manually by hands or other traditional means like rubbing, beating or treading with animals. This method is not only primitive and drudgery laden; the output from the process does not justify effort input.

Over the years, improvement has come over the crude method of maize processing to reduce the burden of grains loss and damage caused by traditional method. Different designs of motorized shellers have been introduced to overcome these difficulties, but those designs have not gained wide adoption by marginal farmers due to prohibitive cost and failure of the shellers to meet the expectation of the processors in terms of design capacity and high efficiency under continued use in the field. Those who even use them by economy of scale cannot afford their high cost of maintenance.

This research endeavour is geared towards designing and fabricating a hand operated maize sheller for farmers in the remote areas of the economy and stake holders who are holder of small farms. This will serve to improve on the activities of maize production and processes in the industry.

## MATERIALS and METHODS

### Design Philosophy

The assembly uses simple machine principle of lever arm or crank system to supply rotational power through the wheel of the arm to the transmission shaft attached to the stripping chute. The lever experiences applied force on one end while the fulcrum

is close to the other end. The fulcrum (ball bearing) is between the applied force on the arm and the load of the chute on the tail end of the transmission shaft.

### Design Consideration

Some relevant factors were considered in the design and development of the hand operated shelling machine. Such factors include power requirement, ease of replacement of various components, labour requirement, ease of mobility, possibility of machine duplication, safety of operation of parts, cost of construction, types of load and stresses, machine kinematics and cost of maintenance. The machine will be very easy to maintain as it does not require mechanical power like oil engine to operate. Mild steel plate of 3 mm thickness was considered for the construction to avoid shearing of parts or machine failure while in operation. The spiral chute operated by lever arm linked to the transmission shaft impacts strong abrasive force to bring about stripping effect as materials are fed in.

### Materials Selection

Table 1 shows the list of materials used for the development of all the minor and major components the machine. The components include transmission shaft, stripping chute, bearing, bearing housing, lever arm, material outlet and top cover. The criteria for material selection of each component of the machine assembly were stated with their specifications and dimensions.

**Table 1.** Major components of the maize sheller assembly.

Machine Element	Criteria for Material Selection	Materials Selected	Dimension	Remark
Transmission Shaft	Machinability, high tensile/compression strength, low notch sensitivity factor, ductile, torsional rigidity, stiffness, etc.	Low carbon steel Iron rod	Ø 25mm, 220mm long	Machined
Stripping chute/Shelling drum	Ability to withstand vibration and abrasive force	Mild steel of 3 mm thickness	Ø 82mm tapered inward	Fabricated
Bearing	Compressive strength, fatigue strength, thermal conductivity, corrosive resistance, etc.	Stainless steel	Øb 68mm Øs 25mmH – 30mm	Bought readymade
Lever Arm/Crank		mild steel rod	Ø 25 mm, 200 mm long	Machined
Support Frame	Compression strength	Galvanized hollow pipe Ø 34 mm	Tripod stand, each being 312 mm long	Constructed
Material Outlet	Must allow free flow of material	Mild steel plate 3 mm thick	249 mm x 37 mm x 3 mm	Constructed
Bearing Housing	Must be strong enough to withstand bearing pressure and protect the bearing from outside particles	Mild steel plate 3 mm thick	Ø 60mm x 70 mm long	Constructed
Top Cover	High shear strength and ability to sustain large permanent deformation to the point of fracture	Mild steel plate 3 mm thick	Ø 86mm(curvature), 81.9mm x 236.5mm	Constructed

## Design Calculations

### Input power requirement

The input power can be determined from the name plate information of a prime mover used to power the machine. It can also be determined from the drive for the transmission shaft of the machine. In this endeavor, the input power for the sheller was found from the Mathematical model by [Belonio \(2004\)](#) on human power estimation for farm work. It is as stated in Equation 1.

$$P_g (Hp) = 0.35 - 0.092 \text{Log}t (min) \quad (\text{Belonio, 2004}) \quad (1)$$

Human power is given as  $P_g (Hp) = 0.35 - 0.092 \text{Log}t (min)$

To find  $P_g$  when  $t = 1 \text{ h} = 60 \text{ minutes}$

$$P_g = 0.35 - 0.092 \log 60 = 0.35 - 0.092 \times 1.7782$$

$$P_g(Hp) = 0.35 - 0.1636 = 0.1864 \text{ HP} = 0.139 \text{ kW} = 139 \text{ W}$$

Hence, human power requirement by one labourer on the sheller for one hour is 139 W.

If the highest material throughput from the machine is  $60 \text{ kg h}^{-1}$  and maximum yield from one hectare of land is 1.69 tonnes ([IITA, 2020](#)), it will take the following number of operators to shell maize from one hectare of farm land in one hour:

$$60 \text{ kg} \rightarrow 1 \text{ h}$$

$$1.69 \times 1000 \text{ kg} \rightarrow x$$

$$x = \frac{1.69 \times 1000}{60} = 28.17 \text{ h} \approx 30 \text{ h}$$

It simply implies 30 of such machines are needed to shell harvested maize from one hectare in 1 hour.

Also, one machine can finish the work in 4 days of 8 hours' work per day.

Power requirement for one hectare of maize farm is:

$$P = 30 \times 139 = 4.17 \text{ kW}$$

### Load Requirement

$$\text{Power, } P = F \times \omega r = F \times v = \frac{F \times \pi DN}{60} \quad (2)$$

Where  $F$  is stripping force on the maize cob,  $\omega$  is angular velocity of the lever arm and  $r$  is radius of the lever arm,  $v$  is linear velocity of the transmission shaft.

$$F = \frac{P}{v} \quad (3)$$

It is assumed that Power,  $P$  transferred to the tripping chute is constant.

Given the following parameters:  $\omega = 120 \text{ rpm}$ ,  $D = 280 \text{ mm} = 0.28 \text{ m}$ , stripping force,  $F$  can be found.

$$\text{At } 120 \text{ rpm, } F = \frac{P}{v} = \frac{P}{\frac{\pi DN}{60}} = \frac{139}{\pi \times 0.28 \times \frac{120}{60}} = 78.98 \text{ N}$$

$$\text{At } 40 \text{ rpm, } F = \frac{139}{\pi \times 0.28 \times \frac{40}{60}} = 237.03 \text{ N}$$

### Torque Requirement

Torque,  $T = \text{Stripping force } F \times \text{radius } r \text{ of the stripping chute}$

$$\text{Torque, } T = F \times r \quad (4)$$

If  $F = 237.03$  and  $r = 80 \text{ mm}$ , then:

$$\text{Torque, } T = 237.03 \times 0.08 = 18.96 \text{ N m}$$

Also, at  $F = 78.98 \text{ N}$ ,

$$\text{Torque, } T = 78.98 \times 0.08 = 7.82 \text{ N}$$

### Machine Description and Operation

The hand operated maize sheller has four main components; the shelling unit, the cranking unit, material outlet and member frame. The selling unit has tripping chute that can accommodate maize cob of varying geometries. The chute on the other hand has four set of blades arranged in a way to create little or no clearance for the cob. The abrasive force generated in the process assists in stripping maize kernel out of the cob, leaving stripped cob behind as waste product of the process. As soon as a batch is completed, another cob is peaked to continue the operation until all kernels are stripped off the cob. The cranking unit is the section of the machine assembly that provides rotational power to the transmission shaft driving the stripping chute. Human power is used to propel the lever arm of the cranking unit. The crank unit is made of 25 mm mild steel rod and two bearings housed by mild steel plate of 4 mm thickness. Material outlet on the other hand provides passage for flow of shelled maize kernels into sack or container provided. The outlet is tilted at an angle to provide free flow of materials by gravity. The member frame is the support for the entire assembly. The design of the frame is in form of a tripod stand. Two mild steel bars of 12 mm diameter assist to hold the tripod in place. The legs of the operator are placed on both sides of the tripod to further strengthen the firmness of the machine while in operation. See figures 1, 2, 3 and 4 for details on all the units of the machine assembly.

### Cost Estimation of the Hand Operated Maize Sheller

Cost of engineering products can broadly be grouped under direct or indirect cost. Direct cost is the cost of factors which are directly attributed to the manufacture of a specific product (i.e. materials and labour costs). Indirect cost on the other hand is that indirectly attributed to the manufacture of a specific product, such as overhead cost (usually expressed in percentage of direct labour cost), (Ajav *et al.*, 2018). The costing of the newly designed and fabricated maize Sheller was based on the detailed factorial estimate method. This is because fabrication of the machine is complete and

detailed breakdown and estimation of component parts is possible. The cost analysis of the machine is as shown in Table 2.

**Table 2. Bill of Engineering Measurement and Evaluation (BEME).**

S/N	Materials	Quantity	Unit Price (₦)	Total (₦)
1	Bearing $\varnothing$ 22mm (internal $\varnothing$ )	2	1 500	3 000
2	Rod $\varnothing$ 22mm & 110 mm long for shaft	$\frac{1}{4}$	8 000	2 000
3	Hollow pipe for body frame $\varnothing$ 35mm	$\frac{1}{2}$	6 000	3 000
4	Mild steel plate 3 mm thickness	$\frac{1}{4}$	28 000	7 000
5	Braising Rod for support 12 mm	$\frac{1}{2}$	4 000	2 000
6	Consumables (Electrode, paint & cutting disc)			2 500
7	Transportation			1 000

Note : 1 US Dollar = ₦ 447.52

Sub-total = ₦ 20,500.00 = \$ 45.81

i. **Materials Cost** : = ₦ 20 500.00 = \$ 45.81

ii. **Direct Labour Cost:**

(Machining of Main Shaft Bending, welding, painting) = ₦2 500 = \$ 5.59

iii. **Indirect/Overhead Cost:** = 20% of ₦ 20 500.00 = ₦4,100 = \$ 9.16

Grand-total = Material cost + Labour cost + Overhead cost = ₦27 100 = \$ 60.56  $\approx$  \$61.00

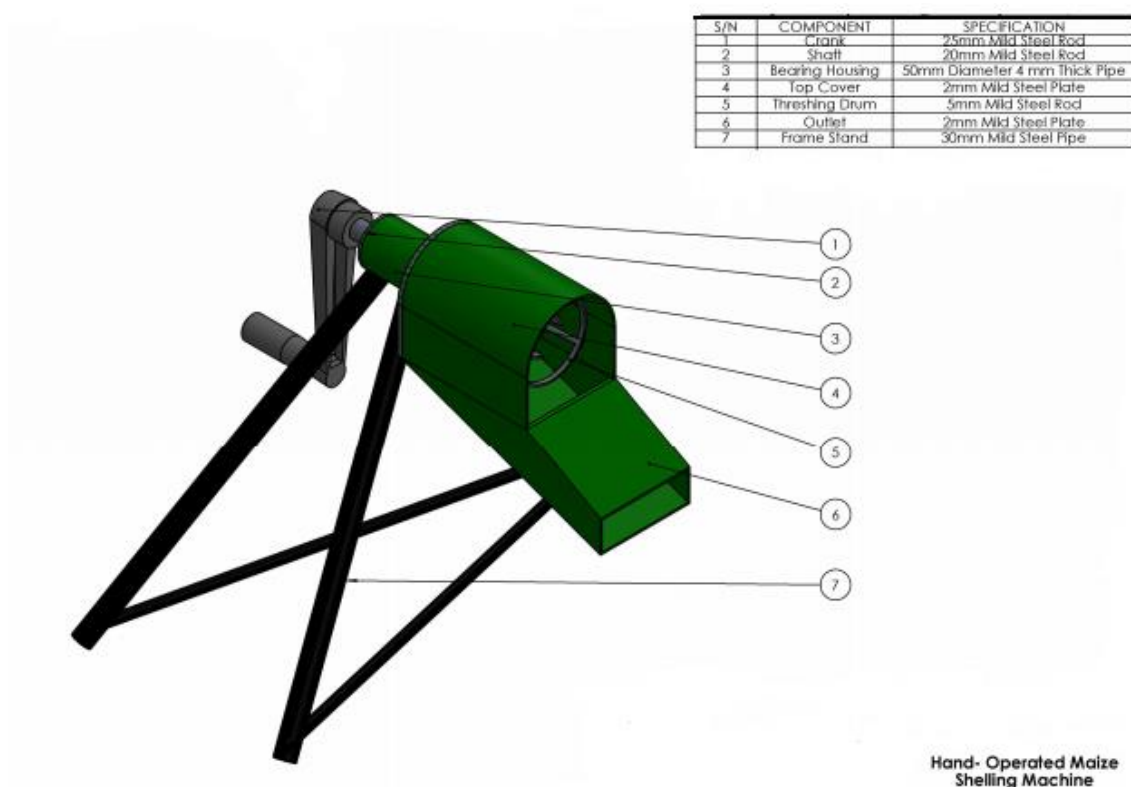


**Figure 1. Pictorial view of the machine.**

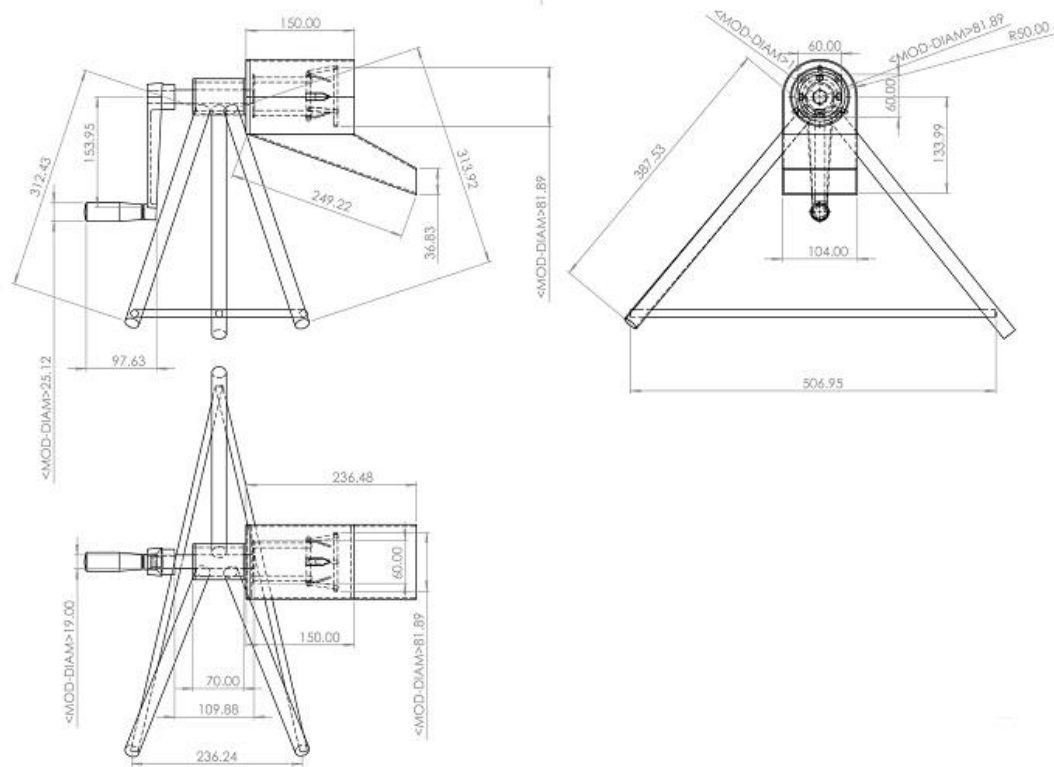


**Figure 2.** Autographic projection of the machine.

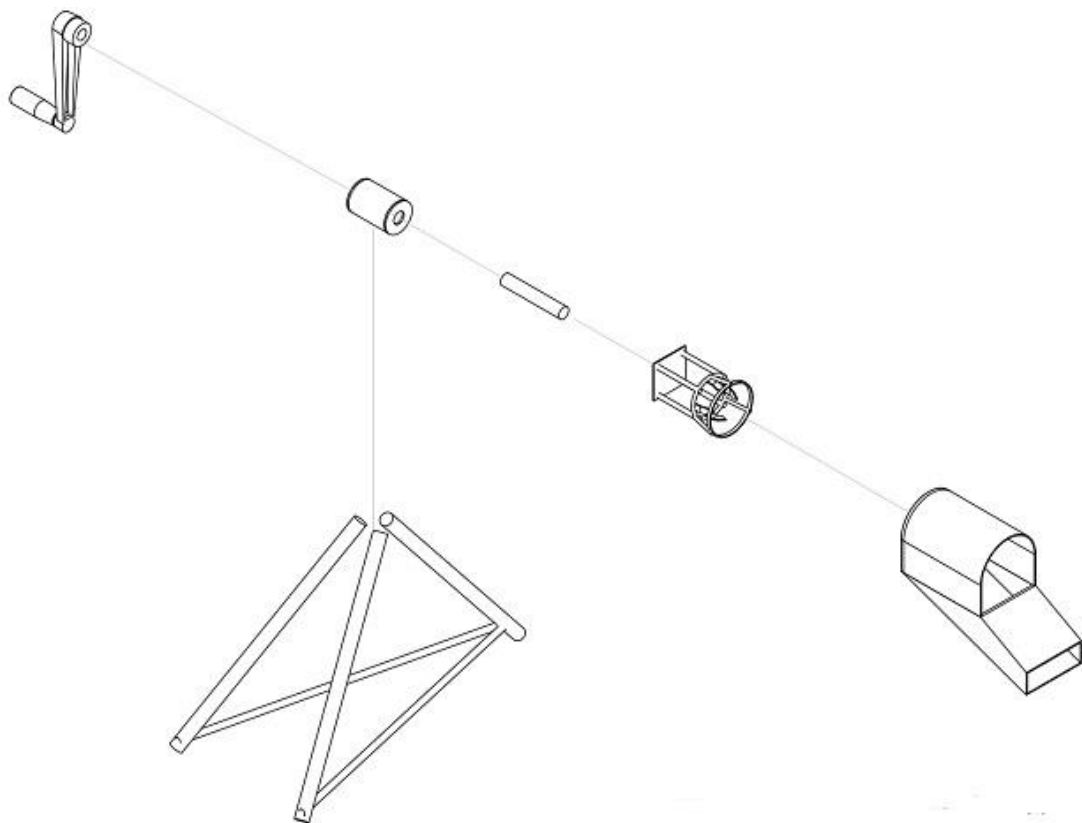


**Figure 3.** Exploded view of the machine.

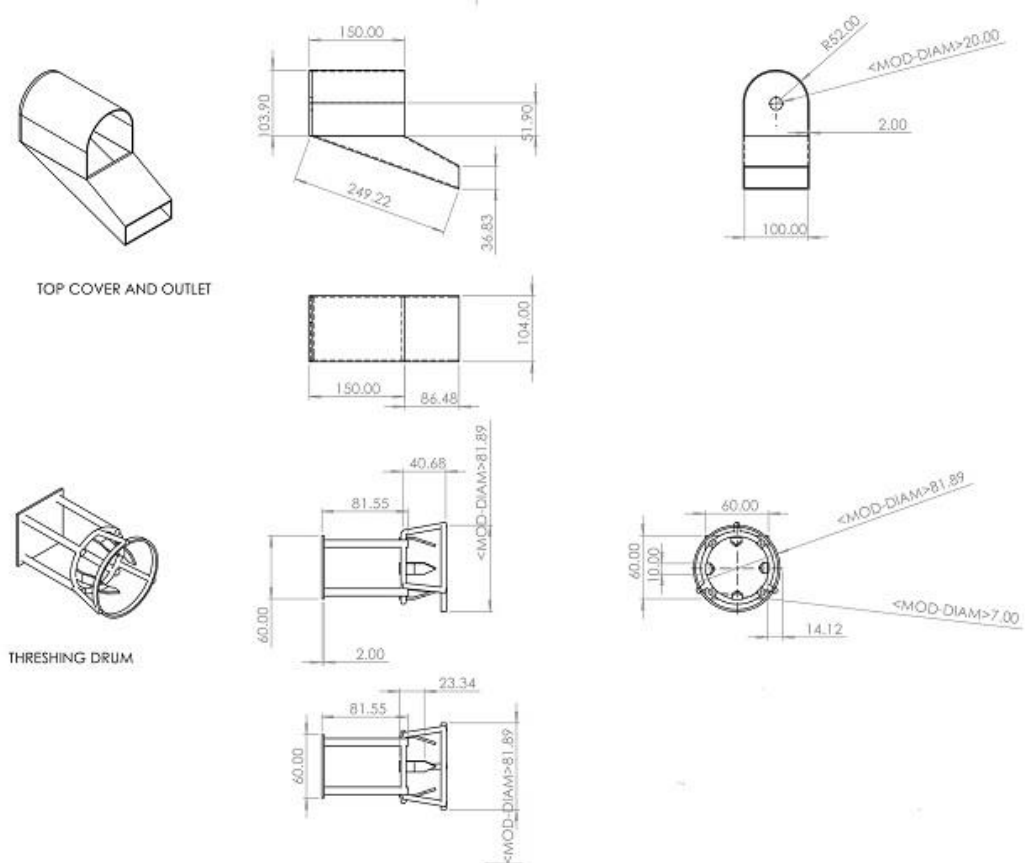


**Figure 4.** Part drawing of the machine.

Figures 1 and 2 are respectively the pictorial view and autographic projection of the machine assembly while Figures 3 and 4 are the exploded view and part drawing of the machine assembly. The dimensions of each component or subcomponents are shown as well. The components include threshing drum, bearing housing, support frame, grain outlet, crank arm, etc.

### Statistical Method for Analysis

Null hypothesis for variables considered is  $H_0: 0.5 \leq r \leq 1$ ; while alternative hypothesis is  $H_1: r < 0.5$ . For  $H_0$  in the range of values stated above. The regression line in Equation 5 and 6 can be determined using statistical method of multiple linear regression by hand using dependence techniques, machine learning algorithm of any applicable application software like excel. A relationship is established between two or more predictors and a response variable for bivariate data (Equation 5). Multivariate linear regression was the statistical model used to understand the relationship between two explanatory variables (speed and moisture content) and a response variable (materials throughput). For the multivariate data, Equation 6 is used.  $y$  is response variable,  $\beta_0$  is intercept on  $y$  axis,  $X_1/X_n$  is the predictor and  $\beta_1/\beta_n$  is the regression coefficient and  $\varepsilon$  is the model error. Microsoft Excel Data Analysis tool pack for multiple regressions was used for analysis of the data.

$$y = bx + a \quad (5)$$

$$y = \beta_0 + \beta_1X_1 + \beta_nX_n + \varepsilon \quad (\text{Zach, 2020}) \quad (6)$$



### Materials for Evaluation

Materials used for evaluation of the sheller are unshelled maize at various MC (14%, 18.5%, and 23.2%), the hand operated sheller, sensitive measuring scale, stop watch, recording materials, veneer caliper, moisture meter. Variables considered during evaluation are material throughput, moisture content, speed of rotation of the crank, stripping force, shelling efficiency, shelling methods and percentage of broken kernel. Equations 7, 8, 9 and 10 below were used for results estimation of the machine evaluation ([Azeez et al., 2017](#)).

$$\text{Materials Throughput} = \frac{\text{Weight of material processed (kg)} \times 60}{\text{Time (minutes)}} \quad (7)$$

$$\text{Percentage of unshelled grains (\%)} = \frac{\{\text{Weight of unshelled kernels (kg)}\}}{\{\text{Total Kernel input (kg)}\}} \quad (8)$$

$$\text{Shelling Efficiency} = 100 - \text{percentage of unshelled kernels} \quad (9)$$

$$\text{Kernel Damage (\%)} = \frac{\{\text{broken grain (kg)}\}}{\text{Weight of shelled maize kernel (kg)}} \quad (10)$$

## RESULTS AND DISCUSSION

Maize sheller developed was evaluated using unshelled maize at various moisture content and speed of rotation of the crank arm to determine the efficiency, shelling capacity and kernel damage. The results of the analysis are as shown in Figures 5 and 6 and Tables 3, 4, and 5.

Tables 3, 4 and 5 show the results of evaluation of the developed maize sheller at various moisture content (MC) ranging from 14% to 23.2%. The results show kernel breakage reduces as the moisture content of various maize samples used for machine evaluation reduces. Also, highest material throughput (60 kg h<sup>-1</sup>.) was obtained at lowest MC (14%) and highest angular speed of rotation. The efficiency of shelling was seen to be highest at lowest MC and time (6-10 seconds).

Table 3 shows reduction in efficiency of shelling from 100 to 94 percent as the speed of rotation increases from 40 rpm and 120 rpm. It can be inferred that the operation of the machine should be kept at barest minimum level to be able to experience optimum shelling efficiency. Also, kernel damage can reduce significantly if the hand operated sheller is kept at optimally low speed while in operation.

**Table 3.** Machine evaluation at moisture content (MC) of 23.2% and time range of 16-22 seconds.

S/N	Material's throughput (kg h <sup>-1</sup> )	Speed (rev min <sup>-1</sup> )	Shelling efficiency (%)	Kernel damage (%)
1	18.61	120	94	0.95 ± 0.01
2	16.52	100	95	0.72 ± 0.01
3	15.72	80	97	0.41 ± 0.01
4	13.85	60	99	0.23 ± 0.01
5	12.00	40	100	0.12 ± 0.01

Table 4 shows reduction in efficiency of shelling from 100 to 95 percent as the speed of rotation increases from 40 rpm and 120 rpm. Kernel breakage also reduced when compared to parameters in Table 3. This could be due to reduction in moisture content of the maize evaluated. It was 23.2% in Table 3 and 18.5% in Table 4. The time it took to shell the same quantity of maize under similar condition also reduced. This shows that the dryer the material to be shelled is, the lesser the time it will take to shell it.

**Table 4.** Machine evaluation at moisture content (MC) of 18.5% and time range of 8-12 seconds for each maize cob.

S/N	Shelling capacity (kg h <sup>-1</sup> )	Speed (rev min <sup>-1</sup> )	Shelling efficiency (%)	Kernel damage (%)
1	27.00	120	95	0.31 ± 0.005
2	22.50	100	96	0.25 ± 0.005
3	18.00	80	97	0.14 ± 0.005
4	15.88	60	100	Nil
5	14.21	40	100	Nil

**Table 5.** Machine Evaluation at MC of 14.0 % and time range of 6-10 seconds for each maize cob.

S/N	Shelling capacity (kg h <sup>-1</sup> )	Speed (rev min <sup>-1</sup> )	Shelling efficiency (%)	Kernel damage (%)
1	60.00	120	96	Nil
2	50.50	100	97	Nil
3	40.00	80	99	Nil
4	30.17	60	100	Nil
5	19.89	40	100	Nil

The result in Table 6 shows various values of shelling capacity at different shelling methods ranging from manual to motorized shelling. The table compared the shelling capacity of the methods. Motorised sheller has the highest capacity (125.0-701.4 kg h<sup>-1</sup>) when compared to all other methods. It can be inferred that what the hand operated sheller does not have in shelling capacity is compensated for in overhead cost - running cost (fuel and maintenance cost).

**Table 6.** Shelling capacity using different shelling methods.

S/N	Shelling method	Shelling capacity (kg h <sup>-1</sup> )	Remarks
1	Rubbing maize against each other	3.0 – 4.0	Evaluated
2	Hand shelling	3.5 – 5.0	Evaluated
3	Hand operated maize shell	18.6 – 60.0	Evaluated and reported by: <a href="#">Rajender et al. (2018)</a> ;
4	Motorized maize sheller	125.0 – 701.4	Reported by: <a href="#">Sedara et al. (2021)</a> ; <a href="#">Dagninet et al. (2008)</a> ;

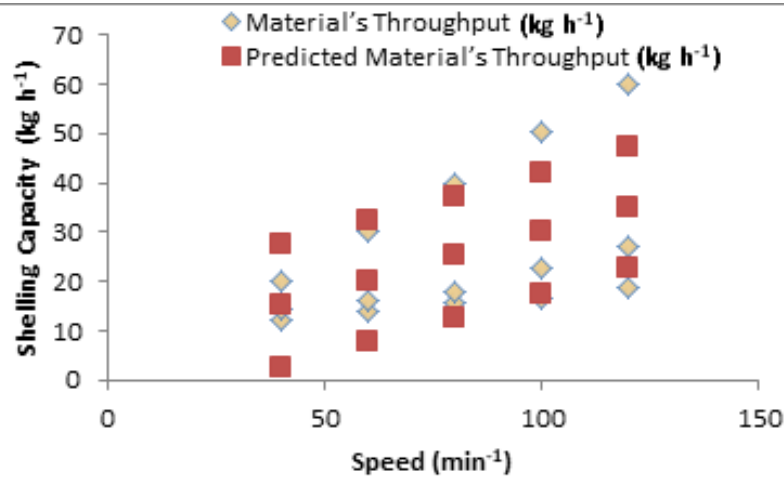


**Figure 5.** Chart of a predictor (speed) and response variable (Shelling Capacity).

In Figure 5, shelling capacity increases as the speed of rotation of cranking arm increases. The highest value was obtained (60 kg h<sup>-1</sup>) at highest speed of rotation (120 rev min<sup>-1</sup>).

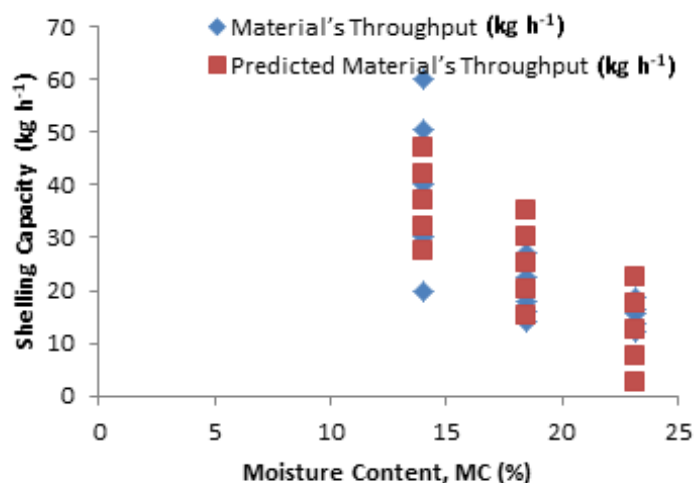


**Figure 6.** Chart of a predictor (moisture content) and response variable (Shelling Capacity).

Figure 6 is the plot of response variable with one of the predictors (MC). Highest value of materials throughput is obtained at lowest MC (14%) possible.

The relationship between the variables also provides the values predicted by the model and the difference between the actual value of the dependent variable and its predicted values by the regression model for each data point.

Results of analysis in Tables 7 and 8 explain the strength of relationship and level of confidence between the two independent variables and the response variable. The results presented in Table 7 shows that 15 observations were used for the model of the predictors and the response variable. The coefficient of determination, R square being 0.777 implies 77.7% of the variation in the materials throughput can be explained by speed of rotation of the crank arm and the moisture content at which the maize was shelled. The multiple R value, 0.883 reveals that there is strong level

of correlation or linear relationship between the two explanatory variables (predictors) and that null hypothesis defined is within acceptable limit. The standard error, 7.35 is larger than the coefficients of the two predictors (speed and MC) which are respectively 0.25 units and 2.68 units. On the average, the observed values of predictors fall 7.35 units from the regression line.

**Table 7. Regression parameters.**

Multiple Regression Statistics	
Multiple R	0.8813
R Square	0.7767
Adjusted R Square	0.7395
Standard Error	7.3511
Observations	15

Table 8 shows the analysis of variance (ANOVA) of the regression statistics. From the table, it can be deduced that the number of independent variables in the model is 2 as regression degree of freedom (df) is 2. F value in the table is 20.87 and the Significance F is 0.00124. The F value assists in testing the hypothesis that the slope of the independent variable is zero. The Significance F is otherwise called the p value for the null hypothesis that assists in confirming that the coefficient of the independent variable is zero. Since the p-value is below 0.05, it implies there is 95% confidence that the slope of the regression line is not zero. Hence, there is significant linear relationship between the explanatory variables (speed and MC) and the response variable (material throughput). For individual p - value in Table 8, it can be deduced that each explanatory variable is statistically significant – meaning the two predictors are applicable for the model.

Coefficients and intercept presented in Table 8 can be used to express linear regression model stated in Equation 6. The response variable, y can be established from the parameters in the table.  $\beta_0$  is 54.92 kg h<sup>-1</sup>,  $\beta_1$  is 0.248 rpm,  $\beta_2$  is - 2.68 % and  $\varepsilon$  being the model error has value of 1.187 kg h<sup>-1</sup>. Therefore, response variable y is expressed as:  $Y = 54.92 + 2.68X_1 - 2.68X_2 \pm 1.187$  (kg h<sup>-1</sup>).

**Table 8. Model parameters.**

	Coefficients	Standard Error	t Stat
Intercept	54.92	10.97	5.00
Speed (rev/min)	0.25	0.07	3.69
MC (%)	-2.68	0.51	-5.30

Variable  $X_1$  in the model is speed of rotation of the crank arm; variable  $X_2$  is the moisture content of maize under evaluation; and variable Y is the material throughput. For example, for every unit increase in cranking speed of the machine at particular moisture content, material throughput increases commensurately. When the experiment is run at much lower moisture content, material throughput increases significantly. The negative sign in the coefficient of variable  $X_2$  indicates that there is inverse relationship between material throughput and moisture content of maize under process. Every unit increase in moisture content will decrease material throughput. The machine reached highest material throughput

(50 kg h<sup>-1</sup>. – predicted, 60 kg h<sup>-1</sup> – estimated) at lowest moisture content (14%) and optimum speed of rotation (80 rpm). From the foregoing, it can be inferred that what the machine does not have in shelling capacity is compensated for by low overhead/running cost when compared to motorized sheller. The machine also has comparative advantage over traditional shelling as it is less stressful to operate; it has shelling capacity higher than any traditional method ever reported (see tables 6 for more details). The shelling capacity (60 kg h<sup>-1</sup>) is also higher when compared to pedal operated maize sheller (40.22 kg h<sup>-1</sup>) reported by [Rajender et al. \(2018\)](#).

## CONCLUSION

From the result of various analysis and evaluations carried out on the machine, it can be deduced that the sheller has comparative advantage over traditional shelling methods ever reported, in terms of shelling capacity, efficiency and shelling drudgery (see Table 4). The hand held Maize Sheller reduces the time required for traditional shelling by more than 10 times and it also protects from injury to fingertips. Also, what the machine does not have in shelling capacity is compensated for by low overhead/running cost when compared to motorized sheller. The operation of the machine should be kept at barest minimum level of speed to be able to experience optimum shelling efficiency. Kernel damage can reduce significantly if the hand operated sheller is kept at optimally low speed while in operation. The moisture content of maize to be shelled play significant role on shelling efficiency, shelling capacity and kernel breakage estimation of the machine. Therefore, maize shelling by the machine is effective when the moisture content is in the range of 10 to 14% the dryer the material to be shelled is the lesser the time it will take to shell it. The machine can be given wide publicity to encourage wide adoption especially among small and medium scale farmers in the rural communities. In view of the federal government policy of local production of grain crops to enhance food sufficiency and security, heavy investment on commercialization of the machine is recommended since it is cost effective and easily affordable.

## DECLARATION OF COMPETING INTEREST

We hereby declare that we have no conflict of interests

## CREDIT AUTHORSHIP CONTRIBUTION STATEMENT

**Muyiwa Abiodun Okusanya** conceptualized this project, did investigation, design and fabrication of the machine.

**Francis Ehis Agbongiaban** contributed to the methodology, data collection/analysis performance evaluation review and editing of the write-up.

## ETHICS COMMITTEE DECISION

This article does not require any ethical committee decision.

## REFERENCES

- Ajav EA, Okusanya MA and Obi OF (2018). Jatropha oil extraction optimization through varied processing conditions using mechanical process. *International Journal of Innovative Research & Development*, 7(9): 227-241. <https://doi.org/10.24940/Ijird/2018/V7/I9/Sep18058>.
- Azeez TM, Uchegbu ID, Babalola SA and Odediran OO (2017). Performance evaluation of a developed maize sheller. Journal of Advancement in Engineering and Technology. Afe Babalola Repository.
- Amare D, Endalew W, Yayu N, Endeblihatu A, Biweta W, Tefera A and Tekeste S (2017). Evaluation and demonstration of maize shellers for small-scale farmers. *MOJ Applied and Biomechanics*, 1(3): 0014. <https://doi.org/10.15406/mojabb.2017.01.00014>.
- Belonio AT (2004). *Agricultural power and energy sources*. Department of Agricultural Engineering and Environmental Management, College of Agriculture, Central Philippines University, Iloilo. City.
- Boluwade E. and Smith G. (2022). Grain and Feed Update. United State Department of Agriculture: Foreign Agricultural Service and Global Agricultural Network.
- Dagninet A, Fentahun T and Abu T (2008). *On-farm evaluation and verification of maize-sorghum thresher*. Proceedings of the 3<sup>rd</sup> Annual Regional Conference on Completed Research Activities on Soil and Water Management, Forestry and Agricultural Mechanization, 1-4 September, 2008. Ethiopia: ARARI
- Danilo M (2003). Maize: Post-Harvest operation. <https://www.aflatoxinpartnership.org/wp-content/uploads/2021/05/Maize-importance-globalv.pdf>. FAO technical Report, Ethiopia. Accessed May, 2022.
- IITA (2020). IITA-BIP Sets record for maize production per hectare in Nigeria. <https://www.iita.org/news-item/iita-bip-sets-record-for-maize-production-per-hectare-in-nigeria/>. Accessed May, 2022.
- Okojie J (2022). Bridging the Nigeria's maize shortfall. <https://businessday.ng/agriculture/article/bridging-nigerias-maize-supply-shortfall/>. Accessed June, 2022.
- Okusanya MA and Oladigbolu AA (2020). Development of a motorised thresher for paddy rice processing. *International Journal of Scientific & Engineering Research (IJSER)*, 11(2): 821-836.
- Rajender G, Anubabu T, Krishna CH, Ali MDM, Thirupathi CH and Vinod V (2018). Performance evaluation of hand operated maize sheller. *International Journal of Agricultural Science*, 10(7): 5676-5678.
- Sedara E, Odediran E and Manuwa S (2021). Design and fabrication of an improved motorized maize sheller/threshing machine. *Journal of Engineering Studies and Research*, 26(4): 120-131. <https://doi.org/10.29081/jesr.v26i4.244>
- USDA (2022). Nigeria's maize production at highest level since independence. United States Department of Agriculture. Foreign Agricultural Service. <https://www.fas.usda.gov/data/nigeria-grain-and-feed-annual-5>
- Zach A (2020). Statology. <https://www.statology.org/author/admin/> Access June, 2022.



## A microcontroller - Based Irrigation Scheduling Using FAO Penman-Monteith Equation

Olugbenga Kayode OGIDAN<sup>a</sup>, Samuel Dare OLUWAGBAYIDE<sup>b\*</sup>,  
Thomas Olabode ALE<sup>c</sup>

<sup>a</sup>Department of Electrical and Electronics Engineering, Elizade University, Ilera Mokin, Ondo State, NIGERIA

<sup>b</sup>Department of Agricultural and Bio-Environmental Engineering, Federal Polytechnic, Ilaro, Ogun State, NIGERIA

<sup>c</sup>Department of Electrical and Electronic Engineering, Federal University of Technology, Akure, NIGERIA

(\*): Corresponding Author: [samuel.oluwagbayide@federalpolyilaro.edu.ng](mailto:samuel.oluwagbayide@federalpolyilaro.edu.ng)

### Article Info

Received: 05.09.2022

Accepted: 10.02.2023

Published: 30.06.2023

## ABSTRACT

This study uses the Food and Agricultural Organization (FAO) Penman-Monteith equation to develop a crop water algorithm needed to automate the supply of specific amount of water to crops, depending on their different crop water requirements. This was done to deviate from the practice of supplying the same amount of water to different crops during irrigation practices which could lead to over-irrigation or under-irrigation resulting in pest infestation and eventually low yield. The crop water requirement for cocoyam, spinach and tomatoes were estimated using data from FAO. A microcontroller-based smart irrigation device incorporated with real-time clock was developed to supply the right amount of water to crops at the right time and duration daily. The implementation was done using a laboratory-scale irrigation test bed and experimental results reveal the effectiveness of the developed system in the automation of crop-specific irrigation systems and in line with their Crop Water Requirement (CWR). Possible applications include greenhouses where researchers have to apply a specific amount of water to crops for experiments; horticultural gardens and nurseries to mention a few.

**Keywords:** Irrigation, Crop water use, Automation, Scheduling, Penman-monteith

**To cite:** Ogidan OK, Oluwagbayide SD and Ale TO (2023). A Microcontroller-Based Irrigation Scheduling Using FAO Penman-Monteith Equation. *Turkish Journal of Agricultural Engineering Research (TURKAGER)*, 4(1): 15-25. <https://doi.org/10.46592/turkager.1170630>



## INTRODUCTION

An automated irrigation is a system of operation with no or just a minimum of manual intervention apart from the surveillance. All systems of irrigation viz drip, sprinkler, and the surface can be automated with the help of timers, sensors or computers, or mechanical appliances (Yogesh *et al.*, 2016; Kamienski *et al.*, 2019). In recent time, there seems to be a paradigm shift from traditional irrigation practices to smart irrigation. This means that certain algorithms are programmed into microcontrollers, making use of sensors, real-time weather, and site data in order to achieve a “smart” and properly scheduled irrigation system (Omid *et al.*, 2020; Zia *et al.*, 2021). These smart controllers sometimes make use of weather or site data to determine when irrigation scheduling will take place for maximum crop production. Some of them also make use of soil conditions, evaporation and crop water use to automatically operate a scheduled irrigation system to meet the needs of a variety of crops.

Agriculture plays very vital role in the economic development of a nation like Nigeria. A good agricultural practice is depended on environmental parameters such as soil moisture, temperature, humidity, pH, and solar radiation (Yogesh *et al.*, 2016). This plays an important role in overall development of the crop and good yield especially as these parameters determined when to irrigate a farm. Successful irrigation practice in any location is very crucial to irrigation scheduling. A smart irrigation system uses information from environment to control when and where irrigation is required (Kizito *et al.*, 2016). The system helps in avoiding wastage of water or energy and low-crop yield, respectively. Water is a critical resource in agriculture, and supplying the right amount is essential for healthy plants and optimum productivity. Rightful application of water to a crop is very important especially during drought (Ewemoje *et al.*, 2018).

Lately, there is rapid growth of research into smart irrigation. The main reasons for this are to increase the crop yield and minimizing human labor. Wastage of water and money spent on labor is avoided in automated irrigation (Sandeep and Deepali, 2017). Also, there is tremendous increase in the rate of adoption of smart technology in agriculture by the developing nations of the world. This has made the market in Asia Pacific to witness a significant intensification in smart agriculture. Countries such as Australia, China, India, Japan, and South Korea are witnessing an extensive growth in the market (Kizito *et al.*, 2016).

However, several works have been done in smart irrigation. For example, (Wardlaw and Bhaktikul, 2004) developed a genetic algorithm for irrigation scheduling with the objective of achieving equity in water delivery throughout the season among the multiple outlets from an irrigation canal system (Torres-Sanchez *et al.*, 2020; Raeth, 2020).

Dorji *et al.* (2017) developed an irrigation scheduling and water requirement-based irrigation system for Citrus Mandarin using tensiometers. This system combines the Food and Agricultural Organization (FAO) Pan Evaporation method and Food and Agricultural Organization (FAO) Penman-Monteith equation in determining the crop water requirement of the plant. The moisture stress readings are obtained at different depths using tensiometers. The project developed a citrus water requirement scheduling irrigation system.



In [Agugo \*et al.\* \(2009\)](#), the authors designed and implemented a theoretical estimate of crop evapotranspiration and irrigation water requirements of Mungbean (*Vigna radiata*) in a low land rain forest location of southeastern Nigeria. The estimation of crops was done in three stages – the calculation of reference crop evapotranspiration, crop coefficient and the maximum evapotranspiration ([Omid \*et al.\*, 2020](#)).

[Rodriguez \*et al.\* \(2015\)](#) developed an automatic irrigation scheduling soilless culture system using a new control algorithm. This system uses a Proportional Integral Derivative (PID) controller and an irrigation control tray with two electrodes (level sensor). Crop water consumption was determined by the process of evapotranspiration. The PID-based irrigation control simulation model included a crop simulation model to estimate the water acceptance of the crop over a given period, water equilibrium in the tray to calculate the drainage water volume and resulting leaching fraction and a PID controller to calculate the dimension intervals between two irrigation events.

In an attempt to judiciously manage the use of water in irrigation practices, the authors in [Ogidan \*et al.\* \(2019\)](#) developed a smart irrigation system with water management capability. The system prioritizes water used for irrigation based on the amount of water available in the reservoir measured by an ultrasonic sensor positioned on the lid of the reservoir. With this type of information about available water, the system was able to determine the number of pumps to be deployed for water supply to the different farms at a particular time ([Ogidan \*et al.\*, 2019](#)).

However, it has been estimated that 40% of the fresh water used for agriculture in developing countries is lost, either by evaporation, water spills, or absorption by the deeper layers of the soil, beyond the reach of plants roots ([Munoth, 2016](#)). This is the reason a drip irrigation system that supplied water directly to the root of crops is more preferred to the sprinkler type of irrigation system when it comes to water management. Another way of ensuring efficient water management in irrigation practice is to ensure that only the exact amount of water required by a particular plant is delivered to it, no more, no less. In order to achieve this, the required water for each crop from planting to maturity must be known. This is what is referred to as crop water requirement (CWR) and the CWR is different from one crop to another.

Many of the automated irrigation systems developed are found to deliver water to crops on a generic basis without taking into consideration their individual water requirements ([Wardlaw and Bhaktikul, 2004](#); [Ogidan and Afia, 2019](#); [Ogidan \*et al.\*, 2019](#)). This means that they deliver the same amount of water to different crops. In reality, all crops do not require the same amount of water for their growth if they would deliver maximum yield. For instance, tomatoes and yam do not require the same amount of water for their growth. Some researchers who have taken time to estimate the crop water use of various types of crops did not implement automation of their watering schedules ([Yadav \*et al.\*, 2018](#); [Agugo \*et al.\*, 2009](#); [Surendran \*et al.\*, 2017](#); [Dorji \*et al.\*, 2017](#); [Raeth, 2020](#)). Manual (unautomated) watering is cumbersome, laborious, and ineffective because the farmer or researcher can forget to wet the crops at the required time. This challenge therefore necessitates the need to develop an irrigation system that is crop specific. The system delivers the right amount of water to different crops based on the specific crop water requirement of each crop and execute an automation system for the irrigation scheduling.

## MATERIALS and METHODS

The approach adopted in this work is divided into three namely: determination of the daily water needs of the crops, determination of irrigation duration for each day and development of a microcontroller-based irrigation scheduling device.

### Determination of the Daily Water Needs of the Crops

The CWR or evapotranspiration rate (mm) is the water needed to meet the water consumption through evapotranspiration (ET<sub>c</sub>) for crops to thrive and to achieve full yield potential under the given growing environment (Brouwer and Heibloem, 1986). The evapotranspiration rate is the amount of water that is lost to the atmosphere per time through the leaves of the plant, as well as the soil surface.

ET<sub>c</sub> data used in estimating the CWR in this research is calculated by using the modified Penman–Monteith equation recommended (Brouwer and Heibloem, 1986; Yadav *et al.*, 2018; Surendran *et al.*, 2017; Omid *et al.*, 2020).

$$ET_c = ET_o \times K_c \quad (1)$$

where: ET<sub>c</sub> refers to crop evapotranspiration or crop water need (mm/day); ET<sub>o</sub> – is the reference evapotranspiration (mm/day); K<sub>c</sub> – indicates Crop Coefficient Factor.

### Determination of ET<sub>o</sub>

Reference evapotranspiration (ET<sub>o</sub>) represents the influence of the climate on crop water needs and it is usually expressed in millimeters per unit of time, e.g. mm/day, mm/month, or mm/season. Grass has been taken as the reference crop (Brouwer and Heibloem, 1986).

In this research, a more simplified version of the Penman-Monteith equation is used in the estimation of ET<sub>o</sub> as shown in Equation 2.

$$ET_o = \frac{0.408\Delta(R_n - G) + \gamma \frac{900}{T + 273} u_2 (e_s - e_a)}{\Delta + \gamma(1 + 0.34 u_2)} \quad (2)$$

where: ET<sub>o</sub> – refers to reference evapotranspiration, mm day<sup>-1</sup>; R<sub>n</sub> - is the net radiation at the crop surface, MJ m<sup>-2</sup> d<sup>-1</sup>; G - indicates soil heat flux density, MJ m<sup>-2</sup> d<sup>-1</sup>; T - is the mean daily air temperature at 2 m height, °C; u<sub>2</sub> – is the wind speed at 2 m height, m/s; e<sub>s</sub> - is saturation vapor pressure, kPa; e<sub>a</sub> is the actual vapor pressure, kPa; e<sub>s</sub> - e<sub>a</sub> - indicates saturation vapor pressure deficit, kPa; Δ - is the slope of saturation vapor pressure curve, kPa °C<sup>-1</sup>; γ - is psychometric constant, kPa °C<sup>-1</sup>.

### Determination of Coefficient Factor, K<sub>c</sub>

The crop coefficient is a mathematical conversion factor that relates and converts the ET of the reference crop to the crop of interest (actual crop water use). The magnitude of the crop coefficient K<sub>c</sub> is not constant all through the season. It varies depending on the growth stage and the relative maturity of the crop as well as some management practices.

Table 1 shows per crop the  $K_c$  values for different growth stages as well as the average  $K_c$  for the total growth period of each of the crops considered in this research namely cocoyam, spinach, and tomatoes.

In order to calculate the Crop Evapotranspiration ( $ET_c$ ) or Crop Water Requirement of various crops under study, the reference evapotranspiration ( $ET_o$ ) is multiplied with the crop coefficient ( $K_c$ ) as illustrated in Equation 1.

Based on equation 1, the estimated crop water requirements ( $ET_c$ ) of different crops under study from planting to maturity is shown in Table 2 (Brouwer and Heibloem, 1986).

**Table 1.** Crop specific coefficients ( $K_c$ ) per crop development stages for various crops under study.

Crop	Initial stage ( $K_c$ )	Days	Crop dev. stage ( $K_c$ )	Days	Mid-season stage ( $K_c$ )	Days	Late season stage ( $K_c$ )	Days	Season average ( $K_c$ )
Cocoyam	0.45	-30	0.85	-40	1.35	-95	0.95	-35	0.9
Spinach	0.45	-20	0.6	-30	1	-40	0.9	-10	0.74
Tomato	0.45	-30	0.75	-45	1.15	-70	0.8	-30	0.79

**Table 2.** Estimated crop water needs of different crops from planting to maturity (Agugo et al., 2009).

Crop	Crop water needs (mm/total growing period)	Average water needs (mm/total growing period)	Total growing period (days)	Average growing period (days)
Cocoyam	600-900	750	200 – 240	220
Spinach	350 – 500	425	60 – 100	80
Tomatoes	400 – 800	600	135 -180	158

From Table 2, it is possible to estimate the daily water needs by dividing the average crop water needs for the total growing period by the average gestation period (number of days from planting to maturity). The result shows  $3.40 \text{ mm day}^{-1}$  for cocoyam,  $5.31 \text{ mm day}^{-1}$  for spinach and  $3.79 \text{ mm/day}$  for tomatoes as shown in Table 2. This means that this is the estimated amount of water needed daily by these crops for maximum yield. Meaning the supply of water more than those specified in table 2 or less than that on a daily basis could adversely affect the yield resulting in low yield.

### Determination of the Duration of Irrigation Per Day

In this work, an automated irrigation scheduling approach is adopted using microcontroller technology. To develop the automated system, certain hardwares were used including Arduino UNO, 1-Channel relay module, soil moisture content sensor, water reservoir, DHT11 sensor, Liquid Crystal Display (LCD), Real-Time Clock (RTC) module. The software used include Arduino sketch. The block diagram of the developed system is shown in Figure 1. The system is divided to three main parts which are the data acquisition, processing, and the system output.

### Data Acquisition

This includes the Digital Humidity and Temperature (DHT) sensor and the moisture content sensors. The DHT measures the environmental temperature and humidity while the moisture content sensors are in form of probes, and they are buried in the (farm) soil to acquire the moisture content of the different farm soils in order to determine if the soil samples have enough moisture (indicating wetness) or it does not (indicating dryness). The sensor readings are fed into the microcontroller for further processing as illustrated in Figure 1.

### Processing

The processing is that part of the system that takes decision about how the device should operate based on the acquired sensor readings and the threshold values at which the system should take decisions. The microcontroller used is an Atmega 328 microcontroller housed in an Arduino Uno board. Interfaced with the microcontroller is a real-time clock (RTC) module. The work of the real-time clock is to assist in keeping track of time (seconds, minutes, hours, days, months, and years) in an accurate manner. RTC can do this for almost a decade. It is a choice component for clocks, calendars, or any other time-keeping project. Here, it is used to keep track of the time (seconds, minutes, hours) the systems are expected to supply water to crops in line with watering schedule. A program of the crop watering schedule is written in the Arduino Integrated Development Environment (IDE) and uploaded into the microcontroller for execution. The schematic circuit of the developed system is shown in Figure 2 while the flowchart of the program is shown in Figure 2. Each of the three moisture content sensors are made to represent different locations in the farm namely cocoyam farm, spinach farm and tomatoes farm. If the moisture content indicates the soil is dry in any of the three farm locations, the system activates the appropriate pump to release water to crops in that location. The specific time irrigation commences is specified by the RTC for example, if the RTC specifies 6:10:05 am, this means 6th hour, 10th minute and 5th second. The system ensures that the water is supplied at this specific time on a daily basis throughout the period of planting. If the moisture content reading indicates a wet soil, the system does not initiate water supply because there is no need for irrigation. The soil moisture content sensor used in this work is the Arduino compatible type shown in Figure 6. Three sensors were used and connected to analog pins A0, A1 and A2 of the Arduino Uno microcontroller board as part of the smart irrigation test bed developed in the Department of Electrical and Electronics Engineering in Elizade University (Ogidan *et al.*, 2019). The purpose of developing this irrigation test-bed is to act as a generalized platform to assist researchers and students in the testing of different algorithms they develop in the field of smart irrigation system. The soil moisture sensors were calibrated with standard digital soil moisture sensor and to give measured moisture values in percentage. If the sensor value falls within 2% to 39%, this indicates that the soil is dry. If the sensor value falls within 40% to 99%, this indicates that the soil is wet. If the moisture content sensor values indicates that the soil is wet, then there is no need for irrigation.

### System Output

The system output comprises of the actuators including relays and pumps, which are used to supply water to the farm site, Liquid Crystal Display (LCD) for display of the system activities for the viewing the system operation. All these are concerned with how the decision of the microcontroller is deployed and made visible to the user. Figure 3 shows the various components of the control unit being coupled, while Figure 4 is the control unit after coupling.

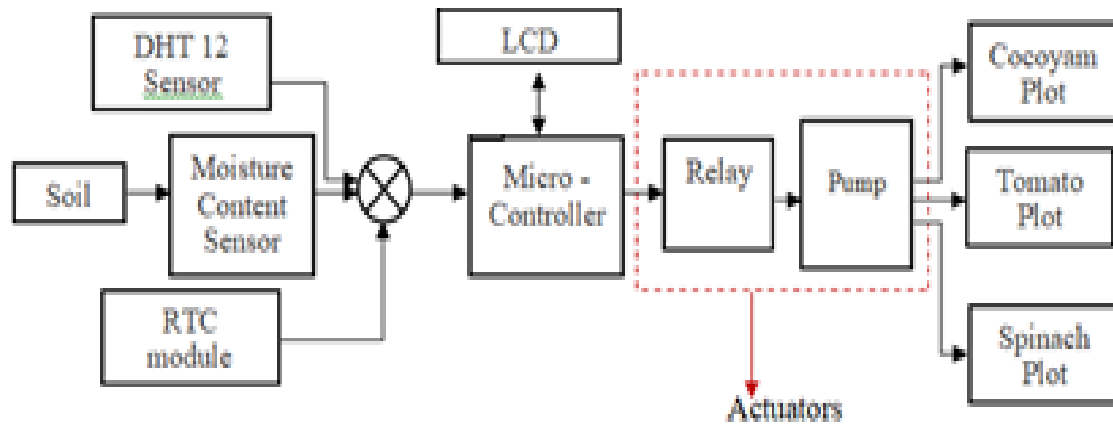


**Figure 1.** Block diagram of the smart irrigation system based on crop water use.

### Testing

For the purpose of testing the developed device, it was connected to the laboratory-scale irrigation test bed as shown in Figure 5. The irrigation test-bed depicts a farm setting with irrigation facilities such as reservoir, pumps, sprinklers, farm sites and so on used for testing irrigation systems in a laboratory setting (Ogidan et al., 2019). The system was set up using three moisture content probes and three soil samples were provided in containers representing soils of different farms (cocoyam, spinach, and tomatoes) soils. The probes were dipped into the soil samples one after the other.

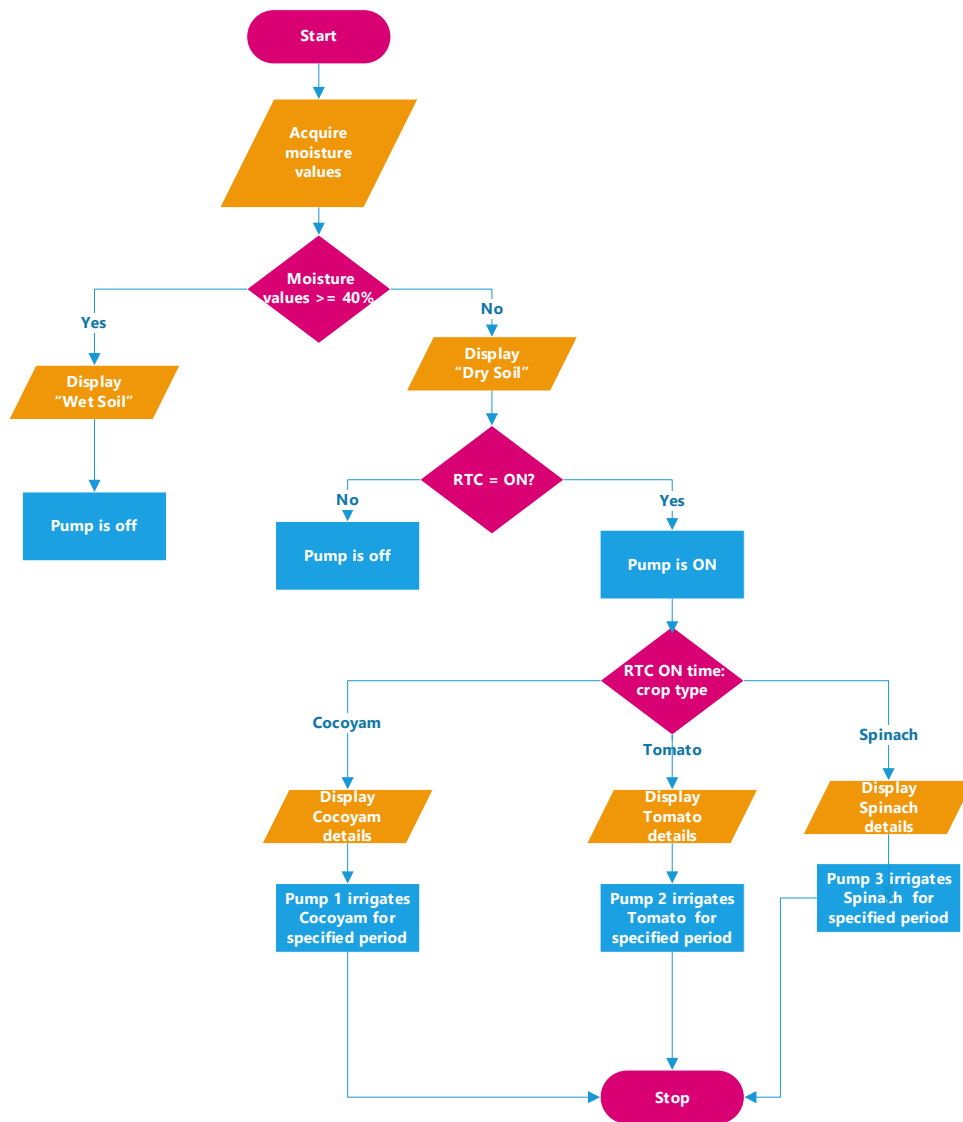
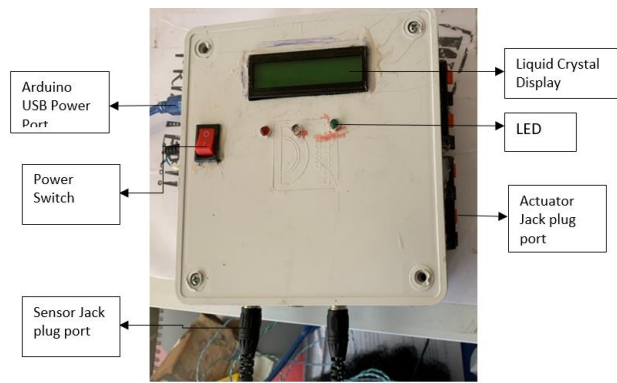


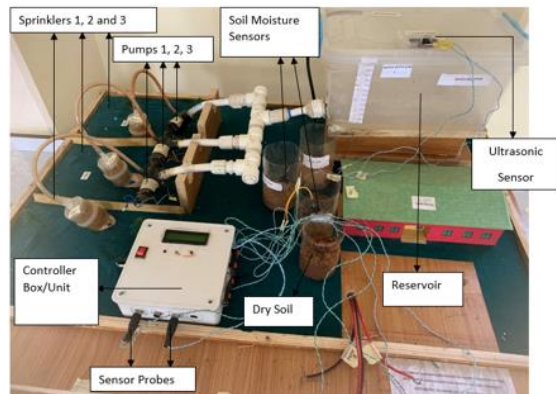
Figure 2. Flowchart of the smart irrigation system based on crop water use.



Figure 3. System being coupled.



**Figure 4.** Developed system after coupling.



**Figure 5.** Laboratory-scale smart irrigation test-bed (Ogidan et al., 2019).

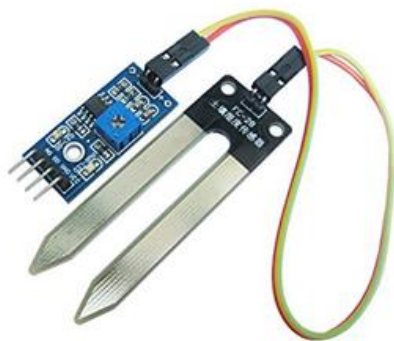


**Figure 6.** Soil moisture sensor.

## RESULTS AND DISCUSSION

Table 5 shows the results for the effect of the moisture content sensors and the real-time clock (RTC) on the pumps connected for each farm Cocoyam, Tomato, and Spinach respectively. With the moisture content sensor dipped in samples of dry soil, irrigation process was initiated in each of the farms, but the water was not supplied until the exact time specified by the RTC is reached. For instance, in case of cocoyam with a soil moisture of 15%, even though the LCD indicates that the soil is dry, water was not supplied to the cocoyam farm until 7:15:13 a.m. When it was 7:16:25 am exactly, the irrigation pump was turned off in line with the time set in the RTC. The watering commenced at 7:15:13 am and stopped at 7:16:50 am daily after supplying water for 97 seconds. The only time the irrigation process was not activated was when the soil was wet (between 84% and 99%) meaning there was no need for

irrigation. The same goes for spinach with 13% soil moisture indicating dry soil that commenced irrigation at 7:45:13 am and stopped water supply at 7:47:01 am after 108 seconds. In the case of tomatoes with moisture content of 20% indicating dry soil, the daily irrigation commenced at 7:30:13 am and stopped at 7:32:44 am after a duration of 151 seconds.

**Table 5.** Irrigation schedule for the three crops based on the RTC.

Soil Moisture (%)	Crop Type	RTC irrigation 'ON' time (hh:mm:ss)	RTC irrigation 'OFF' time (hh:mm:ss)	Irrigation duration per day (s)
15	Cocoyam	7:15:13	7:16:50	97.13
20	Tomato	7:30:13	7:32:44	151.70
13	Spinach	7:45:13	7:47:01	108.28

## CONCLUSION

In this work, a crop-specific crop water requirement algorithm based on data obtained from FAO Penman-Monteith equation was developed and emulated using a laboratory-scale irrigation testbed. RTC was employed in executing the irrigation scheduling by ensuring that the required amount of water was delivered as at when due on a daily basis without human intervention. The system helps to minimise water usage in that the required amount is delivered to the root of crops thus preventing over-irrigation or under-irrigation. Future work would involve implementation of the developed algorithm on a pilot farm and the incorporation of mini-weather station to provide online weather parameters for real-time computation of crop water requirements for different crops.

## DECLARATION OF COMPETING INTEREST

The authors declare that they have no conflict of interest.

## CREDIT AUTHORSHIP CONTRIBUTION STATEMENT

**Olugbenga Kayode Ogidan** designed the concept of entire project. The investigation, methodology and writing of the original draft were done by him, read and approved the final manuscript.

**Samuel Dare Oluwagbayide** was involved in the methodology and former analysis of the experiment. He carried out the review and editing of the original drafted copy, read and approved the final manuscript.

**Thomas Olabode Ale** participated in the designed and investigation of the experiment. He also handled the data curative and validation, read and approved the final manuscript.

## ETHICS COMMITTEE DECISION

This article does not require any ethical committee decision.



## REFERENCES

- Agugo BAC, Muoneke CO, Eno-Obongo EE and Asiegbu JE (2009). A theoretical estimate of crop evapotranspiration and irrigation water requirements of mungbean (*vigna radiata*) in a low land rain forest location of southeastern nigeria. In *Electronic Journal of Environmental, Agricultural and Food Chemistry*, 8(9): 720-729.
- Brouwer C and Heibloem M (1986). Irrigation water management: irrigation water needs. *Training Manual*, 3: 1-5.
- Dorji K, Dorji SD and Tshering P (2017). Irrigation scheduling and water requirements for citrus mandarin (*Citrus reticulata* Blanco) - A case study from Drujegang, Dagana Bhutan.
- Ewemoje TA, Fagbayide SD and Oluwasemire KO (2018). Lysimeter determination of crop coefficient of drip irrigated jatropha curcas. *Federal University Of Technology, Akure, Journal of Engineering and Engineering Technology*, 12(1): 159-170.
- Kamienski C, Soininen JP, Taumberger M, Dantas R, Toscano A, Salmon Cinotti T, Filev-Maia R and Torre-Neto A (2019). Smart water management platform: Iot-based precision irrigation for agriculture. *Sensors*, 19(2), 276; <https://doi.org/10.3390/s19020276>
- Kizito M, Amini N and Taha SU (2016). *Design and implementation of a smart irrigation system for improved water-energy efficiency*. Conference: 4th IET Clean Energy and Technology Conference (CEAT 2016). <https://doi.org/10.1049/cp.2016.1357>
- Munoth P (2016). *Sensor based irrigation: A review*. International Research Journal of Engineering and Technology (IRJET), NCACE Conference Proceedings, Jaipur, India.
- Ogidan OK, Onile AE and Adegboro OG (2019). Smart irrigation system: A water management procedure. *Agricultural Sciences*, 10: 25-31. <https://doi.org/10.4236/as.2019.101003>
- Ogidan OK., and Afia KR (2019). *Smart irrigation system with an android-based remote logging and control*. In IEEE Region 8 Flagship Conference (AFRICON), Gimpa Executive conference Centre, Accra, September, 25<sup>th</sup> - 27<sup>th</sup> 2019.
- Omid A, Pedro F, Luis G and Zita V (2020). Agricultural irrigation scheduling for a crop management system considering water and energy use optimization. *Energy Reports*, 12(1): 133-139. <https://doi.org/10.1016/j.egyvr.2019.08.031>
- Raeth PG (2020). Moving beyond manual software-supported precision irrigation to human-supervised adaptive automation. *African Journal of Agricultural Research*, 16(11): 1548-1553.
- Rodriguez D, Reza J, Martinez J, Lopez-Luque R and Urrestarazu M (2015). Development of a new control algorithm for automatic irrigation scheduling in soilless culture. *Applied Mathematics & Information Sciences*, 9(1): 47-56.
- Sandeep K and Deepali Y (2017). A Survey on automatic irrigation system using wireless sensor network. *International Journal of Current Engineering and Scientific Research*, 4(8): 68-80.
- Surendran U, Sushanth CM, Mammen G and Joseph EJ (2017). FAO-CROPWAT model-based estimation of crop water need and appraisal of water resources for sustainable water resource management: Pilot study for Kollam district-humid tropical region of Kerala, India. *Current Science*, (00113891), 112(1): 76-86.
- Torres-Sanchez R, Navarro-Hellin H, Guillamon-Frutos A, San-Segundo R, Ruiz-Abellón MC and Domingo-Miguel RA (2020). Decision support system for irrigation management. *Analysis and Implementation of Different Learning Techniques*, (12): 548.
- Wardlaw R and Bhaktikul K (2004). Applications of genetic algorithms for irrigation water scheduling. *Scotland*. UK.
- Yadav D, Awasthi MK and Nema RK. (2018). Study on crop water requirement of field crops under different climatic conditions of Madhya Pradesh. *Agricultural Science Digest*, 38(2): 81-87.
- Yogesh GG, Devendra SC and Hitendra CC (2016). A review on automated irrigation system using wireless sensor network. *International Journal of Advanced Research in Electronics and Communication Engineering (IJARECE)* 5(6): 1725-1731.
- Zia H, Rehman A, Harris NR, Fatima S and Khurram M (2021). An experimental comparison of iot-based and traditional irrigation scheduling on a flood-irrigated subtropical lemon farm. *Sensors*, 21(12): 4175. <https://doi.org/10.3390/s21124175>



## AquaCrop Model Validation for Simulating Biomass and Water Productivity Under Climate Change for Potatoes

AbdelGawad SAAD<sup>a\*</sup>, Hani Abdelghani MANSOUR<sup>b</sup>, Elsayed ALI<sup>a</sup>,  
Mostafa Mohamed AZAM<sup>c&d</sup>

<sup>a\*</sup> Department of Biosystem Engineering, Agricultural Engineering Research Institute (AEnRI), Agricultural Research Center (ARC), Dokki, Giza, EGYPT

<sup>b</sup> Department of Water Relations and Field Irrigation, Agriculture and Biological Division, National Research Centre, Cairo, EGYPT

<sup>c</sup> Department of Agricultural Engineering, Faculty of Agriculture, Menofia University, Shibin El-Kom, EGYPT

<sup>d</sup> Department of Agricultural Systems Engineering, College of Agriculture & Food Sciences, King Faisal University, Al-Ahsa, SAUDI ARABIA

(\*) Corresponding Author: [en\\_gawad2000@yahoo.com](mailto:en_gawad2000@yahoo.com)

### Article Info

Received: 05.02.2023

Accepted: 16.05.2023

Published: 30.06.2023

## ABSTRACT

Effective crop development modelling is essential for crop management, water resource planning, assessing climate change's influence on agricultural production, and yield prediction. Validation and simulation of the measured data indicated that AquaCrop software is an effective and reliable program for designing pressurized irrigation systems to increase water application efficiency, system performance and the future prediction. The AquaCrop model was evaluated through a solid-set sprinkler and surface drip irrigation systems at 100%, 80%, and 60% of evapotranspiration (ET<sub>o</sub>) for the potato crop. The AquaCrop model has shown better performance to simulate potato growth and predicting crop variables under various water systems. The surface drip-irrigation system's at 80% of ET<sub>o</sub> (48.00, 8.05 ton ha<sup>-1</sup>) Yield had a substantial impact on the yield of potato and water productivity (WP), matching the yield of potatoes that was irrigated with solid-set sprinklers at 100% of ET<sub>o</sub> (37.39, 7.19 ton ha<sup>-1</sup>), with 20% water savings. Attributes of potatoes (canopy cover, biomass, potato crop factor (K<sub>c</sub>), and water productivity) were affected by increasing water deficit. The simulated of AquaCrop model was a little higher than observed at 80% of ET<sub>o</sub> treatment, but still has a similar deviation, and it was slightly lower than seen for 60% of ET<sub>o</sub> treatment at the mid-season. The AquaCrop model predicted the yield of potatoes and biomass correctly when irrigation is adequate. The results indicated that there may be some changes in AquaCrop model simulation operations over future years based on the climate and irrigation method.

**Keywords:** AquaCrop model, Drip irrigation, Sprinkler irrigation, Potato yield, Water productivity

**To cite:** Saad A, Mansour HA, Elsayed A and Azam MM (2023). AquaCrop Model Validation For Simulating Biomass And Water Productivity Under Climate Change For Potatoes. Turkish Journal of Agricultural Engineering Research (TURKAGER), 4(1), 26-45. <https://doi.org/10.46592/turkager.1247795>



## INTRODUCTION

The impact of current agricultural climate change depends on climatic and weather conditions, as well as crop production and agricultural production are affected by climatic conditions. Precipitation and carbon dioxide concentration both have a direct effect on the production of potatoes. The environment is impacted by climate change, either directly or indirectly. According to [Malhi \*et al.\* \(2021\)](#), climate change will have an effect on agriculture and mitigation strategies. Because of the climate change effect caused by greenhouses, which is actually rising, food security is a global concern. It has been reported that about 1.5-1.8 ppm of carbon dioxide is added to the atmosphere every year. It is crucial to point out that precipitation will fall by 0.7% and 3.0% in 2050, by 5.0% and 7.6% in 2100, and that temperatures will increase by 3-4°C by the end of the 21<sup>st</sup> century. Crop response to water deficit remains to be one of the most reactions to be described by crop models since the water deficit varies in duration, timing, and intensity ([Molden \*et al.\*, 2001](#)). The competitive demand for the limited supply of water is now becoming critically important. The agricultural sector is facing a major difficulty in using less water and produce more food because there are limited opportunities to increase the availability of high water quality. Developing methods to increase the effectiveness of water application in agriculture is therefore required. One of the most effective irrigation techniques for use in agriculture with advanced water-saving technology is pressurised irrigation ([Kemanian \*et al.\*, 2007](#)). Simulation models of crop growth are essential tools for analyzing the consequences of water shortages and for optimizing water use in constrained situations to increase crop production. There is a need to take into consideration about the effectiveness of the use of the available water given the undesirable climate change's effects on current agricultural practices followed by reducing water availability. This is especially important for high-value plants that can be grown in irrigation conditions ([Hsiao, 2000](#); [Hsiao, 2007](#)). The potato crop's yield and biomass were simulated using the AquaCrop model in response to different water application rates. It is also required to calibrate the Aquacrop model for potatoes under limited climatic conditions, as doing so would make it simpler to simulate and predict crop's performance and yield using all of the AquaCrop model's input data parameters ([Steduto, 2003](#)). In recent years, the potato has taken on a significant role in Egypt's crop rotation as a winter crop in both rich and poor fertile soils, alkaline, saline, and calcareous soils. Farmers could then make prior plans for their returns based on every parameter supplied for the model's input data.

A drip irrigation system uses less water than a sprinkler irrigation system. For total and marketable yield, surface drip and subsurface drip were among the most effective techniques. In addition, nitrate leaching under potatoes was reduced by drip irrigation or sprinkler irrigation (at fairly dry soil criteria). Potato yield was unaffected by reducing nitrogen rates when irrigated with a subsurface drip system ([Kaur \*et al.\*, 2022](#)). [Ibrahim \*et al.\* \(2018\)](#) explored the impact of tape depth and emitter spacing on Texas potato (Norgold Russet) yield and quality. Potato yield was unaffected by tape depth or emitter spacing, Nevertheless, when the tape was buried at 0.2 m as opposed to shallower placement, the percentage of tubers that were misshaped was greater. The soil temperature was higher at the tape of 0.2 m, than at 0.1 m or 0.025 m. In comparison to intermediate and greater depths, the drip tape

performed best at depths of 0.08 m (above tubers) and 0.46 m (below tubers), according to [DeTar \*et al.\* \(1996\)](#)'s study. Ten drip irrigation treatments were used by [Fabeiro \*et al.\* \(2001\)](#) to investigate the effect of irrigation deficit timing on tuber productivity and water use efficiency in Spain. Deficits in irrigation that occurred during the mid and late season bulking of tubers were mostly harmful to tuber yield. When irrigation shortfalls are limited to early in the season, good yields are associated with high water usage efficiency. The growth of "Umatilla Russet" in silt loam with drip irrigation. The variables that were investigated included four levels of soil water tension and tape placement (1 tape/ single row or 1 tape/ double row) for automatically beginning irrigation (15, 30 45, and 60 kPa) ([King \*et al.\*, 2020](#)); ([Mansour \*et al.\*, 2015a](#); [Mansour \*et al.\*, 2015b](#); [Mansour \*et al.\*, 2019a](#); [Mansour \*et al.\*, 2019b](#)). They found that drip tape placement significantly affected every measure, with the exception of total yield and bud-end fry colour, where associations between irrigation criterion and tape quantity were significant. Total yield, total marketable yield, and US No. 2 yield were all influenced by the interaction between the tape placement and irrigation criterion. The results revealed that set the silt loam soil and 2.5 mm water applied during each irrigation episode, potatoes should be irrigated at 30.0 kPa. The whole US No. 1 and over 340.0 g tuber size categories were the only ones affected by the irrigation criterion taken into account alone. Different potato cultivars performed considerably differently when subjected to drip irrigation ([Eldredge \*et al.\*, 2002](#)); ([Mansour \*et al.\*, 2016](#)). The AquaCrop model uses a semi-quantitative method to characterize the impact of biomass production but does not predict nutrient cycles and balances ([Rahimikhoob \*et al.\*, 2021](#)). [Mengistu \*et al.\* \(2021\)](#) discovered that the AquaCrop model accurately simulates all observed crop variables. The performance of the AquaCrop model for the potato crop's canopy cover, biomass from dried aboveground and tubers, as well as soil moisture levels.

This study was envisaged to estimate the yield response factor under deficit irrigation in various stressed irrigation systems and validate the AquaCrop model using irrigated potatoes under full and deficit irrigation levels for future prediction.

## **MATERIALS and METHODS**

### **Area of Study and Crop Management**

The potato Spunta variety was planted in an area of 2000 m<sup>2</sup> with split-plot design at the Experimental Farm of National Research Centre, El Nubaria, Egypt, (latitude 30.87 N, longitude 30.17 E) with an altitude of 20 m above sea level. All plots received the normal and recommended care steps for potato growing indicated in the instructions of the official agricultural bulletins. The potato was planted manually to each line at a 15 cm distance between tuber seeds. The potato was cultivated for the growing season on 15<sup>th</sup> Oct. 2021 and harvested on 31<sup>st</sup> Jan 2022. Before cultivation, the soil was plowed three perpendicular times at 20 cm depth, and leveled 100 cm distance apart to extend the lateral tubes of surface irrigation in each experimental plot.

**Table 1.** Some physical properties of the soil.

Depth, cm	Particle Size distribution, %				Texture class	θS % on weight basis					
	C. Sand	F. Sand	Silt	Clay		F.C.	W.P.	AW	HC (cmh <sup>-1</sup> )	BD (g/cm <sup>3</sup> )	"P (cm <sup>3</sup> voids/cm <sup>3</sup> soil)
0-15	8.4	77.6	8.5	5.5	Sandy	14.0	6.0	8.0	6.68	1.69	0.36
15-30	8.6	77.7	8.3	5.4	Sandy	14.0	6.0	8.0	6.84	1.69	0.36
30-45	8.5	77.5	8.8	5.2	Sandy	14.0	6.0	8.0	6.91	1.69	0.36
45-60	8.8	76.7	8.6	5.9	Sandy	14.0	6.0	8.0	6.17	1.67	0.37

Particle Size Distribution according to (Gee and Bauder, 1986) and Moisture retention according to (Klute, 1986), F.C.: Field Capacity, W.P.: Wilting Point, AW: Available Water, HC: Hydraulic conductivity (cm h<sup>-1</sup>), BD: Bulk density (g cm<sup>-3</sup>) and P: Porosity (cm<sup>3</sup> voids/cm<sup>3</sup> soil).

**Table 2.** Some chemical properties of the soil.

Depth, cm	pH 1:2.5	EC dS/m	Soluble Cations, meq/L				Soluble Anions, meq/L			
			Ca <sup>++</sup>	Mg <sup>++</sup>	Na <sup>+</sup>	K <sup>+</sup>	CO <sub>3</sub> <sup>--</sup>	HCO <sub>3</sub> <sup>-</sup>	SO <sub>4</sub> <sup>--</sup>	Cl <sup>-</sup>
0-15	8.3	0.35	0.50	0.39	1.02	0.23	0	0.11	0.82	1.27
15-30	8.2	0.36	0.51	0.44	1.04	0.24	0	0.13	0.86	1.23
30-45	8.3	0.34	0.56	0.41	1.05	0.23	0	0.12	0.81	1.23
45-60	8.4	0.73	0.67	1.46	1.06	0.25	0	0.14	0.86	1.22

Chemical properties according to Rebecca (2004).

**Table 3.** Potato crop factor (Kc) in the semi-arid area.

Stage of growth	Initial	Crop development	Mid-season	Late-season
Periods	1 - 20	21-55	56.0-70	71-110
Total days	35	60	70	45
Kc	0.35	1.2	1.2 > Kc > 0.7	0.5

### Irrigation Systems and Experimental Layout

Standard methods were used to analyze the irrigation water to identify its chemical characteristics. To evaluate the chemical and physical properties of soil, as shown in (Tables 1 and 2) the samples were withdrawn from the soil profile at various layer thicknesses (0, 15, 30, 45, and 60 cm). Every main plot was split into three subplots, each of which contained three treatments and represented three water treatments used to calculate the crop's evapotranspiration (ET<sub>o</sub>) (100, 80, and 60%). The irrigation plan was designed on a two-day interval and applied using pressurized irrigation methods to meet crop water requirements (WR) (solid-set sprinkler and surface drip irrigation). The rotation depends on a shocking stick (kind of sprinkler that can control its rotation and it has a nail to deflect the rush of the water path). The following equation provided by Wu and Gitlin (1975) was used to determine how much irrigation water was used.

$ET_c = ET_o \times K_c$ .  $ET_c$  is evapotranspiration (mm/day),  $ET_o$  is reference evapotranspiration (mm day<sup>-1</sup>) and  $K_c$  is a crop factor.

### Agronomic Data

All agronomic measurements were started after one month from the date of potato planting. Every month, three representative plants were randomly chosen from every plot and measured for height (cm), leaf length (cm), number of leaf plant<sup>-1</sup>, tuber diameter (cm), fresh weight of the top (leaves) /plant (g), dry weight of the top (leaves) /plant (g), total fresh tuber weight (g plant<sup>-1</sup>) and total fresh dry weight (g plant<sup>-1</sup>). At 70°C, plant samples were over-dried until their weight remained constant. A random sample was selected (5 plants) from each plot at harvest to assess the productivity and quality characteristics of the potatoes.

Leaf area index (LAI) = Total area of leaf / Occupied land area (Fang et al., 2019) (1)

By the CC-LAI relationship for canopy cover (CC) of potato was calculated using LAI (García-Vila and Fereres, 2012).

$$CC = 1.005 \times [1 - \exp(-1.2LAI)] \times 100 \quad (2)$$

$$WP = \text{Yield} / \text{Total applied water amount} \quad (3)$$

Where:  $WP$  is productivity of water, (kg m<sup>-3</sup>);  $Y$  is total tuber yield, (kg ha<sup>-1</sup>); and total applied by (m<sup>3</sup> ha<sup>-1</sup>), (Howell, 2001).

Models of the potato plant's reaction to water stress take into account changes in harvest index, canopy cover, and leaf expansion. The model then simulates the yield and biomass using the values of the daily transpiration (Equations 4 and 5).

$$Y = HI \times B \quad (4)$$

$$B = WP \times \sum Tr \quad (5)$$

Where:  $B$  = biomass (g m<sup>-2</sup>),  $Tr$  = potato plant transpiration (m<sup>3</sup> ha<sup>-1</sup>), and  $HI$  = harvest index.

### Climatic Data

The monthly meteorological data for the area of study during the growth period was displayed in Table 4, based on the official data collected by the Central Laboratory for Agricultural Climate. Climatic elements of air temperature (°C), dew point temperature (°C), wind speed (m s<sup>-1</sup>), and rainfall (mm). The evapotranspiration ( $ET_o$ ) was calculated with the use of the  $ET_o$  calculator program depending on the Penman-Monteith equation (Version 3.2, September 2012; Raes et al., 2009).

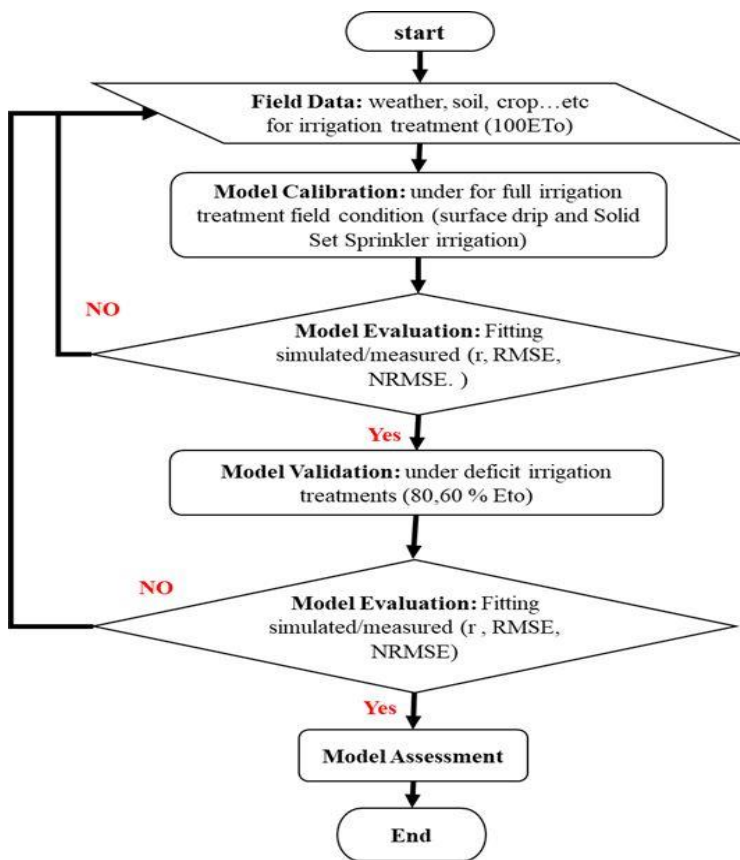
Representative Concentration Pathways (RCPs) 8.5 were chosen for the impact assessment of the climate scenarios 2030, 2050, and 2100. The International Panel on Climate Change adopted the RCPs as greenhouse gas concentration pathways for future climate (Attia and Gobin, 2020).

**Table 4.** Average climate data in the study area.

Month	T <sub>max</sub> °C	T <sub>mean</sub> °C	T <sub>min</sub> °C	T <sub>dew</sub> °C	Wind speed, m s <sup>-1</sup>	Rain, mm
October 2021	28.35	21.88	16.44	5.72	0.45	0.00
November 2021	23.90	17.22	12.14	0.48	0.22	1.89
December 2021	18.45	11.49	6.25	0.64	0.35	2.12
January 2022	17.83	11.36	6.33	0.00	0.45	2.79

### AquaCrop Model

The AquaCrop flow chart for calibration and validation is shown in Figure 1. In order to get the most favourable understanding between the simulated and measured system variables, the model's input parameters must be calibrated ([Shaw et al., 2002](#)).

**Figure 1.** AquaCrop model flow chart processing.

An essential component of model verification is model performance evaluation, which entails contrasting the output produced by the model with independent field measurements. It was calibrated for potatoes using the AquaCrop model (version 6.1).

### The Model Performance Criteria

The performance of the model was then assessed by statistical tools, like Pearson correlation coefficient ( $r$ ), normalized root mean square error (NRMSE), and root mean square error (RMSE).

The Pearson correlation coefficient ( $r$ ), which runs from -1 to 1, indicates strong agreement when values are close to 1 and are normally deemed acceptable in

watershed modelling when values are more than 0.5. (Moriassi et al., 2007). If the measured and simulated values are completely independent, ie they are not correlated or will be zero (Loague and Green, 1991).

$$r = \frac{\sum O_i P_i - n \bar{O} \bar{P}}{\sqrt{\sum O_i^2 - n \bar{O}^2} \sqrt{\sum P_i^2 - n \bar{P}^2}} \tag{6}$$

Where  $P_i$  is the simulated values,  $O_i$  is the observed values,  $\bar{O}$  is the mean of observed values and  $n$  is the number of observations.

The testing of models with various scales is made easier by RMSE and NRMSE. RMSE has a range of zero to positive infinity, with zero signifying excellent model performance and positive infinity, bad model performance. Since RMSE is scale-dependent, it should be used to compare prediction errors of several models of a specific set of data rather than between data sets (Pontius et al., 2008). The variable's observed range and the RMSE are connected by the normalised RMSE (NRMSE). The NRMSE can be seen as a part of the total range that the model normally resolves as a consequence.

$$RMSE = \sqrt{\frac{\sum_{i=1}^n (O_i - P_i)^2}{n}} \tag{7}$$

$$NRMSE = \frac{\sqrt{\frac{\sum_{i=1}^n (O_i - P_i)^2}{n}}}{\bar{O}} \tag{8}$$

Where  $P_i$  is the simulated values,  $O_i$  is the observed values,  $\bar{O}$  is the mean of observed values and  $n$  is the number of observations.

## RESULTS and DISCUSSION

### Reference Evapotranspiration (ETo)

The data shown in Figure 2 shows the daily of (Reference evapotranspiration) ETo. It was calculated by the Penman-Monteith eq., for daily weather data for irrigated potatoes from October 15, 2021, to January 31, 2022. The average of ETo was about 2 mm day<sup>-1</sup> season.

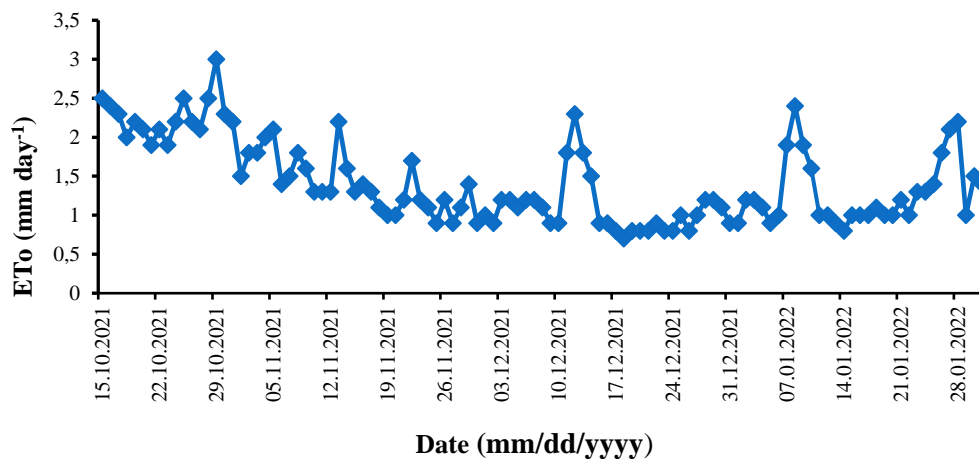


Figure 2. The daily reference evapotranspiration (ETo).



### Applied Water Requirements

The data in Table 5 show the water requirements for irrigated potatoes grown under surface drip and solid-set sprinkler irrigation systems at various water application rates (100, 80, and 60% of ETo) throughout each growth stage. These values were calculated using ETo and Kc. It is evident that due to the high evapotranspiration, the largest amount of water applied was (617 mm) under solid-set sprinkler irrigation and more than (11%) under surface drip irrigation. The irrigation schedule was timed to coincide with the WR applied via surface drip irrigation systems and metered solid-set sprinklers, and it was based on a two-day interval.

**Table 5.** Applied water requirements (WR) under the surface drip and solid-set sprinkler irrigation.

Days from planting	Growing stage	Applied water due to ETo					
		100%		80%		60%	
		Solid-set sprinkler	Surface drip	Solid-set sprinkler	Surface drip	Solid-set sprinkler	Surface drip
1	Initial	68.71	60.63	54.97	47.50	41.23	36.38
20							
21	Development	273.60	244.85	218.88	191.13	164.16	144.85
55							
56							
70	Mid-season	176.26	155.52	141.01	124.52	105.75	93.31
71							
110	Late-season	98.40	86.82	78.72	68.66	59.04	52.09
Total on the season		616.97	547.82	493.58	431.81	370.18	326.63
% of the saved water		0.00	0.00	11.21	20.00	30.01	40.00

### AquaCrop Calibration

The AquaCrop calibration was performed based on measurements of the green canopy cover and data on observed crop growth for the irrigated potato crop under both irrigation systems. The data collected under 80% and 60% of ETo were used to validate the model, while the observed field data under the full irrigation method were used to calibrate the model. The meteorological information, soil properties, CC growth, date of sowing, planting density, CC, biomass (B), and total yield (Y) were used as input for each simulation run. For model calibration, plant density, maximum measured tuber depth, crop development period, and crop water productivity were used. The relationship between the biomass of potato crop, which was determined from samples obtained periodically throughout the growing season, and ETo is given in Figure 3.

According to the data, the WP for surface drip irrigation and solid-set sprinkler irrigation was around 14.1 and 15.1 g m<sup>-2</sup> respectively with an average of about 14.6 g m<sup>-2</sup>. The simulation results for CC, biomass (B), and total yield (Y) were compared to the measured data to evaluate the model's performance.

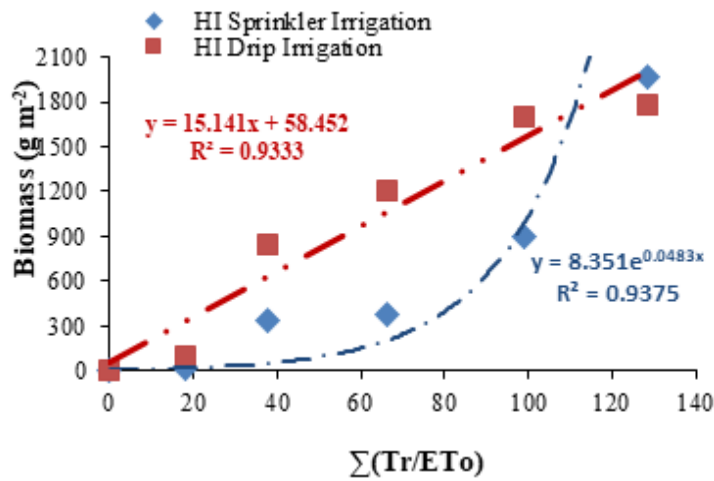


Figure 3. Determination of potato crop biomass.

### Green Canopy Cover (CC)

In Figure 4, with the full irrigation requirement (100% of ETo), the CC analysis results for both irrigation systems are shown. Although there was some variation in the CC between measured (observed) and simulated in the two irrigation systems, it was obvious that surface drip irrigation (S100) had a maximum measured CC of about 80%, while solid-set sprinkler irrigation (S100) had a maximum measured CC of about 75% (D100).

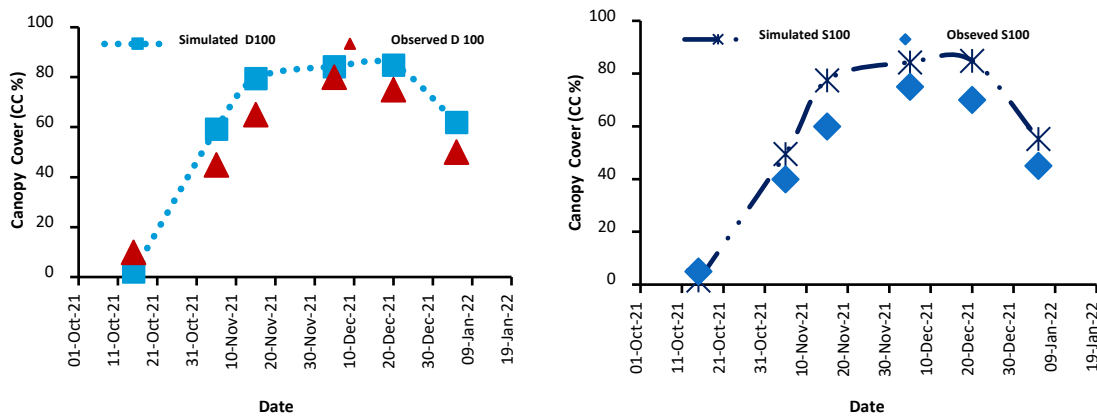


Figure 4. Measured and simulated CC under full irrigation a) surface drip irrigation system b) a solid-set sprinklers irrigation system.

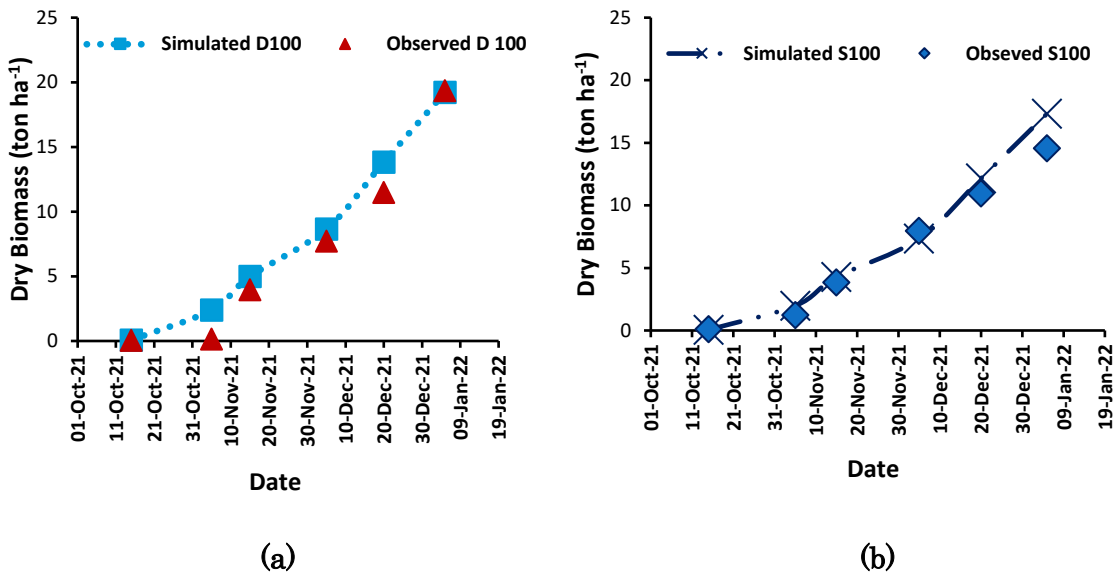
### Dry Biomass (B) and Yield (Y)

Figure 5 shows the results of the dry biomass (B) analysis for both irrigation systems under the full irrigation requirement (100% of ETo). The measured dry biomass and the simulated dry biomass under the surface drip irrigation system differed slightly, as indicated, with the simulated dry biomass being higher than the measured, while there was no difference under the solid-set sprinkler irrigation. Additionally, the maximum measured and simulated dry biomass production of potatoes under surface drip irrigation at harvest was approximately 19.35, 19.23 ton ha<sup>-1</sup>, whereas it was approximately 14.56, 17.33 ton ha<sup>-1</sup> with solid-set sprinkler irrigation. Figure 6 shows the dry yield response to applied water during the growing season. According to the data, both irrigation systems' water applications increased along with the dry

yield. The data obtained calculated that there was no significant difference in the model performances, and the statistical indicators validated the good calibration and performance of AquaCrop in simulating the potato growth and crop water productivity (WP) planted under drip and solid-set sprinkler irrigation systems. The best simulation results were achieved for CC and biomass, with the Pearson correlation coefficient ( $r$ ) being high above 0.99 for both irrigation systems, although it varied for other statistical indicators presented in Table 4. The irrigation treatment had an impact on the simulated values. For two irrigation treatments, the biomass simulation values followed the same trend. On the other hand, the simulated was a little higher than observed at 80% of ETo, but continues to deviate similarly, and it was slightly lower than seen at 60% of ETo treatment at the mid-season. These results agree with those of [Razzaghi et al. \(2017\)](#), who indicated that a variety of simulated biomass from the observed biomass of less than 10% is acceptable.

**Table 6.** Statistical indicators for CC and biomass for full irrigation.

Statistical Indicator	CC, S100	Biomass S100	CC, D100	Biomass D100
$r$	0.99***	0.99***	0.98***	0.99***
RMSE	11.70*	1.30*	11.10*	1.45*
NRMSE	23.80*	20.20*	20.50*	20.30*



**Figure 5.** Measured and simulated dry biomass under full irrigation a) surface drip irrigation system b) a solid-set sprinklers irrigation system.

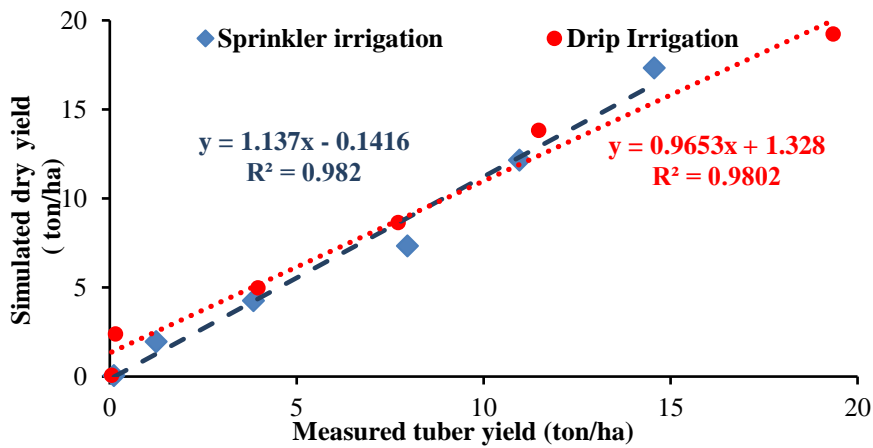


Figure 6. Measured and simulated dry yield under full irrigation.

### AquaCrop Validation

The green yield, biomass, WP, and CC were simulated for different water regimes under both irrigation systems using the calibrated model. Validation of the model was done by contrasting the simulated vs. with measured parameters which included CC and biomass to evaluate the AquaCrop model against the field measured data.

### Comparison of Measured and Simulated CC

The results of the comparison between measured and simulated CC under both irrigation water regimes (80 and 60% of ETo) are shown in Figure 7. The results displayed a significant difference in the CC due to the water stress effect. The crop's increased water transpiration and greater vegetative growth were the causes of this result. The results showed that the model overstimulated CC in all the treatments, especially under 60% of ETo treatment, and the prediction improved with a decline in the water rate application. When compared to the simulated CC, the deficit-irrigated at 60% of ETo yielded lower CC values. As the potato plants developed during growth, the need for water increased, but the supply was insufficient to satisfy crop WR, so the model did not predict properly. However, 80% of ETo treatment of the AquaCrop model had a good prediction of crop growth, especially in the mid and late season. The results of CC model validation are acceptable according to the statistical indicators as shown in Table 7, but the modelling of 60% of ETo treatments was less satisfactory compared to 80% of ETo treatments, which showed the model high performance.

Table 7. Statistical indicators for canopy cover (CC) under deficit irrigation.

Statistical Indicator	CC S80	CC, S60	CC,D80	CC, D60
r	0.98***	0.86**	0.93***	0.80*
RMSE	9.80*	16.00***	12.20*	20.40**
NRMSE	18.10*	45.70***	22.60*	58.30**

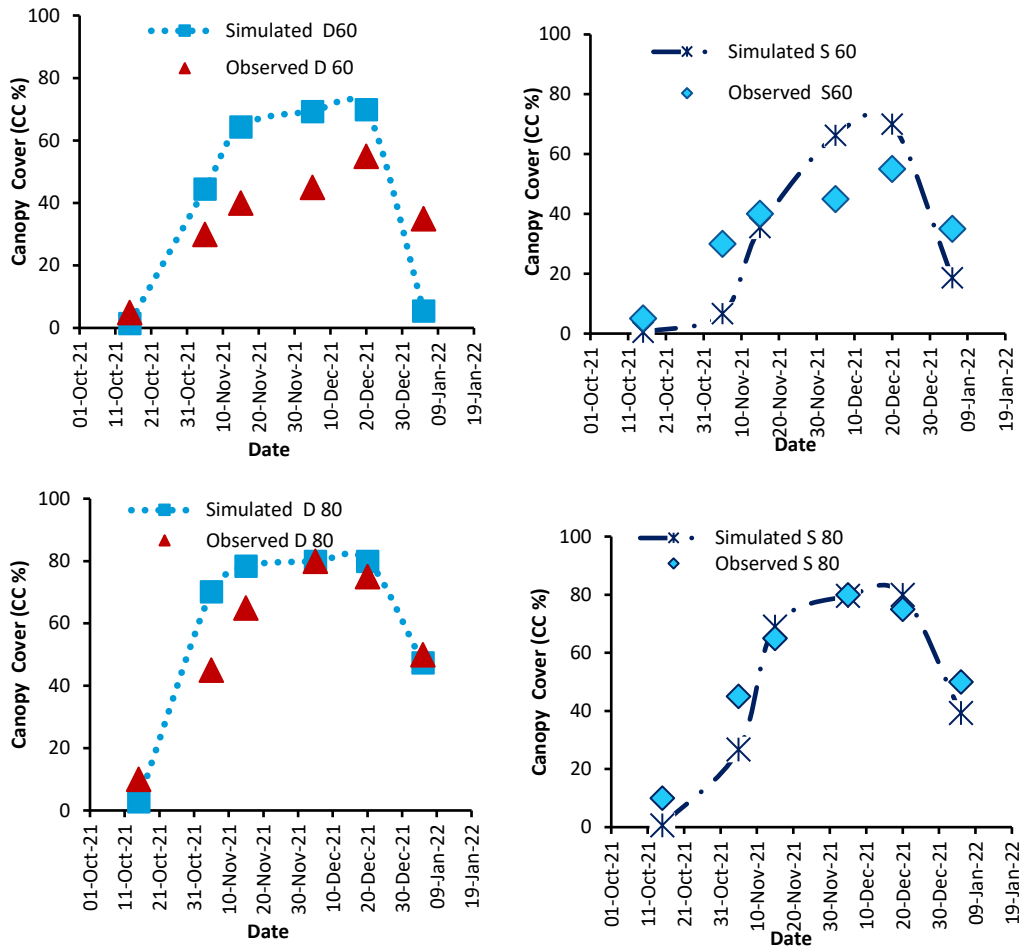


Figure 7. Measured and simulated CC with 80% and 60% regimes.

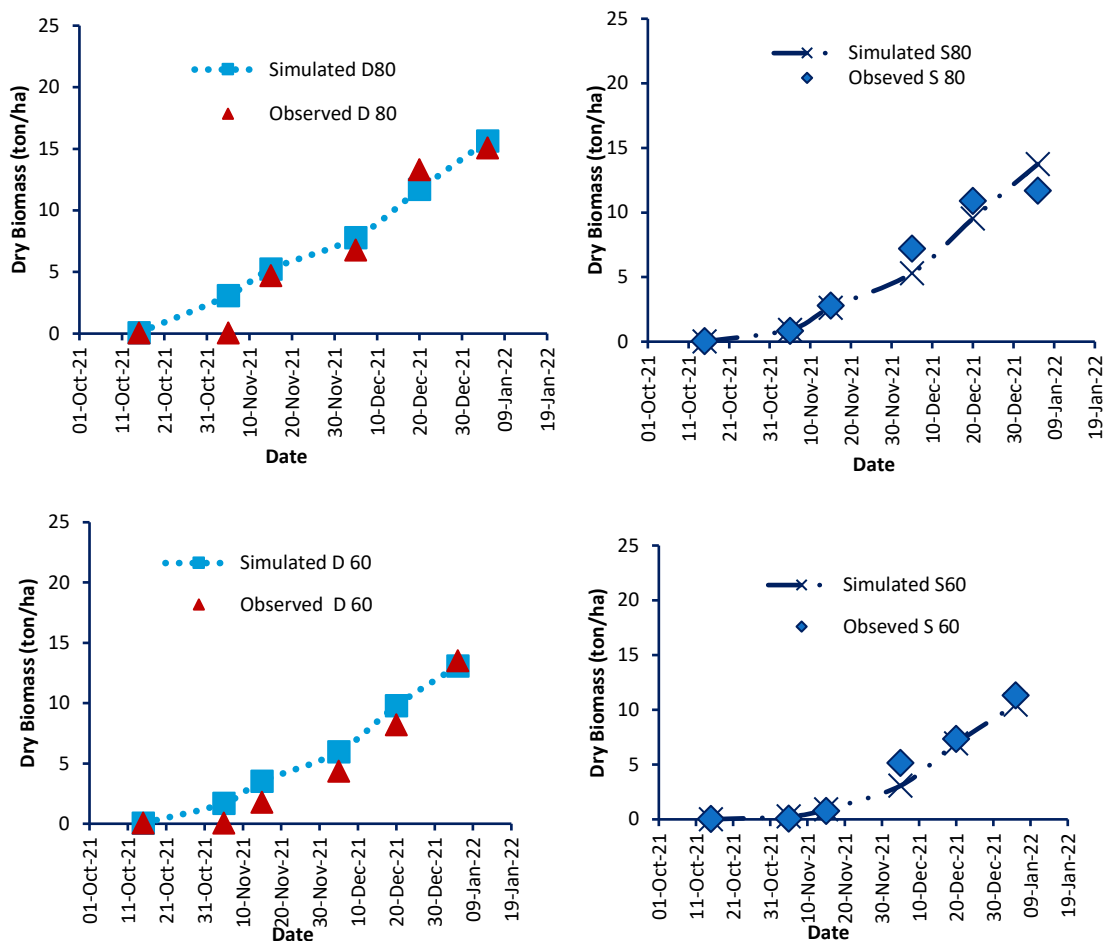


Figure 8. Measured and simulated dry biomass with 80% and 60% of Eto.

Also, the data simulated and measured showed that the dry yield of drip-irrigated potato at 80% of ETo closely matched with the yield of solid-set sprinkler-irrigated potato at 100% of ETo. They was no variation between measured and simulated data under full and deficit irrigation for both irrigation systems. The statistical indicators for different water regimes (80% and 60% of ETo) are presented in Table 8 clarified the results obtained from the model showed that the validation of AquaCrop is acceptable according to the statistical indicators for 80% treatment under both irrigation systems as the simulated dry biomass was slightly the same of the measured and the r-value was about 0.97 and 0.98 for solid-set sprinkler and surface drip irrigation, respectively showing highly significant with the other indicators.

The modelling of the 60% treatment was less successful; the simulated dry biomass was higher than the measured dry biomass in the 60% of ETo solid-set sprinkler irrigation treatment, while it was the opposite in the surface drip irrigation treatment, despite the r value for the sprinkler and surface drip irrigation treatments being approximately 0.99 and 0.98, respectively. This might be because neither 80% of the treatments experienced the acute water stress that would have affected biomass accumulation. Moreover, 60% of ETo experienced water stress through the developing season. Additionally, the AquaCrop model's estimated potato water productivity (WP) for dry yield was significantly higher than the actual value for all irrigation treatments, particularly when deficit irrigation was used, with WP values rising as the water deficit increased. The highest WP was obtained using

surface drip irrigation, particularly when 80% treatment was recorded (11.02 kg m<sup>-3</sup>). In contrast, solid-set sprinkler irrigation had a lower productivity of 7.68, 6.89, and 7.44 at 100%, 80%, and 60% of under water regimens, respectively.

**Table 8.** Statistics for dry biomass under shortage irrigation.

Statistical Indicator	Dry biomass S80	Dry biomass S60	Dry biomass D80	Dry biomass D60
r	0.97***	0.99***	0.98***	0.98***
RMSE	1.30*	0.94*	1.50*	1.35*
NRMSE	22.80*	22.80*	22.50*	29.10*

### Water Stress's Impact on a Potato Yield Component

The results demonstrated how water shortages during the winter of 2021–2022 affected some potato characteristics and yield under surface drip and solid-set sprinkler irrigation methods. Including the mean tuber weight, sucrose, impurities purity percentages, and white sugar yield. According to the measurements, raising the water deficit from 100 to 60% of ETo crop water requirement under two irrigation systems had a substantial impact on potato productivity and white sugar production.

Averaged data over the season revealed at 100% of ETo produced the highest value of tuber yield (54.36, 47.38 ton ha<sup>-1</sup>) under surface drip and solid-set sprinkler irrigation, respectively. Surface drip-irrigated potato plants by 80% of ETo gave the highest percentages of sucrose (19.90%) and purity (84.66%). Additionally, there was no significant variance in the crop ETo at 60% and 80%. The highest WP for white potato yield obtained was under 80% of ETo with about 1.85 kg m<sup>-3</sup> with comparing with all treatment irrigation as shown in Figure 9. Contrarily, when the water deficit grew from 100 to 60% of ETo, the WP raise under both irrigation methods with a few water amount. Additionally, that means there is a big chance to increase the production of white sugar by cultivating a larger area while using the same amount of water (617 mm) under solid-set sprinkle full irrigation, as shown in Table 9. Under surface drip and solid-set sprinkler irrigation systems, the reduction in white sugar yield was 37% and 42.05%, respectively.

Our results were in agreement with those of [Salemi et al. \(2011\)](#), who recommended that the climate, variety of plants planted, and irrigation method might cause some variations in model simulations over dissimilar years. When irrigation is adequate, the AquaCrop model accurately predicts biomass and yield, as shown by [Heng et al. \(2009\)](#), and this result was supported by the results of the current study. Additionally, the measured biomass under various irrigation methods and the simulated Biomass (B) were both consistent (Tables 7 and 8). During this investigation, the CC results were comparable to those found in [Salemi et al. \(2011\)](#). The study found that the AquaCrop model could simulate CC of potato, B, and Tuber Yield (T) under various irrigation methods.

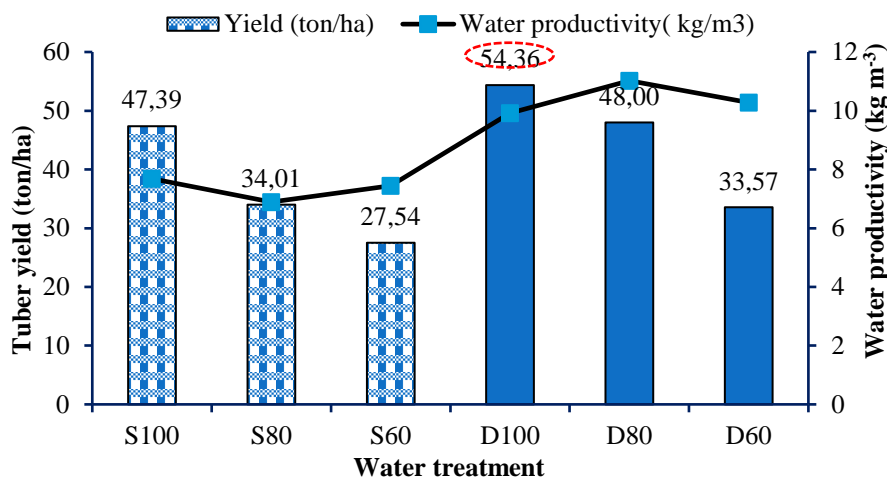


Figure 9. Tuber yield and WP under different irrigation systems regimes.

Table 9. Total area cultivated and total tuber yield using different mean water amounts of solid-set sprinkle full irrigation.

Water applied treatments	S100	S80	S60	D100	D80	D60
Water applied amounts (m <sup>3</sup> ha <sup>-1</sup> )	336.33	269.07	201.79	319.49	235.41	168.15
Total area cultivated (ha)	1.00	1.25	1.76	1.13	1.42	1.89
Total tuber yield (ton)	7.19	6.96	6.96	10.25	11.43	10.79

**The expected scenarios 2030, 2050 and 2100 for WR and WP for winter potato**

The expected scenarios for the WR of the winter potato crop in the study area are displayed in Table 10 and Figure 10 with values of 2544 m<sup>3</sup> ha<sup>-1</sup> in 2030, 2035 m<sup>3</sup> ha<sup>-1</sup> in 2050, and 1527 m<sup>3</sup> ha<sup>-1</sup> in 2100 at 100% of ETo. These values were estimated for the comparative treatment and without water stress. The potato will require 2597 m<sup>3</sup> ha<sup>-1</sup> of water in the year 2030, 2077 m<sup>3</sup> ha<sup>-1</sup> in the year 2050, and 1558 m<sup>3</sup> ha<sup>-1</sup> in the year 2100 if the same treatment was applied in the future, which results in water stress using 80% of ETo. Additionally, if 60% of ETo is adopted, the water quantity needed in 2030, 2050, and 2100 will be 2851, 2281, and 1711 m<sup>3</sup> ha<sup>-1</sup>, respectively.

Table 10 and Figure 11 showed the expected scenarios for the WP of the winter potato crop in the study area were estimated for the comparative treatment and without water stress with the value of WP 129.4 kg m<sup>-3</sup> in the year 2030, the value of 102.9 kg m<sup>-3</sup> in the year 2050, and the value of 77.64 kg m<sup>-3</sup> in the year 2100. In the future, if the treatment is used, water stress 80% of ETo, the crop will be the value of 114.24 kg m<sup>-3</sup> in the year 2030, the value of 91.39 kg m<sup>-3</sup> in the year 2050, and the value of 68.54 kg m<sup>-3</sup> in the year 2100. Also, if a water stress treatment of 60% is used, the value of WP will be 79.89 kg m<sup>-3</sup> in the year 2030, the value will be 63.93 kg m<sup>-3</sup> in the year 2050, and the value will be 47.93 kg m<sup>-3</sup> in the year 2100.

The study found that all of the study regions' potato yield is negatively impacted by climate change, particularly the rise in temperature, average monthly evapotranspiration, and CO<sub>2</sub> rate (Nourani et al., 2020; Stričević et al., 2017). The results of our study, which assessed how several climate change scenarios would affect biomass and potato yield, remain consistent with those of this study. Since the current potato cultivars in Egypt require a period of the chilly climate for tuber start,



it is necessary to change potato planting dates in order to minimize adverse temperature impacts on production of potato and decrease yield losses (Dewedar et al., 2021). Climate change is probable to have an impact on crop yield and quality in relation to temperature, carbon dioxide concentrations, precipitation, the availability of water resources, and climate uncertainty (Luck et al., 2012). As a result of the physiological effects of these expected climatic changes, increasing temperatures during the growing season and shorter times of crop development will result in lower yields in this situation. Due to the detrimental effects of increasing temperatures, it is predicted that potato productivity, growth, and duration will decline (Borus, 2017). In a different study, future climate change scenarios were applied to evaluate the worldwide tuber yield of potatoes, and the results showed that, depending on Representative Concentration Pathways scenarios, the yield will be reduced in 2055 and 2085 by 2 to 6% and 2 to 26%, respectively (El-Shaer et al., 1997).

Table 10. WR and WP under scenarios years 2030, 2050 and 2100.

Years scenarios	WR (m <sup>3</sup> ha <sup>-1</sup> )			WP (kg m <sup>-3</sup> )		
	100 %	80 %	60 %	100 %	80 %	60 %
2030	2544.22	2596.58	2851.24	129.38	114.24	79.89
2050	2035.38	2077.26	2280.99	102.89	91.39	63.93
2100	1526.53	1557.95	1710.74	77.64	68.54	47.93

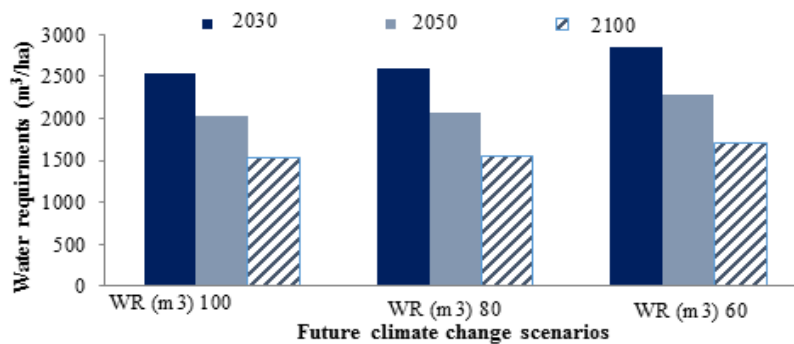


Figure 10. WR of winter potato under climate change scenarios of years 2030, 2050 and 2100.

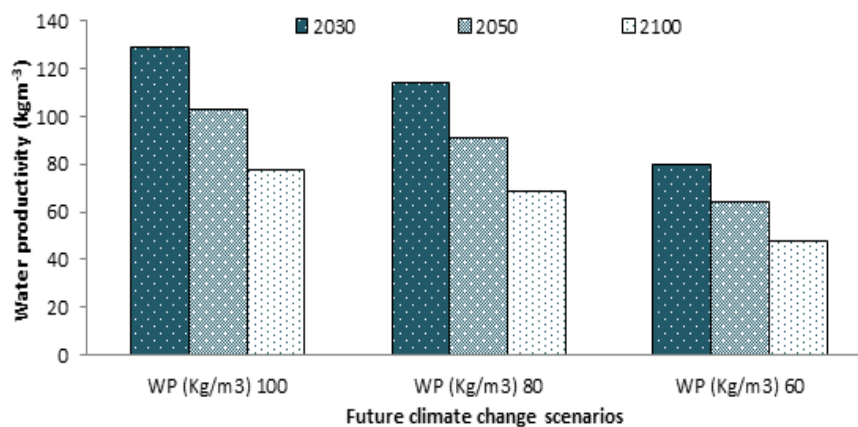


Figure 11. WP of winter potato under climate change scenarios of years 2030, 2050 and 2100.

## CONCLUSION

Under conditions of water shortage, the calibrated AquaCrop model successfully simulated the selected potato crop. As well as, under different irrigation regimes and climatic changes, it is possible to simulate well potato tuber yield, water productivity (WP), and total biomass, but it is unsatisfactory under extreme water stress (intensive water stress). The effects of water management on potato yield and water productivity under deficit irrigation and climate change scenarios can be predicted using this model. Additionally, the potatoe yield cultivated with a surface drip irrigation system using 80% of (Reference evapotranspiration) ETo (48.00, 8.05 ton ha<sup>-1</sup>) was significant compared to the potato yield grown with a solid-set sprinkler irrigation system using 100% of ETo (37.39, 7.19 ton ha<sup>-1</sup>). The AquaCrop model can be dependably applied to predict crop variables and evaluate climate change scenarios for the effectiveness of planning irrigation management strategies for potato crop variables. When describing the results under extreme water stress conditions, the constraints should be taken into consideration.

## ACKNOWLEDGMENTS

The Agricultural Engineering Research Institute (AEnRI) and National Research Centre, which provided the laboratory equipment and chemicals as well as financial support for the achievement of this research work, are sincerely appreciated by the authors.

## APPENDIX

*Symbols and abbreviations.*

Symbol	Detail	Symbol	Detail
ETo	Evapotranspiration	LAI	Leaf area index
WP	Water productivity	CC	Canopy cover
Kc	Potato crop factor	Y	Total tuber yield
WR	Water requirements	B	Biomass
RMSE	Root mean square error	HI	Harvest index
r	Pearson correlation coefficient	Tr	Potato plant transpiration
NRMSE	Normalized root mean square error		

## DECLARATION OF COMPETING INTEREST

There is no conflict of interest between authors.

## CREDIT AUTHORSHIP CONTRIBUTION STATEMENT

The authors declare the contributions to the manuscript such as the following sections:

**AbdelGawad Saad:** Conceptualization, visualization, investigation and review of relevant literatures, methodology, data curation, validation, formal analysis, writing-original draft, review, and editing,

**Hani Abdelghani Mansour:** Visualization, data curation, conceptualization, investigation methodology, formal analysis, validation, writing-original draft, review, and editing,

**Elsayed Ali:** Conceptualization, investigation, methodology, data curation, formal analysis, review, and editing,

**Mostafa Mohamed Azam:** Investigation methodology, formal analysis, data curation, validation, review, and editing.

## ETHICS COMMITTEE DECISION

This article does not require any ethical committee decision.

## REFERENCES

- Attia S and Gobin C (2020). Climate change effects on Belgian households: a case study of a nearly zero energy building. *Energies*, 13(20): 5357.
- Borus DJ (2017). *Impacts of climate change on the potato (Solanum tuberosum L.) productivity in Tasmania, Australia and Kenya*. PhD Thesis. University of Sydney pp. 206.
- DeTar WR, Browne GT, Phene CJ and Sanden BL (1996). *Real-time irrigation scheduling of potatoes with sprinkler and subsurface drip systems*. In Proceeding International Conference on Evapotranspiration and Irrigation Scheduling, eds. CR Camp, EJ Sadler, and RE Yoder (pp. 812-824).
- Dewedar O, Plauborg F, El-Shafie A and Marwa A (2021) Response of potato biomass and tuber yield under future climate change scenarios in Egypt. *Journal of Water and Land Development*. 49(IV-VI): 139-150.
- Eldredge EP, Shock CC and Saunders LD (2002). *Early and late harvest potato cultivar response to drip irrigation*. In XXVI International Horticultural Congress: Potatoes, Healthy Food for Humanity: International Developments in Breeding, 619 (pp. 233-239).
- El-Shaer HM, Rosenzweig C, Iglesias A, Eid MH and Hillel D (1997). Impact of climate change on possible scenarios for Egyptian agriculture in the future. *Mitigation and Adaptation Strategies for Global Change*, 1(3): 233-250.
- Fabeiro CM, de Santa Olalla FM and De Juan JA (2001). Yield and size of deficit irrigated potatoes. *Agricultural Water Management*, 48(3): 255-266.
- Fang H, Baret F, Plummer S and Schaepman-Strub G (2019). An overview of global leaf area index (LAI): Methods, products, validation, and applications. *Reviews of Geophysics*, 57(3): 739-799.
- García-Vila M and Fereres E (2012). Combining the simulation crop model AquaCrop with an economic model for the optimization of irrigation management at farm level. *European Journal of Agronomy*, 36(1): 21-31.
- Gee GN and Bauder JW (1986) Particle Size Distribution. In: Klute, A., Ed., *Methods of Soil Analysis Part 1. Physical and Mineralogical Methods*, 2nd Edition, *Agronomy Society of America/Soil Science Society of America, Madison, Wisconsin*, 383-411.
- Heng LK, Hsiao TC, Evett S, Howell T and Steduto P (2009). Validating the FAO AquaCrop model for irrigated and water deficient field maize. *Agronomy Journal*, 101: 488-498.
- Howell TA (2001). Enhancing water uses efficiency in irrigated agriculture. *Agronomy Journal*, 93: 281-289.
- Hsiao TC (2000). Sensitivity of growth of tubers vs. leaves to water stress: Biophysical analysis and relation to water transport. *Journal of Experimental Botany*, 51: 1595-1616.
- Hsiao TC (2007). *AquaCrop-Model parameterization and testing for maize*. In *ASA-CSSA-SSSA International Annual Meetings (November 4-8, 2007)*. ASA-CSSA-SSSA.
- Ibrahim A, Csúr-Varga A, Jolánkai M, Mansour H and Hamed A (2018). Monitoring some quality attributes of different wheat varieties by infrared technology. *Agricultural Engineering International CIGR Journal*, 20: 201-210.
- IP and Gitlin HM (1975). *Irrigation efficiencies of surface, sprinkler and drip irrigation*. Proceedings Second World Congress, International Water Resources Association, New Delhi: 191-199.

- Kaur A, Singh KB, Gupta RK, Alataway A, Dewidar AZ and Mattar MA (2022). Interactive effects of nitrogen application and irrigation on water use, growth and tuber yield of potato under subsurface drip irrigation. *Agronomy*, 13(1): 11.
- Kemanian AR, Stockle CO, Huggins DR and Viega LM (2007). A simple method to estimate harvest index in grain crops. *Field Crops Research*, 103: 208-216.
- King BA, Stark JC and Neibling H (2020). Potato irrigation management. In *Potato Production Systems* (pp. 417-446). Springer, Cham.
- Klute A (1986). Water Retention: Laboratory Methods, in Klute, A. (ed.): *Methods of Soil Analysis. Part 1. Physical and Mineralogical Methods. ASA and SSSA, Madison, WI, USA*, pp. 635-662.
- Loague K and Green RE (1991). Statistical and graphical methods for evaluating solute transport models: overview and application. *Journal of Contaminat Hydrology*, 7: 51-73.
- Luck J, Asaduzzaman M, Banerjee S, Bhattacharya I, Coughland K, Chakraborty A, Debnath G C, De Boer R F, Dhutta S, Griffiths W, Hossain D, Huda S, Jagannathan R, Khan S, O'leary G, Miah M G, Shana A, Spooner-Hart R (2012). The effects of climate change on potato production and potato late blight in the Asia-Pacific Region. *APN Science Bulletin*, 2: 28-33.
- Malhi GS, Kaur M and Kaushik P (2021). Impact of climate change on agriculture and its mitigation strategies: review. *Sustainability*, 13(3): 1318.
- Mansour HA, Abdallah EF, Gaballah MS and Gyuricza C (2015a). Impact of bubbler discharge and irrigation water quantity on 1-hydraulic performance evaluation and maize biomass yield. *International Journal Geomate*, 9, 1538-1544.
- Mansour HA, Abdel-Hady M, Eldardiry EI and Bralts VF (2015b). Performance of automatic control different localized irrigation systems and lateral lengths for emitters clogging and maize (*Zea mays* L.) growth and yield. *Intenational Journal Geomate*, 9, 1545-1552.
- Mansour HA, Abd-Elmabod SK and Engel BA (2019a). Adaptation of modeling to the irrigation system and water management for corn growth and yield. *Plant Archives*, 19 (Suppl. S1), 644-651.
- Mansour HA, El-Hady MA, Bralts VF and Engel BA (2016). Performance automation controller of drip irrigation system and saline water for wheat yield and water productivity in Egypt. *Journal of Irrigation and Drainage Engineering*, 142, 05016005.
- Mansour HA, Hu J, Ren H, Kheiry AN and Abd-Elmabod SK (2019b). Influence of using automatic irrigation system and organicfertilizer treatments on faba bean water productivity. *Intenational Journal Geomate*, 17: 256-265.
- Mengistu TG, Nigussie TA, Haile A and Seid A (2021). Evaluating the performance of aquacrop model in simulating the productivity of potato (*Solanum tuberosum* L.) crop under various water levels at Debre Birhan, *Amhara Regional State, Ethiopia. Culture*, 5(4), 674-687.
- Molden DJ, Sakthivadivel R and Habib Z (2001). Basin-level use and productivity of water: Examples from South Asia. *Research Report 49, International Water Management Institute, Colombo, Sri Lanka*.
- Moriasi DN, Arnold JG, Liew MWV, Bingner RL, Harmel RD and Veith TL (2007). Model evaluation guidelines for systematic quantification of accuracy in watershed simulations. *Transactions of the ASABE*, 50: 885-900.
- Nourani V, Rouzegari N, Molajou A and Baghanam AH (2020). An integrated simulation-optimization framework to optimize the reservoir operation adapted to climate change scenarios. *Journal of Hydrology*. 587: 125018, 1-19.
- Pontius R, Thontteh O and Chen H (2008). Components of information for multiple resolution comparisons between maps that share a real variable. *Environmental Ecological Statistics*, 15: 111-142.
- Raes D, Steduto P, Hsiao TC and Fereres E (2009). AquaCrop-The FAO crop model to simulate yield response to water: II. Main algorithms and software description. *Agronomy Journal*, 101: 438-447.
- Rahimikhoob H, Sohrabi T and Delshad M (2021). Simulating crop response to nitrogen-deficiency stress using the critical Nitrogen concentration concept and the AquaCrop semi-quantitative approach. *Scientia Horticulturae*, 285, 110194.
- Razzaghi F, Zhou Z, Andersen MN and Plauborg F (2017). Simulation of potato yield in temperate condition by the AquaCrop model. *Agricultural Water Management*, 191: 113-123.
- Rebecca B (2004). *Soil Survey Methods Manual. Soil Survey Investigations Report. No 42 Natural Resources Conservation Services*.
- Salemi H, Mohd-Soom MA, Lee TS, Mousavi SF and Ganji A (2011) Application of AquaCrop model in deficit irrigation management of winter wheat in arid region. *African Journal of Agricultural Research*. 610: 2204-2215.

- Shaw B, Thomas TH and Cooke DT (2002). Responses of potato (*Beta vulgaris* L.) to drought and nutrient deficiency stress. *Plant Growth Regulation*, 37: 77-83.
- Steduto P (2003). Biomass water-productivity. Comparing the growth engines of crop models. *FAO expert consultation on crop water productivity under deficient water supply, Rome*.
- Stričević R, Trbić G, Vujadinović M, Cupać, R, Đurović, N and Čosić M 2017. *Impact of climate change on potato yield grown in different climatic zone in Bosnia and Herzegovina*. In VIII International Scientific Agriculture Symposium, Agrosym (pp. 596-601).



## Development of a Cowpea Threshing Machine

Mohamed Mansour Shalaby REFAAY<sup>a\*</sup>, Ahmed Shawky EL-SAYED<sup>b</sup>,  
Mokhtar Cottb Ahmed AWAD<sup>a</sup>

<sup>a\*</sup> Department of Field and Horticultural Crops Mechanization, Agricultural Engineering Research Institute (AENRI), Agricultural Research Center (ARC), Dokki, Giza, EGYPT

<sup>b</sup> Department of Agricultural Bioengineering Systems, Agricultural Engineering Research Institute (AENRI), Agricultural Research Center (ARC), Dokki, Giza, EGYPT

(\*): Corresponding Author: [d.shalaby85@yahoo.com](mailto:d.shalaby85@yahoo.com)

Received: 20.03.2023

Article Info  
Accepted: 14.05.2023

Published: 30.06.2023

### ABSTRACT

The transmission system of the thresher was developed to suit the process of threshing cowpea seeds. The developed thresher included substantial modifications to the threshing concaves, threshing fan, and threshing drum. The speed of the threshing sieve, suction, and fan were increased while the drum speed was decreased. Concave hole diameters of 20, 24, and 28 mm; drum speeds of 17, 23, and 29 m s<sup>-1</sup>; and feed rates of 360, 540, and 720 kg h<sup>-1</sup> were studied. Threshing efficiency, seed damage, losses of seed, and power requirements were computed. The main findings revealed that increasing the diameter of the concave holes increased threshing efficiency and seed losses while decreasing seed damage and power requirements. Increasing drum speed increases threshing efficiency, reduced seed damage, and lower power requirements while decreasing seed losses. The maximum threshing efficiency reached was 96.75%, while the seed loss was 4.25%, with a minimum seed damage of 1.18%. The power requirement was 7.38 kWh ton<sup>-1</sup> at a moisture content of 14.6%. The operating costs using the developed threshing machine were decreased to 71.33 USD ha<sup>-1</sup> instead of the manually threshed cowpea, which costs about 111 USD ha<sup>-1</sup>.

**Keywords:** Concave, Cowpea, Moisture content, Efficiency, Grain damage, Losses

**To cite:** Refaay MMS, El-Sayed AS and Awad MCA (2023). Development of a Cowpea Threshing Machine. Turkish Journal of Agricultural Engineering Research (TURKAGER), 4(1): 46-60.  
<https://doi.org/10.46592/turkager.1267961>

### INTRODUCTION

Cowpea is essential in securing food security needs and sustaining the balance of global food systems. The cowpea crop in Egypt faces local difficulties as a result of manual threshing. The lack of threshing machines dedicated to the cowpea crop



© Publisher: Ebubekir Altuntas. This is an Open Access article and is licensed (CC-BY-NC-4.0) under a Creative Commons Attribution 4.0 International License.

increases harvest losses and increases the cost of production. Therefore, it is necessary to develop special machines for threshing cowpeas in Egypt. There are many ways to consume the cowpea crop, as it can be used directly as food, fodder, and fuel ([Ayenan \*et al.\*, 2017](#)). The chemical analysis of cowpea seeds includes carbohydrates (57.3%), fats (1.5%), fibers (8.1%), and ash (3.8%) ([Arazu, 2017](#)). There is a direct relationship between the threshing efficiency and the speed of rotation of the threshing drum. Likewise, there is an inverse relationship between the threshing efficiency, feed rate and concavity clearance of the threshing sieves. A directly proportional relationship existed between energy consumption and both drum speed and feeding rate ([Timothy and Olaoye, 2013](#)). Using relatively high speeds leads to an increase in visible grain damage of 5-10%, causing a decrease in the germination rate. Cowpea crop threshed at a standard moisture content of 6.5% ([Morad \*et al.\*, 2007](#)). It is preferable to operate a roller thresher for the cowpea crop at a speed of 496.0 m min<sup>-1</sup> with a sieve clearance of 8.0 mm for the sieves ([Asante \*et al.\*, 2017](#)). Slow speeds are used when threshing cowpeas to use them as seeds, where the rolling speed does not exceed 288.5 m min<sup>-1</sup> and the sieve clearance is 8.0 mm for the sieves ([Onuoha \*et al.\*, 2022](#)). For small-scale farmers, [Dauda \(2001\)](#) assessed the effectiveness of a manually operated cowpea thresher. Results indicated that threshing effectiveness was 85.9%, seed damage was 1.8%, and winnowing effectiveness was 92.35%. It is crucial to use the proper air blowing speed to remove impurities without blowing out seeds because faster cylinder speeds (700-800 rpm) cause more damage to seeds than slower rates (400-500 rpm) ([Herbek and Bitzer, 2004](#)). Moisture content, cylinder speed, feed rate, and sieve clearance all have an impact on how well cowpea seeds germinate ([Ajav and Adejumo, 2005](#)). To keep seed damage levels within the acceptable range of 1.1%, it is also necessary to select the proper drum speed ([Ukatu, 2006](#)). Harvesting the cowpea crop at a forward speed of 2.7 km h<sup>-1</sup> and a seed moisture level of 12.22% is recommended. For threshing, the cowpea crop, the minimal losses, and the least consumed energy were 5.78% and 53.77 kWh ha<sup>-1</sup>, respectively, at a drum speed of 19.1 m s<sup>-1</sup> (500 rpm) and a seed moisture content of 9.52% ([Morad \*et al.\*, 2007](#)). Using a star-shaped fan blower with rotational speeds of 500–1400 rpm, the threshing efficiency was 96.29%. At a feed rate of 74.33-110.86 kg h<sup>-1</sup> for threshing cowpea seeds, there is a minimum damage of 3.55%, a higher cleaning efficiency of 95.60%, and a cleaning loss of 3.71%. The star-shaped fan design is less expensive and more effective ([Irtwange, 2009](#)). When the rotating speed of the threshing drum is increased, the efficiency of threshing the cowpea crop improves. Still, the percentage of visible grain damage rises to 5%, which lowers the germination rate ([Adekanye and Olaoye, 2013](#)). The use of local threshing machines for the cowpea crop is suitable for small farmers because of the ease of maintaining and operating these machines ([Oduma, 2014](#)). Cowpea (*Vigna unguiculata* L.) was threshed at 20.7-12.6% moisture content after harvest. The threshing efficiency reached 99.40%, achieving the highest yield of 77.56 kg h<sup>-1</sup> at the lowest moisture content. Cowpea beans are distinguished by their high protein content of 24.8% and carbohydrates of 63.6% ([Asante \*et al.\*, 2017](#)). A motorized cowpea threshing machine with a power rating of 0.75 kW, a fan speed of 826 rpm, and a beater speed of 418 rpm was developed by [Samuel and Oseme \(2021\)](#) to satisfy the needs of small-scale farmers in developing nations. The results demonstrated average threshing

efficiency, cleaning efficiency, percentage of grain damage, throughput capacity, and successful threshing of several cowpea varieties with less grain loss. The problem with the study is that threshing the cowpea crop manually or with primitive threshing equipment increases grain loss and low germination rates, which drives up production costs and threshing time. The study was aimed at developing, modifying, and evaluating the local wheat threshing machine in order to thresh cowpea to maximize threshing efficiency, reduce grain losses, and reduce operating costs.

## MATERIALS and METHODS

The field experiments were carried out at the El-Serw Agricultural Research Station, Damietta Governorate, Egypt, located at 31.24° N, 31.80° E, during 2022. A threshing machine was developed for separating dry cowpeas. The tractor specifications used in the experiment are shown in Table 1.

**Table 1.** The used tractor specifications.

Power at the PTO (factory observed at 2100 rpm)	(65 HP) universal, manufactured in Romania
Type	Diesel
Cylinders	In Line 4
Compression ratio	15.8:1
Displacement	7.6 L
Lubrication system	Fully pressure - full flow filtration
Fuel system type	Direct injection with rotary injection pump
Electrical system type	12 Volt negative ground
Gear shifting	5 forward, 1 – reverse

### Thresher Description

The developed threshing machine is locally fabricated and comprises a frame loaded on two wheels, as shown in Figure 1. The threshing drum consists of a cylinder with 5 mm of thickness and 800 mm in diameter. The threshing knives are installed axially on the threshing drum with a diameter of 50 mm. The thresher machine consists partly of a threshing concave; a lower flat sieve; a fluidizer; three seed outlet hoppers; the threshing fan; a feeding hopper and a hay exit slot, were shown in Figure 1. Also, as shown in Figure 1, the threshing machine is provided with a flywheel mounted in the transmission system to adjust its balance (Figure1, No. 11).





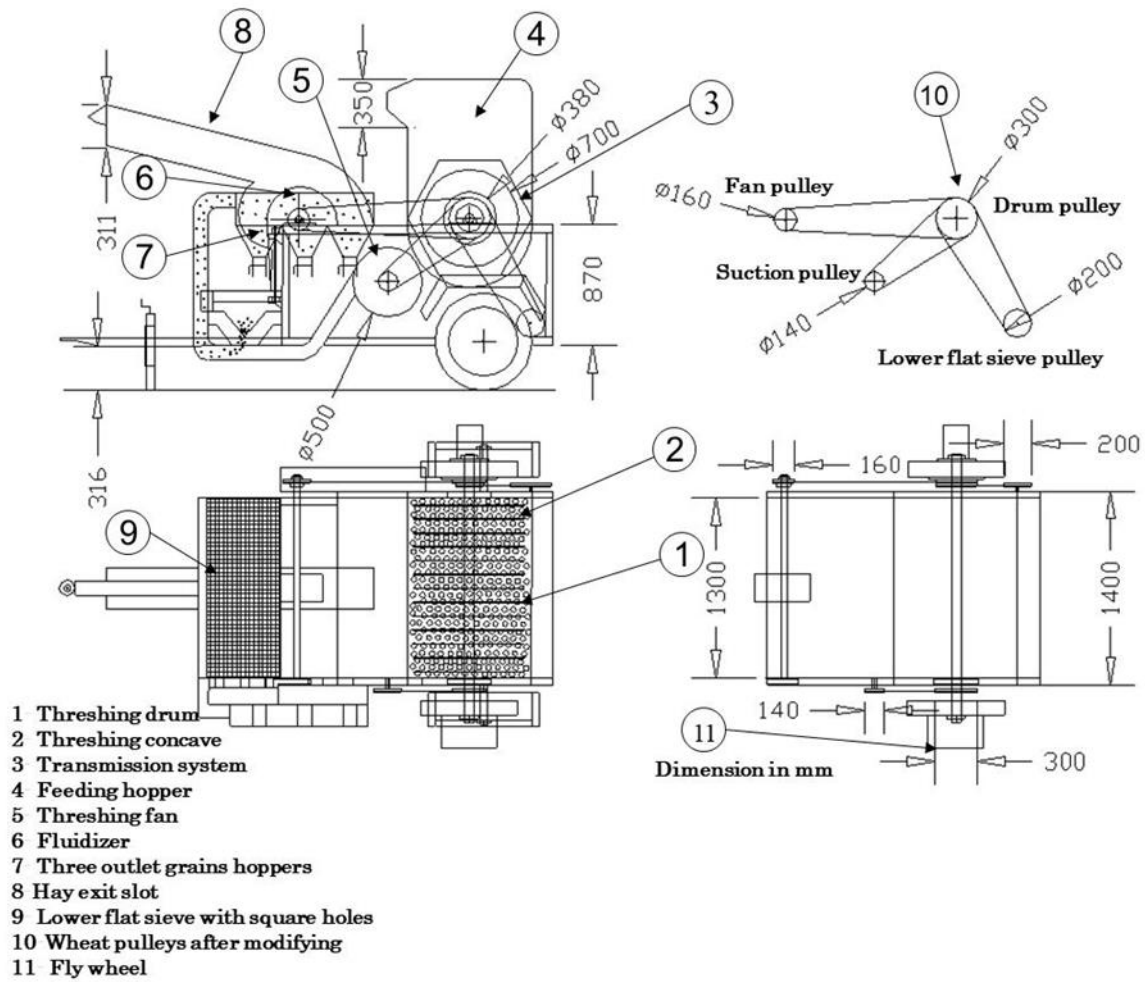


Figure 2. Threshing machine after development.

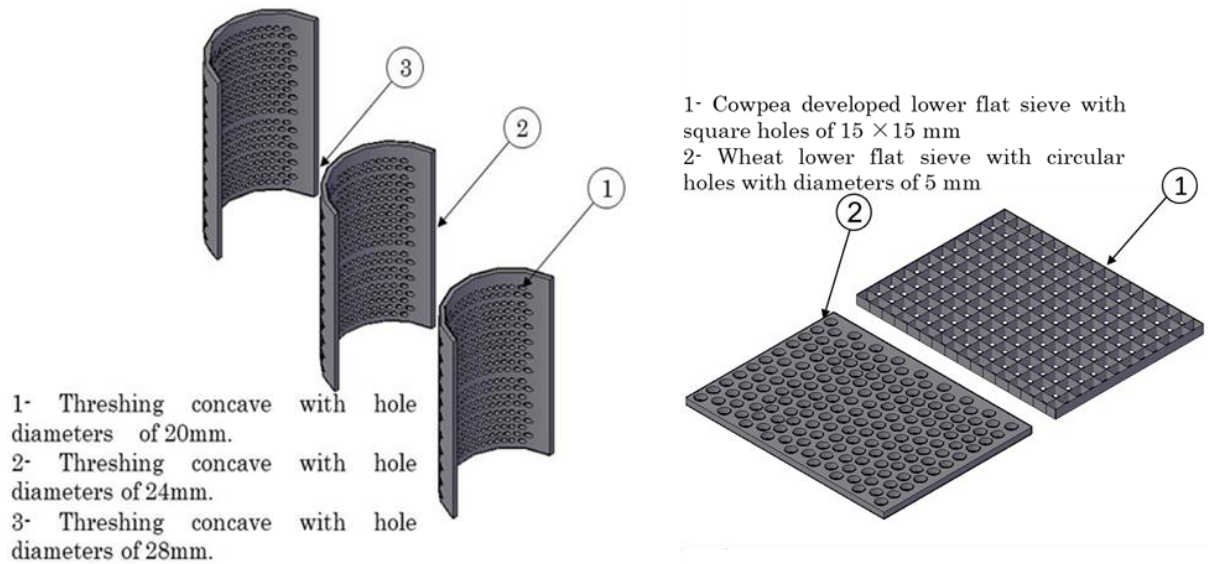


Figure 3. Cowpea-modified concaves.

## Developing Transmission Systems

The transmission system was developed to increase the speeds of the separating concave, separating fan, and the grain suction. To lower the amount of damaged seeds, lower the rate of fuel consumption, and thus lower the cost of threshing and separating dry cowpeas, the threshing drum operates at a slower speed.

The transmission system was developed by fabricating six pulleys with different diameters suitable for threshing cowpea, as shown in the developed thresher machine in Figure 2 and Table 3. The threshing machine transmission modifications were as follows:

1. A pulley with a diameter of 300 mm was manufactured instead of the existing 200 mm pulley and fixed on the threshing drum shaft, which connected directly to the tractor-driven pulley with a wide leather belt (Figure 2).
2. A pulley with a diameter of 200 mm was fabricated and fixed on the separating sieve shaft instead of the existing wheat pulley with a diameter of 300 mm to increase the speed of the separating concave when running the threshing drum at a lower speed (Figure 2).
3. A pulley with a diameter of 300 mm was fabricated and fixed on the threshing drum shaft instead of a pulley with a diameter of 240 mm (Figure 2).
4. A pulley with a diameter of 160 mm was fabricated and fixed on the separating fan shaft instead of a pulley with a diameter of 200 mm to increase the speed of the separating fan (Figure 2).
5. A pulley with a diameter of 140 mm was fabricated and fixed on the grain extractor shaft instead of a pulley with a diameter of 200 mm to increase the speed of the grain extractor to suck out the cowpea when the threshing drum is running at a lower speed (Figure 2).

**Table 2.** Transmission system speeds before and after the development.

No.	Transmission system pulleys	Diameter, mm	Before development					
			Rotational speed			Linear speed		
			S1 rpm	S2 rpm	S3 rpm	S1 m s <sup>-1</sup>	S2 m s <sup>-1</sup>	S3 m s <sup>-1</sup>
1	Drum pulley	200	400	550	700	4.18	5.75	7.32
2	Sieve pulley	300	267	367	467			
3	Fan pulley	200	480	660	840	5.86	8.06	10.25
4	Suction pulley	200	480	660	840			
After development								
1	Drum pulley	300	400	550	700	6.28	8.63	10.99
2	Sieve pulley	200	600	825	1050			
3	Fan pulley	160	750	1031	1312	6.28	8.63	10.99
4	Suction pulley	140	857	1179	1500			

Where: S1-3= rotational and linear speeds.

Notice: the drum linear speeds (17, 23, and 29 m s<sup>-1</sup>) were calculated according to the drum's outer diameter of 800 mm. The threshing drum is a spike-tooth drum type.

Table 3 lists the characteristics of dry cowpea, including, for example, the weight of 1000 seeds of cowpea compared to the weight of 1000 seeds of dry wheat. The cowpea's 1000 seeds weighed twice as much as 1000 seeds of dry wheat.

**Table 3.** Weight of five random samples of 1000 seeds of wheat and cowpea.

Samples	Wheat weight of 1000 seeds (g)	Cowpea weight of 1000 seeds (g)
1	850	1720
2	790	1630
3	930	1580
4	880	1520
5	950	1680

### Tested Variables

Three variables were studied, as follows:

1. Three concave hole diameters (D) of 20, 24, and 28 mm, named D1, D2, and D3, respectively, were adjusted.
2. Three drum speeds (S) of 17, 23, and 29 m s<sup>-1</sup>, respectively, named S1, S2, and S3, were adjusted.
3. Three feed rates (F) of 360, 540, and 720 kg h<sup>-1</sup>, respectively, named F1, F2, and F3, were investigated.

### Measurements

#### Moisture Content (MC)

The threshed cowpea samples were oven dried at 70°C for 72 h using a hot air oven. The samples were weighed before and after drying, and the moisture content was determined by using Equation (1) (dry basis) according to [AOAC \(1990\)](#).

$$MC = \frac{W_1 - W_2}{W_2} \times 100 \quad (1)$$

Where:

MC= moisture content, %;  $W_1$ = sample weight before drying (g);  $W_2$ = sample weight after drying (g).

#### Threshing Efficiency (SE)

The threshing efficiency of a threshing machine is its ability to separate or clear the chaff from the cowpea kernels. The threshing efficiency was measured from Equation 2 according to [Ndirika \(1994\)](#).

$$SE = \frac{W_A - W_B}{W_A} \times 100 \quad (2)$$

Where:

SE= the threshing efficiency, %;  $W_A$  = total weight of the mixture of grain and chaff received at the grain outlet, kg;  $W_B$  = weight of chaff at the chaff outlet of the thresher, kg.

#### Seed Losses (SL)

The seed loss percentage through the chaff outlet is evaluated from Equation 3 according to [Desta and Mishra \(1990\)](#).

$$SL = \frac{W_T - W_B}{W_T} \times 100 \quad (3)$$

Where:

$SL$  = seed losses, %;  $W_B$  = weight of grain losses in chaff in sample, kg;  $W_T$  = total weight of the mixture (seed + chaff) in the sample, kg

### Seed Damage ( $SD$ )

The seed damage percentage was estimated from Equation (4).

$$SD = \frac{W_{bg}}{W_T} \times 100 \quad (4)$$

Where:

$SD$  = the percentage of seed damage, %;  $W_{bg}$  = weight of broken seeds in the sample (kg);  $W_T$  = total weight of the sample seed (kg).

### Power Requirements ( $PR$ )

The consumed power requirements were estimated using Equation 5 according to [Hunt \(1983\)](#).

$$PR = F.C. \times \frac{1}{3600} \times \rho_f \times L.C.V. \times 427 \times \eta_m \times \eta_{th} \times \frac{1}{75} \times \frac{1}{3.6} \times \frac{1}{P} \quad (5)$$

Where:

$PR$  = Power consumption requirements during the threshing operation, kWh ton<sup>-1</sup>;  $F.C.$  = Fuel consumption L h<sup>-1</sup>;  $\rho_f$  = Fuel density, kg L<sup>-1</sup> (for solar = 0.85);  $L.C.V.$  = Lower calorific value of the fuel (kcal kg<sup>-1</sup>) (Solar has an average L.C.V. of 11000 kcal/kg);  $\eta_{th}$  = the thermal efficiency of the engine (considered to be about 35% for diesel engine); 427 = Thermo-mechanical equivalent, kg m kcal<sup>-1</sup>;  $\eta_m$  = mechanical efficiency of the engine, (considered to be 80 percent for a diesel engine);  $P$  = machine productivity, ton h<sup>-1</sup>.

### Statistical Analysis

The measured data for the tested factors were statistically analyzed using the Minitab program version (2019). The tests of analysis of variance (ANOVA) were done using complete randomized design (CRD), three factor model with three replications. The means of treatments were analyzed to estimate the linear regression equations at a 5% level of probability.

## RESULTS AND DISCUSSION

### Factors Affecting Cowpea Threshing Efficiency

As shown in Figure 4A, by increasing the concave hole diameter from  $D1 = 20$  to  $D2 = 24$  mm, the threshing efficiency increased from 83.23 to 87.25%. Also increasing the concave hole diameter from  $D2 = 24$  to  $D3 = 28$  mm, the threshing efficiency increased from 87.25 to 90.35% with drum speed ( $S1 = 17$  m s<sup>-1</sup>) and feed rate ( $F1 = 360$  kg h<sup>-1</sup>). As shown in Figure 4B, by increasing drum speed from  $S1 = 17$  to  $S2 = 23$  m s<sup>-1</sup>, the threshing efficiency increased from 83.23 to 86.99%. Also, by increasing drum speed from  $S2 = 23$  to  $S3 = 29$  m s<sup>-1</sup>, the threshing efficiency increased from 86.99 to 88.43% with a concave hole diameter of 20 mm at the feed rate of  $F1 = 360$  kg h<sup>-1</sup>. As shown in Figure 4C, by increasing the feed rate from

(F1 = 360 to F2 = 540 kg h<sup>-1</sup>), the threshing efficiency decreased from 83.23 to 82.48%, and by increasing the feed rate from (F2 = 540 to F3 = 720 kg h<sup>-1</sup>), the threshing efficiency decreased from 82.48 to 82.02% of drum speed (S1 = 17 m s<sup>-1</sup>) and concave hole diameter (D1 = 20 mm).

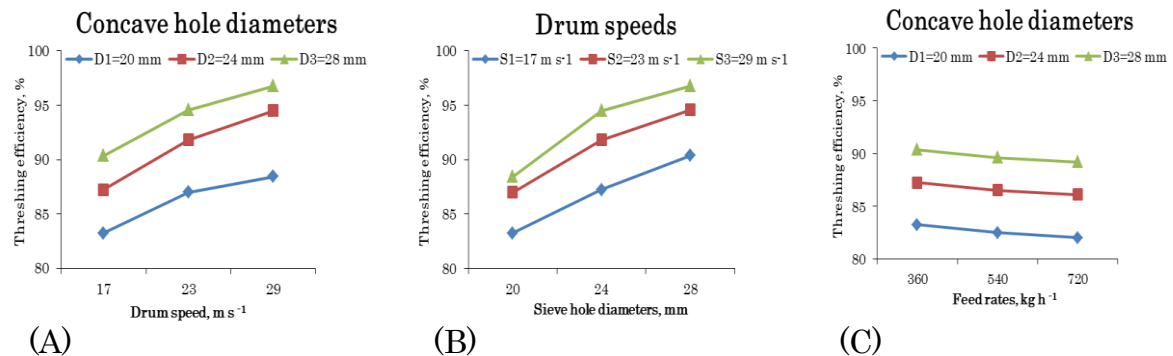


**Figure 4.** (A). Effect of drum speeds on threshing efficiency at concave hole diameters; (B). Effect of concave hole diameters on threshing efficiency at drum speeds; (C). Effect of feed rates on threshing efficiency at concave hole diameters.

The results of threshing efficiency were obtained at a moisture content of 14.6%. The obtained results of threshing efficiency may be due to the decreasing drum speed while increasing both speeds of the threshing concave and the fan, in line with the obtained results of [Herbek and Bitzer \(2004\)](#). Statistically, there are highly significant effects of the total interaction between different treatments ( $P \leq 0.05$ ) for the threshing efficiency values. The regression analysis concluded that the concave hole diameter affects threshing efficiency more than drum speed and feed rate. Also, the feed rate showed less effect on threshing efficiency than drum speed, in agreement with [Ukatu \(2006\)](#). The effects of different parameters on threshing efficiency are arranged as follows: concave hole diameter > drum speed > feed rate. ANOVA analysis for means indicated highly significant differences between the treatments, as listed in Tables 4 and 5. The obtained regression equation for the threshing efficiency was in the form of:

$$SE, \% = 57.818 + 0.957 D + 0.494 S - 0.0048 F. \quad (R^2=0.972).$$

[Where: Threshing efficiency ( $SE, \%$ ), concave hole diameters ( $D$ ), drum speeds ( $S$ ), and feed rates ( $F$ )]

**Table 4.** Means and standard errors for measurements affected by the tested factors.

Factors		Threshing efficiency, %	Seed losses, %	Seed damage, %	Power requirements, kWh ton <sup>-1</sup>
Concave hole diameters	D1	93.12±0.44 <sup>a</sup>	2.66±0.06 <sup>a</sup>	1.08±0.01 <sup>a</sup>	6.46±0.18 <sup>a</sup>
	D2	90.10±0.56 <sup>b</sup>	3.22±0.08 <sup>b</sup>	1.00±0.01 <sup>b</sup>	5.90±0.12 <sup>b</sup>
	D3	85.47±0.51 <sup>c</sup>	3.59±0.08 <sup>c</sup>	0.91±0.01 <sup>c</sup>	5.36±0.08 <sup>c</sup>
	P value	0.0001	0.0001	0.0001	0.0001
Drum speeds	S1	92.24±0.58 <sup>a</sup>	3.47±0.11 <sup>a</sup>	0.95±0.02 <sup>a</sup>	5.33±0.07 <sup>a</sup>
	S2	90.15±0.65 <sup>b</sup>	3.17±0.09 <sup>b</sup>	0.99±0.02 <sup>b</sup>	5.88±0.11 <sup>b</sup>
	S3	86.31±0.68 <sup>c</sup>	2.83±0.08 <sup>c</sup>	1.04±0.02 <sup>c</sup>	6.52±0.18 <sup>c</sup>
	P value	0.0001	0.0001	0.0001	0.0001
Feed rates	F1	90.43±0.81 <sup>a</sup>	2.78±0.09 <sup>a</sup>	1.05±0.02 <sup>a</sup>	5.46±0.09 <sup>a</sup>
	F2	89.58±0.79 <sup>b</sup>	3.22±0.09 <sup>b</sup>	0.99±0.01 <sup>b</sup>	5.84±0.13 <sup>b</sup>
	F3	88.69±0.76 <sup>c</sup>	3.46±0.09 <sup>c</sup>	0.94±0.02 <sup>c</sup>	6.43±0.18 <sup>c</sup>
	P value	0.0001	0.0001	0.0001	0.0001

<sup>a,b</sup> the means with no common subscript within each column differed significantly (P≤ 0.05)

**Table 5.** ANOVA analysis for measurements.

Measurement	Source	Degree of freedom	Adj (ss)	Mean Square (MS)	F value	Probability
Threshing efficiency	Concave holes diameter	1	791.89	791.891	1642.53	0.0001***
	Drum speed	1	475.62	475.616	986.51	0.0001***
	Feed rate	1	40.77	40.768	84.56	0.0001***
	Error	77	37.12	0.482		
	Total	80	25.375			
Seed losses	Concave holes diameter	1	11.5371	11.5371	789.41	0.0001***
	Drum speed	1	5.4722	5.4722	374.43	0.0001***
	Feed rate	1	6.2424	6.2424	427.13	0.0001***
	Error	77	1.1253	0.0146		
	Total	80	24.3770			
Seed damage	Concave holes diameter	1	0.375	0.375	1879.07	0.0001***
	Drum speed	1	0.104017	0.104017	521.21	0.0001***
	Feed rate	1	0.156817	0.156817	785.78	0.0001***
	Error	77	0.015367	0.000200		
	Total	80	0.651200			
Power requirements	Concave holes diameter	1	74.202	74.2017	257.36	0.0001***
	Drum speed	1	77.760	77.7600	269.70	0.0001***
	Feed rate	1	51.627	51.6267	179.06	0.0001***
	Error	77	22.201	0.2883		
	Total	80	225.789			

The significance probability at (P≤ 0.05)

### Factors Affecting Cowpea Seed Losses

As shown in Figure 5A, increasing the diameter of the concave holes from (D1= 20 to D2= 24 mm) increased seed losses from 2.4 to 3.1% when increasing the diameter of the concave holes from (D2= 24 to D3= 28 mm). Also, seed losses increased from 3.1 to 3.7% under drum speed (S1 = 17 m s<sup>-1</sup>) and feed rate (F1 = 360 kg h<sup>-1</sup>). As shown in Figure 5B, with increasing drum speed from S1 = 17 to S2 = 23 m s<sup>-1</sup>, seed losses decreased from 2.4 to 2.3% with increasing drum speed from S2 = 23 to S3 = 29 m s<sup>-1</sup>. Also, seed losses decreased from 2.3 to 2.2% at concave hole diameter (D1 = 20 mm) with feed rate (F1 = 360 kg h<sup>-1</sup>). As shown in Figure 5C, with an

increase in feed rate from ( $F1 = 360$  to  $F2 = 540$   $\text{kg h}^{-1}$ ), the losses of seed increased from 2.4 to 2.96% at an increase in feed rate from ( $F2 = 540$  to  $F3 = 720$   $\text{kg h}^{-1}$ ). Also, seed losses increased from 2.96 to 3.15% under drum speed ( $S1 = 17$   $\text{m s}^{-1}$ ) with a concave hole diameter ( $D1 = 20$  mm).

The results of cowpea seed losses were obtained at a moisture content of 14.6%. These results were due to using an appropriate drum rotation speed that led to a significant decrease in seed losses, as agreed upon by [Adekanye and Olaoye \(2013\)](#); [Oduma \(2014\)](#). Statistically, there are highly significant effects of the total interaction between different treatments ( $P \leq 0.05$ ) for the seed loss values. The regression analysis concluded that the concave hole diameter affects seed losses more than feed rate and drum speed. Also, drum speed showed less effect on seed losses than feed rate. The effects of different parameters on seed losses were arranged as follows: concave hole diameter > feed rate > drum speed. ANOVA analysis indicated highly significant differences between the treatments listed in Tables 4 and 5. The obtained regression equation for seed losses was in the form of:

$$\text{SL, \%} = 0.583 + 0.116 D - 0.0531S + 0.0019 F. \quad (R^2=0.954).$$

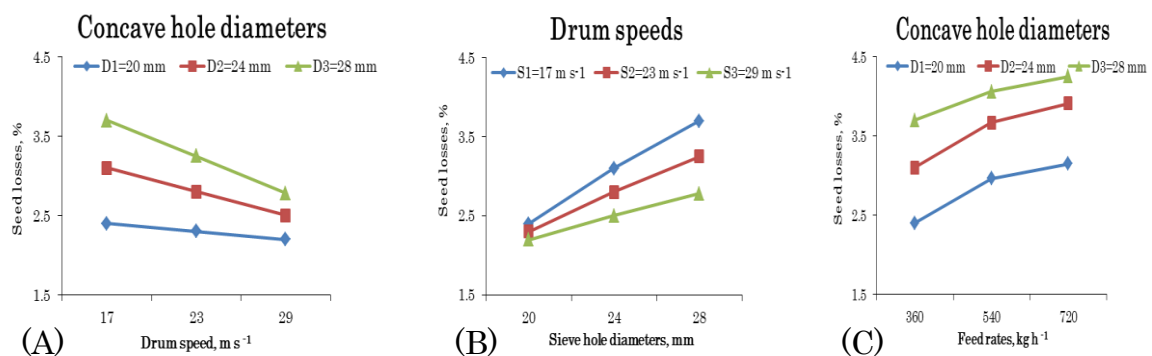


**Figure 5.** (A) Effect of drum speeds on seed losses at concave hole diameters; (B) Effect of concave hole diameters on seed losses at drum speeds; (C) Effect of feed rates on seed losses at concave hole diameters.

### Factors Affecting Cowpea Seed Damage

As shown in Figure 6A, seed damage was reduced from 1.1 to 1.0% by increasing the diameter of the concave holes from ( $D1 = 20$  to  $D2 = 24$  mm) to ( $D2 = 24$  to  $D3 = 28$  mm). Furthermore, seed damage decreased from 1.0 to 0.94% as drum speed ( $S1 = 17$   $\text{m s}^{-1}$ ) increased and feed rate ( $F1 = 360$   $\text{kg h}^{-1}$ ) decreased. As shown in Figure 6B, with increasing drum speed from ( $S1 = 17$  to  $S2 = 23$   $\text{m s}^{-1}$ ), the seed damage increased from 1.1 to 1.15% with increasing drum speed from ( $S2 = 23$  to  $S3 = 29$   $\text{m s}^{-1}$ ). Whereas the seed damage increased from 1.15 to 1.18% under concave hole diameter ( $D1 = 20$  mm) with feed rate ( $F1 = 360$   $\text{kg h}^{-1}$ ). As shown in Figure 6C, increasing the feed rate from ( $F1 = 360$  to  $F2 = 540$   $\text{kg h}^{-1}$ ) reduced seed damage from 1.1 to 1.03% when the feed rate was increased from ( $F2 = 360$  to  $F3 = 720$   $\text{kg h}^{-1}$ ). Furthermore, with the smallest drum speed ( $S1 = 17$   $\text{m s}^{-1}$ ) and concave hole diameter ( $D1 = 20$  mm), seed damage decreased from 1.03 to 0.95%.



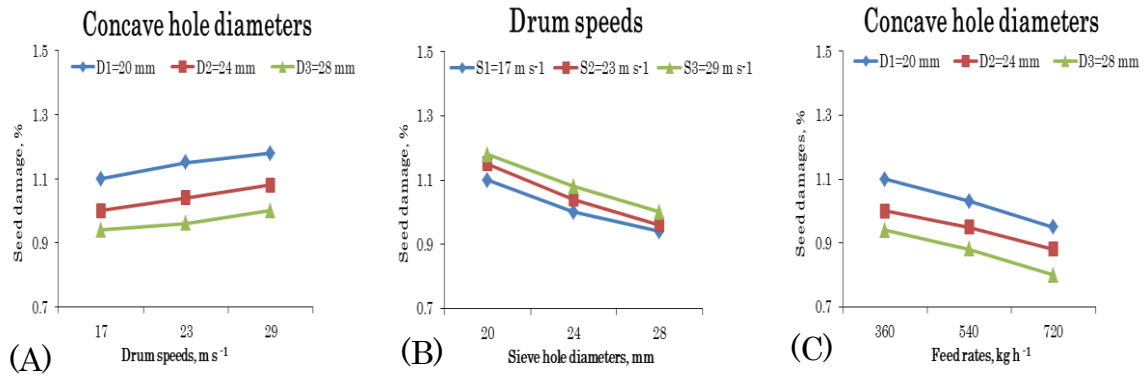


**Figure 6.** (A) Effect of drum speeds on seed damage at concave hole diameters; (B) Effect of concave hole diameters on seed damage at drum speeds (C) Effect of feed rates on seed damage at concave hole diameters.

The results of seed damage were obtained at a moisture content of 14.6%. The results of seed damage were relatively decreased using an appropriate drum rotational speed with an appropriate air fan speed and modifying concaves, in agreement with [Ajav and Adejumo \(2005\)](#); [Morad et al., \(2007\)](#). Statistically, there are highly significant effects of the total interaction between different treatments ( $P \leq 0.05$ ) for the seed damage values. The regression analysis concluded that the concave hole diameter affects seed damage more significantly than feed rate or drum speed. Furthermore, drum speed had the least effect on seed damage when compared to feed rate. The following parameters affected by seed damage: concave hole diameter > feed rate > drum speed. ANOVA analysis indicated highly significant differences between the treatments listed in Tables 4 and 5. The obtained regression equation was in the form of:

$$SD, \% = 1.489 - 0.021 D + 0.0073 S - 0.000299 F. \quad (R^2=0.976).$$

### Factors Affecting Power Requirements

As shown in Figure 7A, by increasing the concave hole diameter from D1 = 20 to D2 = 24 mm, the power requirements decreased from 5.67 to 5.35 kWh ton<sup>-1</sup>. Also increasing the concave hole diameter from D2 = 24 to D3 = 28 mm, the power requirements decreased from 5.35 to 4.97 kWh ton<sup>-1</sup> under drum speed (S1 = 17 m s<sup>-1</sup>) with feed rate (F1 = 360 kg h<sup>-1</sup>). As shown in Figure 7B, by increasing the drum speed from S1 = 17 to S2 = 23 m s<sup>-1</sup>, the power requirements increased from 5.67 to 6.33 kWh ton<sup>-1</sup>. In addition, the power requirements increased from 6.33 to 7.38 kWh ton<sup>-1</sup> as the drum speed increased from (S2= 23 to S3= 29 m s<sup>-1</sup>) with a concave hole diameter (D1= 20 mm) and feed rate (F1= 360 kg h<sup>-1</sup>). As shown in Figure 7C, with an increasing feed rate from (F1 = 360 to F2 = 540 kg h<sup>-1</sup>), the power requirements increased from 5.88 to 6.30 kWh ton<sup>-1</sup>. Also, by increasing the feed rate from F2 = 540 to F3 = 720 kg h<sup>-1</sup>, the power requirements decreased from 6.30 to 7.20 kWh ton<sup>-1</sup> at drum speed (S1 = 17 m s<sup>-1</sup>) with a 20 mm concave hole diameter.

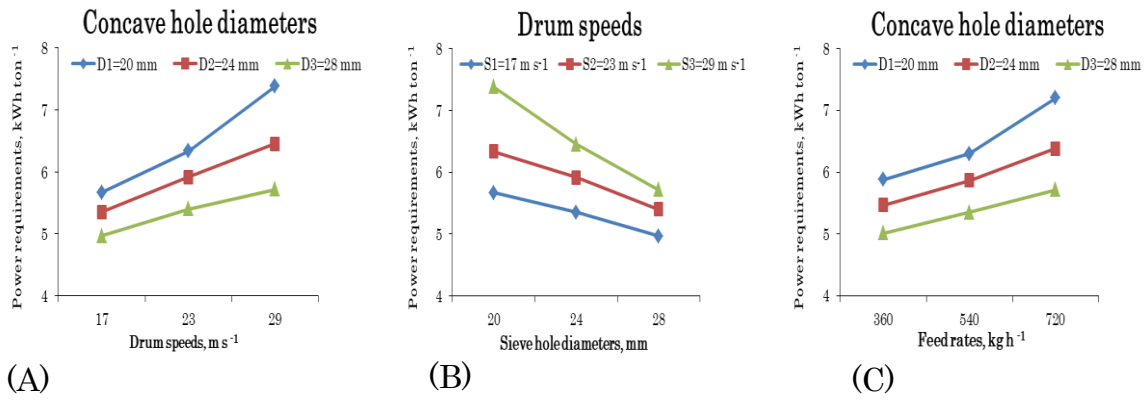


**Figure 7.** (A). Effect of drum speeds on the power requirements at concave hole diameters; (B) Effect of concave hole diameters on the power requirements at drum speeds; (C) Effect of feed rates on the power requirements at concave hole diameters.

The power requirements results were obtained at a moisture content of 14.6%. The consumed power results were due to using appropriate air fan plowing and appropriate concaves and spike tooth drum type rotational speeds while adjusting the transmission system, which led to a decrease in fuel consumption and, thus, a decrease in consumed power, in agreement with [Irtwange, \(2009\)](#); [Samuel and Oseme \(2021\)](#); [Onuoha et al. \(2022\)](#). Statistically, there are highly significant effects of the total interaction between different treatments ( $P \leq 0.05$ ) for the power requirement values. The regression analysis concluded that drum speed consumed more power than the concave hole diameter or feed rate. While the feed rate showed less effect on power requirements than the concave hole diameter, the following parameters affected power requirements: speed > concave holes diameter drum > feed rate. ANOVA analysis indicated highly significant differences between the treatments listed in Tables 4 and 5. The obtained regression equation for power requirements was in the form of:

$$\text{PR, kWh ton}^{-1} = 5.464 \cdot 0.138 D + 0.0991 S + 0.0027F. \quad (R^2=0.885).$$

## CONCLUSION

The highest value of cowpea threshing efficiency was obtained, and it was 96.75% at a concave opening of 28 mm, and the maximum speed of the roller was 29 m s<sup>-1</sup>. The lowest percentage of grain losses was 2.2% when using a concave hole diameter of 20 mm at the lowest feed rate of 360 kg h<sup>-1</sup> and the lowest drum speed of 17 m s<sup>-1</sup>. The lowest value of seed damage percentage was 4.97% when using a concave with 28 mm holes, and the lowest drum speed was 17 m s<sup>-1</sup>. The highest level of energy consumption was 7.38 kWh ton<sup>-1</sup> at the minimum concave holes of 20 mm, with a maximum drum speed of 29 m s<sup>-1</sup> and a maximum feed rate of 720 kg h<sup>-1</sup>. It could be recommended to utilize the wheat threshing machine development process to adapt it to threshing the cowpea crop.

## DECLARATION OF COMPETING INTEREST

The authors declare that they have no conflict of interest.

## CREDIT AUTHORSHIP CONTRIBUTION STATEMENT

**Mohamed Mansour Shalaby Refaay** designed the concept of entire project. The investigation, methodology and writing of the original draft were done by him, read and approved the final manuscript.

**Ahmed Shawky El-Sayed** was involved in the methodology and former analysis of the experiment. He carried out the review and editing of the original drafted copy, read and approved the final manuscript.

**Mokhtar Cottb Ahmed Awad** participated in the designed and investigation of the experiment. He also handled the data curative and validation, read and approved the final manuscript.

## ETHICS COMMITTEE DECISION

This article does not require any ethical committee decision.

## REFERENCES

- Adekanye, TA and Olaoye JO (2013). Performance evaluation of motorized and treadle cowpea threshers. *Agricultural Engineering International: CIGR Journal*, 15(4): 300-306.
- Ajav E A, and Adejumo B A (2005). Performance evaluation of an okra thresher. *Agricultural Engineering International: CIGR Journal Vol 7*, pp 1-8.
- AOAC (1990). Association official Analytical chemists. 15<sup>th</sup> edn. Wash. Dc, U.S.A.  
<https://doi.org/10.1002/0471740039.vec0284>
- Arazu AV (2017). *Comparative studies on the effects of different modifications on the cold water solubility of starch from selected underutilized legumes*. (Doctoral dissertation).
- Asante EA, Kallai WK, Bonney J, and Amuaku R (2017). Performance evaluation of a cowpea thresher at various moisture contents. *International Journal of Technology and Management Research*, 2(2): 32-37. <https://doi.org/10.47127/ijtmr.v2i2.55>
- Ayenán MAT, Ofori K, Ahoton LE and Danquah A (2017). Pigeonpea [(*Cajanus cajan* L. Millsp.)] production system, farmers' preferred traits and implications for variety development and introduction in Benin. *Agriculture & Food Security*, 6(1): 1-11.
- Dauda A (2001). Design, construction and performance evaluation of a manually operated cowpea thresher for small scale farmers in Northern Nigeria. *AMA*, 32(4):47-49.
- Desta K and Mishra TN (1990). Development and performance evaluation of a sorghum thresher. *AMA*, 21(3): 33-37.
- Herbek JH and Bitzer MJ (2004). Soybean production in Kentucky: Part V- Harvesting, drying, storage, and marketing. Lexington, Ky. *Cooperative Extension Service Bulletin AGR 132*.
- Hunt D (1983). Farm power machinery management. *Eighth edition Iowa State Univ Press Ames*. 3-6.
- Irtwange SV (2009). Design, fabrication and performance of a motorized cowpea thresher for Nigerian small-scale farmers. *African Journal of Agricultural Research*, 4(12): 1383-1391.
- Morad MM, El-Kot AS, Ali MM and Salem HM (2007). Study on the mechanization of cowpea crop production under Egyptian conditions. *Misr Journal of Agricultural Engineering*, 24(3): 450-468.
- Ndirika VIO (1994). Development and performance evaluation of a millet thresher. *Journal of Agricultural Technology*, 20-26.

- Oduma O, Nwakuba NR, and Igboke ME (2014). Performance evaluation of a locally developed pigeon pea thresher. *International Journal of Applied Science, Technology and Engineering Research* 3(2): 20-31.
- Onuoha SN, Enaboifo MA, and Ibrahim R (2022). Development of cowpea thresher. *Nigerian Journal of Technology*, 41(2): 385-395. <https://doi.org/10.4314/njt.v41i2.21>
- Samuel B and Oseme OS (2021). Design and simulation analysis of cowpea dehulling machine. *Global Journal of Engineering and Technology Advances*, 7(2): 050-066. <https://doi.org/10.30574/gjeta.2021.7.2.0069>
- Timothy AA, and Olaoye JO (2013). Performance evaluation of motorized and treadle cowpea threshers. *Agricultural Engineering International: CIGR Journal*, 15(4): 300-306.
- Ukatu AC (2006). A modified threshing unit for soya beans. *Biosystems Engineering*, 95(3): 371-377. <https://doi.org/10.1016/j.biosystemseng.2006.06.014>



## Influence of N fertilizing on Single-cut Sorghum × Sudangrass Hybrids' Forage Yield and Nutritive Profile

Ugur OZKAN<sup>a\*</sup>, Nesim YILDIZ<sup>b</sup>, Celal PEKER<sup>c</sup>

<sup>a</sup>Department of Field Crops, Faculty of Agriculture, University of Ankara, Ankara, TURKEY

<sup>b</sup>Medicinal And Aromatic Plants Program, Vocational School, Antalya Belek University, Antalya, TURKEY

<sup>c</sup>Republic of Turkey Ministry of Agriculture and Forestry, Directorate of Provincial Agriculture and Forestry, Range, Pastures and Forage Crops Section Ankara, TURKEY

(\*) Corresponding Author: [ugurozkan@ankara.edu.tr](mailto:ugurozkan@ankara.edu.tr)

Received: 20.02.2023

Article Info  
Accepted: 12.05.2023

Published: 30.06.2023

### ABSTRACT

The study aimed to observe the effects of two forage sorghum hybrids and different nitrogenous (N) fertilizer rates. The current study was set up in randomized complete block (RCB) as a split-plot design with triplicate at the Field Crops Department experimental area, University of Ankara in the 2022 summer season. This experiment included two treatments which had forage sorghum hybrids (Hay day and Super-graze) and nitrogen fertilization rates in the form of 18% ammonium sulfate [control group with no nitrogen (N<sub>0</sub>), 120 kg ha<sup>-1</sup> N (N<sub>1</sub>), 180 kg ha<sup>-1</sup> N (N<sub>2</sub>)]. N fertilizing rates positively influenced in agronomic profiles, yield components and nutritive profiles. The plant height (197.24-221.72 cm), green herbage yield (GHY) (60.42-70.89 ton ha<sup>-1</sup>), dry matter (DM) yield (17.77-23.98 ton ha<sup>-1</sup>), crude protein (CP) yield (0.97-1.90 ton ha<sup>-1</sup>), metabolic energy (ME) yield (33070.17-51840.85 Mcal ha<sup>-1</sup>), net energy production (NE<sub>p</sub>) yield (21164.91-33178.15 Mcal ha<sup>-1</sup>) increased with applied N rates. The maximum of DM (33.83%), CP (7.90%), TDN (58.63%), ME (2.16 Mcal kg<sup>-1</sup> DM), NE<sub>p</sub> (1.80 Mcal kg<sup>-1</sup> DM), and the minimum of ADF (33.09%), NDF (53.17%), ADL (5.14%) were obtained in N<sub>2</sub> rates. In light of the results; "Hay-day" had more GHY. "Sugar-graze" had more DM yield and it was determined more digestible forage. It was inferred that the best yield components and nutritive profiles were obtained in N<sub>2</sub> rate.

**Keywords:** Fertilizing, Sorghum, Yield, Quality

**To cite:** Ozkan U, Yıldız N, Peker C (2023). Influence of N Fertilizing On Single-Cut Sorghum × Sudangrass Hybrids' Forage Yield and Nutritive Profiles. Turkish Journal of Agricultural Engineering Research (TURKAGER), 4(1), 61-72. <https://doi.org/10.46592/turkager.1252187>



## INTRODUCTION

Forage sorghum (*Sorghum bicolor* (L.) Moench × *Sorghum sudanese* (Piper) Stapf) is a beneficial forage crop for livestock production dynamics in many regions around the World owing to the adaptation of different environments ([Fonseca \*et al.\*, 2012](#); [Amelework \*et al.\*, 2015](#)). The capacity to forage from natural rangelands has declined drastically in recent years, on account of water shortage, salinity problems of soil, and degradation ([Zhang \*et al.\*, 2014](#)). As a consequence of natural grassland's poor quality in Turkey, the livestock ecosystem needs more quality feed. In this case, it is reflected a huge production cost for livestock producers. In arid and semiarid environments, forage sorghum is an important alternative plant that has high dry matter (DM) yield and morpho-physiological adaptations that could resist water shortage ([Sankarapandian \*et al.\*, 2013](#); [Ahmeda \*et al.\*, 2016](#)). Also, it is suitable for silage production and it has high nutritive profiles, which has high soluble carbohydrates and low buffering capacity ([Lema \*et al.\*, 2000](#); [Sankarapandian \*et al.\*, 2013](#); [Brocke \*et al.\*, 2014](#); [Kumar \*et al.\*, 2015](#)).

While agronomic specifications of forage sorghum are necessary, economic specifications must be considered too. Forage sorghum is known to be more economical than other cereal forages because of the fewer requirements in irrigating and fertilizing. It was demonstrated by [Iqbal \*et al.\* \(2015\)](#) that seed usage, fertilizing amount, irrigation, total expenditures and net earnings are cheaper than maize ([Iqbal, 2015](#); [Iqbal \*et al.\*, 2015](#)). Some agronomic practices, especially fertilizing, have the potential to increase the green herbage yield and nutritive value of sorghum ([Iqbal, 2015](#)). Particularly, N fertilizer is essential for the plant's growth during the growing season. Sorghum utilizes nitrogen more efficiently than maize ([Noori, 2020](#)). Increasing N fertilizing positively affect to plant height, shoot elongation, palatability, yield components and nutritive profiles of forage crops ([Ikanovic \*et al.\*, 2014](#)). It also increases protein content, digestibility of dry matter, and decreases crude fibre ([Sher \*et al.\*, 2016](#)). Deficit of soil N leads to lower forage sorghum biomass in result of reductions on leaf area, chlorophyll index ([Mahama \*et al.\*, 2014](#)). Other than that, forage sorghum has an ability to regrow after cutting, especially when fertilization is applied ([Afzal \*et al.\*, 2012](#)). Forage sorghum hybrids is fertilized for optimal forage with application of 50 to 100 kg·N·ha<sup>-1</sup>, applied in two equal rates, which is recommended by [OMAF \(2002\)](#).

The first objective of the current research was to study the effect of forage sorghum hybrids and N fertilizer rates on agronomic profiles, yield components, and nutritive profiles of the Central Anatolian region, Ankara. The second objective was to determine which parameters had a relationship with growing degree days (GDD).

## MATERIALS and METHODS

### Experimental Design and Agronomic Practices

The experimental site was established at Ankara University, Faculty of Agriculture, Field Crops Department's experimental area in summer season of 2022. Köppen-Geiger climate classification of Ankara province is Csa which has a temperate, dry, and hot summer climate ([Rahimi \*et al.\*, 2020](#)). The latitude of Ankara, Turkey is 39° 97' north, the longitude is 32° 86' east and the elevation is 891 m. Mean

temperature and total accumulated precipitation were 23.20°C and 77.30 mm between planting time to harvest. Soil of the experimental area is clay-sandy (sand 23.12, clay 44.60) with 8.02 pH. Organic matter contents were low, particularly in the layers to below given depth. There was rich in potassium (582 ppm), medium phosphorus (13.28 ppm), and low nitrogen (0.074%).

Forage sorghum hybrids were planted 30 kg ha<sup>-1</sup>; with row spacing of 35 cm; a mean plot size of 5.75 m<sup>2</sup> keeping a distance of 1m gap among 3 replicates in a randomized complete block design with split plots. In order to prevent the side effect in the study, one more row was added to the borders of the experimental area. Two forage sorghum hybrids, which are certified, Hay day and Super-graze (n=2) were established in the field. Forage sorghum hybrids were all planted on May 30, 2022, and harvested on September 16, 2022. Before planting; phosphorous (P) fertilizer (120 kg ha<sup>-1</sup> in the form of 46% di-ammonium phosphate) was applied to the all plots. Control treatment (N<sub>0</sub>) (0 kg ha<sup>-1</sup>) and two different N rates [N<sub>1</sub> (120 kg ha<sup>-1</sup> N); N<sub>2</sub> (180 kg ha<sup>-1</sup> N)] (n=3), which were in the form of 18% ammonium sulfate, were applied to the soil. N was applied into two different times; half of it was applied during the planting and the second part was applied when the plants reached up to 20-30 cm in length. The mechanical weeding operation by hand was done at the vegetative growth stage of the plants, specifically when the plants reached a height range of 30 to 40 cm. Forage sorghum hybrids are harvested at the dough stage. Silking date (days), which is described as the beginning of the flowering time, and plant height (cm) were measured for obtaining an agronomic profile. Plant height was measured for twenty sorghum plants and then taken as an average per plot. All plants per plot were harvested, then weighed to determine GHY on a hectare basis (ton ha<sup>-1</sup>). The dry matter (DM) yield (ton ha<sup>-1</sup>) was calculated per plot by multiplying the dry matter (%) and GHY. Growing degree days (GDD) were calculated per all plots in accordance with seedling emergence date in the field to the harvest date (GDD = [(T<sub>max</sub>, °C + T<sub>min</sub>, °C)/2 - 5]) ([McMaster and Wilhelm, 1997](#)) (data now shown).

### Sampling and Nutritive Profile Analysis

Twenty plants per plot were separated at the harvest stage. The collected sample (500 g) was retained and dried at 70°C for 48 h to determine the constant weight ([Avei, 2000](#)). Dried samples were ground to pass through a 1-mm screen in the mill. All the collected samples were analyzed for DM, CP, ADF, NDF, ADL, and TDN. DM was analyzed from the collected sample (10 g) (135°C for 2 hours) ([AOAC, 2005](#) method 930.15). The traditional Kjeldahl acid digestion method was used for obtaining nitrogen compound, then it was converted to ammonia, which is distilled and titrated ([AOAC, 2005](#) method 2001.11), and CP was calculated with  $N \times 6.25$  equation. [Van Soest \*et al.\* \(1991\)](#)'s a sequential procedure applied to determine the ADF and NDF with the ANKOM200 Fiber Analyzer (Ankom Technology Corp, Macedon, NY, USA) after pre-treatment with sodium sulfite and  $\alpha$ -amylase and expressed inclusive of residual ash. ADL was analyzed with the direct sulphuric acid (72%) method using ADF residues by [Robertson and Van Soest \(1981\)](#). By [Horrocks and Valentine \(1999\)](#); TDN was calculated [(TDN = (-1.291 × ADF %) + 101.35)]. Metabolic energy (ME) and net energy production (NE<sub>p</sub>) were calculated in accordance with [NRC \(1989\)](#). After identifying CP, and ME, NE<sub>p</sub> values; these values

were multiplied with dry matter yield, then converted on a hectare basis for obtaining yield values of these parameters (ton ha<sup>-1</sup> and Mcal ha<sup>-1</sup>).

### Statistical Analysis

The data obtained from the current study were subjected to analysis of variance in accordance with the randomized completely block design (RCB) with split plots as triplicate (n=3) via JMP v.13 computer software (SAS, 2017). For each forage sorghum hybrid; agronomic profiles (the silking date, plant height) and yield components (GHY, DM yield, CP yield, ME yield, NE<sub>p</sub> yield) and nutritive profiles (DM, CP, ADF, NDF, ADL, TDN, ME, NE<sub>p</sub>) were analyzed. DM, CP, ADF, NDF, ADL, and TDN were arcsine-transformed before the statistical analysis to stabilize variances and normalize proportional data. Probabilities equal to or less than 0.05 were considered significant (\* P<0.05, \*\* P<0.01). If ANOVA indicated differences between treatment means, LSD test was performed to separate them. Correlations (r) between GDD to agronomic profiles, yield components, and nutritive profiles were determined. The dependent variable of this observation was GDD. Its relationship with agronomic profiles, yield components and nutritive profiles are presented in Table 2.

## RESULTS AND DISCUSSION

### Agronomic Profile and Yield Components

The effect of the forage sorghum hybrids on agronomic profiles; significant differences were not detected for all parameters (ns), excluding GHY (P<0.05). But, the effect of the N rates had significant differences in plant height, DM yield, CP yield, ME yield, and NE<sub>p</sub> yield (P<0.01) in accordance with one-way ANOVA, excluding silking date (ns) and GHY (P<0.05). The interaction of forage sorghum hybrids × N fertilizer rates were found non-significant for all parameters. “Hay day” and “Sugar-graze” generally showed similar agronomic and yield values due to their non-differences in statistical data. An earliest silking date (66.89 days) was observed in “Hay day”. The longest plant height (212.25 cm), the maximum GHY (68.05 ton ha<sup>-1</sup>), the maximum yield of DM (20.91 ton ha<sup>-1</sup>), CP (1.44 ton ha<sup>-1</sup>) were obtained in “Sugar-graze” (Figure 1, Figure 2). The minimum agronomic profiles and yield components were noted in “Hay day”, excluding ME (42567.55 Mcal ha<sup>-1</sup>), and NE<sub>p</sub> (27243.23 Mcal ha<sup>-1</sup>). “Hay day” had the smallest plant height (210.37 cm), the minimum GHY (63.86 ton ha<sup>-1</sup>), the minimum yield of DM (20.78 ton ha<sup>-1</sup>), and CP yield (1.41 ton ha<sup>-1</sup>) (Table 1, Figure 2).

The silking date (69.83-64.14 days), plant height (197.24-221.72 cm), GHY (60.42-70.89 ton ha<sup>-1</sup>), DM yield (17.77-23.98 ton ha<sup>-1</sup>), CP yield (0.97-1.90 ton ha<sup>-1</sup>), ME yield (33070.17-51840.85 Mcal ha<sup>-1</sup>), NE<sub>p</sub> yield (21164.91-33178.15 Mcal ha<sup>-1</sup>) were varied among N fertilizer rates (N<sub>0</sub> to N<sub>2</sub>) (Table 1). N<sub>2</sub> fertilizer gave more GHY (10.47 ton ha<sup>-1</sup>), the yield of DM (6.21 ton ha<sup>-1</sup>), and CP (0.93 ton ha<sup>-1</sup>) over non-fertilizing (N<sub>0</sub>) plots (Figure 2).



**Table 1.** Mean values of agronomic profiles, yield component and nutrient values of Forage sorghum hybrids and N fertilizer rates.

Agronomic profile and yield components	Hybrids		Fertilizer			MEAN	± SD
	Hay day	Sugar-graze	No (Control)	N <sub>1</sub> (120 kg ha <sup>-1</sup> )	N <sub>2</sub> (180 kg ha <sup>-1</sup> )		
Silking date, (day)	66.89	67.11	69.83	67.00	64.17	67.00	± 4.77
Plant height, (cm)	210.37	212.25	197.24b	214.97a	221.72a	211.31	± 15.45
GHY, ton ha <sup>-1</sup>	63.86b	68.05a	60.42b	66.56ab	70.89a	65.96	± 6.38
DM yield, ton ha <sup>-1</sup>	20.78	20.91	17.77b	20.79ab	23.98a	20.85	± 3.38
CP yield, ton ha <sup>-1</sup>	1.41	1.44	0.97c	1.41b	1.90a	1.42	± 0.43
ME yield, Mcal ha <sup>-1</sup>	42567.55	41778.95	33070.17c	41608.73b	51840.85a	42173.25	± 8991.78
NE <sub>p</sub> yield, Mcal ha <sup>-1</sup>	27243.23	26738.53	21164.91c	26629.58b	33178.15a	26990.88	± 5754.75
<b>Nutrient Profile</b>							
DM, %	32.53	30.67	29.41b	31.23ab	33.83a	31.50	± 3.16
CP, % DM	6.66	6.77	5.48b	6.77a	7.90a	6.72	± 1.13
ADF, % DM	35.30b	36.14a	38.23a	35.83ab	33.09b	35.72	± 2.48
NDF, % DM	55.82	56.43	58.98a	56.21ab	53.17b	56.13	± 2.89
ADL, %DM	5.77	5.64	6.21a	5.75ab	5.14b	5.70	± 0.59
TDN, % DM	55.78a	54.69b	51.99b	55.09ab	58.63a	55.24	± 3.21
ME, Mcal kg <sup>-1</sup> DM	2.03a	1.99b	1.86b	2.00ab	2.16a	2.01	± 0.14
NE <sub>p</sub> , Mcal kg <sup>-1</sup> DM	1.30a	1.27b	1.20b	1.28ab	1.38a	1.29	± 0.10

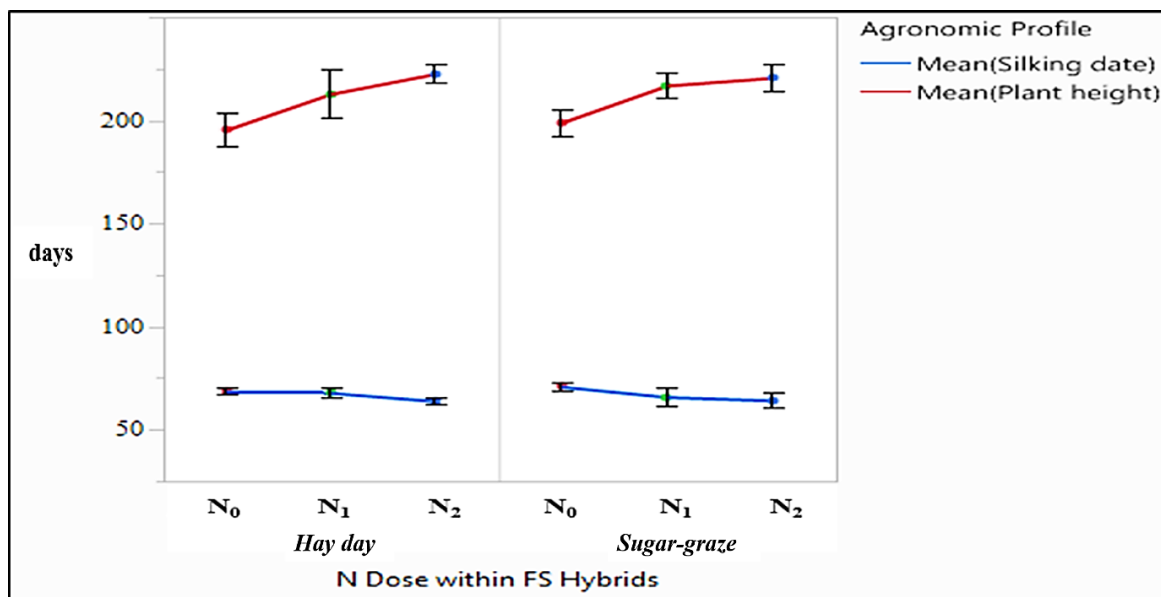
GHY: green herbage yield, DM: Dry matter, CP: Crude protein, ME: Metabolic energy, NE<sub>p</sub>: Net energy production, SD: Standart deviation.

An agronomic profile such as plant height reached the longest level in N<sub>2</sub> compared to non-fertilizing plots (Figure 1), for “Hay day” and “Sugar-graze” (210.37 and 212.25 cm). [Silva et al. \(2011\)](#) evaluated plant height in 25 forage sorghum hybrids and noted that was an average of 207 cm, which was below the forage sorghum hybrids in current study. The plant height findings of [Chaudhary et al. \(2018\)](#) (161.06-173.98 cm) were also lower, yet the findings of [Atis et al. \(2012\)](#) (257.70-278.00 cm) and [Singh et al. \(2016\)](#) (274.9-354.8 cm) were higher than the current study. “Hay Day”, which was used in the current study, was stated the plant height as 284.60 cm by [Keskin et al. \(2018\)](#). [Shivprasad and Singh \(2017\)](#) also obtained the plant height as 234.00 cm with the same row spacing and N rate, which was similar to current study.

[Monteiro et al. \(2004\)](#) defined that plant height is an essential agronomic parameter for the GHY. It is also influenced positively by higher nitrogen rates ([Cheema et al., 2010](#)). But a greater plant height does not always refer to a higher DM yield. “Sugar-graze” had a longer plant height (212.25 cm) and GHY (68.05 ton ha<sup>-1</sup>) than the plant height (210.37 cm) and GHY (63.86 ton ha<sup>-1</sup>) of “Hay day”. But the DM yield of “Sugar-graze” (20.91 ton ha<sup>-1</sup>) was very close to the DM yield of “Hay day” (20.78 ton ha<sup>-1</sup>). The similarity of DM yield in forage sorghum

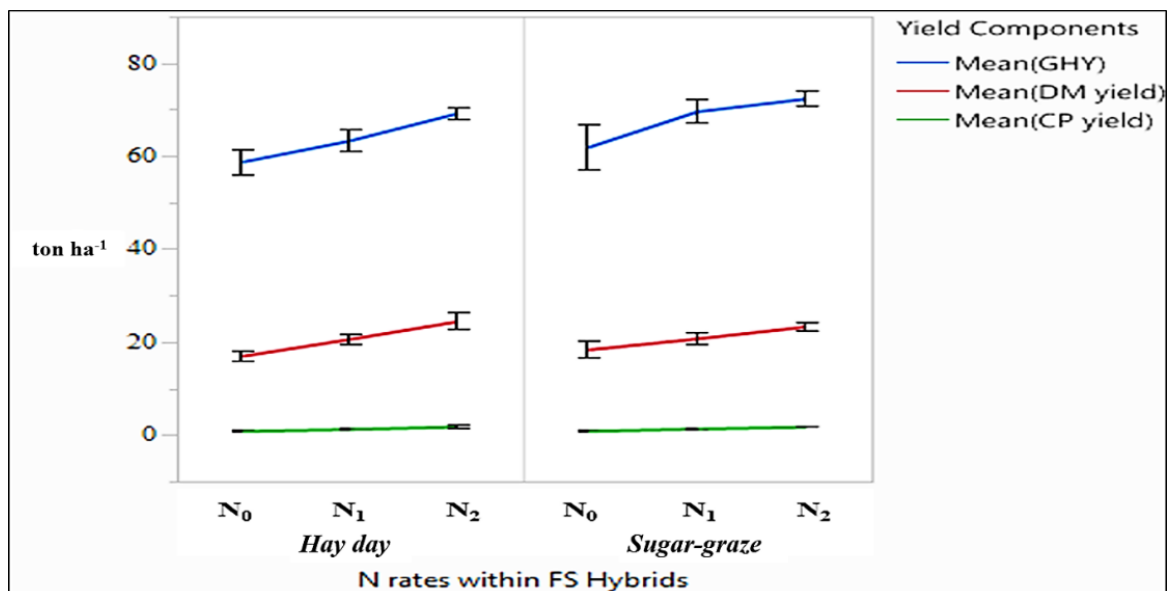
hybrids emanated from the DM content of the “Sugar-graze” (30.67%) and “Hay day” (32.53%).

GHY, DM yield, CP yield, ME yield, and  $NE_p$  yield tended to increase in applied N fertilizer [ $N_0$  to  $N_2$  (0 to 180 kg ha<sup>-1</sup>)] (Figure 2). But individual hybrids' influence was less effective compared to different N rates on these yield components. With the parallel findings of [Holman \*et al.\* \(2019\)](#) and [Almodares \*et al.\* \(2009\)](#); GHY, and DM yield showed significant differences with the applied N rates. The GHY and DM yield results of [Keskin \*et al.\* \(2018\)](#) (83.37 ton ha<sup>-1</sup> and 26.58 ton ha<sup>-1</sup> for “Hay day”) and [Atis \*et al.\* \(2012\)](#) (84.69 ton ha<sup>-1</sup> and 21.0 ton ha<sup>-1</sup>) showed higher yield potential from the current study. Similar agronomic practices to the current study by [Shivprasad and Singh \(2017\)](#), who conducted their study with row spacing of 30 cm and 120 kg ha<sup>-1</sup> N rate, reported that GHY was as 36.90 ton ha<sup>-1</sup>. CP yields of forage sorghum hybrids were very similar to each other, while N rates showed significant differences. The response of CP yield to the N rates is related to the increase in DM and CP content. When nutrient uptake is boosted in the plants with some agronomic practices like fertilizing, protein synthesis in the plants is disposed to increase which is resulted in higher protein content, CP yield per area also increases as a consequence of this ([Książak \*et al.\*, 2012](#); [Sher \*et al.\*, 2017](#); [Pal \*et al.\*, 2014](#)) demonstrated that CP yield ranged 0.98-1.04 ton ha<sup>-1</sup> and 1.02-1.76 ton ha<sup>-1</sup>, which were below the CP yield of  $N_2$  rate in the current study.



$N_0$ : control treatment,  $N_1$ : 120 kg ha<sup>-1</sup> N,  $N_2$ : 180 kg ha<sup>-1</sup> N.

**Figure 1.** Expression of agronomic profiles.



N<sub>0</sub>: control treatment, N<sub>1</sub>: 120 kg ha<sup>-1</sup> N, N<sub>2</sub>: 180 kg ha<sup>-1</sup> N, GHY: Green herbage yield, DM: Dry matter, CP: Crude protein.

**Figure 2.** Expression of yield components.

### Nutritive Profile

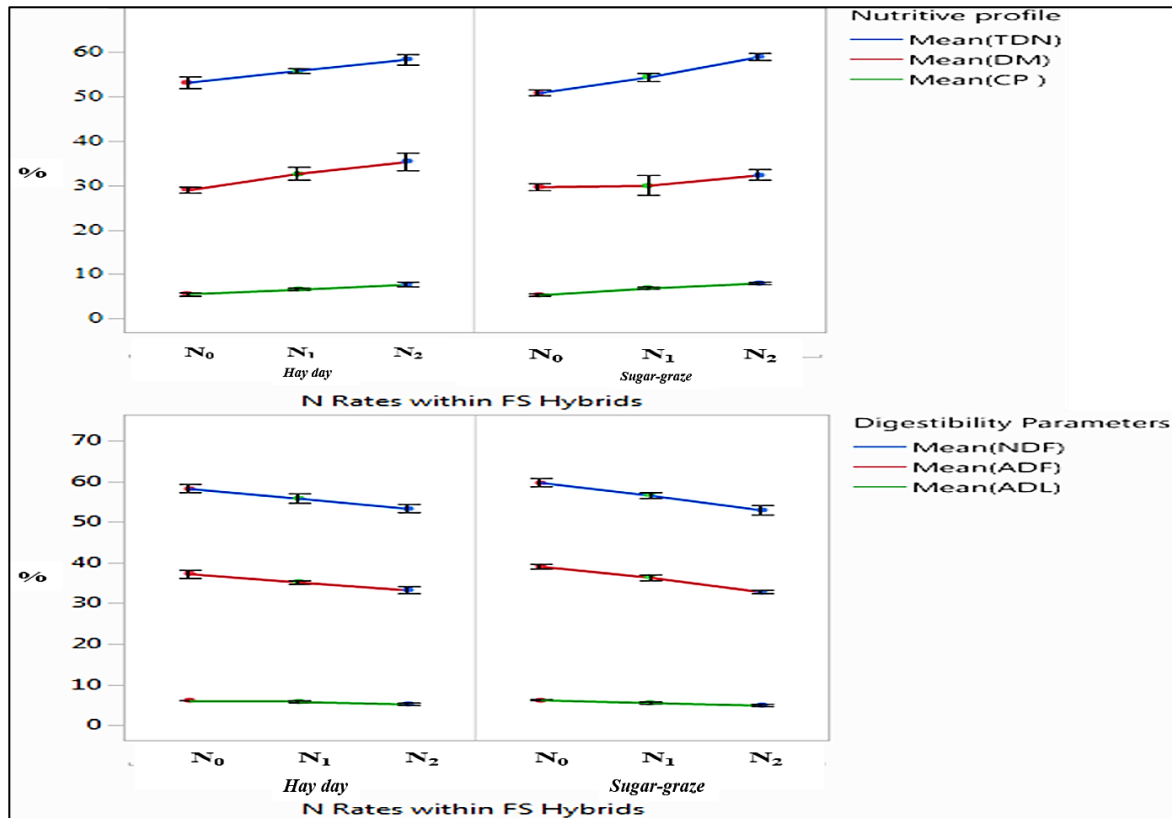
The effect of the forage sorghum hybrids on nutritive profile; ADF, TDN, ME, and NE<sub>p</sub> had significantly different ( $P < 0.05$ ), while DM, CP, NDF, and ADL were not (ns). The N rates effect on CP, ADF, NDF, ADL, TDN, ME, and NE<sub>p</sub> detected significant differences ( $P < 0.01$ ) in accordance with one-way ANOVA, excluding DM ( $P < 0.05$ ). The interaction of forage sorghum hybrids  $\times$  N fertilizer rates were found non-significant for all parameters. “Hay day” and “Sugar-graze” had more than 30% DM (32.53% and 30.67%) (Figure 3). The maximum CP content (6.77%), ADF (36.14%), NDF (56.43%) were obtained in “Sugar-graze”. “Hay day” had a maximum ADL (5.77%), TDN (55.78%), ME (2.03 Mcal kg<sup>-1</sup> DM), and NE<sub>p</sub> (1.30 Mcal kg<sup>-1</sup> DM) compared to “Sugar-graze”.

It was indicated that the maximum of DM (33.83%), CP (7.90%), TDN (58.63%), ME (2.16 Mcal kg<sup>-1</sup> DM), NE<sub>p</sub> (1.38 Mcal kg<sup>-1</sup> DM) in N<sub>2</sub> rate. N<sub>0</sub> had the maximum ADF (38.23%), NDF (58.98%), and ADL (6.21%). N<sub>2</sub> plots gave 30% more CP, %11 TDN, %14 ME, %13 NE, and less %13 ADF, %10 NDF, % and 17% ADL over non-fertilizing (N<sub>0</sub>) plots (Figure3).

Forage sorghum hybrids did not affect DM content, while N fertilizer rates did [N<sub>0</sub> to N<sub>2</sub> (0 to 180 kg ha<sup>-1</sup>)]. “Hay day” and “Sugar-graze” showed a little variation of each other on DM content. In the contrast to current study; [Costa et al. \(2016\)](#) and [Tolentino et al. \(2016\)](#) indicated that 12 and 24 different sorghum genotypes might show wide variation in DM content (30.14-42.33%) (36.31-50.25%), in the same order. This type of wide variation makes predicting nutritive profile and dry matter intake non-confident. In addition, this is one of the main reasons why livestock producers choose corn rather than forage sorghum as silage for their total mixed rations ([Govea et al., 2010](#)).

The nutritive quality increase when N fertilizers should be so properly applied that they should improve the efficient use of plant nutrients. This application preserves also feed digestibility as well as silage quality ([Kaplan et al., 2019](#)). ADF, NDF, and ADL percentages are inversely related to DM intake, palatability and digestibility. Under these circumstances, low fiber contents ([Ahmad et al., 2016](#)) and

higher CP are more acceptable for better quality, and vice versa. The current study indicated that CP increased and digestibility parameters (ADF, NDF, ADL) decreased with applied N rates (Figure 3). The more digestible product, which had lower ADF (35.30%), NDF (55.82%) was “Hay day”. The findings of [Holman \*et al.\* \(2019\)](#) and [Damian \*et al.\* \(2017\)](#) about increasing CP content with applied N rates showed similar trends to the current study. CP contents were also documented by [Celik and Turk \(2021\)](#) (10.72% in 5 cultivars), [Costa \*et al.\* \(2016\)](#) (8.03% in 15 genotypes), [Tolentino \*et al.\* \(2016\)](#) (8.14% in 24 genotypes).



$N_0$ : control treatment,  $N_1$ : 120 kg ha<sup>-1</sup> N,  $N_2$ : 180 kg ha<sup>-1</sup> N, DM: Dry matter, CP: Crude protein, TDN: Total digestible nutrient, ADF: Acid detergent fiber, NDF: Neutral detergent fiber, ADL: Acid detergent lignin.

**Figure 3.** Expression of nutritive profile and digestibility parameters.

In the current study, there were variations among N fertilizer rates [ $N_0$  to  $N_2$  (0 to 180 kg ha<sup>-1</sup>)] in digestibility parameters, which were ADF, NDF, and ADL. Increasing N rates declined ADF, NDF, and ADL content, in contrast to the findings of [Tang \*et al.\* \(2018\)](#) and [Marsalis \*et al.\* \(2010\)](#). These rates in the current study also made forage sorghum hybrids more digestible for animal feed. The findings of [Tang \*et al.\* \(2018\)](#) (40.60% ADF, 65.20% NDF) and [Sher \*et al.\* \(2016\)](#) (43.80% ADF, 53.95% NDF) were higher than the current study. [Kir and Sahan \(2019\)](#) indicated the ADL content of “Sugar-graze” was 5.20%, which is lower for the same hybrid in the current study. TDN defines the available nutrients for livestock and the energy content of forages ([Sayar \*et al.\*, 2014](#); [Posada \*et al.\*, 2012](#)); therefore, the highest TDN (55.78%) was observed in “Sugar-graze”. N fertilizer rates [ $N_0$  to  $N_2$  (0 to 180 kg ha<sup>-1</sup>)] increased TDN in the current study. The TDN content of the current study had %11 more TDN (55.78%) compared to the finding of [Bilen and Turk \(2021\)](#) for “Sugar-graze” (49.52%). [Tang \*et al.\* \(2018\)](#) (49.00%) and [Sher \*et al.\* \(2016\)](#) (44.80%) also stated lower TDN content over the current study.

Similar to TDN, which is highly desirable quality components, ME and NE<sub>p</sub> are beneficial to forage quality by improving animals' ability to utilize the forage nutrients (Carmi *et al.*, 2006, Lithourgidis *et al.*, 2006). Applied N rates increased energy values in agreement with Kaplan *et al.*, 2016; Kaplan *et al.*, 2019). They also determined ME values as 2.11 and 1.56 Mcal kg<sup>-1</sup> DM, which were higher compared to the control treatment and lower than N<sub>2</sub> rates in the current study.

### Growing Degree Days (GDD) Relationship with Agronomic Profile, Yield Components and Nutritive Profile

**Table 2.** Correlation co-efficients of some important parameters with growing degree days (GDD).

	SD	PH	DM	GHY	DMY	CPY	MEY	NE <sub>p</sub> Y	CP	ADF	TDN	NDF	ADL
<b>GDD</b>	-0.44	0.71	0.41	0.50	0.54	0.38	0.45	0.45	0.17	-	0.13	-	-
										0.13		0.10	0.30
<b>p level</b>	0.03*	0.001***	0.09	0.03*	0.02*	0.13	0.06	0.06	0.50	0.60	0.61	0.72	0.23

**SD:** silking date, **DM:** dry matter, **GHY:** green herbage yield, **DMY:** dry matter yield, **CPY:** crude protein yield, **MEY:** metabolic energy yield, **NE<sub>p</sub>Y:** net energy production yield, **CP:** crude protein, **ADF:** acid detergent fibre, **TDN:** total digestible nutrient, **NDF:** neutral detergent fibre, **ADL:** acid detergent lignin

GDD had a relationship with some agronomic profiles and yield components, while all nutritive profiles were not (ns) (Table 2). Plant height ( $r = 0.71$ ,  $P < 0.001$ ) showed a positive strong correlation. GHY ( $r = 0.50$ ,  $P = 0.03$ ), DM yield ( $r = 0.54$ ,  $P = 0.02$ ) showed a positive weak correlation, while silking date ( $r = -0.44$ ,  $P = 0.03$ ) showed a negative weak correlation with GDD (Table 2). Lyons *et al.* (2019) noted a positive weak relationship between GDD to sorghum biomass yield and DM yield, similar to the current study.

## CONCLUSION

The two forage sorghum hybrids cultivated with three different N rates were evaluated for agronomic profiles, yield components, and nutritive profiles in Ankara. The results indicated that all agronomic profiles, yield components, and nutritive profiles were influenced by N fertilizing and its rates. But forage sorghum hybrids just affected GHY, ADF, TDN, ME, NE<sub>p</sub>. "Hay day" was determined more nutritive in DM, ADF, NDF, TDN, ME, and NE<sub>p</sub> compared to "Sugar-graze". In contrast to the nutritive profile, "Sugar-graze" had more GHY, DM yield, and CP yield. Forage sorghum hybrids were affected positively by applied N rates [N<sub>0</sub> to N<sub>2</sub> (0 to 180 kg ha<sup>-1</sup>)]. In the current study, more digestible forage was expressed by "Hayday" than "Sugar-graze" with lower ADF, NDF. In the progress of control treatment (N<sub>0</sub> to 180 kg ha<sup>-1</sup> (N<sub>2</sub>); digestibility and quality increased. This progress also positively affected the agronomic profiles and yield components of forage sorghum hybrids.

## DECLARATION OF COMPETING INTEREST

Authors declare that they have no conflict of interest.

## CREDIT AUTHORSHIP CONTRIBUTION STATEMENT

**Ugur Ozkan:** Investigation, methodology, formal analysis, writing, editing,  
**Nesim Yildiz:** Investigation, data curation, writing,  
**Celal Peker:** Data curation, laboratory analysis.

## ETHICS COMMITTEE DECISION

This article does not require any ethical committee decision.

## REFERENCES

- Afzal M, Ahmad A and Ahmad AH (2012). Effect of nitrogen on growth and yield of sorghum forage (*Sorghum bicolor* (L.) Moench cv.) Under three cuttings system. *Cercetări Agronomice*, 45: 57-64.
- Ahmeda IAM, Eltiliba AMA, Ganawab FHS and Islamd KR (2016). Utilization of industrial waste aqueous ammonia for irrigated forage sorghum production. *Archives of Agronomy and Soil Science*, 62: 93-07.
- Almodares A, Jafarinia M and Hadi MR (2009). The effects of nitrogen fertilizer on chemical compositions in corn and sweet sorghum. *American-Eurasian Journal of Agricultural and Environmental Sciences*, 6(4): 441-446.
- Amelework B, Shimelis H, Tongoona P, Mark Laing M and Mengistu F (2015). Genetic variation in lowland sorghum (*Sorghum bicolor* (L.) Moench) landraces assessed by simple sequence repeats. *Plant Genetic Resources*, 13: 131-141.
- AOAC (2005). Official methods of analysis (930.15 and 2001.12). 18th ed. *AOAC International, Gaithersburg, MD, USA*.
- Atis I, Konuskan O, Duru M, Gozubenli H and Yilmaz S (2012). Effect of harvesting time on yield, composition and forage quality of some forage sorghum cultivars. *International Journal of Agriculture and Biology*, 14(6): 879-886.
- Avcı M (2000). *Determination of winter perennial wheatgrass- leguminous forage crops mixtures that can be cultivated to establish temporary artificial pasture in Çukurova*. Çukurova University, Graduate School of Natural and Applied Sciences, 113 p., Adana.
- Bilen Y and Turk M (2021). A research on possibilities of second crop sorghum-sudangrass hybrids growing on banaz condition. *SDU Journal of the Faculty of Agriculture*, 16(1): 46-51.
- Brocke KV, Trouche G, Weltzien E, Barro CPK, Sidibe A, Zougmore R (2014) Helping farmers adapt to climate and cropping system change through increased access to sorghum genetic resources adapted to prevalent sorghum cropping systems in Burkina Faso. *Experimental Agriculture*, 50: 284-305.
- Carmi A, Aharoni Y, Edelstein M, Umiel N, Hagiladi A, Yosef E, Nikbachat M, Zenou A, Miron J (2006). Effects of irrigation and plant density on yield, composition and in vitro digestibility of a new forage sorghum variety, Tal, at two maturity stages. *Animal Feed Science Technology*, 131: 121-133.
- Celik B and Turk M (2021). The determination of forage yield and quality of some silage sorghum cultivars in ecological conditions of uşak province. *Turkish Journal of Range and Forage Science*, 2(1): 1-7.
- Chaudhary JD, Pavaya RP, Malav JK, Dipika G, Chaudhary N, Kuniya NK and Jat JR (2018). Effect of nitrogen and potassium on yield, nutrient content and uptake by forage sorghum (*Sorghum bicolor* (L.) Moench) on loamy sand. *International Journal of Chemical Studies*, 6(2): 761-765.
- Cheema MA, Farhad W, Saleem MF, Khan HZ, Munir A, Wahid MA, Rasul F and Hammad HM (2010). Nitrogen management strategies for sustainable maize production. *Crop Environment*, 1: 49-52.
- Costa RF, Pires DADA, Moura MMA, Sales ECJD, Rodrigues JAS and Rigueira JPS (2016). Agronomic characteristics of sorghum genotypes and nutritional values of silage. *Acta Scientiarum- Animal Sciences*, 38: 127-133.
- Damian JM, Ros COD, Silva RFD, Coldebella, IJ and Simon DH (2017). N, P or K doses on the dry matter and crude protein yield in maize and sorghum for silage. *Pesquisa Agropecuária Tropical*, 47: 53-61.





- Fonseca, L, Mezzalira JC, Bremm C, Filho RSA, Gonda HL and Carvalho PCF (2012). Management targets for maximising the short-term herbage intake rate of cattle grazing in *Sorghum bicolor*. *Livestock Science*, 145: 205–211.
- Govea FE, Marsalis MA, Lauriault LM and Bean BW (2010). Forage sorghum nutritive value: A review. Online. *Forage and Grazinglands*, 8(1): 1-6.
- Horrocks RD and Vallentine JF (1999). Harvested Forages. *Academic Press*, London, UK.
- Holman JD, Obour AK and Mengel DB (2019). Nitrogen application effects on forage sorghum production and nitrate concentration. *Journal of Plant Nutrition*, 42(20): 2794-2804.
- Ikanović J, Janković S, Popović V, Rakić S, Dražić G, Živanović L and Kolarić L (2014). The effect of nitrogen fertilizer rates on green biomass and dry matter yield of *Sorghum* ssp. at different growth stages. *Biotechnology in Animal Husbandry*, 30(4): 743-749.
- Iqbal MA (2015). Agronomic management strategies elevate forage sorghum yield: A review. *Journal of Advanced Botany and Zoology*, 3: 1-6.
- Iqbal MA, Ahamd B, Shah MH and Ali K (2015). A study on forage sorghum (*Sorghum bicolor* L.) production in perspectives of white revolution in Punjab, Pakistan: Issues and future options. *American-Eurasian Journal of Agricultural and Environmental Sciences*, 15(4): 640-647.
- Kaplan M, Baran O, Unlukara A, Kale H, Arslan M, Kara K and Ulas A (2016). The effects of different nitrogen doses and irrigation levels on yield, nutritive value, fermentation and gas production of corn silage. *Turkish Journal of Field Crops*, 21(1): 101-109.
- Kaplan M, Kara K, Unlukara A, Kale H, Beyzi SB, Varol IS and Kamalak A (2019). Water deficit and nitrogen affects yield and feed value of sorghum sudangrass silage. *Agricultural Water Management*, 218: 30-36.
- Keskin B, Akdeniz H, Temel S and Baris, E (2018). Determination of agricultural characteristics of some silage sorghum and Sudan grass varieties grown as second product. *Yuzuncu Yil University Journal of Agricultural Sciences*, 28(4): 412-418.
- Kir H and Sahan BD (2019). Yield and quality feature of some silage sorghum and sorghum-sudangrass hybrid cultivars in ecological conditions of Kırşehir province. *Turkish Journal of Agricultural and Natural Sciences*, 6(3): 388-395.
- Książak J, Matyka M, Bojarszczuk J and Kacprzak A (2012). Evaluation of productivity of maize and sorghum to be used for energy purposes as influenced by nitrogen fertilization. *Žemdirbystė-Agriculture*, 99(4): 363-370.
- Kumar TVA, Samuel DVK, Jha SK and Sinha JP (2015). Twin screw extrusion of sorghum and soya blends: a response surface analysis. *Journal of Agricultural Science Technology*, 17: 649-662.
- Lema M, Felix A, Salako S and Bishnoi U (2000). Nutrient content and in vitro dry matter digestibility from various grain sorghum and sweet sorghum cultivars. *Journal of Sustainable Agriculture*, 17: 55-70.
- Lithourgidis AS, Vasilakoglou IB, Dhima KV, Dordas CA, Yiakoulaki MD (2006). Forage yield and quality of common vetch mixtures with oat and triticale in two seeding ratios. *Field Crop Research*, 99: 106-113.
- Lyons SE, Ketterings QM, Godwin GS, Cherney JH, Cherney DJ, Meisinger JJ and Kilcer TF (2019). Double-cropping with forage sorghum and forage triticale in New York. *Agronomy Journal*, 111(6): 3374-3382.
- Mahama GY, Vara Prasad PV, Mengel DB and Tesso TT (2014). Influence of nitrogen fertilizer on growth and yield of grain sorghum hybrids and inbred lines. *Agronomy Journal*, 106(5): 1623-1630.
- Marsalis MA, Angadi SV and Contreras-Govea FE (2010). Dry matter yield and nutritive value of corn, forage sorghum, and BMR forage sorghum at different plant populations and nitrogen rates. *Field Crop Research*, 116: 52-57.
- McMaster GS and Wilhelm WW (1997). Growing degree-days: one equation, two interpretations. *Agricultural and Forest Meteorology*, 87(4): 291-300.
- Monteiro MCD, Anunciação Filho CJ, Tabosa JN, Oliveira FJ, Reis OV and Bastos GQ (2004). Avaliação do desempenho de sorgo forrageiro para o semiárido de Pernambuco. *Revista Brasileira de Milho e Sorgo*, 3: 52-61. (In Spanish)
- National Research Council (NRC) 1989. Nutrient requirements of dairy cattle. *National Academies Press, Washington, DC, USA*.
- Noori MS (2020). Effect of nitrogen fertilization on growth and forage yield of sorghum [*Sorghum bicolor* (L.) Moench.] under takhar agro-ecological conditions. *Turkish Journal of Range and Forage Science*, 1(2): 66-71.
- Ontario Ministry of Agriculture and Food (OMAF) (2002) *Annual Report*.

- Pal MS, Reza A, Joshi YP and Panwar UBS (2014). Production potential of forage sorghum (*Sorghum bicolor* L.) under different intercropping systems. *Agriculture for Sustainable Development*, 2(2): 87-91.
- Posada OS, Rosero NR, Rodríguez N and Costa CA (2012). Comparison of methods to determine the energy value of feeds for ruminants. *Revista MVZ Cordoba*, 17(3): 3184-3192.
- Rahimi J, Laux P and Khalili A (2020). Assessment of climate change over Iran: CMIP5 results and their presentation in terms of Köppen–Geiger climate zones. *Theoretical and Applied Climatology*, 141(1): 183-199.
- Robertson JB and Van Soest PJ (1981). The detergent system of analysis and its application to human foods. In *The Analysis of Dietary Fiber in Food*; James, WPT, Theander O, Eds; Marcel Dekker: New York, NY, USA, 123-158.
- Sankarapandian R, Audilakshmi S, Sharma V, Ganesamurthy K, Talwar HS and Patil JV (2013). Effect of morpho-physiological traits on grain yield of sorghum grown under stress at different growth stages, and stability analysis. *Journal of Agricultural Science*, 151: 630-647.
- SAS Institute, Inc (2017). JMP® Statistical Discovery Software (v.13.0). Cary, NC.
- Sayar MS, Han Y, Yolcu H and Yucel H (2014). Yield and quality traits of some perennial forages as both sole crops and intercropping mixtures under irrigated conditions. *Turkish Journal of Field Crops*, 19(1): 59-65.
- Sher A, Ansar M, Ijaz M and Sattar A (2016). Proximate analysis of forage sorghum cultivars with different doses of nitrogen and seed rate. *Turkish Journal of Field Crops*, 21(2): 276-285.
- Sher A, Hassan FU, Ali H, Hussain M and Sattar A (2017). Enhancing forage quality through appropriate nitrogen dose, seed rate and harvest stage, in sorghum cultivars grown in Pakistan. *Grassland Science*, 63(1): 15-22.
- Shivprasad M and Singh R (2017). Effect of planting geometry and different levels of nitrogen on growth, yield and quality of multi-cut fodder sorghum (*Sorghum bicolor* (L.) Monech). *Journal of Pharmacognosy and Phytochemistry*, 6(4): 896-899.
- Silva TC, Santos EM, Azevedo JAG, Edvan RL, Perazzo AF and Pinho RMA (2011). Agronomic divergence of sorghum hybrids for silage yield in the semiarid region of Paraíba. *Revista Brasileira de Zootecnia*, 40: 1886-1893.
- Singh KP, Chaplot PC, Sumeriya HK and Choudhary GL (2016). Performance of single cut forage sorghum genotypes to fertility levels. *Forage Research*, 42(2): 140-142.
- Tang C, Yang X, Chen X, Ameen A and Xie G. (2018). Sorghum biomass and quality and soil nitrogen balance response to nitrogen rate on semiarid marginal land. *Field Crops Research*, 215: 12-22.
- Tolentino DC, Rodrigues JAS, Pires DADA, Veriato FT, Lima LOB and Moura MMA (2016). The quality of silage of different sorghum genotypes. *Acta Scientiarum- Animal Sciences*, 38: 143-149.
- Van Soest PJ, Robertson JB and Lewis BA (1991). Methods for dietary fiber, neutral detergent fiber, and non starch polysaccharides in relation to animal nutrition. *Journal of Dairy Science*, 74: 3583-3597.
- Zhang YJ, Zhang XQ, Wang XY, Li N and Kan HM (2014). Establishing the carrying capacity of the grasslands of China: a review. *The Rangeland Journal*, 36(1): 1-9.





## Performance and Cost Comparison of Photovoltaic and Diesel Pumping Systems: In Central Rift Valley of Ethiopia

Maney Ayalew DESTA<sup>a\*</sup>, Getachew Shunki TIBA<sup>b</sup>, Mubarek Mohammed ISSA<sup>a</sup>  
Wariso HEYI<sup>a</sup>

<sup>a</sup> Department of Agricultural Engineering Research, Melkassa Agricultural Research Centre, Ethiopian Institute Agricultural Research, Addis Ababa, ETHIOPIA

<sup>b</sup> Department of Mechanical Engineering, College of Electrical and Mechanical Engineering, Addis Ababa Science and Technology University, Addis Ababa, ETHIOPIA

(\*): Corresponding Author: [maneyayalew58@gmail.com](mailto:maneyayalew58@gmail.com)

Received: 29.03.2022

Article Info  
Accepted: 29.05.2023

Published: 30.06.2023

### ABSTRACT

Diesel pumps have extensively used for irrigation water pumping. However, this causes challenges both in terms of economic factors (fuel costs) and environmental impacts (emits air pollution). An alternative solution is using renewable energy sources. In this regard, a battery less solar PV energy system was designed and evaluated for the geographic location and metrological data of Dugda woreda, representing the central rift valley of Ethiopia. Performance testing were conducted on sunny days of April month and with time intervals of from 9:00 am to 5:00 pm, again the respective solar radiation ranges between 385.8 to 862.2 W m<sup>-2</sup> h<sup>-1</sup>. The solar photovoltaic pumping has been evaluated with the head levels of 10, 12, 15, and 18 m. Accordingly the result showed that, PV system size can irrigate a tomato field of 0.33-0.75 ha with a mean daily water use of 8.7 and 17.4 m<sup>3</sup> day<sup>-1</sup> at head levels of 10 and 18 meters, respectively. After evaluation, the maximum water flow rate has been at the midday day from 12:00 am to 1:00 pm. Comparative economic evaluation of the solar-powered water pump system and diesel pump devices were done using cycle cost breakdown and the cost of water per unit volume. Thus the long term economics of water pumping using solar photovoltaic and diesel pumping systems showed a cost of 1.33 ETB m<sup>-3</sup> and 3 ETB m<sup>-3</sup>, respectively. The result demonstrated that photovoltaic water pump systems are more affordable for the long-term services of small to medium-scale farms than gasoline water pumps.

**Keywords:** Photovoltaic, Solar radiation, Pumps, Life cycle cost

**To cite:** Desta MA, Tiba GS, Issa MM and Heyi W (2023). Performance and Cost Comparison of Photovoltaic and Diesel Pumping Systems: In Central Rift Valley of Ethiopia *Turkish Journal of Agricultural Engineering Research (TURKAGER)*, 4(1), 73-90. <https://doi.org/10.46592/turkager.1272864>



## INTRODUCTION

Energy is a fundamental and essential desire of human life. It is one of the most valuable inputs in agricultural production. More than one quarter of the energy used globally is expended on food production and supply. Energy can be generated from renewable and non-renewable sources. The conventional fossil fuels cannot sustain any more in the near future because of environmental impacts and depletion of the reserves. On the other hand energy generated from renewable sources is an alternative way for sustainable, feasible and pollution free uses.

Ethiopia is endowed with many rivers and all year round abundant sunlight due to its geographical location in equator. According to recent survey, Ethiopia's annual solar potential is estimated to be over 2 trillion MW hours (Zegeye et al., 2014). The potential irrigable land of the basin is only 2.64%; and the gross hydro-electric potential of the basin is found to be 800 GWh/year. The water resources of the basin have enough potential for irrigation, hydropower and domestic water supply (Hulluka et al., 2023).

Because Ethiopia does not produce oil, it must rapidly develop its industrial economy to fulfill this aim. The farm segment leads the Ethiopian investment, accounting for 47.7% of the overall growth development program, with 13.3% from industries and 39% from commerce. However, farming is the most important sector, and Ethiopia practices local farming irrigation (Zegeye et al., 2014).

Ethiopian has recently assessed that around 11 mega hectares is appropriate for irrigation, with groundwater accounting for 48% of the total. According to the compatibility maps and current land use data, 18% (3.74 million ha) of Ethiopia irrigated rain-fed land would be appropriate for a solar photovoltaic watering system (Otoo et al., 2018).

For instance, while components like pump can last a year from 5-15, solar cells can last 20-25 years, and control panels usually have a lifespan of about seven years. Solar photovoltaic systems are highly durable. In contrast, around 20% of hand pumps was malfunctioned within less than one year after installation. They have a drawback in running high maintenance costs, unreliable fuel supply, and causes to environmental pollution (Zadi and Bamford, 2016).

A study conducted in Ethiopia for irrigation purposes of potato crops using ground water with a renewable energy of solar PV system indicated that, water pumping with solar system is better prime chance in terms of solar accessibility, carbon release control, and economic effectiveness (Nasir, 2016). On the other hand, in the Indian Himalayan region the performance of DC solar pumping showed that, a variation in pumping efficiencies and overall efficiency between directly measured and PVsyst simulated is 47.7% and 22.1%, respectively (Chandel et al., 2017).

This research aims to compare the size, experimental inquiry, and economics of solar photovoltaic devices and gasoline engine pump systems in outdoor conditions in Dugda wereda, in Oromia regional state for tomato crop irrigation. This place is approximately 8 km east of Meki town and 140 km northeast of Addis Ababa.

## MATERIALS and METHODS

### Study Area

The Central Rift Valley (CRV) lake basin system is part of the Main Ethiopian Rift (MER) that includes four presentday enduring lakes, Zeway, Langano, Abijata, and Shalla; and a tectonically controlled endorheic basin. The study was bounded by  $7^{\circ} 00' 56''$  to  $8^{\circ} 28' 8''$  N latitude and  $38^{\circ} 03' 38''$  to  $39^{\circ} 24' 48''$  E longitude.

The rift valley has a wide-range socio-economic and ecology amenities. In terms of area coverage, 76.8% of its part is dominantly under rain-fed farming. Irrigated farming covers <3% of the basin. About 44% of the existing irrigated areas depend on surface water from streams. Moreover, 31% pumps uses directly from Lake Zeway, and about 25% from groundwater ([Hulluka \*et al.\*, 2023](#)). The overall shallow water resource of the rift valley lake basin is estimated at just over 5.6 billion  $\text{m}^3 \text{ year}^{-1}$  and the predicted groundwater potential of the basin is 0.1 billion  $\text{m}^3 \text{ year}^{-1}$ .

This system was designed and tested with the stated ranges of central rift valley area of Dugda wereda in specific geographical coordinates, Latitude= $8.13^{\circ}$ N and  $38.81^{\circ}$ E, and an altitude of 1644 m.a.s.l. Ethiopia has a great daily solar potential of receiving 5000-7000  $\text{Wh m}^{-2}$  on PV tilt surfaces ([Zegeye \*et al.\*, 2014](#)).

### Test Condition of the System

The system was composed of a PV power generator of 150 watt power submersible helical pump PS2-100 AHRP-23S, an Apogee data acquisition system linked to a laptop, an IR thermometer temperature sensor, a hygrometer for humidity measurement, a clamp meter for measuring the current and voltage, and water flow rate directly to the plastic container. All this data has been obtained based on the maximum water requirement of the worst irrigation months ([Zaki and Eskander, 1996](#)). Accordingly, the current study is conducted between the months of February and May 2021 to evaluate the implications of pump heads on solar pump capacities.

It was tested at four pump heads of 10, 12, 15, and 18 m using a submersible pump (PS2-100 AHRP 23S) for deep good purposes. The effect of head on the operation of solar photovoltaic pumping systems was investigated and economically evaluated against the conventional diesel power system.

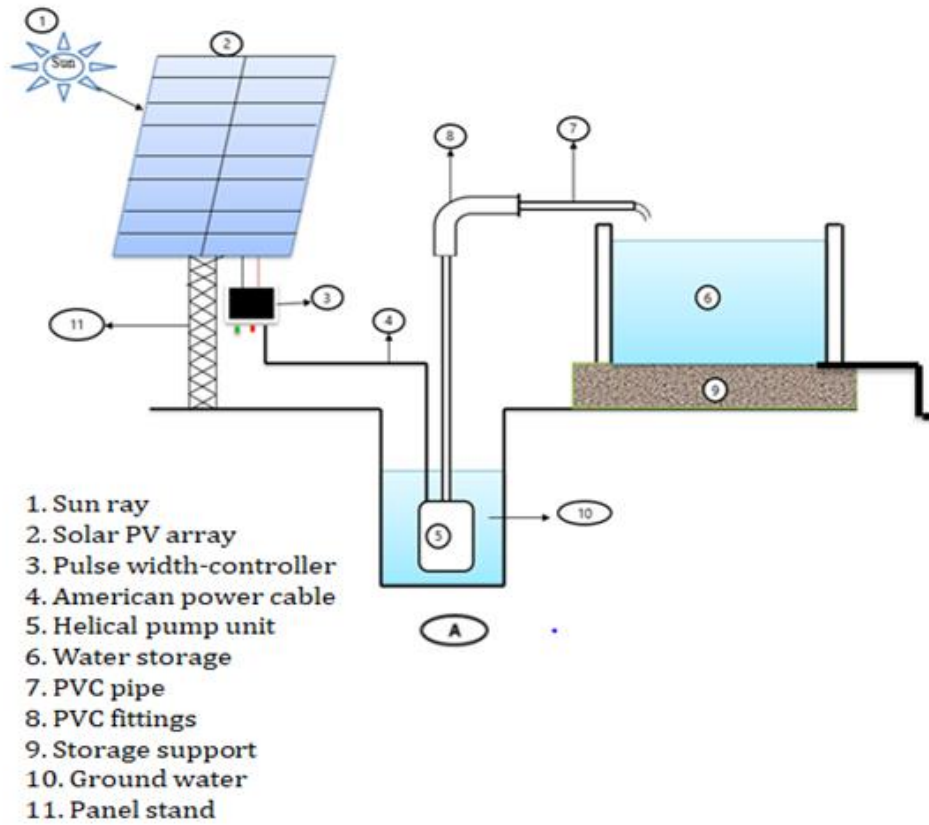


Figure 1. Solar PV pumping system schematics.

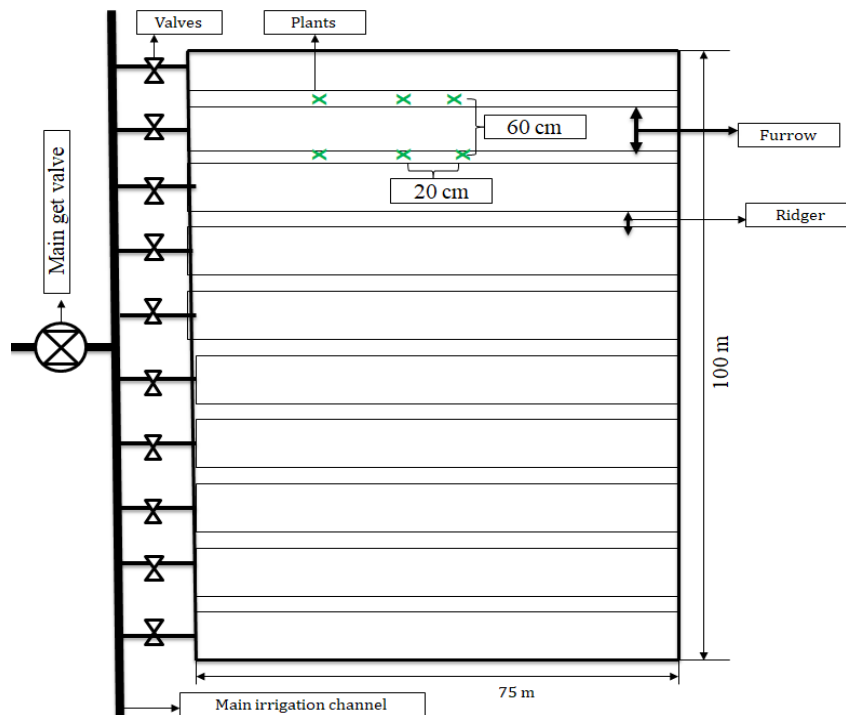


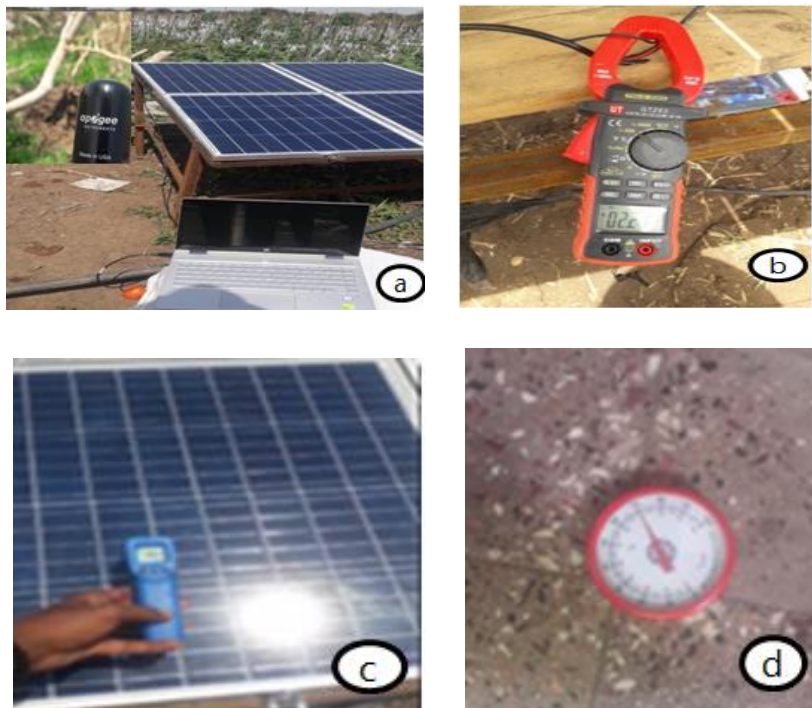
Figure 2. Irrigation system and planting layouts.

Figure 1 shows that solar photovoltaic water pumping system schematic diagrams which includes, solar panel, controller, pump, water storage, pipes with fittings, panel stand, and storage support. Again Figure 2 describes that, the irrigation system layout as per the standards.



**Figure 3.** Photographs during experiemntal testing.

As shown in Figure 3, each photograph indicates overall system installation, submersible pump testing, and measurements tools taken during experiemnt test. And, Figure 4 shows that, different measuring instruments used during data collection such as; a. Apogee instrument for measuring solar intensity b. clamp meter for measuring V and I c. IR-thermometer for measuring temperature d. hygrometer used to measure humidity.



**Figure 4.** Instruments used during data records.

### Determining the Maximum Crop Water Requirement

To determine the maximum water requirement, one has to be prior to calculate evapotranspiration ( $ET_o$ ). If it is in the extreme climatic condition of the Blaney-Criddle method, estimated as 52% (inaccurate, dry, and sunny areas), it is assumed to be 40% for humid areas.

$$ET_o = p (0.46T_{mean} + 8) \quad (1)$$

$$ET_c = K_c \times ET_o \quad (2)$$

$$ET_c = 5.75 \text{ mm day}^{-1}$$

Through this, the eventual water requirements for the specific crop will be calculated using Equation 3.

$$W_r = \frac{\text{crop area} \times ET_c \times W_c}{E_u} \quad (3)$$

$$W_r = 17.4 \text{ m}^3 \cdot \text{day}^{-1}$$

Where,

$ET_o$ , Evapotranspiration,  $\text{mm day}^{-1}$ ,  $T_{mean}$ , daily average temperature,  $23.9^\circ\text{C}$  p, average of day fraction of yearly period in hours taken as 28% for latitude angle of  $8.13^\circ$  for the specific Equation 1 the value for  $ET_o$  was about  $5 \text{ mm day}^{-1}$ ,  $W_r$ , Irrigation demand of water,  $\text{m}^3 \text{ day}^{-1}$ , irrigated space,  $\text{m}^2$ ,  $K_c$ , coefficient of a specific crop,  $ET_c$ , evapotranspiration,  $\text{mm day}^{-1}$ ,  $W_c$ , percentage of wetted space,  $E_u$ , uniformity emission.

According to [Foster et al. \(2001\)](#), the percentage of wetted area is assumed be depending on the crop type; and the percentage of uniformity emission ([Gouws and Lukhwareni, 2012](#)).

### Irrigation scheduling

The basic thing of an irrigation system is just scheduling before water deficiency arises. This will control when and how much water is applied. This depends on the water holding capacity of the loam soil type, with an average value of about  $80 \text{ mm m}^{-1}$  ([Nasir, 2016](#)).

The maximum irrigation interval of tomato crops can be determined using [Maughan et al. \(2015\)](#). Accordingly, the average root depth ([Villalobos and Fereres, 2016](#)) and is calculated at about three days.

$$\text{Maximum irrigation interval} = \frac{H_w \times D_r \times D_a}{ET_c} \quad (4)$$

### The Design of Flow Rate

According to the specific location obtained by inserting into CROPWAT software, the reasonable peak daily sun hours of the month was about eight hour per day. The discharge flow rate can be obtained as follows,

$$Q = \frac{W_r}{n_{PSH}} \quad (5)$$

$$Q = 2 \cdot 175 \text{ m}^3 \text{ h}^{-1}$$

Where,

$W_r$ , Water absorption capacity,  $\text{mm m}^{-1}$ ,  $D_r$ ,  $D_a$ , acceptable depletion for tomato crops the percentage of permissible allowable depletion available moisture in the soil with insignificant yield (Morales et al., 2010).

$Q$ , discharge rate,  $\text{m}^3 \text{ h}^{-1}$ ,  $n_{PSH}$ , Net peak sun hours, hour

### Determination of Hydraulic Energy

The hydraulic energy at the outlet of the pump could be calculated using (Gouws and Lukhwareni, 2012).

$$P_h = \frac{\rho \times g \times W_r \times H}{3.6 \times 10^6 (\text{J} \cdot \text{kWh}^{-1})} \quad (6)$$

$$\eta_{pm} = \frac{P_h}{P_{EL}} \quad (7)$$

$P_{el}$  is motor power

$P_h$ , hydraulic power required ( $\text{kWh day}^{-1}$ ),  $W_r$ , water demand,  $\text{m}^3 \text{ day}^{-1}$ ,  $H$ , dynamic head, in meter,  $\rho$ , water density,  $1000 \text{ kg day}^{-1}$ ,  $g$ , gravity,  $\text{m s}^{-2}$ .

Again calculating the power motor for the pump by considering the normal working condition of pump to be 0.57 (Nasir, 2016).

### Solar PV Power Requirements

In determining the better possible tilt angle of a PV panel, which would be a non-adjustable PV panel and to collect the greatest year-round solar radiation energy, it should be inclined on the way to the southern side similar to the latitude axis in order to obtain the most year-round solar radiation energy (Sass et al., 2020).

Determine the required solar array peak power produced using the relation of the average solar radiation based on incident solar radiance at STC, A.M 1.5, cell temperature  $25^\circ\text{C}$ , and with a panel area of  $1.3 \text{ m}^2$  (Elrefai et al., 2016).

$$P_{PV} = \frac{P_h}{F * G} \times 1000 \text{ W m}^{-2} \quad (8)$$

$$\eta_{PV} = \frac{P_{PV}}{G \times A_{array}} \quad (9)$$

Where,

$\eta_{PV}$ , solar module efficiency,  $A_{array}$ , area of solar panel,  $\text{m}^2$ .

$P_{PV}$ , peak solar power produced, watt,  $F$ , percentage of mismatch factor (0.8),  $G$ , average monthly solar radiation based on worst moth of irrigation  $5.33 \text{ kWh m}^{-2} \text{ day}^{-1}$ . Calculating the solar PV panel efficiency using the formula (Osaretin, 2016).

$\eta_{pm}$ , Motor pump efficiency,  $P_{EL}$ , electrical power produced from the panel, W.

**Table 1.** PV panel and pump specifications.

Specifications	
<b>1. Solar panels</b>	<b>PV Panel: OPES 36CPdef</b>
<b>Modules, number</b>	<b>4</b>
Total ultimate produced power, watt	200
Open voltage, voltage	45.22
Nominal volt, $V_{mc}$	36.66
Short current, $I_{sc}$ , ampere	2.94
Open circuit current, $I_{mp}$ , ampere	2.73
<b>2. Pump</b>	<b>PS2-100 AHRP-23S</b>
The maximum head, m	18
Flow rate, $m^3 h^{-1}$	2.8
The aximum pump efficiency, %	57

Table 1 shows that the overall specifications of photovoltaic panel and submersible pumps. It is as per the manufacturers manual of power rated, open & nominal voltage, short & open circuits, maximum head, pump efficiency, and flow rate.

### Statistical Analysis

Statistical computing (ANOVA) and graphics were performed using open-source integrated development environment for R-4.0.2 programming language software. When the treatment effects were found significant, the least significance difference test was performed to assess the difference among the treatments at 5% significance.

## RESULTS and DISCUSSION

The amount of discharged water is primarily determined by the pumping head and the hourly radiation from the sun. Evaluations of solar photovoltaic systems at various heads and irradianations have been conducted using the obtained experimental results and optimized photovoltaic module array. There are various characteristics that determine the performance of the solar photovoltaic pump system, but the most essential are heads, discharge rate, peak power, and solar radiation.

The following data shows; the measured hourly solar radiation (directly measured using Apogee instrument) from 9:00 am to 5:00 pm, and designates that there have been no significant variations between the sample days of April month.



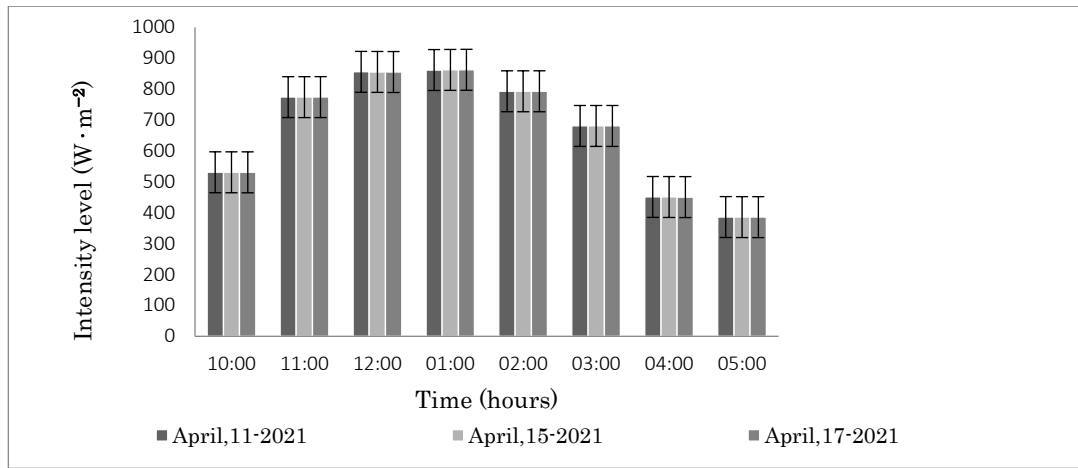


Figure 5. Average hourly solar radiation for different sample days.

Figure 5 shows that, data has been taken for different three days with in the maximum crop demand months. Accordingly, there no significance variation in solar intensity of different days but, it has much more variation in between hours. The maximum peak power produced (solar intensity produced) was in the mid-day time of 12:00 am to 1:00 pm and the solar intensity level ranges from 855 to 862 W m<sup>-2</sup> respectively. Again, the minimum solar intensity was in the late after-noon at 5:00 pm is about 385.7 W m<sup>-2</sup> and in the morning time the mean hourly solar irradiance was measured about 530 W m<sup>-2</sup>.

**PVsystr Simulated Analysis of Photovoltaic Panel**

The specific site data recorded using the, PVsystr 7.1 system energy tool were used to generate a simulation report for the specific photovoltaic array illustrated in Figure 6 using parallel and series adjacent connections (2S\*2P).To produce a single solar module with a power variation from 19 watt to 100 watt power, the current (I) and voltage (V) will occurred due to variation of incident irradiancies.

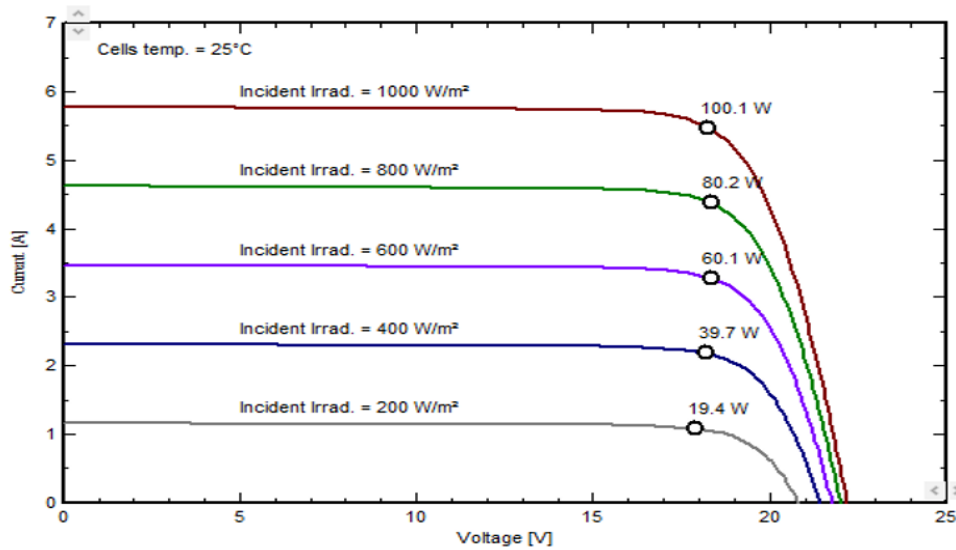
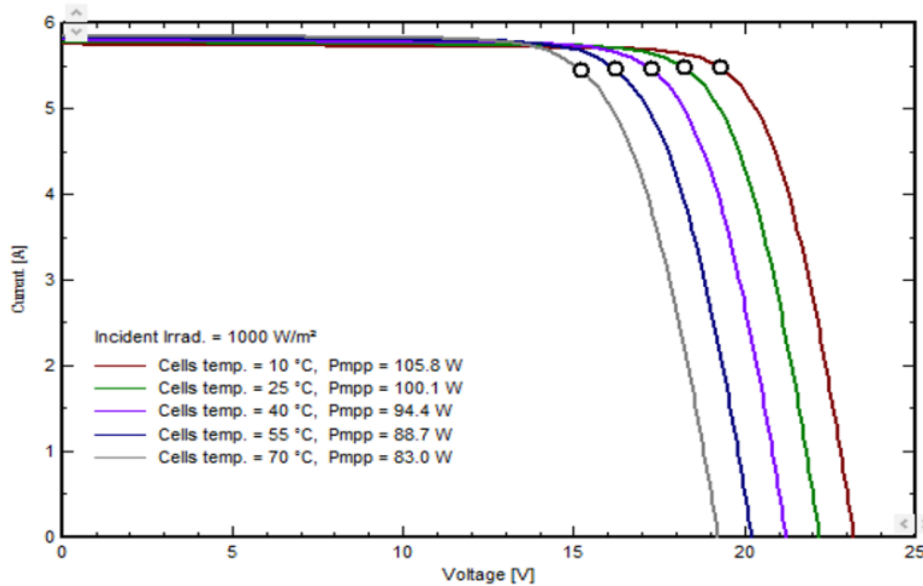


Figure 6. I-V characteristics curves with different irradiance levels.

Figure 6 I-V model curve shows for a constant cell temperature of 25°C, at various solar irradiation levels the short circuit current increases in proportion to the solar incident while open circuit voltage logarithmically with solar radiation. As long as curved portions in the figure show that the I-V does not intersect the short circuit current is proportional to incident irradiation. On the other hand, if the incident irradiance is assumed to be persistent spectral scatterings the short circuit current can be used as extent to incident irradiances.



**Figure 7.** I-V characteristics curves at different temperature.

I-V characteristics curves both for incident irradiance and temperatures were showed in Figure 7. It has been perceived that the temperature linearly decreased the produced voltage as compared to current. Subsequently, the maximum power point of photovoltaic module decreases as the voltage decreases with a constant solar irradiance. Though, the effect of temperature is lesser on short circuit current but upturns with increase in incident solar irradiance.

Figure 8 illustrated those P-V curve features for different solar irradiances at fixed cell temperature of 25°Cs. It was founded that, as increase in solar irradiance and open circuit voltage the power also increases.

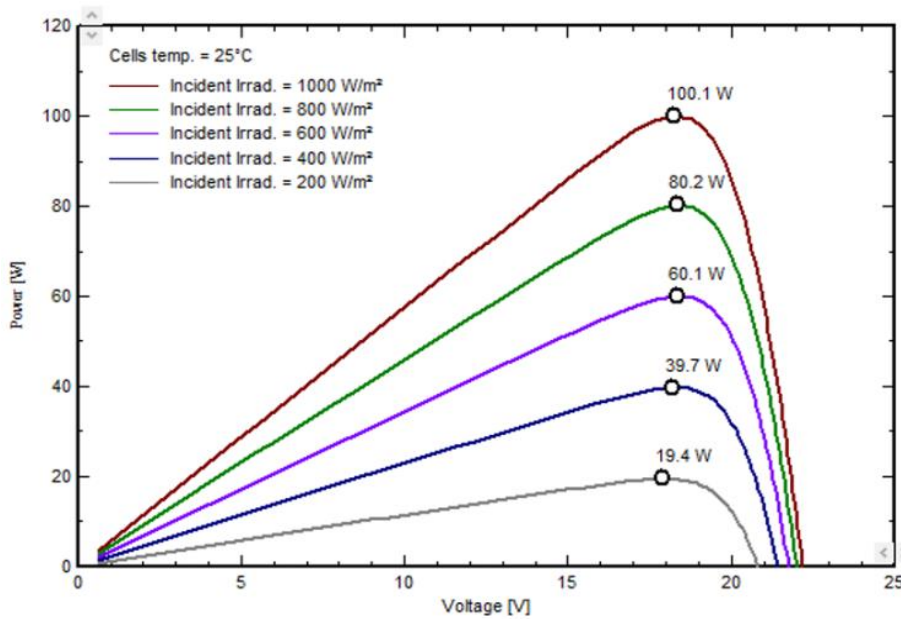


Figure 8. P-V characteristics curve at different set of incident radiations.

### Effects of Solar Radiation

In practical situations, it is difficult to obtain  $1000 \text{ W m}^{-2}$ , as a result, research is required to determine the most effective pumping operations for specific levels of radiation.

According to the experiment test results, the solar radiation is dynamically affected by the time of each hour. The correlation model indicated that solar radiation significantly affected the flow rate at each different head level ( $P < 0.05$ ). The best-fit equation of each level head is presented here in Figure 9. It can be seen that the pump discharge rates rise exponentially with the rising solar radiation. It could be concluded that, at the same level of irradiance the flow rate decreases with increasing each head levels.

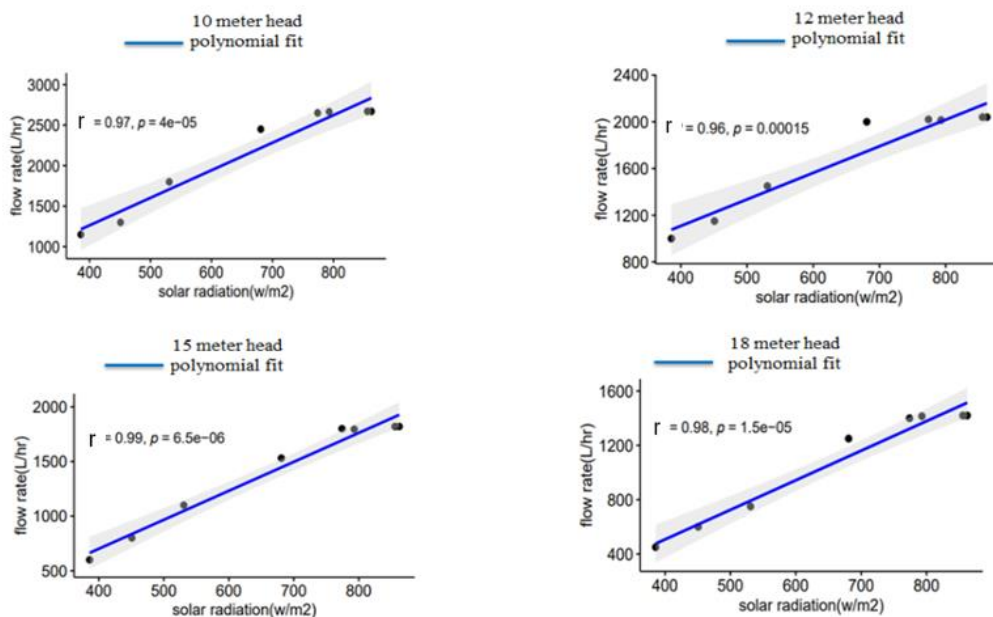


Figure 9. Discharge versus solar radiation at different head levels.

The data collected from the field experiment test of Table 2 showed that, the flow rate in each group also varied significantly in dependent with solar intensity. Also, the flow rate of the pump at different levels of head varies when the solar radiation varies from 385.8-862.2  $\text{W m}^{-2}$ . The minimum and maximum flow rate obtained at 10 m head is 1150 and 2670  $\text{L h}^{-1}$  with the respective solar intensity of 385.8 and 862.2  $\text{W m}^{-2}$ .

**Table 2.** Discharge of solar pump system at various heads and solar radiations.

Head level (m)	Discharge flow ( $\text{L h}^{-1}$ ) At 385.8 ( $\text{W m}^{-2}$ )	Discharge flow ( $\text{L h}^{-1}$ ) At 862.2 ( $\text{W m}^{-2}$ )
10	1150	2670
12	1000	2040
15	600	1820
18	450	1420

### Effects of Time on Hourly Solar Radiation

Figure 10 shows that, the hourly solar radiation produced by the PV array versus time, where the input power to the pump has gained a minimum level in the morning and afternoon time and a maximum result at the mid-day time, similar result to that of power vs. time.

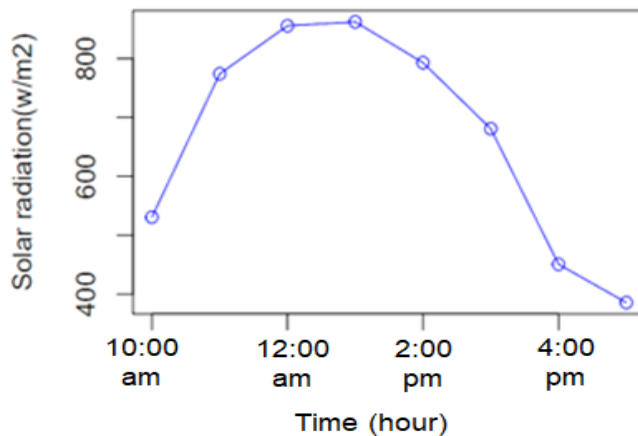


**Figure 10.** Panel output power obtained on an hourly basis.

Visualize the best fit equation and correlation effects between different heads on flow rate, the pump efficiency, and total system efficiency.

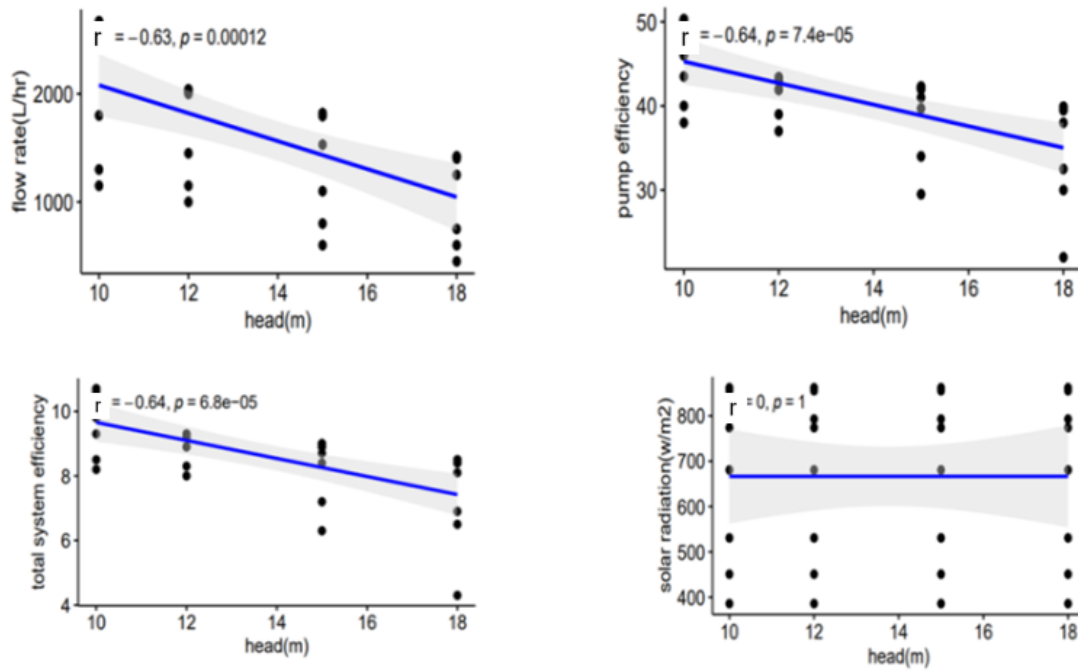


Figure 11. Correlation effects of head in various dependent variables.

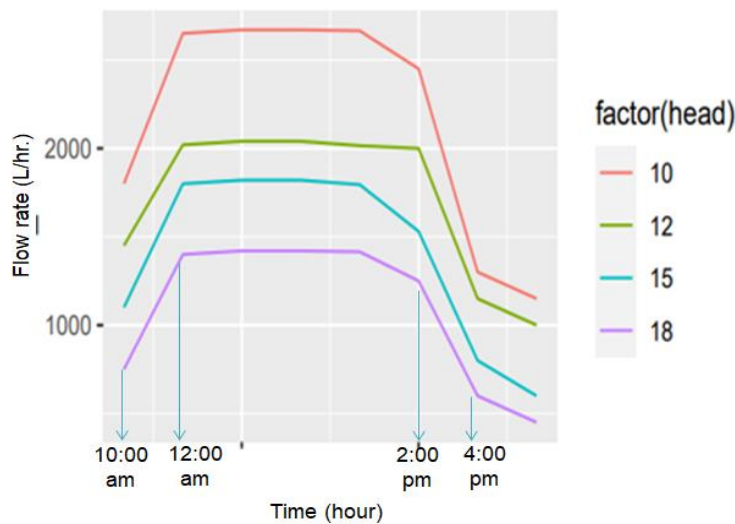
The pump power varies every hour of the day. It increases during the morning hours, rapidly peaks in the middle of the day, and rapidly declines in the late afternoon. The pump and overall system performance are reduced for all pump head.

Table 3. Mean and level of significance of dependent variables at various heads.

Head (m)	Mean flow rate (L h <sup>-1</sup> )	Mean pump efficiency (%)	Mean of total system efficiency (%)
10	2169.38 <sup>a</sup>	46.04 <sup>a</sup>	9.8 <sup>a</sup>
12	1714.38 <sup>ab</sup>	41.59 <sup>ab</sup>	8.89 <sup>ab</sup>
15	1408.13 <sup>bc</sup>	39.10 <sup>bc</sup>	8.3b <sup>c</sup>
18	1088.13 <sup>c</sup>	35.16 <sup>c</sup>	7.45 <sup>c</sup>

Means results by the similar words superscript were not predominantly affected and alpha level=0.05, and letters “a, ab, bc, and c” indicate that the level of average mean followed by the same letters is not significantly different.

The working time significantly affects the overall capacity of the photovoltaic pump. As mentioned in Table 3 above, the data collected and analyzed using ANOVA for the mean and significance effects. Table 3 shows that, the mean pump efficiency and total system efficiency operating at 10 m head were 46.04% and 9.8% respectively. Again, at 10 meter head, the mean hourly flow rate was obtained 2169.38 L h<sup>-1</sup>. The reason for the lower pump efficiency at 18 m head is due to the lower underutilization of limited power produced by the solar photovoltaic array.



**Figure 12.** Flow rate variation on an hourly basis at varying head.

From the experiment test result obtained, for different pumping heads and pumping time, the result shows there was a variation in flow rate. Figure 12 illustrated that, the flow rate increases gradually somehow remains constant during midday as well as rapidly decline later after 3:00 pm. This result shows that, the flow rate decreases with increasing in pumping head proportionally.

### Economic Comparisons Between Photovoltaic and Diesel Pumps

For this analysis, it should achieve an economic evaluation and compare solar PV with existing diesel-pumping system technology for the feasibility study. The economic evaluation is accompanied by investment cost, lifetime cycle cost, energy cost, as well as consistent profitability per the determined volume of water.

The assessment for diesel-pumping system information is gathered from the end users/ farmer field. The 6.7 Hp power diesel pump was tested within eight operating hours per day, and its initial cost with its component was (ETB) 26000. Obtained from the field-test result, the diesel pump has a fuel consumption of  $0.8 \text{ L h}^{-1}$ , and its volume of water pumping capacity is about  $6 \text{ m}^3 \text{ h}^{-1}$ .

The following mathematical equation can be used to determine lifecycle expense analysis (Maughan et al., 2015).

$$LCC=CC+MC+EC+RC-SC \quad (10)$$

Where;

$CC$  stands for initial cost,  $MC$  stands for cost of maintenance,  $EC$  stands for fuel costs,  $RC$  stands for replacement value, and  $SC$  stands for recovery cost.

The following major assumption factors have been considered to be needed for an optimum cost analysis of the photovoltaic water pumping system using (Narale et al., 2013) and (Park, 2013).

- The operating life of the PV panel and solar pump has been considered twenty and ten-years, respectively.

- The operational cost for a solar photovoltaic pump system is supposed to 0.1% of its investment across a year.
- The operational cost for the engine generator is supposed to 10% of the investment charge.
- The recovery price a solar pump is 5% of its overall original procuring charge.
- The specific area-based accessibility of sunlight days was measured to be 2920 h per year.
- The repairing charge of engines is expected to be 10% of the overall investment charge in year
- The recovery charge of diesel pumping was presumed to be 20% of its investment value, and it is replaced every 10 years.

According to [Girma et al. \(2015\)](#) financial comparisons were made between solar photovoltaic and diesel pumping systems for ground water use of 20 years life cycle. It was analyzed using life cycle cost analysis in different areas of Siadberand Wayu in Amhara, Wolmera in Oromia, and Enderta in Tigray regions. The findings, using life cycle cost analysis for solar photovoltaic and diesel generator pump systems were \$ 1295.66 and \$ 7812 respectively. Again, the cost of pumped water (\$ m<sup>-3</sup>) were 0.1, 0.16, & 0.16 and 0.2, 0.23, and 0.27 for each respective regions of pumping systems. Based on the variation of life cycle cost comparisons made, PV water pumping was economically feasible than diesel pumping system.

**Table 4.** System cost comparison using life cycle cost analysis.

No.	Cost types (ETB)	The cost of solar PV system	The cost of diesel engine system
1	Capital cost (CC)	117780	26000
2	Maintenance cost (MC)	2332.04	52000
3	Fuel/energy cost (EC)	None	1244160
4	Replacement cost (RC)	46000	52000
5	Total cost	166112.04	1374160
	Salvage cost (SC)	5889	5200
	Life cycle cost (LCC)	172001.04	1379360

### Cash Flow

It is important to consider the net present value of money as an option for worth economic comparison. Just using an economic equivalent to some present and future amount can be expressed using the following relations ([Girma et al., 2015](#)).

$$F = P (1 + i)^N \quad (11)$$

Where,

$F$ -Future value

$P$  Present value

$N$ -years, and  $i$ -rate of interest

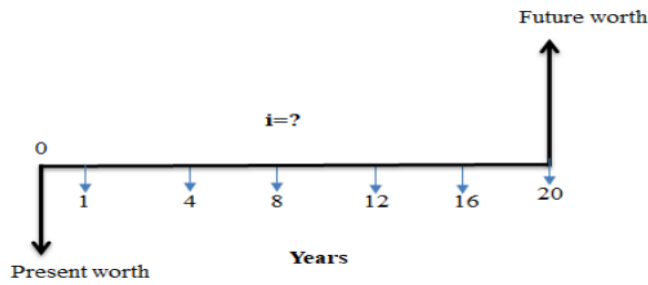


Figure 13. Cash flow diagram.

Table 4 indicates that, the solar photovoltaic pumps have higher initial investment costs than diesel pumping systems. But, other costs (maintenance, operation, and replacement) were significantly lower than those of the diesel pumping system. Additionally, there is no energy cost needed for the solar pump and the solar-driven pump has more reliability and long-term life. Diesel pumps have higher total cost as compared to solar photovoltaic system. From the results, about 85% of the life cycle cost for the diesel pump is fuel cost, and this shows that the pump charge in the extended life for the system is due to energy cost, unless the initial and other costs during the operation were very low. The economic comparison result between solar and diesel water pumping systems has a cost of water 1.3 (ETB) m<sup>-3</sup>, and 3 (ETB) m<sup>-3</sup> respectively, using life cycle cost analysis for 20 years.

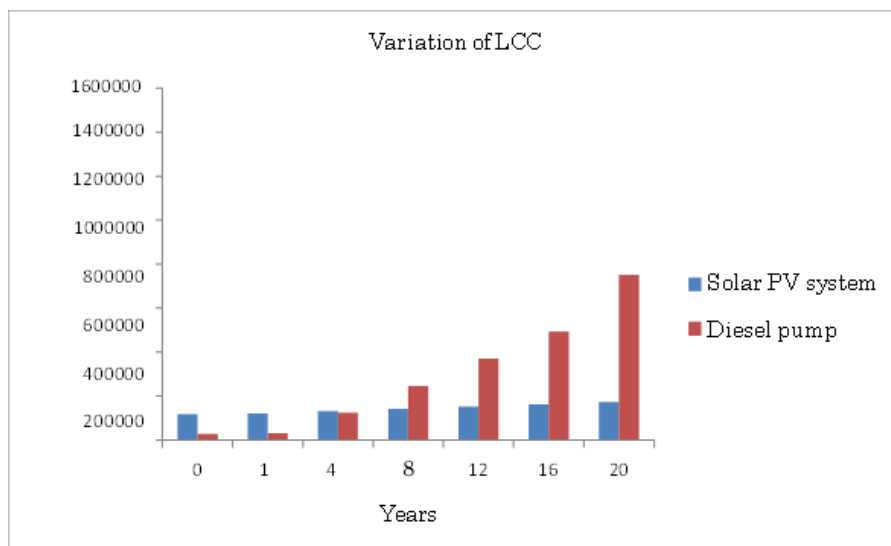


Figure 14. Variation of cash flow life cycle cost for solar photovoltaic and diesel pumps.

### The Cost of Pumped Water

The cost of water pumping for both diesel and solar pumps can be calculated using the annuity technique of LCC analysis (Narale et al., 2013).

$$\text{Water cost} = \frac{\text{Annual period series scheme}}{\text{Overall discharged water}} \tag{12}$$



By considering the total life cost of solar PV, diesel engine pumping systems were about ETB 172001.04 and 1379360, respectively. Accounting for the life cycle time of twenty years, an average twelve-month PV pump has about ETB 8600 with a monthly cost of about ETB 716.67, and the cost of pumped water ( $\text{m}^3$ ) is about  $1.3 \text{ birr m}^{-3}$ . Also, for the diesel-pumping system, the average yearly value cost was calculated as ETB 68968, and its monthly cost is ETB of 5747.33. The cost to pump water using DP system was 3 Birr  $\text{m}^{-3}$ , which is three times as costly as a solar PV pumping system to pump a unit volume of water.

## CONCLUSION

Through the performance of market-available direct-coupled solar pump systems, this paper studied the economic feasibility of the existing engine pumping system. These results have been investigated through operation in the actual and under conditions of the Dugda site. Evaluations have been conducted under four different levels of the head (10 m, 12 m, 15 m, and 18 m) on a sunny day. Heads and solar intensity at hourly bases can be determined flow rate of the solar photovoltaic pumps. The designed photovoltaic pump was accomplished by watering 0.75 hectares of tomato for eight hours with the cost of pumped water 3 ETB  $\text{m}^{-3}$ . From the evaluation results, the maximum daily water requirement was about  $2.169 \text{ m}^3 \text{ h}^{-1}$  at 10 m head. If it rises to of 18 m, the average flow rate reduces to  $1.088 \text{ m}^3 \text{ h}^{-1}$  with the irrigation area less than  $1/3 \text{ ha}$  of tomato farm. The best pump and total system efficiencies is in 10 m head is about 46.04% and 9.8% respectively. Hereafter, it can be decided that time has a significant influencing on solar radiation, dominantly influencing the overall efficiency of PV system. It is summarized that for locations representing central rift valley of Ethiopia, solar pump systems could size as per irradiance range  $385.8\text{-}862.2 \text{ W m}^{-2}$ . Using life cycle cost analysis with durations of twenty years, the life cycle cost of solar system was cost-ineffective than diesel-pump system. The study shows that, watering of vegetables through solar photovoltaic pump systems is a valuable again fit for extended reserves in contrast to a diesel generator. For the future, it is advantageous to model the system using internet of things for better efficient improvements. Therefore, governmental and non-governmental institutions could access to loan and create awareness about the technology.

## DECLARATION OF COMPETING INTEREST

The authors declare that they have no conflict of interest.

## CREDIT AUTHORSHIP CONTRIBUTION STATEMENT

**Maney Ayalew Desta:** Investigation, formal analysis, writing original draft, and conceptualization,

**Getachew Shunki Tiba:** Validation, review,

**Mubarek Mohammed Issa:** Visualization, paper editing,

**Wariso Heyi:** Data collection, paper editing.

## ETHICS COMMITTEE DECISION

This article does not require any ethical committee decision.

## REFERENCES

- Benghanem M, Daffallah O, Alamri N and Joraid A (2014). Effect of pumping head on solar water pumping system. *Energy Conversion and Management*, 77: 334-339.
- Chande S, Naik N and Chandel R (2017). Review of performance studies of direct coupled photovoltaic water pumping systems, a case study. *Renewable Sustainable Energy Reviews*, 76: 163-175.
- Elrefai M and Hamdy R (2016). *Design and performance evaluation of a solar water pumping system: A case study*. Eighteenth International Middle East Power Systems Conference (MEPCON).
- Foster R, Argaw N, and Ellis A (2001). Renewable energy for water pumping applications in rural villages: period of performance. April 1, 2001-September 1, 2001. United States: N. p., 2003. Web. <https://doi.org/10.2172/15004054>
- Girma M, Assefa A and Molinas M (2015). Feasibility study of a solar photovoltaic water pumping system for rural Ethiopia. *AIMS Environmental Science*, 2(32): 697-717.
- Gouws R and Lukhwareni T (2012). Factors influencing the performance and efficiency of solar water pumping systems : A review. *International Journal of Physical Sciences*, 7(48): 69-80.
- Hartung H and Pluschke L (2018). The benefits and risks of solar powered irrigation-a global review. Food and Agricultural Organization.
- Hulluka TA, Balcha SK, Yohannes B, Bantider A and Negatu A (2023). Review: Groundwater research in the Ethiopian Rift Valley Lakes region. *Frontiers in Water*, 5: 819568.
- Maughan T, Drost D and Allen N (2015). Vegetable irrigation; Sweet pepper and sizing and testing of solar photovoltaic water pumping system for irrigation purposes tomato. *Horticulture*, 3: 1-5.
- Morales D and Busch J (2010). Design of small photovoltaic solar-powered water pump systems', United States Department Agriculture and Natural resources Conservation Service.
- Narale P, Rathore S and Kothari S (2013). Study of solar pv water pumping system for irrigation of horticulture crops. *International Journal of Engineering Science Invention*, 2(12): 54-60.
- Nasir A (2016). *Design, simulation and analysis of photovoltaic water pumping system for irrigation of a potato farm at Gerenbo*. Masters Thesis, Addis Ababa Institute of Technology School of Graduate Studies School of Mechanical and Industrial Engineering, p.98.
- Osaretin A and Edeko F (2016). Design and implementation of a solar charge controller with variable output. *Journal of Electrical and Electronic Engineering*, 12(2): 40-50.
- Otoo M, Lefore N, Schmitter P, Barron J and Gebregziabher G (2018). Business model scenarios and suitability: smallholder solar pump-based irrigation in Ethiopia. Agricultural Water Management- Making a Business Case for Smallholders.
- Park S (2013). Fundamentals of engineering economics. Pearson International Edition, England.
- Sass J and Hahn A (2020). Solar Powered Irrigation Systems (SPIS), Deutsche Gesellschaft für Internationale Zusammenarbeit (GIZ) GmbH, Bonn.
- Villalobos J and Fereres E (2016). Principles of Agronomy for Sustainable Agriculture, Springer, Switzerland.
- Zadi D and Bamford E (2016). Scaling up solar powered water supply systems: A review of experiences, UNICEF.
- Zaki M and Eskander N (1996). Matching of photovoltaic motor-pump systems for maximum efficiency operation. *Renewable Energy*, 7(3): 279-288.
- Zegeye M, Tadiwos T and Aman A (2014). Optimal sizing of solar water pumping system for small scale irrigation : Case study of Dangila. *International Journal of Sustainable and Green Energy*, 3(5): 99-107.



## Mathematically Predicting the Performance Rate of Plow-Type Trenchless Machine

Mohamed GHONIMY<sup>a\*</sup>

<sup>a</sup>Department of Plant Production and Protection, College of Agriculture and Veterinary Medicine, Qassim University, P.O.Box 6622, Buraydah, Al-Qassim 51452, SAUDI ARABIA; Agricultural Engineering Dept., Faculty of Agriculture, Cairo University, Giza, EGYPT

(\*): Corresponding Author: [mohamed.ghonimy@agr.cu.edu.eg](mailto:mohamed.ghonimy@agr.cu.edu.eg)

Received: 21.02.2023

Article Info  
Accepted: 29.05.2023

Published: 30.06.2023

### ABSTRACT

*This research was aimed to identify the main factors that influence the performance rate of plow-type trenchless machine and mathematically correlate these variables to predict performance rate. The mathematical analysis ended with an equation correlating the performance rate with the factors affecting it. The derived relationship was checked in various operational circumstances. The performance rate's practical experiments revealed that only for the 0.92 and 0.76 m disturbed soil depths, respectively, did the theoretical performance rate variation from the actual performance rate range from -3.0 to -0.7%. Also, for the 0.92 and 0.76 m disturbed soil depth, respectively, the field efficiency of plow type trenchless machine ranged from 49.7 to 45.4%. The novelty and innovativeness of this article is in the use of an analytical method to deduce a mathematical equation that can predict the performance rate; in determining the actual factors affecting the performance rate of plow type trenchless machine.*

**Keywords:** *Mathematical analysis, Modeling, Performance rate, Plow, Trenchless*

**To cite:** Ghonimy M (2023). Mathematically Predicting The Performance Rate of Plow-Type Trenchless Machine. *Turkish Journal of Agricultural Engineering Research (TURKAGER)*, 4(1): 91-103. <https://doi.org/10.46592/turkager.1254292>

### INTRODUCTION

To maintain the ideal soil moisture-air balance for the crop that is growing, drainage in agriculture refers to the process of removing free water from soil that is present in the root zone of plants above the field capacity. The water excess is removed by a subsurface pipe drainage system placed at a suitable slope and depth to help get rid of the excess water which is drained to an open channel drain



© Publisher: Ebubekir Altuntas. This is an Open Access article and is licensed (CC-BY-NC-4.0) under a Creative Commons Attribution 4.0 International License.

([Rokochinskiy et al., 2019](#)). Trenching machines typically come in three different types; plow type, wheel type, and chain type trenching machines, which vary in their design and methods of operation ([Islam et al., 2019](#)).

The advantage of a trenching machine is its high-performance rate due to it digs the trench, installs the drainage pipes, and, in the case of a plow type, it also fills the ditches with soil. In other words, the machine carries out its' entire task at the same time. It is distinguished by its great level of accuracy when placing the pipes at the necessary depth and slop. There are a number of obvious advantages when contrasting the trenching machine with other excavating machinery. A more precise control of trench depth and width is provided by the trenching machine, which enables a significantly greater output rate ([Naghshbandi et al., 2021](#)). However, due to the inherited characteristics of the machine itself, trenching machines' efficiency and output rates are generally regarded as low compared to other types of agricultural equipment. Most of the attempts to boost the productivity and efficiency of trenching machines were a trial and error types of attempts, and only a small number of early researches relied on descriptive analysis of variables influencing the effectiveness and performance of trenching machines. According to [Sitorus et al. \(2016\)](#), the three most important elements affecting the power and speed of digging machines are the trench depth and width, machine forward speed, and uniaxial compressive strength. Some mathematical models were used to describe the performance of the trenching machines. [Ghonimy et al. \(2022\)](#) concluded that the theoretical excavation force calculated by the mathematical model was lower than the actual excavating force by 4.0 kN and 3.5 kN for the 1.2 m and 1.5 m trench depths, respectively, for chain-type trenching equipment. And at trench depths of 1.2 m and 1.5 m, respectively, the theoretical excavation power was lower than the actual excavating power by 3.8% and 2.8%. [Diep \(2017\)](#) linked a number of digging unit specifications, such as the cutting assembly's angle, the distance between teeth, the speed of the tangential teeth, and the forward speed to the chain trenching machine's chipping depth. [Reddy and Shailesh \(2018\)](#) performed a study to find how long a bucket tooth on a backhoe digger would last. They observed that the costs related to the product lifecycle might be significantly reduced through computer-aided engineering (CAE). [Ghonimy \(2021\)](#) found that the machine chain-type trenching machine field efficiency ranged from 46.7 to 57% for the 150.7 cm and 120.7 cm trench depths, respectively. The goal of this research was to identify the main factors that influence the performance rate of plow-type trenchless machine and to mathematically correlate these variables to predict performance rate.

## MATERIALS and METHODS

### Approach of the Mathematical Analysis

The rate of performance of plow-type trenchless machine depends on the trencher's forward speed, trenching width, and field efficiency. The machine's forward speed is correlated with the size of the power source and the amount of power used to operate it. Thus, the mathematical analysis relied on the mathematical relationship which related the tractor brake power and each of the forward speeds and the total forces acting on the plow-type trenchless machine during field operation. Equation 1 allows the estimation of the highest forward speed of the machine ([Revenko et al., 2022](#)) as

well as the performance rate of plow-type trenchless machines by correlating the size of the power source with the overall amount of power necessary for machine functioning.

$$P_b = P_c + P_r + P_i + P_s + P_t \pm P_a + P_n \quad (1)$$

Where:  $P_b$  is the tractor brake power, kW;  $P_c$  is the required power to overcome cutting resistance, kW;  $P_r$  is the required power to overcome rolling resistance, kW;  $P_i$  is the power necessary to overcome the resistance of the soil surface slope, kW;  $P_s$  is the lost power in slipping, kW;  $P_t$  is the transmission systems lost power, kW;  $P_a$  is the required power to confrontation air resistance, kW;  $P_n$  is necessary power for the trenchless machine to reach its operational speed because of its inertia, kW.

Since the forward speed of plow-type trenchless machine during operation was so low in comparison to other moving trucks, both  $P_a$  and  $P_n$  were disregarded. Thus, Equation 1 could be simplified to Equation 2:

$$P_b = P_c + P_r + P_i + P_s + P_t \quad (2)$$

### Construction and Mechanical Theory of the Plowing Unit of Plow-type Trenchless Machine

Figure (1) showed the plowing unit of the plow-type trenchless machine. Its consists of a cutting blade with an attached pipe chute. The cutting blade moves horizontally at a velocity ( $V_m$ ) in the same forward direction of the trenching machine. The cutting edge starts vertically in front of the blade shank and extends to the plow bottom to a depth ( $d$ ). The performance theory of this type of the trenchless machine is that, while the machine travels horizontally at a speed ( $V_m$ ), the cutting edge of the blade causes fracturing of the soil. The shank pushes the soil, creating fracture lines from the trench bed to the surface Figure 2. The wedge-shaped fractures of the soil are lifted upwards without reaching the surface. Through the lifting and fracturing of the soil, impermeable layers are lastingly destroyed. These fracture lines create easy access for the flow of water to the subsurface drainage pipes. The pushing and lifting action of the shank prevents soil compaction.

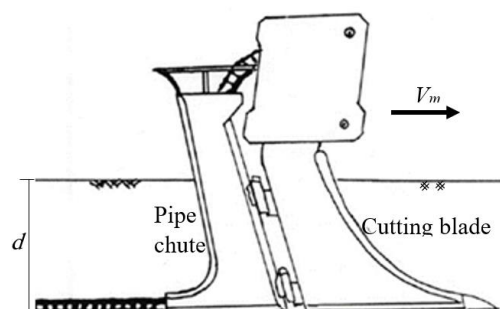


**Figure 1.** The mechanism of the plow-type trenchless machine.

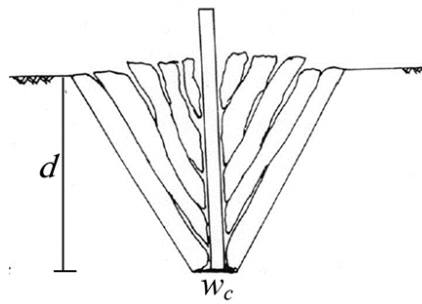


**Figure 2.** The wedge-shaped fractures of the soil due to the plow-type trenchless machine action.

### Factors Impacting the Plow-type Trenchless Machine's Performance Rate

The performance rate of plow-type trenchless machinery is affected by variety of factors. These factors can be divided into two categories; **soil factors** which encompass; unit draft of soil ( $U$ ),  $N\ m^{-2}$ , specific weight of soil ( $\omega$ ),  $N\ m^{-3}$ , coefficients of friction between soil and soil ( $f_{ss}$ ) and between metal and soil ( $f_{ms}$ ), inclination angle of soil surface with the horizontal direction ( $\psi$ ), degree, and coefficient of rolling resistance ( $RR$ ). **Machine factors**; which encompass; weight of tractor and machine ( $W_m$ ),  $N$ , brake power of tractor ( $P_b$ ),  $kW$ , trench cutting width ( $w_c$ ),  $m$ , machine forward speed ( $V_m$ ),  $m\ s^{-1}$ , vertical cutting depth ( $d$ ),  $m$ , tractor transmission efficiency ( $\eta_t$ ), slip ratio of the tractor contact device with the ground ( $S$ ), and field efficiency ( $\eta_f$ ).

To make mathematical manipulation easier, several presumptions and simplifications were made. These simplifications were constant unit draft of soil, homogeneous and isotropic soil, and constants of machine forward speed, and disturbed soil depth.

### Mathematical Analysis Steps

Equation 3 was used to calculate the theoretical performance rate ( $PR_{th}$ ) of the plow-type trenchless machine according to (Ghonimy, 2021):

$$PR_{th} = 60 \times V_m \times \eta_f \quad (3)$$

Where:

$PR_{th}$  = theoretical performance rate,  $m\ min^{-1}$ ;

$V_m$  = forward speed of plow-type trenchless machine,  $m\ s^{-1}$ ;

$\eta_f$  = the field efficiency, decimal.

The parts of Equation 2 were obtained as the following in order to determine the value of  $V_m$ .

#### a) Determination of $P_c$

The required power to overcome cutting resistance ( $P_c$ ), Equation 4, depends on the cutting force ( $F_c$ ) and the machine forward speed ( $V_m$ ) (Ranjbarian, et al., 2017).

$$P_c = 0.001 \cdot F_c \cdot V_m \quad (4)$$

$$F_c = U \cdot A \quad (\text{Ghonimy, 2021}) \quad (5)$$

Referring to Figure 3, the cross-section area ( $A$ ) of the disturbed soil due to cutting can be calculated as follows:

$$A = d^2 \cdot \left( \frac{w_c}{d} + \frac{1}{\tan \theta} \right) \quad (6)$$

Thus,

$$F_c = K^* \cdot U \cdot d^2 \cdot \left( \frac{w_c}{d} + \frac{1}{\tan \theta} \right) \quad (7)$$

Where:  $F_c$  is the cutting force, N;  $K^*$  is the dimensionless coefficient =  $\frac{U^*}{U}$ ;  $U^*$  is the unit draft of soil including the friction forces acting on bucket metal during cutting, N m<sup>-2</sup>;  $U$  is the unit draft of soil, N m<sup>-2</sup>;  $U^* = K^* \cdot U$ ;  $d$  is disturbed soil depth, m;  $w_c$  is the cutting width, m;  $\theta$  is the soil shear angle, degree =  $\frac{\pi}{2} - \left( \frac{\beta + \zeta + \phi}{2} \right)$ , (Equation 8) according to [Das and Luo \(2016\)](#);  $\beta$  is the tool cutting angle, degree;  $\zeta$  is the metal soil friction angle, degree; =  $\tan^{-1} \left( \frac{\tan \phi}{2} \right)$ , (Equation 9), according to [Das and Luo \(2016\)](#);  $\phi$  is the internal soil friction angle, degree; = 12 degree for clay soil.

Substituting from Equation 7 into Equation 4 gives:

$$P_c = 0.001 V_m \cdot K^* \cdot U \cdot d^2 \cdot \left( \frac{w_c}{d} + \frac{1}{\tan \theta} \right) \quad (10)$$

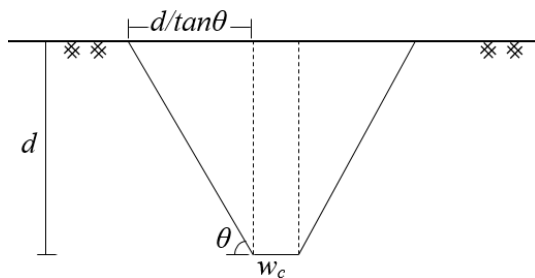


**Figure 3.** Cross sectional area of the disturbed soil.

There is a draft force on the shank of the plow due to the effect of the friction of the cut soil on it. However, this draft resisting force was included in the unit draft ( $U^*$ ) used in the analysis. This resisting draft force on the shank depends on many factors such as the repose angle ( $\epsilon$ ) of the pulverized soil, the friction coefficient ( $f_{ss}$ ) between soil and soil, the friction coefficient ( $f_{ms}$ ) between soil and metal, and the width of the plow shank.

Referring to Figure 4, the weight of the disturbed soil ( $W^*$ ) by the plow action can be calculated as:

$$W^* = w_{sh} \cdot \omega \cdot d^2 \cdot \left( \frac{w_c}{d} + \frac{1}{\tan \theta} \right) \quad (11)$$

Where,  $w_{sh}$  is the shank width in meter.

Referring to Figure 4, weight of this disturbed soil causes a resisting draft force on both sides of the plow shank as shown in Figure 4. The inclined resultant force ( $F_{rt}$ ) acting on one side of the shank is:

$$F_{rt} = \frac{W^*}{2} \cdot (\sin \epsilon - f_{ss} \cdot \cos \epsilon) \quad (12)$$

The resisting friction force ( $F_{rs}$ ) acting on the shank is:

$$F_{rs} = f_{ms} \cdot w_{sh} \cdot \omega \cdot d^2 \cdot \cos \epsilon \cdot \left( \frac{w_c}{d} + \frac{1}{\tan \theta} \right) \cdot (\sin \epsilon - f_{ss} \cdot \cos \epsilon) \quad (13)$$

When substituting reasonable values for the parameters in Equation 13, the magnitude of the draft resisting force will be very limited compared with the force needed for cutting, and it can be ignored.

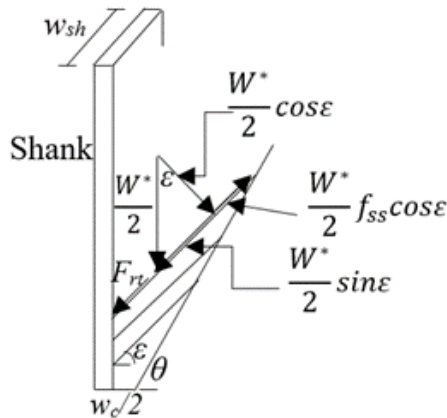


**Figure 4.** The normal force acting on the shank of the plow.

#### a) Determination of $P_r$

The required power to overcome rolling resistance ( $P_r$ ) was calculated from Equation 14 (Srivastava *et al.*, 2006; Kepner *et al.*, 2017).

$$P_r = 0.001 F_r \cdot V_m \quad (14)$$

$$F_r = RR \cdot \cos \psi \cdot (W_m + F_{cv}) \quad (15)$$

Where:

$F_r$  = The resistance force due to rolling, N;

$W_m$  = Tractor and machine weight, N;

$RR$  = Rolling resistance coefficient;

$F_{cv}$  = The vertical component of the cutting force;

$\psi$  = The inclination angle of soil surface with the horizontal direction, degree.

Referring to Figure 5, the  $F_{cv}$  was calculated as follows

$$F_{cv} = F_c \cdot \tan \theta = K^* \cdot U \cdot d^2 \cdot \left( 1 + \frac{w_c \cdot \tan \theta}{d} \right) \quad (16)$$

Substituting from Equation 16 into Equation 15 gives:

$$F_r = RR \cdot \cos \psi \cdot \left( W_m + K^* \cdot U \cdot d^2 \cdot \left( 1 + \frac{w_c \cdot \tan \theta}{d} \right) \right) \quad (17)$$



Substituting from Equation 17 into Equation 14 gives:

$$P_r = 0.001 V_m \cdot RR \cdot \cos\psi \cdot \left[ W_m + K^* \cdot U \cdot d^2 \cdot \left( 1 + \frac{w_c \cdot \tan\theta}{d} \right) \right] \quad (18)$$

#### b) Determination of $P_i$

The  $P_i$ , Equation 19, depends on the machine weight ( $W_m$ ), the machine forward speed ( $V_m$ ), and the angle ( $\psi$ ) between the inclined soil surface and the horizontal direction ([Kepner et al., 2017](#)).

$$P_i = 0.001 W_m \cdot \sin\psi \cdot V_m \quad (19)$$

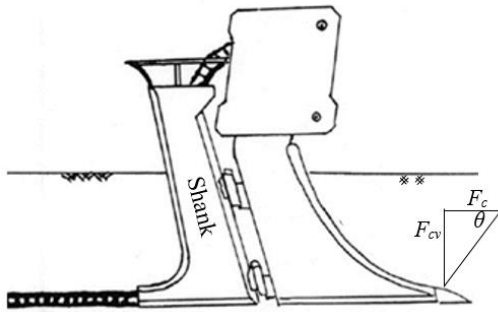


**Figure 5.** The component of the cutting force acting vertically on the share for the plow.

#### c) Determination of $P_s$

The power lost in slipping ( $P_s$ ) and loss in machine speed due slippage ( $V_s$ ) are calculated from Equations 20 and 21 ([Baek et al., 2022](#))

$$P_s = 0.001 F_s \cdot V_s = 0.001 (F_c + F_r) \cdot V_s \quad (20)$$

Where  $P_s$  is the power lost in slip resistance,  $F_c$  is the cutting force,  $F_r$  is the resistance force due to rolling and  $V_s$  is the loss in machine speed due slippage ( $S$ ).

$$V_s = \left( \frac{S}{100-S} \right) \cdot V_m \quad (21)$$

Substituting from Equations 7, 17, and 21 into Equation 20 gives:

$$P_s = 0.001 \left( \frac{S}{100-S} \cdot V_m \right) \cdot \left[ K^* \cdot U \cdot d^2 \cdot \left( \frac{w_t}{d} + \frac{1}{\tan\theta} \right) + RR \cdot \cos\psi \cdot \left[ W_m + K^* \cdot U \cdot d^2 \cdot \left( 1 + \frac{w_c \cdot \tan\theta}{d} \right) \right] \right] \quad (22)$$

#### d) Determination of $P_t$

The  $P_t$  was calculated from Equation 23 according to [Srivastava et al. \(2006\)](#) and [Kepner et al. \(2017\)](#) as follows:

$$P_t = P_b \cdot (1 - \eta_t) \quad (23)$$

Where,  $\eta_t$  is the machine transmission efficiency.

From Equations 2, 10, 18, 19, 22 and 23;

$$\begin{aligned}
1000P_b \cdot \eta_t &= V_m \cdot \left\{ K^* \cdot U \cdot d^2 \cdot \left( \frac{w_c}{d} + \frac{1}{\tan \theta} \right) + RR \cdot \cos \psi \cdot \left[ W_m + K^* \cdot U \cdot d^2 \cdot \left( 1 + \frac{w_c \cdot \tan \theta}{d} \right) \right] \right. \\
&\quad + W_m \cdot \sin \psi \\
&\quad + \left( \frac{S}{100 - S} \right) \cdot \left[ K^* \cdot U \cdot d^2 \cdot \left( \frac{w_c}{d} + \frac{1}{\tan \theta} \right) \right. \\
&\quad \left. \left. + RR \cdot \cos \psi \cdot \left( W_m + K^* \cdot U \cdot d^2 \cdot \left( 1 + \frac{w_c \cdot \tan \theta}{d} \right) \right) \right] \right\} \\
1000P_b \cdot \eta_t &= V_m \cdot \left( \frac{100}{100 - S} \right) \cdot \left\{ \left[ K^* \cdot U \cdot d^2 \cdot \left( 1 + \frac{w_c \cdot \tan \theta}{d} \right) \cdot \left( \frac{1}{\tan \theta} + RR \cdot \cos \psi \right) \right] + \left[ W_m \cdot \left( RR \cdot \cos \psi + \right. \right. \right. \\
&\quad \left. \left. \left. \sin \psi \cdot \frac{S}{100 - S} \right) \right] \right\} \tag{24}
\end{aligned}$$

**Solving for  $V_m$ :**

$$V_m = \frac{1000P_b \cdot \eta_t}{F_t} \tag{25}$$

$$\begin{aligned}
F_t &= \left( \frac{100}{100 - S} \right) \cdot \left\{ \left[ K^* \cdot U \cdot d^2 \cdot \left( 1 + \frac{w_c \cdot \tan \theta}{d} \right) \cdot \left( \frac{1}{\tan \theta} + RR \cdot \cos \psi \right) \right] + \left[ W_m \cdot \left( RR \cdot \cos \psi + \right. \right. \right. \\
&\quad \left. \left. \left. \sin \psi \cdot \frac{100 - S}{100} \right) \right] \right\}, \text{ N.} \tag{26}
\end{aligned}$$

Using Equations 3, and 23, the actual performance rate of the machine ( $PR$ ) can be obtained as follows:

$$PR_{th} = 6 \times 10^4 \times \frac{P_b}{F_t} \times \eta_t \times \eta_f \tag{27}$$

Where:  $PR_{th}$  is the theoretical machine performance rate ( $\text{m min}^{-1}$ ),  $P_b$  is the tractor brake power (kW),  $\eta_t$  is the transmission efficiency,  $\eta_f$  is the field efficiency,  $F_t$  is total forces affecting the trenchless machine (N),  $S$  is the loss in machine speed due to slippage (%),  $K^*$  is the dimensionless coefficient,  $U$  is the unit draft of soil ( $\text{N m}^{-2}$ ),  $d$  is disturbed soil depth (m),  $w_c$  is the cutting width (m),  $\theta$  is the soil shear angle (degree),  $RR$  is the rolling resistance coefficient,  $\psi$  is the angle between inclined soil surface and the horizontal direction (degree), and  $W_m$  is the tractor and machine weight (N).

Experiments work is the second step of this scientific approach's plan. This experimental work is considered as a way to validate Equation 27.

### Field Experimental Work

The plow-type trenchless machine (Figure 6) was tested in two experimental areas in Beheira Governorate, Egypt. Table 1 shows the specifications of the tractor and machine used. The plow-type trenchless machine was tested at two disturbed soil depths 0.75, and 0.90 m for first and second site respectively.



**Figure 6.** Plow-type trenchless machine.

**Table 1.** Technical specifications of the machine and tractor

Plow model	Soil Max Zd Plow Tilling
Boot, mm	101.6, 152.4, and 203.2
Machine weight, daN	275
Ploughing depth, mm	Up to 1250
Blade Length, mm	965
Blade width, mm	190
Tractor model	CaseIH MX230
Factory	Racine, Wisconsin, USA
Chassis	4WD
Weight, daN	8935
Height, m	3.16
Gears	18 forward and 4 reverse
Brake power, kW	174.5
Power at PTO, kW	141.7
Power at Drawbar, kW	123.2
Transmission efficiency, %	70.5

## Measurements and Calculations

### Soil texture and physical properties

Some of the soil's mechanical and physical characteristics, which were listed in Equation 27, were determined in this research work.

### Unit draft of soil ( $U$ )

The average value of soil unit draft was taken  $10 \text{ N cm}^{-2}$  according to [Jia et al. \(2018\)](#).

### Rolling resistance coefficient ( $RR$ )

The values of rolling resistance coefficient ( $RR$ ) ranged between 3.0 and 5.0% according to [Jia et al. \(2018\)](#). Thus, it was taken the experimental field's average  $RR$  4.0%

**Dimensionless coefficient ( $K^*$ )**

The value of  $K^*$  was taken as 9 since it was found ranging between 5 to 15 (Ghonimy, 2021).

**Soil shear angle ( $\theta$ )**

The  $\theta$  angle was calculated from Equation 8.

**Disturbed soil depth ( $d$ )**

Five trenches with three measurements each were used to measure the average disturbed soil depth for two experimental sites.

**Slip percentage ( $S$ )**

The  $S$  of the traction device was calculated from Equation 28, (Baek et al., 2022)

$$S = \frac{D_1 - D_2}{D_1} \times 100 \quad (28)$$

Where:  $D_1$  is the distance travelled by the machine with no load as the tracks had three complete rotations (m), and  $D_2$  is the distance travelled by the machine with a load as the tracks had three complete rotations (m).

**Machine weight ( $W_m$ ) and transmission efficiency ( $\eta_t$ )**

The  $W_m$  and  $\eta_t$  were taken from specification catalogue.

**The machine field efficiency ( $\eta_f$ )**

The  $\eta_f$  was calculated from Equation 29.

$$\eta_f = \frac{\text{net excavating time}}{\text{total time}} \times 100 \quad (29)$$

**RESULTS AND DISCUSSION****Soil Particle Size Distribution and Texture**

The average values of soil texture for two experimental areas are shown in Table 2.

**Table 2.** Soil mechanical analysis and texture for field experiments.

Operating depth, m	Particle size distribution (%)			Texture class
	Sand	Silt	Clay	
0.76	19.2	27.1	53.7	clay
0.92	17.7	27.3	55.0	Clay

**Field measurements**

Table 3 shows the average values of field measurements.

**Table 3.** Average values of field measurements for plow-type trenchless machine.

Nominal disturbed soil depth, m	0.75		0.90	
Field measurements	Average	SD	Average	SD
$d$ , m	0.76	+0.02	0.92	+0.04
$w_c$ , m	0.323	+0.04	0.323	+0.04
$S$ , %	5.00	---	5.00	---
$RR$ , %	4.00	---	4.00	---
$U$ , $N m^{-2}$	100000	---	100000	---
$K^*$	9.00	---	9.00	---
$\theta$ , degree	80	---	80	---
$W_m$ , $N$	92100	---	92100	---
$\phi$ , degree	0.00	---	0.00	---

$d$  = Disturbed soil depth,  $w_c$  = cutting width,  $S$  = slip percentage,  $RR$  = traction rolling resistance,  $U$  = unit draft of soil,  $K^*$  = a dimensionless coefficient,  $\theta$  = soil shear angle,  $W_m$  = tractor and machine weight,  $\psi$  = inclination angle of soil surface with the horizontal direction.

### Actual Performance Rate ( $PR$ ) and Field Efficiency ( $\eta_f$ )

Table (4) shows the average values of the breakdown items of the daily machine time, machine performance rate ( $PR$ ), and field efficiency ( $\eta_f$ ) as they were really observed in the field. It is evident that the average  $PR$  values were 13.6 and 10.1  $m \min^{-1}$  for disturbed soil depths of 0.76 and 0.92 m, respectively, while the  $\eta_f$  values were 54.4 and 49.7% for disturbed soil depths of 0.76 and 0.92 m, respectively. The field results showed decrease (about 50%) in the field efficiency of the plow-type trenchless machine due to the low of speed operation to control the depth and slope of the pipe drain that have been installed. These results were similar to those found by Ghonimy (2021); Ghonimy et al. (2023). Ghonimy (2021) indicated that the chain-type trenching machine's field efficiency ranged from 46.7 to 57% for the 150.7 cm and 120.7 cm trench depths, respectively. Also, Ghonimy et al. (2023) found that the wheel-type trenching machine field efficiency ranged from 43.0 to 50.1% for the 90.5 cm and 60.4 cm trench depths, respectively.

**Table 4.** Breakdown of the plow-type trenchless machine's daily machine item, performance rate, and field efficiency.

Activities	*Average consumed time, $\min \text{ day}^{-1}$		SD, $\min \text{ day}^{-1}$	
	Disturbed soil depth, m		Disturbed soil depth, m	
	0.76	0.92	0.76	0.92
Net installed time	286	252	6.17	4.22
Turning and travelling to start digging another trench	60	63	0.62	1.51
Setup time for reaching the depth	30	42	2.42	2.65
Rest periods	75	75	2.36	3.74
Field quick maintenances	30	35	1.82	1.23
Refill of fuel tank	25	25	3.27	2.54
Other lost time	20	15	2.65	3.72
Average total time, $\min \text{ day}^{-1}$	526	507	8.33	12.36
**Total installed length, $m \text{ day}^{-1}$	7153	5100	5.87	6.17
Actual performance rate, $m \text{ min}^{-1}$	13.6	10.1	0.12	1.12
*** Field efficiency, %	54.4	49.7	1.65	2.33

\* Average value of ten estimates, each for a different operating day.

\*\*Average value ( $m \text{ day}^{-1}$ ) of the total excavated trench lengths within the ten days period.

\*\*\* Average field efficiency within the ten days period.

**Theoretical Estimation of the Performance Rate of Plow-type Trenchless Machines**  
Equations 26, and 27, which theoretically predicted the performance rate, were used. Table 1 displays the applicable plow-type trenchless machine's specifications (1). Also, the experimental field's measured results are displayed in Table 3.

#### **For 0.76 m disturbed soil depth**

Theoretically,  $13.5 \text{ m min}^{-1}$  was predicted for the  $PR_{th}$  of the plow-type trenchless machine using Equations 26, and 27. This estimate was extremely near to the actual performance rate that was experimentally determined to be  $13.6 \text{ m min}^{-1}$  for the 0.76 m disturbed soil depth. The deviation of predicted for the performance rate from the actual performance rate was only -0.7%.

#### **For 0.92 m disturbed soil depth**

Theoretically, the  $PR_{th}$  of the plow-type trenchless machine was predicted to be  $10.1 \text{ m min}^{-1}$  using Equations 26), and 27. This number was extremely near to the actual performance rate that was experimentally determined to be  $9.8 \text{ m min}^{-1}$  for the 0.92 m disturbed soil depth. The deviation of theoretical prediction of the performance rate from the actual performance rate was only -3.0%. These results were similar to those found by [Ghonimy \(2021\)](#); [Islam et al. \(2019\)](#); [Ghonimy \(2021\)](#) in their study indicated that the chain-type trenching machine's theoretical performance rate was 3.4% and 2% lower than its actual performance rate at disturbed soil depths of 120.7 cm and 150.7 cm, respectively.

## **CONCLUSION**

**The following conclusions can be made:**

1. The predicted performance rate ( $PR_{th}$ ) was  $13.5$  and  $10.1 \text{ m min}^{-1}$  for 0.76 m and 0.92 m disturbed soil depth, respectively. While the actual values of performance rate were  $13.6$  and  $9.8 \text{ m min}^{-1}$  for 0.76 m and 0.92 m disturbed soil depth respectively.
2. The actual field efficiency ( $\eta_f$ ) was 54.4 and 49.7 % for 0.76 m and 0.92 m disturbed soil depth, respectively.
3. The predicted performance rate from the actual performance rate ranged from -3.0 to -0.7 % only for the 0.92 and 0.76 m disturbed soil depth, respectively.

The resultant equation can be used to theoretically predict the performance rate of a plow-type trenchless machine with a high degree of confidence.

## **DECLARATION OF COMPETING INTEREST**

There is no conflict of interest because the manuscript has only one author.

## **CREDIT AUTHORSHIP CONTRIBUTION STATEMENT**

**Mohamed Ghonimy** is responsible for the various parts of this paper including.

## ETHICS COMMITTEE DECISION

This article does not require any ethical committee decision.

## REFERENCES

- Baek SY, Baek SM, Jeon HH, Kim WS, Kim YS, Sim TY, Sim TY, Choi KH, Hong SJ and Kim YJ (2022). Traction performance evaluation of the electric all-wheel-drive tractor. *Sensors*, 22(3): 785. <https://doi.org/10.3390/s22030785>
- Das BM and Luo Z (2016). Principles of soil dynamics. *Cengage Learning*.
- Diep DD (2017). Analysis the factors affecting conveyance rate of unbucket chain trenching machine. In *Agricultural, Forest and Transport Machinery and Technologies*, 4(1): 38-44.
- Ghonimy M (2021). Prediction the performance rate of chain type trenching machine. In *Turkish Journal of Agricultural Engineering Research*, 2(2): 390-402. <https://doi.org/10.46592/turkager.2021.v02i02.012>
- Ghonimy M, Abd El Rahman E and Alzoheiry A (2022). Mathematical prediction of excavating force and power of chain type trenching machine. *Acta Technologica Agriculturae*, 25(4): 197-204. <https://doi.org/10.2478/ata-2022-0029>
- Ghonimy M, Morcos MA, and Badr AE (2023). Mathematical analysis for prediction performance rate of wheel type trenching machine. *Journal of Agricultural Machinery*, 13(1): 1-13. <https://doi.org/10.22067/jam.2021.71081.1049>
- Islam MN, Iqbal MZ, Kabir MSN, Jung KY, Mun DH and Chung SO (2019). Performance evaluation of trenchless subsurface drainage piping machine. *Journal of Biosystems Engineering*, 44(4): 218-225.
- Jia J, Jia and Schmidt (2018). Soil dynamics and foundation modeling. New York: *Springer*.
- Kepner RA, Bainer R and Barger EL (2017). Principles of Farm Machinery. Published by Satish Kumar Jain and produced by Varun Jain for *CBS Publishers & Distributors Pvt. Ltd*.
- Naghshbandi SN, Varga L and Hu Y (2021). Technologies for safe and resilient earthmoving operations: A systematic literature review. *Automation in Construction*, 125: 103632. <https://doi.org/10.1016/j.autcon.2021.103632>
- Ranjbarian S, Askari M, and Jannatkhah J (2017). Performance of tractor and tillage implements in clay soil. *Journal of the Saudi Society of Agricultural Sciences*, 16(2): 154-162. <https://doi.org/10.1016/j.jssas.2015.05.003>
- Reddy Y and Shailesh P (2018). Design and analysis of excavator bucket tooth. In *International Journal of Modern Trends in Engineering and Research*, 5(4): 79-86.
- Revenko VU, Ivanov AB, and Petukhov DA (2022, June). Power balance of all-wheel drive mobile power vehicle. In *IOP Conference Series: Earth and Environmental Science*, 1045(1): 012080. IOP Publishing. <https://doi.org/10.1088/1755-1315/1045/1/012080>
- Rokochinskiy A, Jeznach J, Volk P, Turcheniuk V, Frolenkova N and Koptiuk R (2019). Reclamation projects development improvement technology considering optimization of drained lands water regulation based on BIM. *Przegląd Naukowy. Inżynieria i Kształtowanie Środowiska*, 28(3): 85. <https://doi.org/10.22630/PNIKS.2019.28.3.40>
- Sitorus PE, Ko JH and Kwon OS (2016). Parameter study of chain trenching machines of underwater construction robots via analytical model. In *OCEANS 2016 MTS/IEEE Monterey*. Monterey, CA, USA: IEEE, pp. 1–6. ISBN: 978-1-5090-1537-5. <https://doi.org/10.1109/OCEANS.2016.7761072>
- Srivastava AK, Goering CE, Rohrbach RP and Buckmaster DR (2006). Engineering principles of agricultural machines. 2<sup>nd</sup> ed., pp. i-xiv. St. Joseph, Michigan: ASABE. Copyright 2006 American Society of Agricultural and Biological Engineers, *St. Joseph, Mich.*



Research Article

## Simulation-Optimization Modelling of Yield and Yield Components of Tomato Crop

Nura Jafar SHANONO<sup>a\*</sup>, Lawal AHMAD<sup>b</sup>, Nuraddeen Mukhtar NASIDI<sup>a</sup>,  
Abdul'aziz Nuhu JIBRIL<sup>a</sup>, Mukhtar Nuhu YAHYA<sup>a</sup>

<sup>a</sup>. Department of Agricultural and Environmental Engineering, Bayero University Kano, NIGERIA

<sup>b</sup> Department of Agricultural and Bioenvironmental Engineering, Waziri Umaru Federal Polytechnic, Birnin-Kebbi, NIGERIA

(\*): Corresponding Author: [njshanono.age@buk.edu.ng](mailto:njshanono.age@buk.edu.ng)

Received: 16.04.2023

Article Info  
Accepted: 14.06.2023

Published: 30.06.2023

### ABSTRACT

This study simulate and optimize the yield and yield parameters of tomato using AquaCrop model and genetic algorithm (GA) respectively. The AquaCrop model was firstly calibrated using the data obtained from the field and was later used to simulate the observed yield, water productivity and biomass of tomato. The Root Mean Square Error (RMSE), Coefficient of Residual Mass (CRM) Normalized Root Mean Square Error (NRMSE) and Modelling efficiency (EF) were used to compare the observed and simulated values. The governing equation of AquaCrop simulation software was then optimized using the evolutionary optimization method of GA with MATLAB programming software. All the statistical indices except CRM used in comparing the simulated and observed values indicated good agreement. The CRM values of -0.11, -0.06 and -0.20 were obtained for the yield, biomass and water productivity of tomato which indicated a very slight over-estimation of the observed results by the AquaCrop model. The optimization algorithm terminated when the optimal values of yield and biomass were 4.496 ton ha<sup>-1</sup> and 4.90 ton ha<sup>-1</sup> respectively. The GA revealed that the yield and biomass of tomato can be increased by 57% and 23% respectively if the optimized parameters were either attained on the field experiment or used during simulation. Thus, the study ascertained that crop simulation models such as AquaCrop and optimization algorithms can be used to identify optimal parameters that if maintained on the field could improve the yield of crops such as tomato.

**Keywords:** AquaCrop model, Drip irrigation, Genetic algorithm, Optimization, Simulation, Tomato yield

**To cite:** Shanono NJ, Ahmad L, Nasidi NM, Jibril AN and Yahya MN (2023). Simulation-Optimization Modelling of Yield and Yield Components of Tomato Crop. *Turkish Journal of Agricultural Engineering Research (TURKAGER)*, 4(1), 104-124. <https://doi.org/10.46592/turkager.1283793>





## INTRODUCTION

Sustainable agricultural production of food with the aim to meet the ever-increasing population could be achieved when more food is produced with less water. This can be realized through an optimal irrigation water management ([Shanono \*et al.\*, 2022](#)). In irrigation practice, crop models are important tools developed to improve the efficiency of irrigation systems through water saving and improved water delivery, reduce the operating and labour costs and ensure sustainable agricultural production that will enhance the food security and socio-economic status of the farmers and nation ([Shanono \*et al.\*, 2014](#); [Perea \*et al.\*, 2017](#)). These models simulate the physiological processes of a given crop growth parameter, and matter and water transport, predict yield, and yield components (leaves, roots, and stems) of crop ([Seidel, 2012](#)).

Different crop simulation models have been developed some decades ago coupled with the advances achieved in crop sciences and computing technologies to improve crop productivity ([Shanono, 2019](#); [Reynolds \*et al.\*, 2018](#); [Singels \*et al.\*, 2013](#)). Some of these crops simulation models include the soil vegetation–atmosphere transfer (SVAT) model, AquaCrop model, decision support systems for agrotechnology transfer (DSSAT), the agricultural production systems simulator (APSIM), and Environmental Policy Integrated Climate model (EPIC). These crop simulation models offer the opportunity to investigate the effects of cultivar potential for new areas, droughts and other factors affecting the yield and crop production which will save the energy, water, time and other resources required for experiments ([Kephe \*et al.\*, 2021](#); [Kloss \*et al.\*, 2014](#); [Shanono \*et al.\*, 2012](#)). DSSAT is one of the irrigation simulation models developed to enhance crop water use efficiency. The use of DSSAT in agriculture has increased across the world during the last three decades. The DSSAT has been applied for balancing the water allocation for irrigation and in minimizing pollution while adding value to nutrient-use efficiency ([Ara \*et al.\*, 2021](#)).

[Ko \*et al.\* \(2009\)](#) applied EPIC simulation model in Texas to assess the effect of water consumption variables including crop evapotranspiration (ET<sub>c</sub>) and crop water-use efficiency (WUE) on the yield of maize and cotton. The EPIC was applied to simulate the response of crop yield to various irrigation levels and the results prove EPIC to be a remarkable decision support tool. [Walser \*et al.\* \(2011\)](#) used Soil–Vegetation–Atmosphere Transfer (SVAT) models were used to simulate a rain-out experimental field of wheat and barley to maximize water productivity. The SVAT performed remarkably well to a slightly water-stressed crop. The AquaCrop model stands to be the most popularly known and widely used crop simulation model due to its ease of operation, and high accuracy ([Raes \*et al.\*, 2022](#)). AquaCrop incorporates the effects of various crop production factors including water-stress, salinity, climate, field management and does not consider nutrients cycle or balances to determine soil fertility stress but its expected effects on crop biomass production ([Gaelen \*et al.\*, 2015](#)). AquaCrop has been used widely by different researchers under different climatic and soil conditions and has been confirmed to accurately simulate plant yield, biomass and water productivity ([Bitri \*et al.\*, 2014](#)).

In addition, optimization algorithms are also effective tools for solving problems of irrigation water management ([Jiang \*et al.\*, 2016](#)). The optimization tool describes

and generalizes the irrigation process using a series of mathematical expressions and optimization algorithms to obtain the best results ([Li \*et al.\*, 2020](#); [Singh, 2012](#)). According to [Seidel \(2012\)](#), efficient irrigation water management can further be sustained by optimizing the operational parameters such as irrigation threshold and amount of irrigation water. Water-sharing or scheduling optimization models have been developed, using optimization techniques such as genetic algorithms, and dynamic, linear and non-linear programming ([Li \*et al.\*, 2020](#)). Optimization can change conventional irrigation systems to optimal ones while maintaining high crop yields and ensuring little or no water is lost by deep percolation. Genetic algorithms (GA) is a popular optimization tool used for searching optimum decision results thereby solving diverse challenges that relate to the planning, design and management of resources ([Whitley, 2001](#)). GA is a form of Evolutionary algorithm (EA) that is a well-known device for the effective optimization of irrigation water. Evolutionary algorithms search for the optimum results from the population in parallel but not from a single point ([Ikudayisi and Adeyemo, 2015](#)).

An improved irrigation system that will minimise the inputs while maximizing the output can be best achieved by linking simulation models with optimization algorithms thereby searching optimal results. Studies related to the development and usage of the simulation-optimization approach to the management of drip irrigation are still few ([Akbari \*et al.\*, 2018](#); [McCarthy \*et al.\*, 2013](#)). Most of the experiments carried out to improve water productivity in irrigation systems focused on either simulating or optimizing the system separately but rarely integrate simulation with optimization modelling for crop and water productivity. To this end, this study intends to employ a simulation-optimisation approach to simulate and optimize yield and yield components of tomato for optimum production. Such a study is particularly important for addressing water scarcity in the semi-arid area of northwestern Nigeria which occasionally experiences climatic uncertainties such as drought and erratic rainfall.

## **MATERIALS and METHODS**

### **Study Location and Experimental Set-up**

#### **Study location**

This study was conducted at the training farm of the Department of Agricultural and Environmental Engineering, Bayero University, Kano. Kano is located in the northwestern part of Nigeria and lies between latitude 12° 0' 0.0000" N and longitude 8° 31' 0.0012" E and it is 472.45 m amsl. Kano is situated in a semi-arid zone with an average yearly rainfall of 898 mm which is below the average evaporation of 1560 mm. The average maximum and minimum temperatures are 32°C and 26°C respectively ([Ahmad and Haie, 2018](#); [Lawal and Shanono, 2022](#)).

#### **Experimental set-up**

The field study was carried out from 24<sup>th</sup> February to 31<sup>st</sup> May 2022 on a 3 m × 15 m experimental plot which was divided into two units (UA and UB). The drip system is a gravity-driven irrigation method which consists of 2000 litres (2 m<sup>3</sup>) tank capacity mounted 2 m above the ground connected to the main pipeline which was also connected to the submarine pipeline. The submarine pipeline has 20 junctions and

each junction was connected to a lateral, and the laterals were spaced at 0.75 m apart as recommended row spacing of the tomato crop. Each lateral has a length of 3 m and 9 emitters that are spaced 0.3 m apart based on the recommended crop spacing of the tomato crop. Figure 1 shows the schematic of the experimental plot.

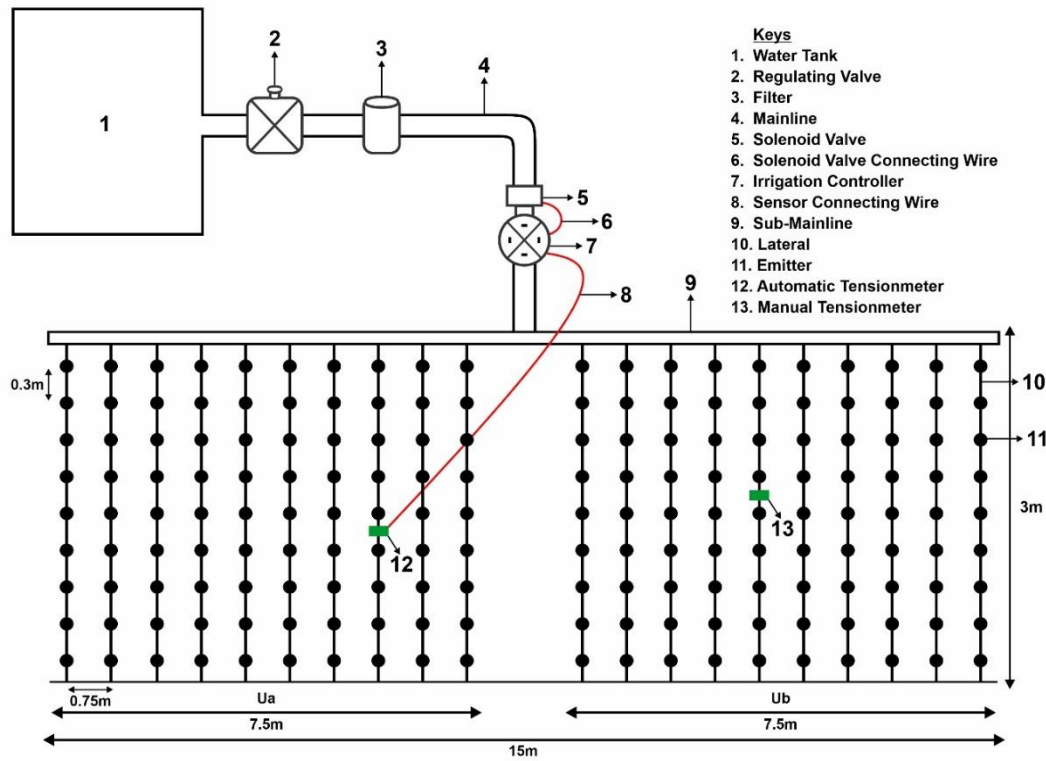


**Figure 1.** The layout of the experimental plot.

### Soil Analysis of the Experimental Site

The soil analyses of the experimental field show that the soil has a textural class of sandy loam (82.4% sand, 4% silt and 13.76% clay) and an average bulk density of  $1.65 \text{ g cm}^{-3}$ . The average soil moisture at saturation, field capacity and the permanent wilting point was found to be 30.09%, 17.77% and 7.48% respectively. The NPK: 15-15-15 fertilizer was applied at the rate of  $250 \text{ kg ha}^{-1}$  as recommended by [Isah et al. \(2014\)](#). The pesticide and fungicide chemicals were applied based on the advice of the experts in the study area. The weeding was also conducted based on the advice of the experienced local farmers in the study area. All other standard agronomic procedures were strictly followed.

### Soil Water Retention Curve for the Experimental Sites

The automatic tensiometer was installed in the experimental plot at a depth of 15 cm and set at -15 kPa and -10 kPa as the lower and upper soil moisture limits respectively for sandy loam soils ([Thompson and Gallardo, 2005](#)). The automatic tensiometer was connected to an irrigation controller that is also connected to the solenoid valve which was installed at the mainline of the experimental field. The manual tensiometer was also installed at depth of 15 cm in the field to serve as a control. Both automatic and manual tensiometers were calibrated by determining the soil moisture using a gravimetric method of the sample taken at the exact depth

of the ceramic tips of the sensors and the results were related to the soil-water characteristic curve of the experimental site. The soil moisture characteristic curve of the experimental site is shown in Figure 2.

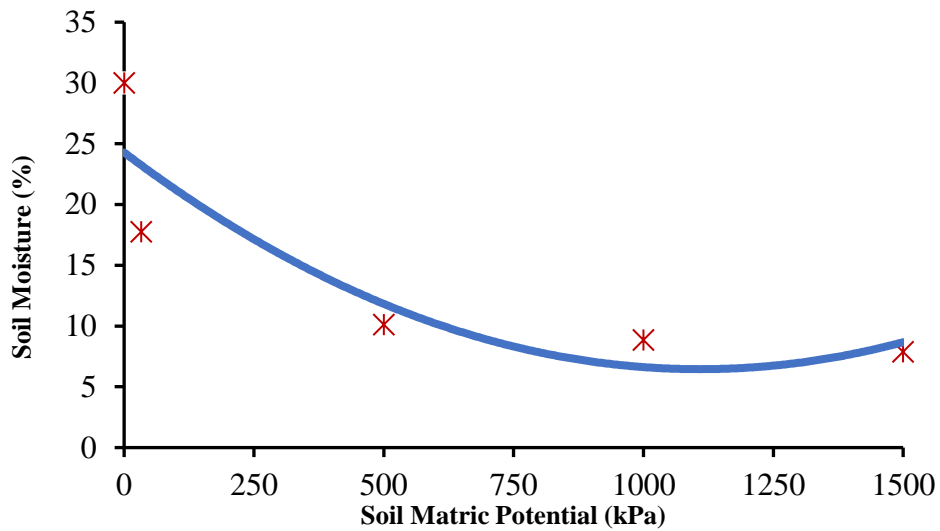


**Figure 2.** Soil water retention curves of the experimental site.

The automatic tensiometer signals the irrigation controller to trigger or interrupt/stop irrigation events based on the set limits and the controller will either open or close the solenoid valve to initiate or suspend the irrigation events. Figure 3, 4, 5 and 6 show the automatic sensor, irrigation controller, solenoid valve and manual tensiometer installed in the experimental plot.



**Figure 3.** Automatic tensiometer.



**Figure 4.** Irrigation controller.



**Figure 5.** Solenoid valve



**Figure 6.** Manual tensiometer

### Yield Measured in the Experimental Site

The yield from the experimental plot ( $Y_e$ ) was measured in both its fresh and dry state. The fresh yield was determined by weighing all the harvested tomato using a weighing scale and divided by the experimental field area ( $\text{kg m}^{-2}$  or  $\text{ton ha}^{-1}$ ). Measurement of dry yields and aboveground biomass were carried out from the plants selected from four laterals of each unit. In each of the selected laterals, three plants were randomly selected and their yields and aboveground biomass were oven-dried at  $70^\circ\text{C}$  for 24 hours. The water productivity ( $WP_e$ ) was computed as the ratio of yield ( $\text{ton ha}^{-1}$ ) to the amount of water applied ( $\text{m}^3$ ).

### Simulation of Yield and Yield Components of Tomato using AquaCrop

#### The AquaCrop

The AquaCrop simulation model was used for the simulation. The model estimates crop yield, crop water requirement, and crop water use efficiency (WUE) in water-stressed conditions. It has also been used under supplementary irrigation and rainfed farming ([Heng \*et al.\*, 2009](#); [Hadebe \*et al.\*, 2017](#)).

#### Calibration of the AquaCrop Model

The AquaCrop model was calibration to account for adjustment of the local varieties or local environmental and management conditions. The parameters for AquaCrop calibrations were divided into two and include crop parameters and non-conservative parameters. The conservative crop parameters include crop growth, transpiration, yield formation, water stresses, biomass and temperature stress. Generally and in principle, the conservative variables do not require adjustment to the local situations and can be used in simulations ([Steduto \*et al.\*, 2012](#)).

The FAO has calibrated crop parameters for several crops including tomato which is the test crop for this study. In this study, the crop variables used in calibrating the AquaCrop are summarized in Table 1 and they include transplanting, emergence, flowering and maturity dates, initial canopy and maximum canopy cover, harvested index, plant density and the effective rooting depth of the plants. The meteorological data that include the wind speed, rainfall, solar radiation and minimum and maximum temperature were obtained from the Centre for Dryland Agriculture, Bayero University, Kano which is in proximity to the study area.

**Table 1.** Field parameters for calibration of AquaCrop model.

S/No.	Parameter	Value
1	Transplanting	24 <sup>th</sup> February, 2022
2	Emergence	3 <sup>rd</sup> March, 2022
3	Maximum Canopy cover	25 <sup>th</sup> April, 2022
4	Maturity	10 <sup>th</sup> May, 2022
5	Flowering	5 <sup>th</sup> April, 2022
6	Time to start of canopy senescence	7 <sup>th</sup> May, 2022
7	End of flowering	11 <sup>th</sup> May, 2022
8	Maximum Canopy cover	0.80
9	Harvested Index, HI	51.40 %
10	Initial Canopy cover	0.25%
11	Plant density (plant m <sup>-2</sup> )	4 plant m <sup>-2</sup>
12	Effective rooting depth (mm)	0.6 m

### Field and Climatic Data for Simulation

The input parameters used in simulating the yield, water productivity and biomass of tomato in the AquaCrop model are shown in Table 2 and they include soil parameters, crop parameters, amount of irrigation water applied and climatic data. All the input parameters except climatic data were obtained from the study area while the climatic data which include the rainfall, wind speed, maximum and minimum temperature and solar radiation were obtained from the Centre for Dryland Agriculture, Bayero University, Kano which is in proximity to the study.

**Table 2.** The AquaCrop model input data.

S/No.	Parameters	Value
1	Saturated hydraulic conductivity, $K_{sat}$ (mm h <sup>-1</sup> )	41.5 mm h <sup>-1</sup>
2	Saturation (%)	30.09 %
3	Field capacity, FC (%)	17.77 %
4	Permanent wilting point, PWP (%)	7.48 %
5	Soil texture	Sandy loam (82.4% sand, 4% silt and 13.76% clay)
6	Plant density (plant m <sup>-2</sup> )	4 plant m <sup>-2</sup>
7	Harvest index	50.20 %
8	Effective rooting depth (mm)	0.6 m
9	Flowering time (days)	40 days
10	Maturity time (days)	75 days
11	Irrigation method	Drip
12	Amount of irrigation water applied (m <sup>3</sup> )	20.847 m <sup>3</sup>

### Comparison Between the Observed and Simulated Tomato Yield and Yield Component

The comparison between experimental (observed - O) and simulated (predicted - P) results of the yield and yield components of tomato were carried out using four statistical indices;

#### i) The Root Mean Square Error (RMSE)

This is to measure the precision of the outcomes. If RMSE tends towards 0, the measure of precision between the predicted and measured values increase.

$$RMSR = \left[ \frac{1}{n} \sum_{i=1}^n (P_i - O_i)^2 \right]^{0.5} \quad (1)$$

Where  $P_i$  = simulated value,  $O_i$  = observed value,  $n$  = number of the observation.

### ii) Normalized Root Mean Square Error (NRMSE)

This is a statistical index that facilitates the comparison between the models of different scales. The NRMSE classified the comparison into excellent, good, acceptable and poor based NRMSE percentage. The value of  $NRMSE < 10\%$  is termed as Excellent,  $NRMSE 10\%$  to  $20\%$  is Good,  $NRMSE 20\%$  to  $30\%$ , is Acceptable and  $NRMSE > 30\%$  is poor. Equation 2 shows the formula for computing NRMSE.

$$NRMSE = 100 \times \frac{\sqrt{\left[ \frac{1}{n} \sum_{i=1}^n (P_i - O_i)^2 \right]}}{O_m} \quad (2)$$

Where  $P_i$  = simulated value,  $O_i$  = observed value and  $O_m$  = mean of the observed values.

### iii) Modelling Efficiency (EF)

This is also known as the Coefficient of Nash-Sutcliffe (Nash and Sutcliffe, 1970), which is used to measure the fitness between the measured and predicted values and it ranges from  $-\infty$  to 1. When EF is 0 shows results are as good as the mean value of the measured data, while an EF of less than 0, implies that the measured value is better than the simulated. But when EF is 1 indicates a perfect match of the predicted to the measured data.

$$EF = 1 - \frac{\sum_{i=1}^n (O_i - P_i)^2}{\sum_{i=1}^n (O_i - O_m)^2} \quad (3)$$

### iv) Coefficient of Residual Mass (CRM)

This is the measure if the model under or over-predict measured values. A given value of zero (0) shows a perfect model, a negative value reveals overestimation whereas a positive value indicates underestimation.

$$CRM = \frac{\sum_{i=1}^n O_i - \sum_{i=1}^n P_i}{\sum_{i=1}^n O_i} \quad (4)$$

Where;  $O_i$  = observed value,  $P_i$  = model predicted value,  $O_m$  = mean of measured values and  $n$  = number of data.

## Optimization of the Simulated Parameters using Genetic Algorithm

The dry yield, aboveground biomass and crop water productivity of tomato crops were simulated using AquaCrop model. The simulated AquaCrop model was then optimized using the evolutionary optimization method of genetic algorithm (GA). The general procedures for solving any optimization problem using genetic algorithms include the initialization process, mutation, crossover and selection.

Firstly, populations of individuals as potential solutions are randomly generated. Fitness function is used to assess each generated solution. During each iteration process, a selection process is then applied to generate a new population which is more optimum compared to the previous population. The solutions will then pass through mutation and crossover and this is to mimic the natural evolution process. Such a process of iteration will continue until a stoppage criterion is reached (Eiben and Smith, 2015). The Operational framework of the genetic algorithm is summarised in Figure 7.

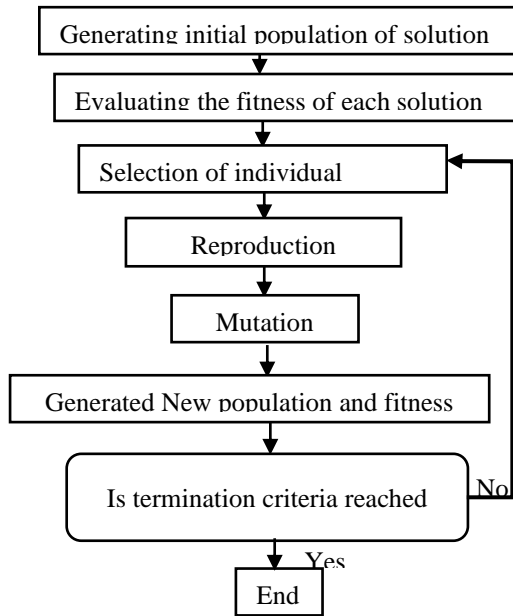


Figure 7. Operational framework of genetic algorithm.

The operational principle of the coupled simulation-optimization model of tomato production under a sensor-based drip irrigation system via genetic algorithm is shown in Figure 8.

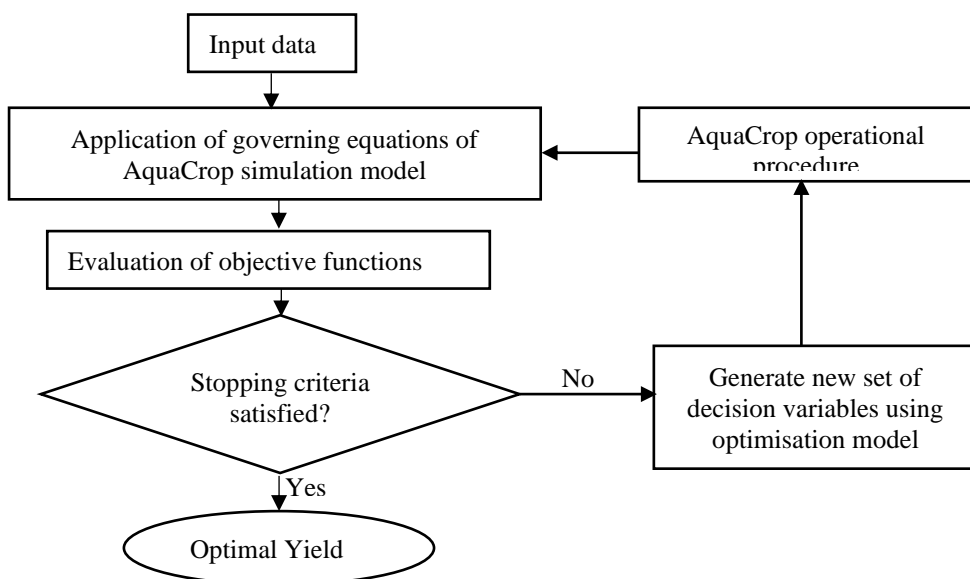


Figure 8. Operational framework of the simulation-optimization model via AquaCrop-Genetic Algorithm.



The parameterizations and ranges of the parameters affecting the model are shown in Table 3 below.

**Table 3.** Optimization parameters and ranges.

S/No.	Parameter	Symbol	Ranges
1	Soil fertility stress	$K_{S_{wp}}$	0 - 1
2	Yield	$Y_{expt}$	3000 - 200000 kg ha <sup>-1</sup>
3	Crop transpiration	ET	4000 - 8000 m <sup>3</sup> ha <sup>-1</sup> season <sup>-1</sup>
4	Daily transpiration	$Tr_i$	4.0 - 8.0 mm day <sup>-1</sup>
5	Daily reference evapotranspiration	$ET_{oi}$	4.0 - 9.0 mm day <sup>-1</sup>
6	Total Fresh plant weight	$TFPW$	1.28 - 29.8 ton ha <sup>-1</sup>
7	Marketable yield	$MY$	2.7 - 18 ton ha <sup>-1</sup>
8	Non-marketable yield	$NMY$	0 - 2.7 ton ha <sup>-1</sup>

The objective function of the optimization is the governing equation of the AquaCrop simulation model is stated in Equation 5.

$$\text{Maximise, } Y = K_{S_{wp}} \frac{Y(expt)}{ET} \sum \left( \frac{Tr_i}{ET_{oi}} \right) \times \frac{MY}{FPW+MY+NMY} \quad (5)$$

Where;  $Y$  = optimised yield (ton ha<sup>-1</sup>),  $MY$  = marketable yield,  $FPW$  = fresh plant weight,  $NMY$  = non-marketable yield,  $K_{S_{wp}}$  = coefficient of soil fertility stress,  $Y(expt)$  = expected yield.

## RESULTS AND DISCUSSION

### Dry Yield, Water Productivity and Dry Biomass of Tomato from AquaCrop

#### Simulated yield, and yield components of tomato

Table 4 shows the simulated dry yield, water productivity and dry biomass of tomato using the AquaCrop model. The AquaCrop simulation results show an average dry yield of 2.10 and 1.76 ton ha<sup>-1</sup> for units A and B respectively. The average value of the yield for the whole experiment is 1.93 ton ha<sup>-1</sup>. The values of the simulated dry biomass for units A and B are 3.65 and 4.00 ton ha<sup>-1</sup> averaging 3.83 ton ha<sup>-1</sup> for the study. The water productivity obtained from the simulation is 0.7 and 0.5 kg m<sup>-3</sup> for units A and B respectively. The average value of water productivity of the simulated result is 0.60 kg m<sup>-3</sup>.

**Table 4.** Simulated yield, water productivity and dry biomass of tomato.

Unit	Dry Yield (ton ha <sup>-1</sup> )	Water Productivity (kg m <sup>-3</sup> )	Dry Biomass (ton ha <sup>-1</sup> )
Unit A	2.10	0.70	3.65
Unit B	1.76	0.50	4.00
Average	1.93	0.60	3.83

### Observed Dry Yield, Dry Biomass and Water Productivity of Tomato

Table 5 shows the observed dry yield, dry biomass and water productivity of tomato from the field. The average observed dry yields for units A and B are 1.95 and

1.52 ton ha<sup>-1</sup> respectively. The average value of the observed dry yield for the whole experiment is 1.74 ton ha<sup>-1</sup>. The values of observed dry biomass for units A and B are 3.40 and 3.85 ton ha<sup>-1</sup> averaging 3.63 ton ha<sup>-1</sup> for the study. The water productivity obtained from the simulation is 0.65 and 0.35 kg m<sup>-3</sup> for units A and B respectively. The average value of water productivity of the observed dry yield is 0.50 kg m<sup>-3</sup>.

**Table 5.** Observed dry yield, water productivity and dry biomass of tomato.

Unit	Observed dry yield (ton ha <sup>-1</sup> )	Observed water productivity (kg m <sup>-3</sup> )	Observed dry biomass (ton ha <sup>-1</sup> )
Unit A	1.95	0.65	3.40
Unit B	1.52	0.35	3.85
Average	1.74	0.50	3.63

### Simulated and Observed Dry Yield, Water Productivity and Biomass of Tomato

#### *Simulated and observed dry yield of tomato*

Figure 9 showed the simulated and observed dry yield of tomato. The figure represents the average yield of the simulated and observed values for units A and B and the average yield of the observed and simulated value for the whole study. The values of the average simulated dry yield for units A and B are 2.10 and 1.76 ton ha<sup>-1</sup> respectively. The average dry simulated yield for the study is 1.93 ton ha<sup>-1</sup>. The average observed dry yield for units A and B are 1.95 and 1.52 ton ha<sup>-1</sup> averaging 1.74 ton ha<sup>-1</sup> for the whole experiment.

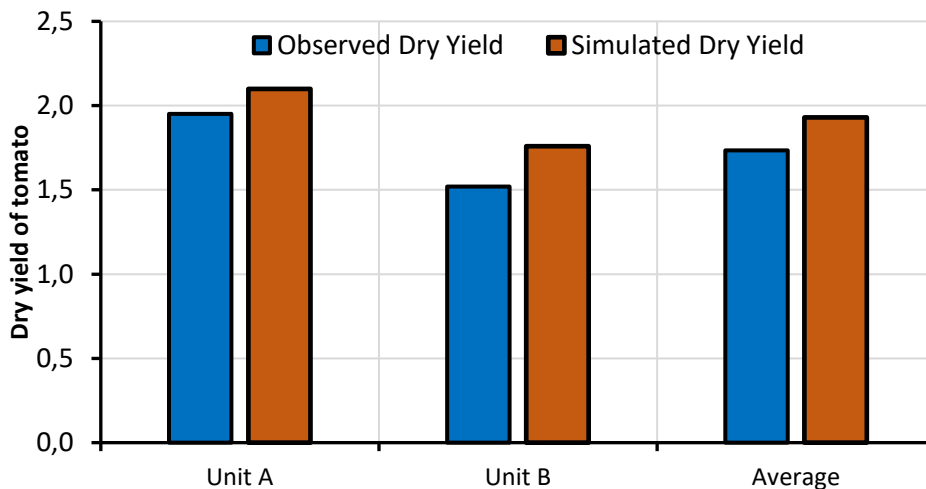


**Figure 9.** Simulated and observed dry yield of tomato.

#### *Simulated and observed water productivity of tomato*

Figure 10 showed the simulated and observed water productivity of tomato. The figure represents the average values of the observed and simulated water productivity of tomato for units A and B and the average simulated and observed water productivity for the whole study. The average simulated water productivity for units A and B are 0.7 and 0.5 kg m<sup>-3</sup> respectively. The average simulated water productivity for the study is 0.6 kg m<sup>-3</sup>. The average observed water productivity for unit A and B are 0.65 and 0.35 kg m<sup>-3</sup> respectively. The average observed water productivity for the whole experiment is 0.5 kg m<sup>-3</sup>.

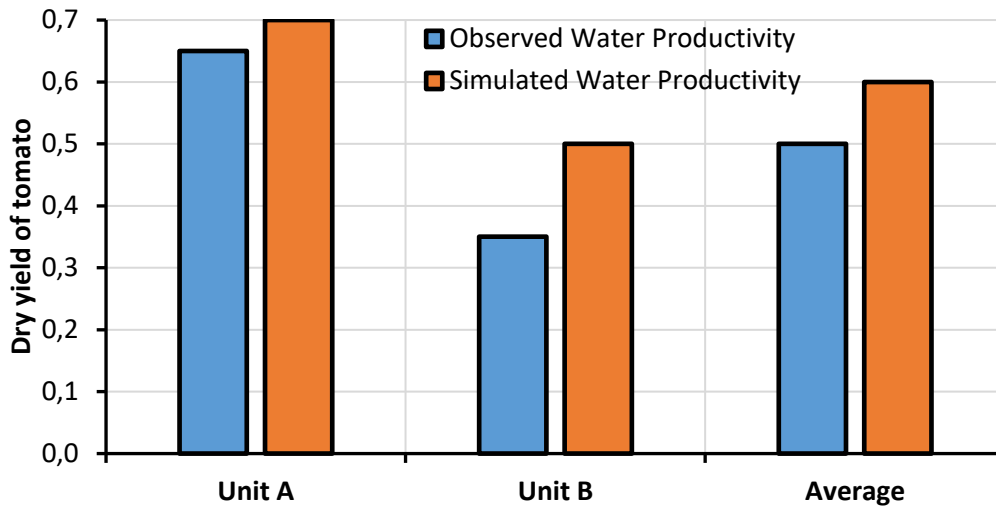


Figure 10. Observed and simulated water productivity of tomato.

**Simulated and observed dry biomass of tomato**

Figure 11 showed the simulated and observed biomass. The figure represents the average dry observed and simulated biomass of tomato for units A and B and the average biomass of the simulated and observed value for the whole study. The averages simulated dry biomass for units A and B are 3.65 and 4.00 ton ha<sup>-1</sup>, respectively. The average dry simulated aboveground biomass for the whole study is 3.83 ton ha<sup>-1</sup>. The average observed dry biomass for units A and B are 3.4 and 3.85 ton ha<sup>-1</sup> respectively. The average observed dry biomass for the whole experiment is 3.63 ton ha<sup>-1</sup>.

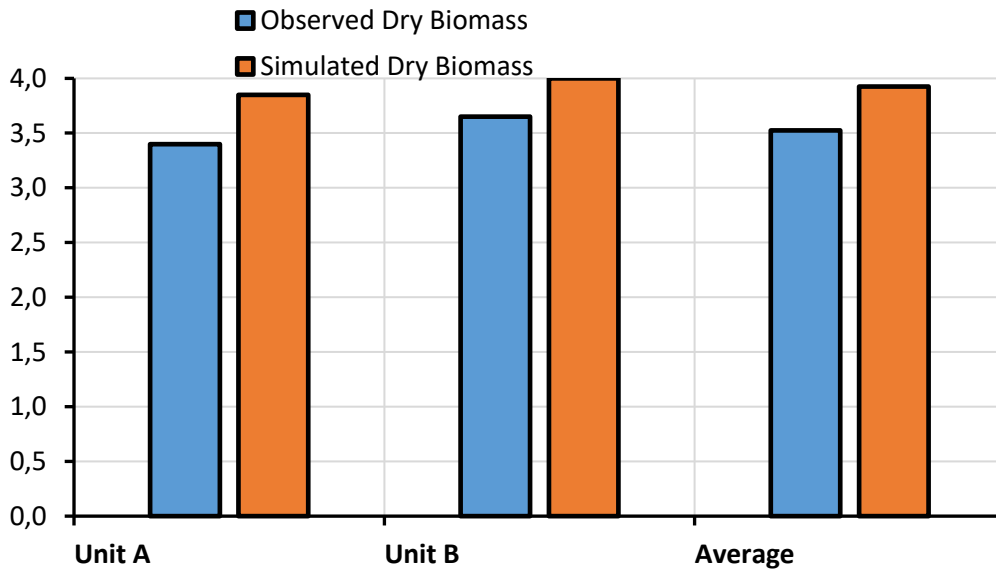


Figure 11. Observed and simulated dry biomass of tomato.

**Statistical Comparison Between Simulated and Observed Results**

The observed and simulated results were subjected to comparison using four statistical indices to determine the accuracy of AquaCrop simulation model.

### Comparing Observed and Simulated Dry Yield of Tomato

The results of statistical indices (RMSE=0.2, EF= 0.13, CRM=-0.11, NRMSE=11%) used in comparing the simulated and observed dry yields of tomato revealed good agreement between the observed and simulated values. The value of the normalized root means square error, NRMSE of 11% is classified as good (10 to 20%) and is similar to what has been established by [Takács et al. \(2021\)](#) who obtained an NRMSE value of 13.6% for comparing the observed-field and AquaCrop simulated yields of tomato. The value of NRMSE of 11% obtained for the comparison contradicts the works of [Vegu et al. \(2018\)](#); [Hendy et al. \(2019\)](#); [Thangaraju \(2020\)](#); [Farrokhi et al. \(2021\)](#) and [Ebrahimipak et al. \(2022\)](#), whose when compared between the AquaCrop simulated and the observed yield of tomato recorded an excellent value of NRMSE (< 10%) of 3.1%, 9.5%, 3.76 %, 9.97% and 0.07%, respectively.

The value of the root means square error, RMSE of 0.20 obtained for the comparison is similar to the works of [Sang \(2020\)](#); [Thangaraju \(2020\)](#); [Cheng et al. \(2022\)](#); [Muroyiwa et al. \(2022\)](#); [Ebrahimipak et al. \(2022\)](#) who used AquaCrop to simulate tomato yield and obtained RMSE values of 0.13, 0.40, 0.34, 0.34, and 0.42 respectively for comparison between the observed and simulated yields. This revealed a strong relationship between simulated and observed yield as the degree of precision of the comparison increase as the RMSE tends toward zero. The value of modeling efficiency, EF between the simulated and observed dry yields of tomato is 0.13 which is in line with the work of [Ebrahimipak et al. \(2022\)](#) whose studies recorded an EF value of 0.41 for comparing AquaCrop simulated and the observed dry yield of tomato. The modeling efficiency ranges from  $-\infty$  to 1 with an EF value of 1 corresponding to a perfect match of the predicted to the observed value. The closer the efficiency approximation is to 1, the better the model's values. The coefficient of residual mass, CRM between the observed and the simulated result is -0.11 which indicated that AquaCrop slightly overestimated the dry yield and this is consistent works of [Rinaldi et al. \(2011\)](#) and [Jadhav et al. \(2022\)](#) who obtained CRM values of -0.31 and -0.06 for comparing the observed and simulated yields. The CRM values range from  $-\infty$  to 1 with an optimum value of 0. A CRM value greater than 0 indicates underestimation. A negative value revealed an overestimation of the model. The observed and simulated results for the dry yield of tomato are presented in Figure 12.

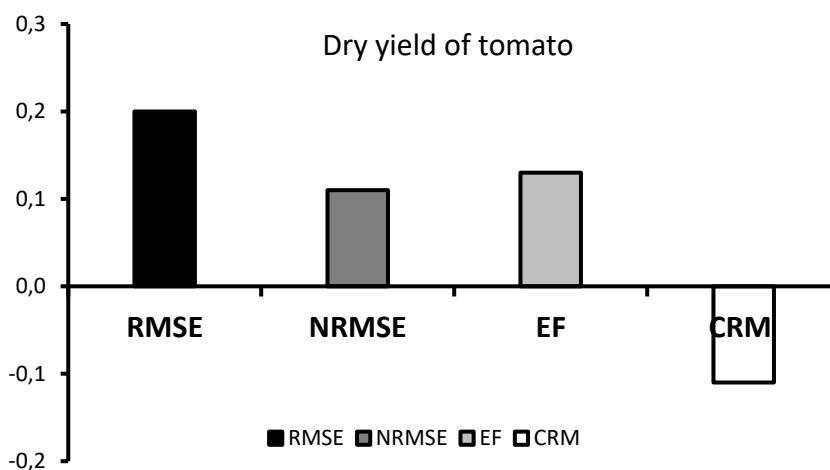


Figure 12. Observed and simulated comparative results for the dry yield of tomato.

In addition to statistical indices used to compare the simulated and observed yields, the t-test was also conducted with the aim to determine if there is a significant difference between the simulated and observed yields and the result of the t-test ( $p > 0.05$ ) reveals no significant difference between the simulated and observed tomato yield.

### Comparing Simulated and Observed Water Productivity of Tomato

The values of RMSE, NRMSE, EF and CRM used in comparing the observed and the AquaCrop water productivity of tomato are 0.11, 22%, 0.44 and -0.20. The value of the RMSE of 0.11 shows good agreement the simulated is compared with the observed values of water productivity and has concur with the works of [Sang \(2020\)](#); [Farrokhi et al. \(2021\)](#) and [Ebrahimipak et al. \(2022\)](#) whose studies recorded RMSE values of 0.04, 0.23 and 0.02 respectively for comparing the simulated and observed values of water productivity of tomato. The NRMSE value obtained from the comparison is 22% which is termed acceptable (20% to 30%). This value of NRSME (22%) contradicts the values of NRMSE obtained by [Vegu et al., \(2018\)](#) and [Ebrahimipak et al. \(2022\)](#) of 3.1% and 0.03% respectively.

The value of EF obtained is 0.44 which is considered average and is consistent with the value of EF obtained by [Farrokhi et al. \(2021\)](#) and [Ebrahimipak et al. \(2022\)](#) of 0.23 and 0.19 respectively for comparing the observed and AquaCrop simulated water productivity of tomato. The value of CRM obtained for the comparison is -0.20 which shows that AquaCrop slightly overestimated the water productivity of tomato and this is in line with what was reported by [Salemi et al. \(2011\)](#) who obtained CRM of -0.20 for comparing the simulated and observed water productivity. The t-test was further conducted to determine whether there is a significant difference between the observed and simulated value and the result of the t-test ( $p > 0.05$ ) shows that there is no significant difference between the simulated and observed water productivity of the tomato. The observed and simulated comparative results of water productivity of tomato are shown in Figure 13.

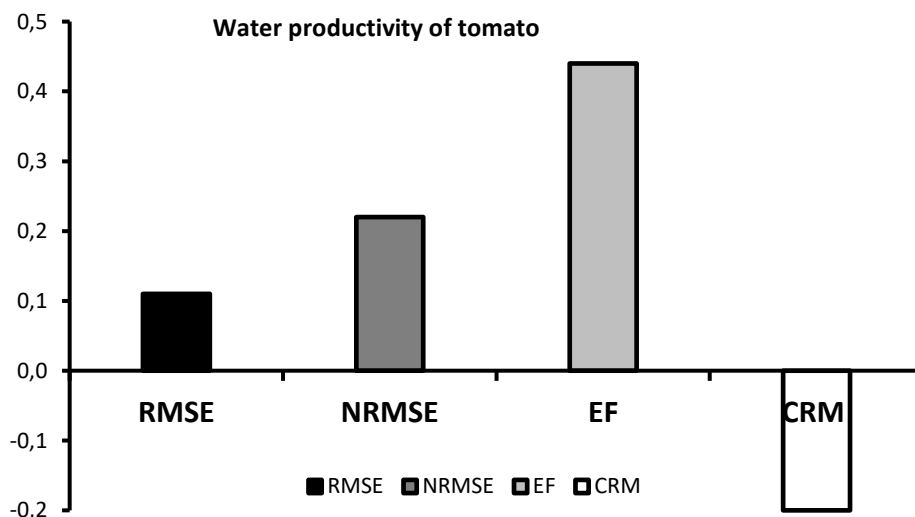


**Figure 13.** Observed and simulated comparative results for the water productivity of tomato.

### Comparing Observed and Simulated Dry Biomass of Tomato

The values of the RMSE, NRMSE, EF and CRM used in comparing the observed and the simulated results of the aboveground dry biomass are 0.21, 5%, 0.16 and -0.06 respectively. The simulated and observed values are approximately similar as indicated by the values of the statistical indices used in their comparison. The value of RMSE (0.21) obtained from the comparison agrees with the works of [Hendy \*et al.\* \(2019\)](#); [Takács \*et al.\* \(2019\)](#); [Sang \(2020\)](#) and [Cheng \*et al.\* \(2022\)](#) whose comparison between the observed and simulated aboveground biomass of tomato recorded RMSE of 0.20, 0.45, 0.60 and 0.53 respectively. The value of NRMSE (5%) obtained shows that the comparison is excellent ( $NRMSE < 10\%$ ) and is in line with the works of [Vegu \*et al.\* \(2018\)](#); [Hendy \*et al.\* \(2019\)](#); [Thangaraju \(2020\)](#); [Cheng \*et al.\* \(2022\)](#); [Muroyiwa \*et al.\* \(2022\)](#) who used AquaCrop to simulate aboveground biomass of tomato and obtained NRMSE value of 4.7%, 1.9%, 5.9%, 9.7% and 5.2% respectively by comparing the simulated and observed biomass. However, the value of NRMSE (5%) obtained from the comparison contradicts the works of [Takács \*et al.\* \(2021\)](#) and [Farrokhi \*et al.\* \(2021\)](#) whose NRMSE ( $> 10\%$ ) values are 12.1% and 16.26% respectively.

The EF value obtained from the comparison is 0.16 which is similar to the values obtained by [Sang \(2020\)](#); [Cheng \*et al.\* \(2022\)](#) when compared between the observed and AquaCrop simulated aboveground biomass of 0.16 and 0.77 respectively. The CRM value obtained between the results obtained from the simulated and observed biomass result is -0.06 which indicated a very little overestimation of the biomass by the AquaCrop model. The value of CRM obtained from the comparison is in agreement with the values of CRM obtained by [Rinaldi \*et al.\* \(2011\)](#) of -0.20 who also compared observed and simulated biomass of tomato. AquaCrop is known to overestimate biomass for tomato crops at the final stage of its growing season as reported by [Katerji \*et al.\* \(2013\)](#). The t-test ( $p > 0.05$ ) conducted shows no significant difference between the simulated and observed aboveground biomass of tomato. The simulated and observed comparative results for the dry biomass of tomato are presented in Figure 14.

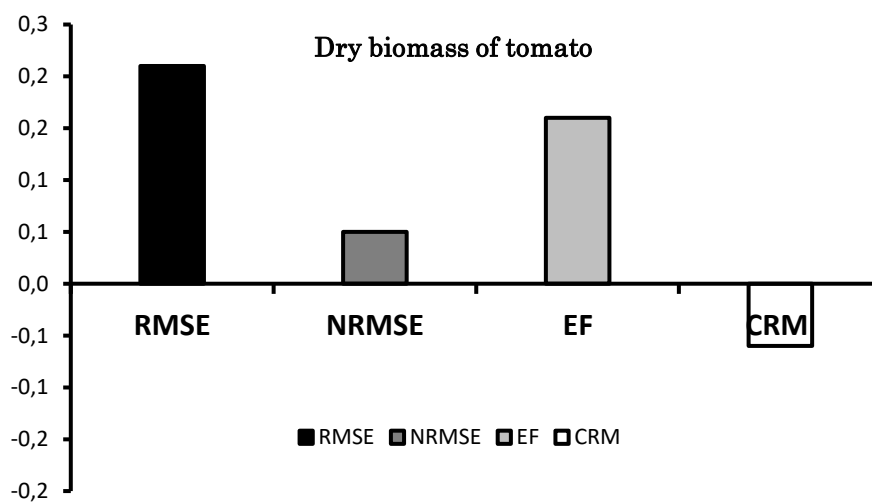


**Figure 14.** Observed and simulated comparative results for the dry biomass of tomato.

Generally, the AquaCrop simulation model performed remarkably well in simulating the dry yield, dry biomass and water productivity of the tomato crop. All the statistical indices except CRM used in comparing the observed and simulated values revealed a good agreement between the simulated and observed values. The CRM value of -0.11, -0.06 and -0.20 was obtained for the dry yield, dry biomass and water productivity although indicate a slight overestimation of the model they are also closer to the optimum value of 0. More so, the t-test ( $p > 0.05$ ) conducted shows no significant difference between the simulated and observed dry yield, dry biomass and water productivity of the tomato.

### Optimized Yield and Yield Components of Tomato

Table 6 presents the optimal values of the simulated dry yield (objective function) and the dry yield parameters obtained using the evolutionary optimization algorithm (genetic algorithm) using MATLAB programming software. The objective function set to maximise the dry yield which is the AquaCrop governing equation is expressed below.

$$\text{Maximise, } Y = K_{S_{wp}} \frac{Y(\text{expt})}{ET} \sum \left( \frac{Tr_i}{ET_{O_i}} \right) \times \frac{MY}{FPW + MY + NMY}$$

The value of the optimized dry yield of 4.496 ton ha<sup>-1</sup> is higher than the simulated yields of 2.10 ton ha<sup>-1</sup> and 1.76 ton ha<sup>-1</sup> for units A and B respectively. This shows that the GA has maximized the simulated yields by about 53 and 61% respectively. The dry biomass computed from the optimal parameters is 4.90 ton ha<sup>-1</sup> which is also higher than the simulated values of 3.6 ton ha<sup>-1</sup> and 4.0 ton ha<sup>-1</sup> for units A and B respectively. This also indicates that dry biomass has been maximized by 27% and 18% for units A and B. The study conforms with the work of [Abdollah et al. \(2022\)](#) who recorded an increase of 63% and 22% in water conservation and yield for optimizing irrigation practices.

This study further agrees with the work of [Seidel \(2012\)](#) who achieved 22% and 76% for water productivity and nitrogen use efficiency using an optimization framework. [Saber et al. \(2020\)](#), also recorded a remarkable increase in the water use efficiency of 14.2% using a simulation–optimization framework.

**Table 6.** Optimal values of the simulated dry yield and the optimization parameters.

S/No.	Parameters	Symbol	Optimal values	Unit
1	Soil fertility stress coefficient	$K_{S_{wp}}$	1	
2	Yield	$Y_{\text{expt}}$	19,025.308	kg ha <sup>1</sup>
3	Crop transpiration	$ET$	4,000.001	m <sup>3</sup> ha <sup>-1</sup> season <sup>-1</sup>
4	Daily transpiration	$Tr_i$	8.247	mm day <sup>-1</sup>
5	Daily reference evapotranspiration	$ET_{O_i}$	8.000	mm day <sup>-1</sup>
6	Total Fresh plant weight	$TFPW$	29.800	ton ha <sup>-1</sup>
7	Marketable yield	$MY$	2.700	ton ha <sup>-1</sup>
8	Non-marketable yield	$NMY$	0.000	ton ha <sup>-1</sup>
9	Objective function (dry yield)	$Y$	4.496	ton ha <sup>-1</sup>

Figure 15 shows the fitness value of the optimization result (optimal dry yield of tomato) after 800 iterations. The figure indicates the best function in each generation versus the iteration during the optimization process. Thus, the fitness value of an individual corresponds to the fitness function for that particular individual. The black dots/marks indicate the best fitness values whereas the blue dots/marks indicate the mean fitness values in each generation. The fitness function is a measure of how close a given solution is to the optimum solution of the desired problem and the best fitness value is equal to the objective function. The fitness value improves rapidly in the early generations and more slowly in later generations which is quite similar to the general optimization problems (Hanan et al., 2016). The MATLAB programming software searches for the minimum of the function and hence, the best fitness value for a given population is the smallest value for a given individual in that particular population. The best fitness value of dry yield of tomato was found to be -4.960 which translates to 4.960 ton ha<sup>-1</sup>ton because the objective function of the optimization process was to maximize the dry yield of tomato.

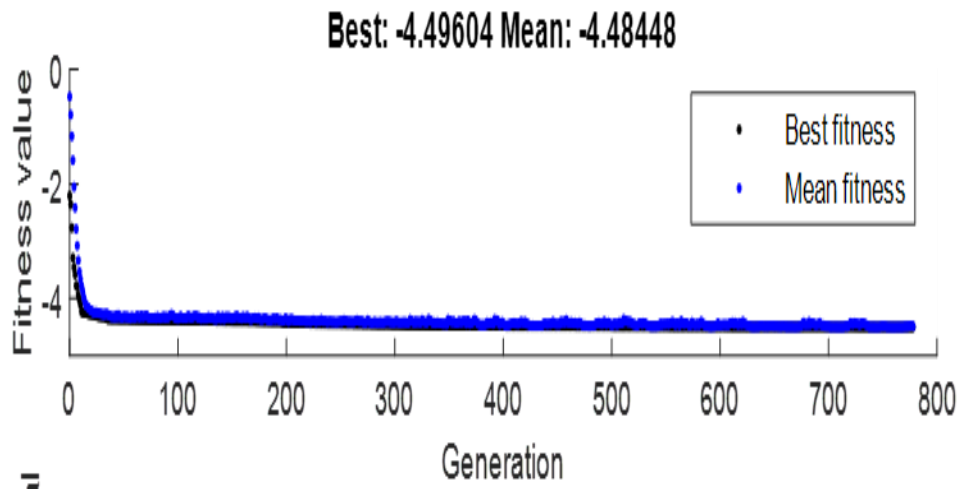


*Figure 15. Best and the mean fitness of the dry yield of tomato.*

## CONCLUSION

The AquaCrop simulation model performed remarkably well in simulating the observed yield, aboveground biomass and water productivity of tomato based on results of RMSE (0.20, 0.21 and 0.11), NRMSE (11%, 5% and 22%), EF (0.13, 0.16 and 0.44) and CRM (-0.11, -0.06 and -0.20) used in comparing the simulated and observed results. All the statistical indices except CRM show good agreement between the observed and simulated results. The CRM value of -0.11, -0.06 and -0.20 was obtained for yield, biomass and water productivity although indicate a very slight overestimation of the model they are also closer to the optimum value of zero (0). The t-test ( $p > 0.05$ ) conducted between the observed and simulated results also shows that there is no significant difference between the simulated and observed results.

The result of the optimization revealed the optimal values of yield and aboveground biomass of 4.49 ton ha<sup>-1</sup> and 4.90 ton ha<sup>-1</sup> respectively. This shows that



the GA has maximized the simulated yields by 53% and 61% respectively for units A and B. The GA has also maximized aboveground biomass by 27% and 18% for units A and B. The GA has therefore proved to be an effective tool for improving the yield and the yield components of tomato crops.

## DECLARATION OF COMPETING INTEREST

We hereby declare that we have no conflict of interests

## CREDIT AUTHORSHIP CONTRIBUTION STATEMENT

**Nura Jafar Shanono**, Investigation, methodology, conceptualization, data curation, validation, review, and editing, visualization,

**Lawal Ahmad**, Investigation, methodology, data curation, review, and editing, visualization,

**Nuraddeen Mukhtar Nasidi**, Formal analysis, data curation, review, and editing, visualization,

**Abdul'aziz Nuhu Jibril**, Methodology, formal analysis, validation, review, and editing, visualization,

**Mukhtar Nuhu Yahya**, Investigation, methodology, validation, writing - original draft.

## ETHICS COMMITTEE DECISION

This article does not require any ethical committee decision.

## REFERENCES

- Abdollah S, Ali A, Ritzema H, Dam J Van and Hellegers P (2022). A combined model approach to optimize surface irrigation practice: SWAP and WinSRFR. *Agricultural Water Management*, 271 (December 2021), 107741. <https://doi.org/10.1016/j.agwat.2022.107741>
- Ahmad MT and Haie N (2018). Assessing the impacts of population growth and climate change on performance of water use systems and water allocation in Kano River basin, Nigeria. *Water (Switzerland)*, 10(12). <https://doi.org/10.3390/w10121766>
- Akbari M, Gheysari M, Mostafazadeh-Fard B and Shayannejad M (2018). Surface irrigation simulation-optimization model based on meta-heuristic algorithms. *Agricultural Water Management*, 201 (January), 46-57. <https://doi.org/10.1016/j.agwat.2018.01.015>
- Ara I, Turner L, Harrison MT, Monjardino M, deVoil P and Rodriguez D (2021). Application, adoption and opportunities for improving decision support systems in irrigated agriculture: A review. *Agricultural Water Management*, 257 (June), 107161. <https://doi.org/10.1016/j.agwat.2021.107161>
- Bitri M, Grazhdani S and Ahmeti A (2014). Validation of the aquacrop model for full and deficit irrigated potato production in environmental condition of Korça Zone, South-Eastern Albania. *International Journal of Innovative Research in Science, Engineering and Technology*, 3(4): 1-8.
- Cheng M, Wang H, Fan J, Xiang Y, Liu X, Liao Z, Elsayed A, Zhang F and Li Z (2022). Evaluation of AquaCrop model for greenhouse cherry tomato with plastic film mulch under various water and nitrogen supplies. *Agricultural Water Management*, 274 (July), 107949. <https://doi.org/10.1016/j.agwat.2022.107949>
- Ebrahimipak NA, Egdernezhad A, Tafteh A and Ansari MA (2022). The effect of irrigation water management and fertilizer amount on aquacrop accuracy and efficiency for tomato yield and water use efficiency simulation. *Iranian Journal of Irrigation and Water Engineering*, 47(3): 121-136. <https://doi.org/10.22125/IWE.2020.243948.1405>



- McCarthy AC, Hancock NH and Raine SR (2013). Advanced process control of irrigation: the current state and an analysis to aid future development. *Irrigation Science*, 31: 183-192.  
<https://doi.org/dx.doi.org/10.1007/s00271-011-0313-1>
- Muroyiwa GATM, Mashonjowa E and Muchuweti M (2022). Evaluation of FAO AquaCrop Model for ability to simulate attainable yields and water use for field tomatoes grown under deficit irrigation in Harare, Zimbabwe. *African Crop Science Journal by African Crop Science Society*, 30(2), 245-269.  
<https://doi.org/https://dx.doi.org/10.4314/acsj.v30i2.10>
- Perea RG, Daccache A, Di'az JAR, Poyato EC and Knox JW (2017). Modelling impacts of precision irrigation on crop yield and in-field water management. *Precision Agriculture*, 19: 497-512.  
<https://doi.org/https://doi.org/10.1007/s11119-017-9535-4>
- Raes D, Steduto P, Hsiao TC and Feres E (2022). AquaCrop Version 7.0 Reference manual; Chapter 1 FAO crop-water productivity model to simulate yield response to water (Issue August). Food and Agriculture Organization of the United Nations. <https://www.fao.org/3/br246e/br246e.pdf>
- Reynolds M, Kropff M, Crossa J, Koo J, Kruseman G, Molero Milan A, Rutkoski J, Schulthess U, Singh B, Sonder K, Tonnang H and Vadez V (2018). Role of modelling in international crop research: Overview and some case studies. *Agronomy* 8(12): 291.
- Rinaldi M, Garofalo P, Rubino P and Steduto P (2011). Processing tomatoes under different irrigation regimes in Southern Italy: agronomic and economic assessments in a simulation case study. *Italian Journal of Agrometeorology* 3(3): 39-56.
- Saberi E, Khashei Siuki A, Pourreza-Bilondi M and Shahidi A (2020). Development of a simulation-optimization model with a multi-objective framework for automatic design of a furrow irrigation system. *Irrigation and Drainage*, 69(4): 603-617. <https://doi.org/10.1002/ird.2460>
- Salemi H, Amin M, Soom M, Mousavi S and Ganji A (2011). Irrigated silage maize yield and water productivity response to deficit irrigation in an arid region. *Polish Journal of Environmental Studies*, 20(5). <https://doi.org/https://www.researchgate.net/publication/275953655>
- Sang HJ (2020). *Optimisation of tomato water productivity under deficit sub-surface drip irrigation and mulching systems*. Egerton University.
- Seidel S (2012). *Optimal simulation based design Dresdner Schriften zur Hydrologie*.
- Shanono NJ (2019). *Assessing the impact of human behaviour on reservoir system performance using dynamic co-evolution*. A PhD Thesis Submitted to University of the Witwatersrand, Johannesburg.  
<https://doi.org/http://wiredspace.wits.ac.za/handle/10539/29043>
- Shanono NJ, Nasidi NM, Zakari MD and Bello MM (2014). Assessment of field channels performance at watari irrigation project Kano, Nigeria. 1st International Conference on Dryland, Center for Dryland Agriculture, Bayero University Kano, Nigeria. 8<sup>th</sup>-12<sup>th</sup> December, 2014, 144-150.
- Shanono NJ, Othman MK, Nasidi NM and Isma'il H (2012). *Evaluation of Soil and water quality of watari irrigation project in semi-arid region, Kano, Nigeria*. Proceedings of the 33<sup>rd</sup> National Conference and Annual General Meeting of the Nigerian Institute of Agricultural Engineers (NIAE) Bauchi., 181-186.
- Shanono NJ, Abba BS and Nasidi NM (2022). Evaluation of Aqua-Crop Model using onion crop under deficit irrigation and mulch in semi-arid Nigeria. *Turkish Journal of Agricultural Engineering Research (TURKAGER)*, 3(1): 131-145. <https://doi.org/10.46592/turkager.1078082>
- Singels A, Annandale JG, Jager JM De, Schulze RE, Durand W, Rensburg LD Van, Heerden PS Van, Crosby CT, Green GC and Steyn JM (2013). Modelling crop growth and crop water relations in South Africa: Past achievements and lessons for the future. 1862.  
<https://doi.org/10.1080/02571862.2010.10639970>
- Singh A (2012). An overview of the optimization modelling applications. *Journal of Hydrology*, 466-467(August), 167-182. <https://doi.org/10.1016/j.jhydrol.2012.08.004>
- Steduto P, Hsiao TC and Fereres E (2012). Crop yield response to water. Food and Agricultural Organisation. [www.fao.org](http://www.fao.org)
- Takács S, Csengeri E, Pék Z, Bíró T, Szuvandzsiev P, Palotás G and LH (2021). Performance evaluation of aquacrop model in processing tomato biomass, fruit yield and water stress indicator modelling. *Water*, 13(3587). <https://doi.org/https://doi.org/w13243587>
- Takács S, Rác I, Csengeri E and Bíró T (2019). Biomass production estimation of processing tomato using AquaCrop under different irrigation treatments. *Acta Agraria Debreceniensis*, 2: 131-136.  
<https://doi.org/10.34101/actaagrar/2/3691>
- Thangaraju NKA (2020). *Predicting crop water requirements and yield for tomato under a humid climate (Issue April)* [McGill University, Montreal]. <https://escholarship.mcgill.ca/theses>

- Thompson RB and Gallardo M (2005). Use of Soil moisture sensors for irrigation scheduling. "improvement of water use efficiency in protected crops, January, 1–6. [https://doi.org/https://www.researchgate.net/publication/285422793\\_Use\\_of\\_soil\\_sensors\\_for\\_irrigation\\_scheduling/link/566481dc08ae418a786d6a93/download](https://doi.org/https://www.researchgate.net/publication/285422793_Use_of_soil_sensors_for_irrigation_scheduling/link/566481dc08ae418a786d6a93/download)
- Vegu G, Geethalakshmi V and Bhuvanewari K (2018). Evaluation of the AquaCrop Model for simulating yield response of tomato crop over Thiruchirapalli District Of Tamilnadu. *Journal in Science, Agriculture & Engineering*, 7(Special issue).
- Walser S, Schütze N, Marcus G, Susanne L and Schmidhalter U (2011). Evaluation of the transferability of a SVAT model--results from field and greenhouse applications. *Irrigation and Drainage*, 60(Suppl. 1): 59-70. <https://doi.org/10.1002/ird.669>
- Whitley D (2001). An overview of evolutionary algorithms: Practical issues and common pitfalls. *Information and Software Technology*, 43(14): 817-831. [https://doi.org/10.1016/S0950-5849\(01\)00188-4](https://doi.org/10.1016/S0950-5849(01)00188-4)



## Design and Development of a Model Smart Storage System

Omokaro IDAMA<sup>a</sup>, Ovuakporaye Godwin EKRUYOTA<sup>a\*</sup>

<sup>a</sup>Department of Computer Engineering, Delta State University of Science and Technology, Ozoro, NIGERIA

(\*): Corresponding Author: [g.o.softsystem@gmail.com](mailto:g.o.softsystem@gmail.com)

Received: 15.05.2023

Article Info  
Accepted: 15.06.2023

Published: 30.06.2023

### ABSTRACT

Food security has become a global major problem, due to the rapid increase in population growth. This has necessitated the development of an effective agricultural products' storage system, to alleviate the problem of food wastage. This study was embarked upon to develop a prototype of universal smart storage system for farm products, by using the internet of thing (IoT). The storage structure consists of four principal constituents which were: the power source, storage chamber, central processing system, and peripheral component interconnect (PCI) heater and PCI fan. The developed model was tested at a pre-set temperature and relative humidity of 32°C and 62% RH respectively. The results revealed that the developed system had an efficiency of 85%. Though, the smart model had a failure rate of 15%, this smart prototype is a major breakthrough in the production of automated storage system for agricultural products.

**Keywords:** Automation, Environmental conditions, Food security, Smart system, Storage structure

**To cite:** Idama O and Ekruyota OG (2023). Design and Development of a Model Smart Storage System. *Turkish Journal of Agricultural Engineering Research (TURKAGER)*, 4(1), 125-132. <https://doi.org/10.46592/turkager.1297511>

### INTRODUCTION

Food insecurity is rising daily mostly due to decrease in food production and increase in human population. Apart from increase in food production, appropriate storage and processing conditions, may help to alleviate the problem of food wastage. [Ekruyota and Uguru \(2021a\)](#) reported that food wastage, probably caused by poor storage and handling conditions, is one of the major causes of food insecurity. This is because more than 30% of the crops produced globally, are susceptible to rapid deterioration, due to poor harvesting, transportation and storage operation. Nigeria is losing billions of Dollars annually due to food waste, resulting from inadequate storage structures, and scandals in crops processing ([Ijabo et al., 2019](#)).



Soft tissue fruits and vegetable are highly prone to mechanical damage – which is one of the major causes of food wastage, when harvested and/or handled with inappropriate machines and methods ([Ekruyota et al., 2021](#)). Likewise, [Golf \(2019\)](#) stated that adequate storage facilities, which modern equipment to monitor the interior environmental condition are necessary to combat the menace of food insecurity. Some of the vital factors inside storage houses which are regularly monitored, in order to increase the shelf-life of the stored products are; carbon oxides, humidity, water vapour, volatile gases, and temperature. Citing [Hagstrum and Subramanyam \(2006\)](#), the interior of a standard storage structure should be designed to preserve the quality and quantity of the stored agricultural product; hence, the heat of respiration of agricultural products is an important parameter to be considered during the development of any storage system.

Remarkably, results from the shortage of human power to accomplish the task of massive food production, automation of agricultural business is gaining foothold. Most of these automated systems uses artificial intelligence (AI) to provide food security, through substantial food production and protection ([Bezboruah and Bora 2020](#); [Idama et al., 2021](#)). Internet of things (IoT) is of the techniques used for the automation of agricultural activities (smart farming). It incorporates hardware (devices), software, and other relevant technologies, with the aim of monitoring the farm operations through the internet. Designing a functioning smart agriculture operation required adequate knowledge of the intended crop engineering properties, prevailing environmental conditions, and the farming system (method) employed ([Nwanze and Uguru, 2020](#); [Ekruyota and Uguru, 2021b](#)).

[Mabrouk et al. \(2017\)](#) reported that poor monitoring techniques are contributing greatly to the quality deterioration of crops stored inside storage structures. [Mabrouk et al. \(2017\)](#) listed the advantages of an automated farm operation as, extraordinary proficiency of sensing errors, reduced human health risks, and an elaborate structure; while design complexity and high cost of corrective maintenance, are some of the delimitation of smart systems. Though several researchers have designed or developed smart systems for various crops storage ([Onibonoje et al., 2019](#); [Zhao et al., 2014](#); [Ekuewa et al., 2022](#)), there is still serious necessity to develop universal smart machine, that can handle to storage if various agricultural crops. Therefore, the main purpose of this research work is to design and developed a prototype of smart storage structure for different crops, where the temperature and humidity can be regulated.

## MATERIALS and METHODS

The prototyping methodology, as explained by [Boehmer \(2015\)](#) and shown in Figure 1, was adopted for this research work, to develop a prototype of an automated storage structure.

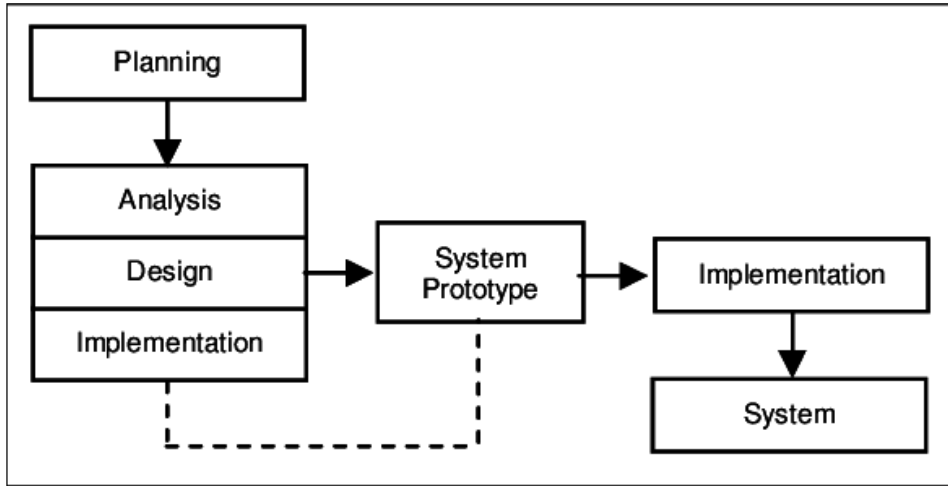


Figure 1. Prototyping methodology (Boehmer, 2015).

### System Analysis

The automated storage structure has four main components, which are:

- I. the power source,
- II. the storage chamber,
- III. the central processing system that consists of the relays, sensors and microcontroller, and
- IV. peripheral component interconnect (PCI) heater and PCI fan.

The smart system performance rating (efficiency) was calculated with Equation 1.

$$PR = \frac{\text{observed output}}{\text{expected output}} \times 100 \quad (1)$$

Where  $PR$  = system performance rating.

The failure rate of the system was calculated through Equation 2.

$$\text{Failure rate} = 100 - PR \quad (2)$$

### System Description

Figure 2 shows that the system comprises of an arduino microcontroller that acts at the brainbox. The arduino device receives information from the environmental sensors (temperature and humidity sensors), and send them to the main station through the GSM module. Additionally, the PCI heater and fan will switch on if the temperature and humidity exceeded the pre-set values.

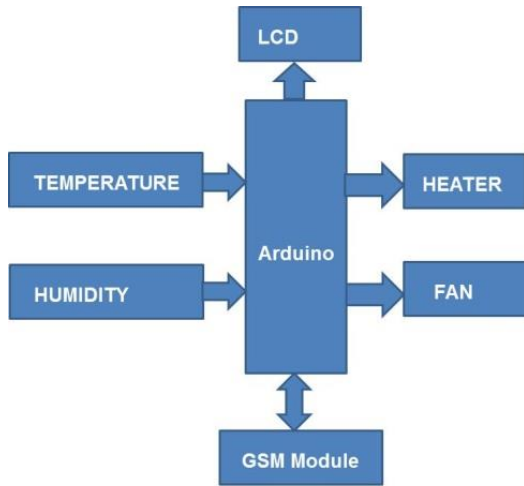


Figure 2. System design architecture.

**Component Specification**

The components were used for the building of the prototype with their specification are presented in Table 1.

Table 1. The smart system components.

S/No	Component	Specification
1	NodeMCU	Model ESP8266
2	Arduino uno Microcontroller	Arduino Mega 2560
3	Relay module	5 V
4	Humidity sensor	5V DC SL module
5	Gas sensor	CCS811 module sensor
6	Temperature sensor	DHT11 sensor
7	Jumper Wire	
8	Liquid crystal display (LCD)	16x2 LCD screen
9	Wi – fi module	ESP8266 01S
10	Bread board	
11	Storage chamber	Capacity of 0.2 m <sup>2</sup> , and made from aluminum sheet
12	Heater	100°C, sensitivity of ± 0.1°C
13	Fan	SL-PCI-02_SML, DC 12 V, speed 2500 rpm

**Development of the Internet of Things (IoT) System**

The language use for the design was the C++ language, while the framework was the arduino IDE and blynk App. The blynk application (App) for Android was used to develop the GUI Interface, while the arduino IDE was used to build instruction for the board (Jenkins and Kurasaki, 2018). The blynk app is compatible with numerous IoT applications. Blynk app has effective pins that emulate the Arduino pins, which are used to transfer information between itself and the Arduino.

Furthermore, a Wi-Fi module (powered by 3V DC dry cell) which is an extremely integrated chip was used link the smart storage system to the web (internet), to facilitate the communication with the mobile app distantly. All the system hard ware (fan and heater) were powered by a 12 V battery; while the PIC heater and fan were switch “OFF” and “ON” through the help of the relay modules. Humidity and



temperature sensors are sensitive devices, which were incorporated into smart system to monitor the temperature and humidity level inside the storage system. The graphical user interface (GUI) used in selecting commands in this system is presented in Figure 3. On the System dashboard is the Switch “ON” and “OFF” buttons, which allows the user to switch on the heater and fan from anywhere, provided there is internet network.



*Figure 3. System dashboard design.*

### **Testing of the Smart Storage System**

The storage system was test run at the research center of the Delta State University of Science and Technology, Ozoro, Nigeria. The internal temperature and humidity of the system were pre-set at 32°C and 62% RH respectively. It took the system about 3 h to attain this pre-set state. Few potatoes tubers were put inside the storage chamber, and the system was allowed to run a period of 20 hours.

## **RESULTS AND DISCUSSION**

The results obtained through the testing of the automated storage chamber are presented in Table 2. It was noted that the heating system automatically switched on when the temperature inside the storage chamber fell below 32°C; but when the temperature rose above 32°C due to heat of respiration of the stored material, the heater was switched on. Table 2 depicted that the heating system operated for 13 h,

during the 20 h during which the system was test-run. Nevertheless, as presented in Table 2, the smart storage structure has efficiency of 85%. These results are similar to earlier observations made by [Mabrouk et al. \(2017\)](#), who recorded approximately 90% success in a design smart storage system. Similarly, [Karim et al. \(2018\)](#) reported about 91% success in using IoT to monitor the temperature and humidity inside storage chamber.

**Table 2.** The environmental conditions measurement.

Time (h)	Humidity (%)	Temperature (°C)	Heater	Fan
0	75	35	OFF	ON
1	71	38	OFF	ON
2	68	33	OFF	ON
3	72	34	OFF	ON
4	57	30	ON	ON
5	59	31	ON	ON
6	63	29	ON	ON
7	65	28	ON	ON
8	54	31	OFF	OFF
9	50	30	OFF	OFF
10	51	25	ON	OFF
11	52	24	ON	OFF
12	60	23	ON	ON
13	61	24	ON	ON
14	63	25	ON	ON
15	62	20	ON	ON
16	67	25	ON	ON
17	62	27	ON	ON
18	55	29	ON	OFF
19	49	33	OFF	OFF
20	51	32	OFF	OFF

Based on the programmed temperature (32°C) and humidity of 62%, it was noted that the system operated at the right temperature setting in 17 occasions.

Efficiency of the system based on the heater performance =  $\frac{17}{10} \times 100 = 85\%$ .

Failure rating of the system based on the heater performance =  $100 - 85 = 15\%$ .

It was observed that the humidity sensor failed in some cases, as the humidity increases with increased in the chamber temperature. This could be linked to transmission speed of the sensors used for the prototype construction.

## CONCLUSION

The research was carried out to develop a model smart storage structure. Heat and humidity sensors were incorporated into the storage structure, to effectively monitor the temperature and relative humidity inside the storage system. These two parameters are crucial factors to be considered during the design and development of any storage structure for agricultural products. The system was tested with potato tubers, and results obtained revealed that based on temperature regulation, the smart system has 85% accuracy. Although, 15% failure rate was recorded, this smart prototype is a major breakthrough in the production of smart storage system for agricultural products.

## DECLARATION OF COMPETING INTEREST

We hereby declare that we have no conflict of interests.

## CREDIT AUTHORSHIP CONTRIBUTION STATEMENT

**Ovuakporaye Godwin Ekruyota** data analysis and review of the original draft, **Omokaro Idama** designed the research and writing the original draft.

## ETHICS COMMITTEE DECISION

This article does not require any ethical committee decision.



## REFERENCES

- Bezboruah T and Bora A (2020). Artificial intelligence: the technology, challenges and Applications. *Transactions on Machine Learning and Artificial Intelligence*, 8(5): 44-51.
- Boehmer E (2015). Basics of software engineering principle and research. *Lookman Publication*, USA.
- Ekruyota OG and Uguru H (2021a). Characterizing the mechanical properties of eggplant (Melina F1) fruits, for the design and production of agricultural robots. *Direct Research Journal of Engineering and Information Technology*, 8: 21-29.
- Ekruyota OG and Uguru H (2021b). Development of an autonomous multifunctional fruits harvester. *Journal of Agricultural Research*, 6(2): 1-7.
- Ekruyota OG, Akpenyi-Aboh ON and Uguru H (2021). Evaluation of the mechanical properties of tomato (cv. Roma) fruits as related to the design of harvesting and packaging autonomous system. *Direct Research Journal of Agriculture and Food Science*. 9: 174-180.
- Ekuewa OI, Ogunti EO and Ekuewa JB (2022). Development of internet of things systems for monitoring agricultural silos. *European Journal of Electrical Engineering and Computer Science*, 6(1): 6-15.
- Golf D (2019). Automated green house system. *International Journal of Engineering Research & Technology*, 4(3): 45-60.
- Hagstrum DW and Subramanyam B (2006). Fundamentals of stored-product entomology. Woodhead publishing and AACC International Press. Elsevier Inc.
- Idama O, Uguru H and Akpokodje OI (2021). Mechanical properties of bell pepper fruits, as related to the development of its harvesting robot. *Turkish Journal of Agricultural Engineering Research*, 2(1): 193-205. <https://doi.org/10.46592/turkager.2021.v02i01.015>
- Ijabo J, Irtwange SV and Uguru H (2019). Effects of storage on physical and viscoelastic properties of yam tubers. *Direct Research Journal of Agriculture and Food Science*, 7(7): 181-191.
- Jenkins, D and Kurasaki R (2018). ABE-VIEW: Android interface for wireless data acquisition and control. *Sensors*, 18(8): 2647-2667.

- Karim AB, Hassan Z, Akanda M and Mallik A (2018). Monitoring food storage humidity and temperature data using IoT. *MOJ Food Process Technology*, 6(4): 400-404.
- Mabrouk S, Abdelmonsef A and Toman C (2017). Smart grain storage monitor and control. *American Scientific Research Journal for Engineering, Technology, and Sciences*. 31(1): 156-162.
- Nwanze NE and Uguru H (2020). Optimizing the efficiency of eggplant fruits harvesting and handling machines. *Journal of Materials Science Research and Reviews*, 6(3): 1-10.
- Onibonoje MO, Nwulu NI and Bokoro PN (2019). A wireless sensor network system for monitoring environmental factors affecting bulk grains storability. *Journal of Food Process Engineering*, 42(7): 1-13.
- Zhao Q, Liu Y, Yu Y, Song J and Zhou G (2014). *Intelligent system for monitoring and controlling of the grain condition based on ARM9*. The 26<sup>th</sup> Chinese Control and Decision Conference.



## Development and Performance Evaluation of Hand Operated Screw Juicer for Small Scale Application

Muyiwa Abiodun OKUSANYA<sup>a</sup>, Francis Ehis AGBONGIABAN<sup>a\*</sup>

<sup>a</sup>. Department of Agricultural and Bio-Environmental Engineering, School of Engineering  
The Federal Polytechnic, Ilaro, Ogun State, NIGERIA

(\*): Corresponding Author: [agbons75@gmail.com](mailto:agbons75@gmail.com)

Received: 19.12.2022

Article Info  
Accepted: 15.06.2023

Published: 30.06.2023

### ABSTRACT

Nutrients from fruits are lacking in most African diets despite their importance. This results in malnutrition and diseases. Some of the factors responsible for these dietary deficiencies are income level and technologies to address postharvest losses. A hand-operated screw juicer was developed in this technical brief to address some of the problems. The machine developed uses screw principle for fruits mastication and juice extraction. The screw juicer performance was tested based on extraction capacity, efficiency and number of runs. Bivariate linear regression was the statistical model used to understand the relationship between the explanatory variable,  $x$  (number of pass/runs) and the response variable,  $y$  (extraction capacity/efficiency). For orange, cucumber, pineapple, golden melon and watermelon, the efficiencies (%) are respectively 79.30, 48.68, 68.96, 56.41 and 56.52 at single pass. Also, the extraction capacities of the machine ( $L h^{-1}$ ) are respectively 6.38, 5.08, 9.16, 7.84 and 10.48 for the fruits. The efficiencies are higher with orange and pineapple due to fibrous nature of the fruits. Pineapple and watermelon gave higher extraction capacity due to higher water content and juicy nature, at 5 and 7 runs respectively. The model ( $Y = -49.29X1 + 295.71 \pm 89.75$ ) from the analysis using watermelon reveals machine extraction capacity in volume is a function of number of runs. The machine reached its highest extraction capacity of 10.48 liters in 1 hour at 7 runs. This extraction capacity makes the machine fit to meet daily dietary requirements (400 g per person, an equivalence of 380 ml) of more than 4 households if operated for one hour. The machine can be adopted for use by small scale processors as it is affordable, less stressful and easy to maintain.

**Keywords:** Crank, Mastication, Juicer, Hand-operated, Extraction-capacity

**To cite:** Okusanya MA and Agbongiaban FE (2023). Development and Performance Evaluation of Hand Operated Screw Juicer for Small Scale Application. *Turkish Journal of Agricultural Engineering Research (TURKAGER)*, 4(1), 133-150. <https://doi.org/10.46592/turkager.1220141>



## INTRODUCTION

Fruits and vegetables lose a lot of their nutrients quickly since they continue to metabolize and breathe after harvest. At this stage, oxygen in the atmosphere is consumed by the fruits to produce heat, carbon dioxide, ethylene gas and moisture. When the process continues for prolonged time, the produce ripens and the quality degrades. Aerobic respiration of the fruits causes breakdown of organic compounds in the fruits to simpler molecules to cause decay with the release of energy ([Delphine et al., 2020](#)).

Postharvest losses in fruits and vegetables in Nigeria are estimated to be about 50% annually. This is a worrying situation because fruits and vegetables that are meant to complement other food items for healthy diets are wasting away. Unfortunately, fresh preservation of the fruits requires a lot of investment ([NSPRI, 2023](#)).

From empirical facts gathered, it can be inferred that some of the factors responsible for postharvest losses of these highly perishable products are seasonal glut, lack of storage facilities, lack of habit of value addition on harvested products through processing, lack of processing facilities, poor market structure and information on products sales, poor post-harvest handling and management, etc. ([Yahaya and Mardiyya, 2019](#)). Postharvest losses from food crops and fruits should be seen as a disservice to humanity, most especially in a country like Nigeria where sizable number of citizens is suffering from lack of access to quality foods. If appropriate technologies are not explored for value addition, the loss may be very unbearable for farmers and stakeholders in the nearest future.

According to World Health Organization ([WHO, 2021](#)), it was recommended that at least 400 g of fresh fruit juice should be taken each day by an average individual to boost his or her health for nutritional benefits. Report by [WHO \(2019\)](#) also reveals that 3.9 million of deaths cases recorded worldwide in 2017 were attributed to not eating enough fruit and vegetables. Further, insufficient intake of fruit and vegetables was estimated to cause around 14% of death cases from gastro-intestinal cancer worldwide; 11% of ischemic heart disease, and 9% of stroke cases ([Afshin et al., 2019](#)).

Health benefits of fresh fruit juice cannot be overemphasized. Antioxidants in fruits can prevent cell damage caused by oxidants and unstable molecules moving in the body ([Labo et al., 2010](#)). The juice also contains most of the vitamins, minerals and plant chemicals (phytonutrients) found in the fruit. According to [Zeratsky \(2022\)](#), it is believed that drinking fresh fruit juice is better than eating whole fruits because the body can absorb the nutrients better than stressing digestive system to process the fibers in fruits for onward absorption into the body. However, there is a need for scientific evidence on the power fruit juice has in reducing risk of being prone to cancer, boosting immune system, removing toxins from the body, aiding digestion and helping to lose weight.

Over the years, different designs of motorized juicers have been introduced to the market to overcome the challenges of poor post-harvest handling and processing of fruits; but those designs have not gained wide adoption by marginal farmers due to highly prohibitive cost. Those who even use them by economy of scale cannot afford their high cost of maintenance. [Eyeowa et al. \(2017\)](#) developed a juice extractor with

polytetrafluoroethylene (PTFE) to beat down the cost of production so as to make it affordable for orchard farmers. However, researches have proven that human exposure to Teflon is carcinogenic since chemical used in the manufacturing process (perfluorooctanoic acid, PFOA) has a link with cancer ([Pietrangelo, 2020](#)). According to [Bochanic \(2022\)](#), the United State National Health and Nutrition Examination Survey found PFOA in the blood samples of 98% of participants examined. The use of Teflon as a major component of food processing machine should therefore be discouraged.

A juicer is a machine used in extracting juice out of different types of fruits, leaving pulp, seeds and peels behind as byproducts. Juice extraction can be through tapered screw principle, pneumatic pressing, centrifuge separation, rotating blades, triturating discs, masticating teeth, etc. This research endeavour is therefore geared towards designing and fabricating a low cost screw juicer for small scale application to aid the culture of value addition. This will serve to address post-harvest losses of fruits during the time of seasonal glut and as well assist in contributing to dietary requirements of food by nutritionists.

## **MATERIALS and METHODS**

### **Design Philosophy**

The screw juicer uses the change of gap of the tapered screw shaft to build pressure sufficient enough to squeeze the flesh of fruits fed in, to extract the juice. The two operating principles combined by the transmission shaft are material transport within the squeezing chamber and squeezing effect via compression. This type of extraction principle is the most widely used for fruits as the design and operating principle are suitable for small scale application.

### **Design Consideration**

Some relevant factors were considered in the design and development of the hand operated juice extractor; such factors include power requirement, ease of replacement of various components, labour requirement, ease of mobility, possibility of machine duplication, safety of operation of parts, cost of construction, types of load and stresses, machine kinematics and cost of maintenance. The machine will be very easy to maintain as it does not require mechanical power like an oil engine or electric motor to operate. Stainless steel plate of 2 mm thickness was considered for the construction of hopper and the squeezing chamber to avoid shearing of parts or machine failure while in operation. The tapered screw shaft operated by lever arm impacts strong squeezing force in fruits fed in to achieve extraction effect by the juicer assembly. The shaft of the screw juicer was made of stainless steel to avoid food contamination.

## Materials Selection

**Table 1.** Materials used for machine fabrication.

Machine Element	Criteria for Material Selection	Materials Selected	Dimension	Remark
Hopper	Must allow free flow of materials into squeezing chamber	Stainless steel of 2 mm thickness	240 mm x 75.5 mm x 2 mm thickness	Machined
Transmission Shaft	Machinability, high tensile/compression strength, low notch sensitivity factor, ductile, torsional rigidity, stiffness, etc.	Stainless steel rod	$\varnothing$ 25mm, 220mm l	Machined
Squeezing Chamber	Ability to withstand vibration and squeezing force	Stainless steel of 2 mm thickness	diameter, $\varnothing$ 82mm tapered inward	fabricated
Bearing	Compressive strength, fatigue strength, thermal conductivity, corrosive resistance, etc.	Stainless steel shaft diameter, $\varnothing$ 60 mm Check and write	Outer diameter, $\varnothing b$ 60mm Inner diameter, $\varnothing s$ 25mm, width, $H$ – 30mm	Bought readymade
Lever Arm/Crank	Must be firm, free to rotate and must have torsional rigidity	mild steel rod	Diameter, $\varnothing$ 25 mm, 200 mm long	Machined
Support Frame and Base	Strong ability to withstand compression strength	Galvanized hollow pipe $\varnothing$ 34 mm & stainless steel rectangular platform	Rectangular platform dimension: L x B x T, where L is length, B, breadth and T width	Constructed
Pulp Outlet	Must allow free flow of material	Stainless steel plate folded into cone like hollow pipe (2 mm thick)	249 mm 37 mm x 3 mm	Constructed
Juice Outlet	High shear strength and ability to sustain large permanent deformation to the point of fracture.	Stainless steel screen of 3 mm pore space	15 mm x 10 mm	Bought
Bearing Housing	Must be strong enough to withstand bearing pressure and protect the bearing from outside particles	Mild steel plate 3 mm thick	$\varnothing$ 60mm x 70 mm long	Constructed
Screen	Must have ability for both laboratory scale and industrial scale size separation (strong sieving ability)	Stainless steel of 3,000 micron (pore space)	3 mm screen in the dimension of squeezing chamber	Bought readymade and cut to size



## Design Calculations

### Input power requirement

The input power can be determined from the name plate information of a prime mover used to power a machine. It can also be determined from the drive for the transmission shaft of the machine. In the design, the input power for the hand operated screw juicer was found from the Mathematical model by [Belonio \(2004\)](#) on human power estimation for farm work. It is as stated in Equation 1.

$$P_g (Hp) = 0.35 - 0.092 \text{Logt}(min) \quad \text{Belonio (2004)} \quad (1)$$

Human power is given as  $P_g (Hp) = 0.35 - 0.092 \text{Logt}(min)$

To find  $P_g$  when  $t = 1 \text{ h} = 60 \text{ minute}$ .

$$P_g = 0.35 - 0.092 \log 60 = 0.35 - 0.092 \times 1.7782$$

$$P_g (Hp) = 0.35 - 0.1636 = 0.1864 \text{ Hp}$$

$$1 \text{ Hp} = 0.746 \text{ kW}$$

$$0.1864 \text{ HP} = x$$

$$x = 0.746 \times 0.1864$$

$$P_g = 0.139 \text{ kW}$$

$$P_g = 139 \text{ W}$$

Hence, human power requirement by one human operator on the screw juicer for one hour is **139 W**.

### Load requirement

In estimating load requirement, the squeezing force of the screw shaft is calculated using power requirement of the entire machine assembly.

$$\text{Power, } P = F \times \omega r = F \times v = \frac{F \times \pi DN}{60} \quad (2)$$

Where  $F$  is squeezing force on the flesh of the fruit,  
 $\omega$  is angular velocity of the lever arm

$r$  is the radius of the lever arm,  $v$  is the linear velocity of the transmission shaft and  
 $P$  is the power transferred from the cranking arm to squeezing chamber.

$$F = \frac{P}{v} = \frac{P}{\frac{\pi DN}{60}} (N) \quad (3)$$

Where  $p$  is the power from the cranking arm and  $v$  is the velocity of transmission.

It is assumed that Power,  $P$  transferred from the cranking arm to squeezing chamber is constant.

Given the following parameters:  $\omega$  is 75 rpm,  $D$  is 20 mm = 0.02 m, squeezing force,  $F_{sq}$  can be found.

$$\text{At } 75 \text{ rpm, } F = \frac{P}{v} = \frac{P}{\frac{\pi DN}{60}} = \frac{139}{\pi \times 0.02 \times \frac{75}{60}} = 1.769 \text{ kN}$$

### Torque requirement

The torque requirement is found using the formula given below.

Torque,  $T$  transmitted through shaft = squeezing force  $F$  x radius,  $R$  of screw shaft

$$\text{Torque, } T = F \times R \quad (4)$$

For squeezing force,  $F$  is 1,769 and  $R$  is 0.02 m, then:

$$\text{Torque, } T = 1,769 \times 0.02 = 35.38 \text{ Nm}$$

### Design capacity of the screw juicer

A screw juicer compresses fresh fruits between the layers of screw and the squiring chamber to separate pulp from juice. The design capacity of the screw juicer is as estimated in Equation 5 below:

$$Q = 60 \times \left(\frac{\pi}{4}\right) \times D^2 \times S \times N \times \alpha \times \rho \times C \quad (\text{Eyeowa et al., 2017}) \quad (5)$$

$Q$  = screw capacity (kg h<sup>-1</sup>.)

$D$  = screw diameter (m) = 20 mm = 0.02 m

$S$  = screw pitch (m) = 0.01 m (see Equation 7 for details)

$N$  = screw speed (rpm) = 72.5 rpm (estimated from crank arm rotation)

$\alpha$  = loading ratio = 0.3 (materials is averagely a flow-able material)

$\rho$  = material loose density ( $\frac{kg}{m^3}$ ) = 1030 kg m<sup>-3</sup> (orange fruit)

$C$  = inclination correction factor = 1.0 (since the screw has zero inclination)

$$Q = 60 \times \left(\frac{\pi}{4}\right) \times 0.02^2 \times 0.01 \times 72.5 \times 0.3 \times 1030 \times 1$$

$$Q = 4.22 \frac{kg}{h}$$

$$V = \frac{Q}{\rho} \quad (6)$$

where  $V$  is the volumetric capacity (m<sup>3</sup> h<sup>-1</sup>.) and  $\rho b$  is the bulk density of fruit

if  $\rho b$  (orange juice) = 440 kg m<sup>-3</sup>

$$V = \frac{Q}{\rho} = \frac{4.22}{440} = 0.0096 \frac{m^3}{h}$$

$V = 9.6 \frac{L}{h}$ . Therefore, the extraction capacity for fruit processed is 9.6 liters per hour.

The value is subject to type fruit processed since loose density varies for the type of fruit processed.

### Screw pitch design

$$S = \frac{4VDL}{\pi \times (D^2 - d^2)N} \quad (\text{Eyeowa et al., 2017}) \quad (7)$$

Screw pitch,  $S$  = ?, the inlet velocity of raw material,  $V$  is 0.025 m/s (Assumed).

Outside diameter of screw,  $D$  is 30 mm, the inside diameter of screw,  $d$  is 20 mm.

The length of the screw shaft,  $L$  is 100 mm, the shaft speed,  $N$  is 75 rpm.

$$S = \frac{4VDL}{\pi \times (D^2 - d^2)N}$$

$$S = \frac{4 \times 0.025 \times 0.03 \times 0.1}{\pi \times (0.03^2 - 0.02^2) \times 75}$$

$$S = 0.0102 \text{ m} = 10.2 \text{ mm}$$

### Shaft diameter design

$$d = \left( \frac{16}{\pi \tau_{max}} \times T \right)^{\frac{1}{3}} \quad (\text{Khurmi and Gupta, 2005; Adetola et al., 2014}) \quad (8)$$

From Equation 4, Torque,  $T$  is 35.38 N m. If maximum allowable stress of the screw shaft,

$\tau$  max is 6.67MPa, then diameter of screw shaft can be calculated using Equation 8

$$d = \left( \frac{16}{\pi \times 6.67 \times 10^6} \times 35.38 \right)^{\frac{1}{3}}$$

$$d = 0.030005 \text{ m} \approx 30 \text{ mm}$$

For torsional rigidity, the deflection angle of transmission shaft is given as  $\theta = \frac{\tau L}{GR}$  (Khurmi and Gupta, 2005). (9)

$G$  = Modulus of rigidity for stainless steel =  $120 \times 10^9$  Pa

$R$ , radius of screw shaft is 15 mm

$L$ , length of shaft is 100 mm

$\theta = \frac{\tau L}{GR} = \frac{6.67 \times 10^6 \times 0.1}{120 \times 10^9 \times 0.015} = 0.000371$  - Since the value is less than 0.003, it is within acceptable region.

### Machine Description and Operation

The hand operated screw juicer has four main components: a cranking unit, squeezing unit, pulp outlet, juice outlet and member frame. The squeezing unit has a screw shaft inside a barrel made of stainless steel to avoid food contamination. The squeezing chamber accommodates diced fruit flesh of varying geometries fed into it through the hopper to masticate the fruit and at the same time squeeze out the juice. The screw shaft is powered by the rotation of the cranking arm operated manually at the peripheral of the machine assembly. The masticating and compression force generated in the process assists in squeezing the juice out of the flesh. The juice is afterwards collected through juice outlet while pulp is allowed to be discharged through pulp outlet.

As soon as a batch is completed after many runs depending on the type of fruit processed, another batch of diced fruits is fed in to continue the operation until all the juice contained in the batch is fully squeezed out. The cranking unit is the section of the machine assembly that provides rotational power to the screw shaft masticating and squeezing the fruit flesh. Human power is used to propel the lever arm of the cranking unit. The crank unit is made of 25 mm mild steel rod and two bearings housed by stainless steel plate of 4 mm thickness. The juice outlet provides the passage for flow of juice out of the squeezing chamber through the 3 mm screen at the outlet section directly under the chamber. The outlet for pulp is immediately after the screw shaft at the peripheral of the compression chamber (see Figures 1, 2 and 3 for details of the design). It is made of stainless steel and formed into shape of 25 mm diameter to create pressure sufficient enough to squeeze out the juice and release the pulp. The member frame is the support for the entire assembly. The design of the frame is in form of a pew with rectangular base platform. The pipe linked to the base helps to hold the squeezing chamber in place. The legs of the operator are placed on both sides of the base to further strengthen the firmness of the machine while in operation. See Figures 1, 2 and 3 for details on all the units of the machine assembly.

### Cost Estimation of the Hand Operated Screw Juicer

Cost of engineering products can broadly be grouped under direct or indirect costs. The costing of the newly designed and fabricated screw juicer was based on the detailed factorial estimate method. This is because fabrication of the machine is complete and detailed breakdown and estimation of component parts is possible. The cost analysis of the machine is as shown in Table 2.

**Table 2.** Bill of Engineering Measurement and Evaluation (BEME) for the screw juicer.

S/N	Materials	Quantity	Unit Price (\$)	Total (\$)
1	Cranking Arm ( $\phi$ 25mm rod & 110 mm long)	1/8	17.32	2.16
2	Hopper, Pulp Outlet, Extraction Barrel and Support Base (3 mm stainless steel plate)	1/8	173.32	21.6
3	Screw Shaft (20 mm stainless steel rod) with 10 mm pitch	$\frac{1}{4}$	21.64	5.41
4	Braising Rod for support (30 mm stainless steel pipe)	$\frac{1}{4}$	51.95	12.99
5	Juice Outlet (3 mm thick stainless steel screen)	1/8	86.58	10.82
6	Bearing $\phi$ 25mm (internal $\phi$ )	2	3.25	6.50
7	Consumables (electrodes, paint & cutting disc, body filler, etc.)			5.41
8	Transportation			2.16

Sub-total = \$ 67.10

Materials Cost = \$ 67.10

Direct Labour Cost: (Machining of Main Shaft, Bending, welding, painting) = \$ 7.58

Indirect/Overhead Cost: = 20% of \$ 67.10 = \$13.42

Grand-total = Material cost + Labour cost + Overhead cost = \$ 67.10 + \$ 7.58 + \$ 13.42 = \$ 88.10

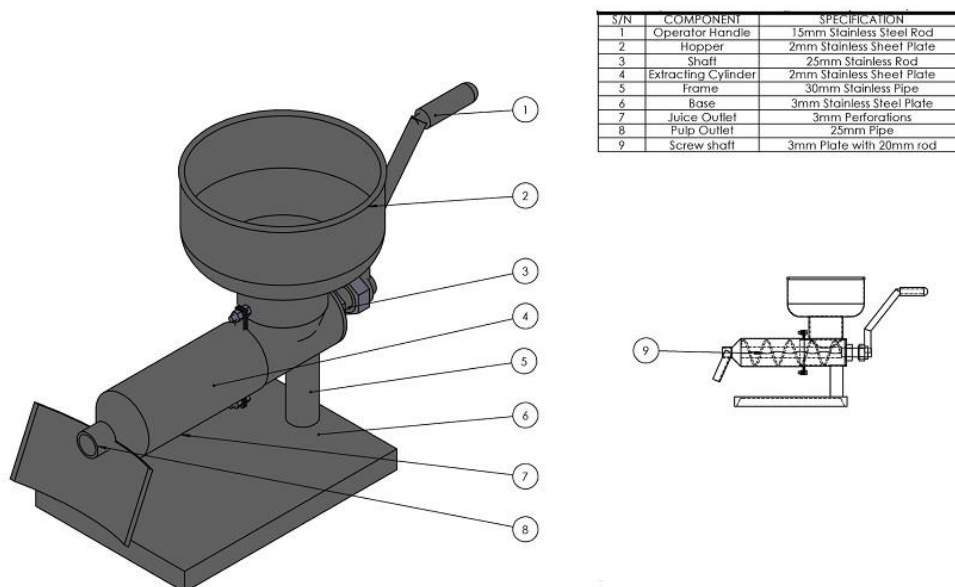


**Figure 1.** Pictorial view of screw juicer.

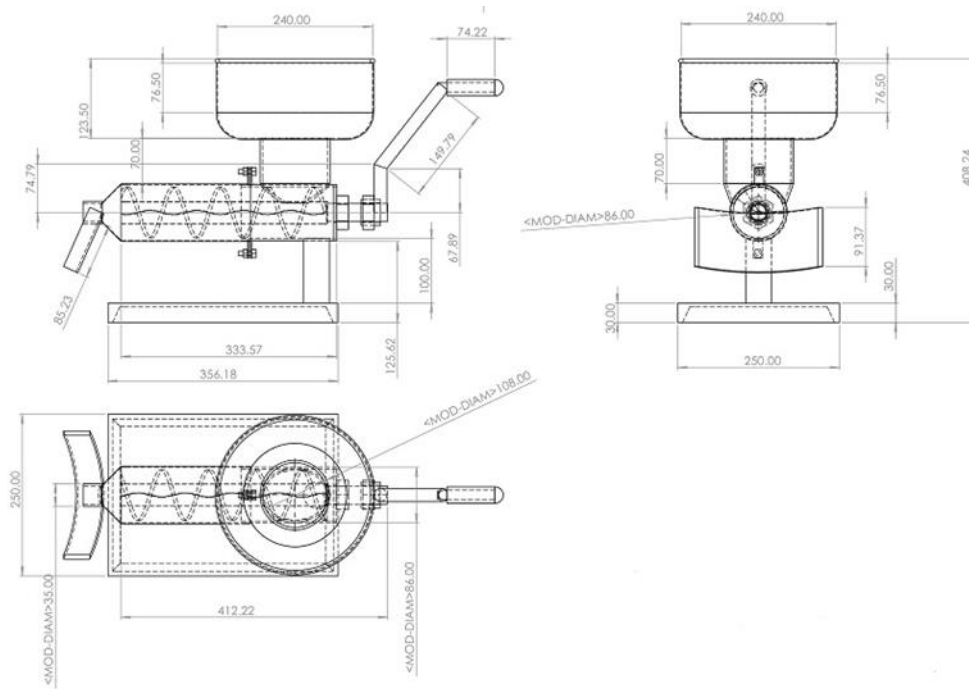


**Figure 2.** Autographic projection of the screw juicer (All dimensions are in mm).

**Statistical Analysis**

Null hypothesis for variables considered is  $H_0: 0.5 \leq r \leq 1$ ; while alternative hypothesis is  $H_1: r < 0.5$ . Bivariate Linear regression was the statistical model used to understand the relationship between the predictor and the response variable. Y is response variable,  $\beta_0$  is intercept on y axis,  $X_1 / X_n$  is the predictor and  $\beta_1 / \beta_n$  is the regression coefficient and  $\varepsilon$  is the model error (see Equation 10 and 11 for the regression model). Other statistical instrument used is the diagrammatic representation of the evaluation data in quantities (descriptive statistics).

$$Y = \beta_0 + \beta_1 X_1 \quad (\text{Zach, 2020}) \tag{10}$$

$$Y = \beta_0 + \beta_1 X_1 + \dots + \beta_n X_n + \varepsilon \quad (\text{Zach, 2020}) \tag{11}$$

**Materials for Evaluation**

The fruits used for evaluation of the screw juicer are orange, pineapple, cucumber, golden-melon and watermelon fruits. The instruments for materials evaluation are sensitive measuring scales, stopwatch, recording materials, vernier caliper and measuring cylinder. Variables considered during material’s evaluation are material throughput, extraction capacity, speed of rotation of the cranking arm, extraction efficiency, etc.

$$\text{Materials throughput} = \frac{W \times 3600}{t} \left( \frac{kg}{h} \right) \quad \text{Eyeowa et al. (2017)} \tag{12}$$

Where W is weight of material processed(kg) and t is extraction time (s)

$$\text{Extraction Efficiency (\%)} = \frac{V_s}{V_t} \times 100 \quad \text{Eyeowa et al. (2017)} \tag{13}$$

$V_s$  is volume of juice extracted at single pass and  $V_t$  is total volume of juice in the fruit

$$\text{Juice Extraction Capacity} = \frac{V \times 3600}{t} \left(\frac{Ll}{h}\right) \text{ Eyeowa et al. (2017)} \quad (14)$$

Where  $V$  is the total volume of juice extracted and  $t$  is extraction time in seconds

$$\text{Density of Juice} = \frac{m}{v} \left(\frac{kg}{m^3}\right) \text{ Eyeowa et al. (2017)} \quad (15)$$

## RESULTS AND DISCUSSION

The screw juicer developed was evaluated with various types of fruits which include orange, cucumber, watermelon, pineapple and golden-melon. Parameters evaluated are materials throughput, extraction capacity and extraction efficiency. The results are shown in Tables 3 and 4.

Maize sheller developed was evaluated using unshelled maize at various moisture content and speed of rotation of the crank arm to determine the efficiency, shelling capacity and kernel damage. The results of the analysis are as shown in Figures 5 and 6 and Tables 3, 4, and 5.

Tables 3, 4 and 5 show the results of evaluation of the developed maize sheller at various moisture content (MC) ranging from 14 % to 23.2%. The results show kernel breakage reduces as the moisture content of various maize samples used for machine evaluation reduces. Also, highest material throughput (60 kg h<sup>-1</sup>.) was obtained at lowest MC (14%) and highest angular speed of rotation. The efficiency of shelling was seen to be highest at lowest MC and time (6 - 10 seconds).

Table 3 shows reduction in efficiency of shelling from 100 to 94 percent as the speed of rotation increases from 40 rpm and 120 rpm. It can be inferred that the operation of the machine should be kept at barest minimum level to be able to experience optimum shelling efficiency. Also, kernel damage can reduce significantly if the hand operated sheller is kept at optimally low speed while in operation.

**Table 3.** Material evaluation of screw juicer using different types of fruits.

S/N	Type of Fruit	Mass of fruits to be processed (g)	Volume of juice extracted (ml)	Number of Pass/runs	Revolution (Crank arm)	Time taken (s)	Mass of juice extracted (g)	RPM (rev min <sup>-1</sup> )
1.	Orange	581.11	245	1	127	110	330.80	69.27
			55	2	38	35	50.00	65.14
			10	3	36	30	13.65	72.00
2.	Cucumber	561.23	180	1	110	112	255.87	58.93
			85	2	36	39	89.53	55.38
			35	3	38	30	44.07	76.00
			40	4	29	26	28.00	66.92
			20	5	30	28	28.38	64.28
			10	6	28	27	15.25	62.22
3.	Pineapple	390.86	200	1	45	48	208.0	56.25
			40	2	20	20	43.5	60.00
			20	3	20	20	31.7	60.00
			20	4	16	17	15.61	56.47
			10	5	13	14	5.0	55.71
4.	Golden-melon	603.20	220	1	86	79	222.8	65.31
			100	2	36	28	107.7	77.14
			20	3	25	25	30.35	60.00
			40	4	25	24	34.22	62.50
			10	5	28	23	9.83	73.04
5.	Watermelon	910.24	390	1	108	87	476.5	74.48
			130	2	53	45	126.0	70.66
			60	3	38	32	66.93	71.25
			40	4	34	28	44.82	72.85
			40	5	22	19	44.82	69.47
			20	6	17	14	22.41	72.85
			10	7	15	12	11.21	75.00
6.	Orange + Cucumber	549.00	220	1	103	97	197.0	63.71
			40	2	25	26	58.0	57.69
			20	3	30	24	16.0	75.00
			10	4	25	16	8.0	93.75
7.	Pineapple + Watermelon	982.54	540	1	160	172	527.41	55.81
			100	2	40	46	98	52.17
			40	3	36	38	40	56.84
			20	4	30	28	25	64.29
			10	5	23	24	13	60.00

The results in Table 3 show volume of juice extracted at different number of passes ranging from three to seven depending on type of fruit processed. The time taken and the revolution of the cranking arm at each number of runs were recorded. Water melon has the highest number of runs followed by cucumber. When either the cucumber or water melon was combined with fibrous fruits like orange or pineapple, the number reduced to 5 for water melon and 4 for cucumber. The implication from this is that the fibrous property lacking in the fruits was compensated for by other fruits combined with them during evaluation.

**Table 4.** Extraction efficiency and extraction capacity of the screw juicer for various types of fruits processed.

S/N	Type Fruit	Density of juice (kg m <sup>-3</sup> )	Extraction capacity (at all possible runs) (L h <sup>-1</sup> )	Materials throughput (at all possible runs) (Kg h <sup>-1</sup> )	Number of Pass	Average RPM	Extraction efficiency (at Single Pass/Runs) (%)
1	Orange	1272.42	6.38	11.95	3	68.80	79.03
2	Cucumber	1170.54	5.08	7.71	6	63.96	48.65
3	Pineapple	1047.62	9.16	12.34	5	57.69	68.96
4	Golden-melon	1038.21	7.84	19.04	5	67.60	56.41
5	Watermelon	1083.87	10.48	13.83	7	72.37	56.52
6	Orange + Cucumber	962.07	6.41	12.12	4	72.54	75.86
7	Pineapple + Watermelon	990.72	8.30	12.24	5	57.82	76.06

Table 4 gives the average value of extraction capacity, materials throughput, and angular speed of rotation and extraction efficiency for each fruit. Orange has the highest extraction efficiency (79.03%) followed by pineapple (68.96%). Also, the machine has the highest extraction capacity for water melon, followed by pineapple. The high extraction volume can be attributed to juicy nature of the fruits. The speed of rotation of the cranking arm ranges from 57.69 to 72.52 rpm. On the average, the cranking arm of each extraction process completes 60 revolutions and above in one minute.

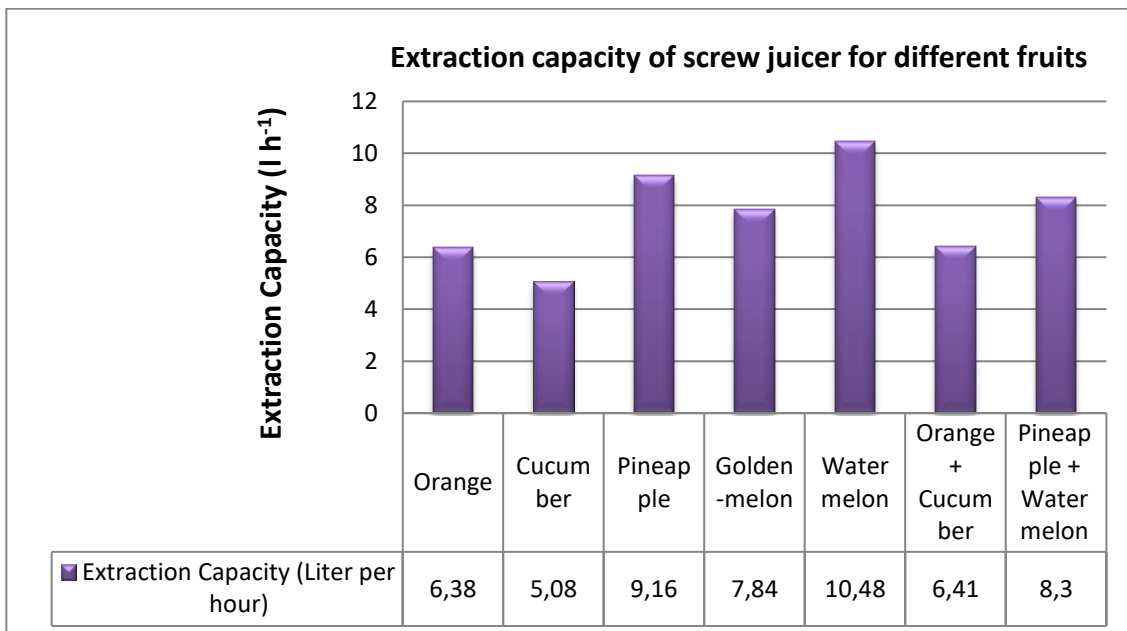
**Figure 3.** Chart of extraction capacity of the screw juicer for different fruits.

Figure 3 is the chart of extraction capacity of the screw juicer for various fruits processed. The machine extraction capacity was highest with watermelon (10.48 L h<sup>-1</sup>) and lowest with cucumber (5.08 L h<sup>-1</sup>). The reasons for the differences



in the extraction capacity are due to soluble solid content and water content of the fruits.

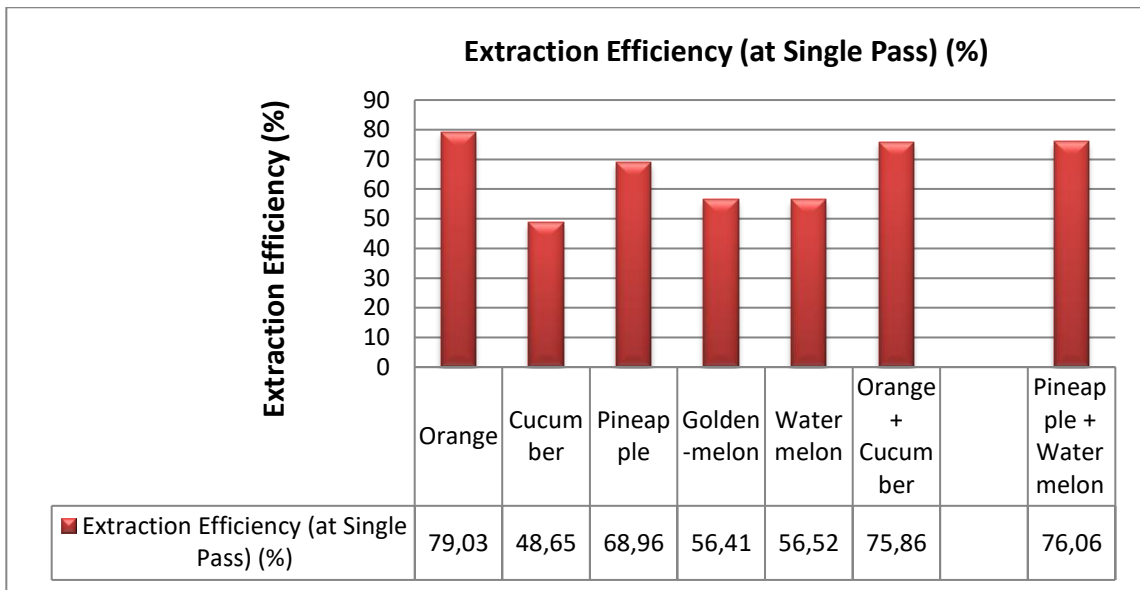


Figure 4. Chart of extraction efficiencies of various fruits.

Figure 4 is the chart of extraction efficiencies of the fruits. The screw juicer efficiency was highest with orange (79.03%) and lowest with cucumber (48.65%). The reasons for the differences in the extraction capacity are due to fibrous nature orange fruit over cucumber and other fruits with low extraction efficiency. Also, pineapple is close to orange in efficiency due to its fibrous property - the property assists in generating enough friction required to masticate and squeeze the juice out of the fruit.

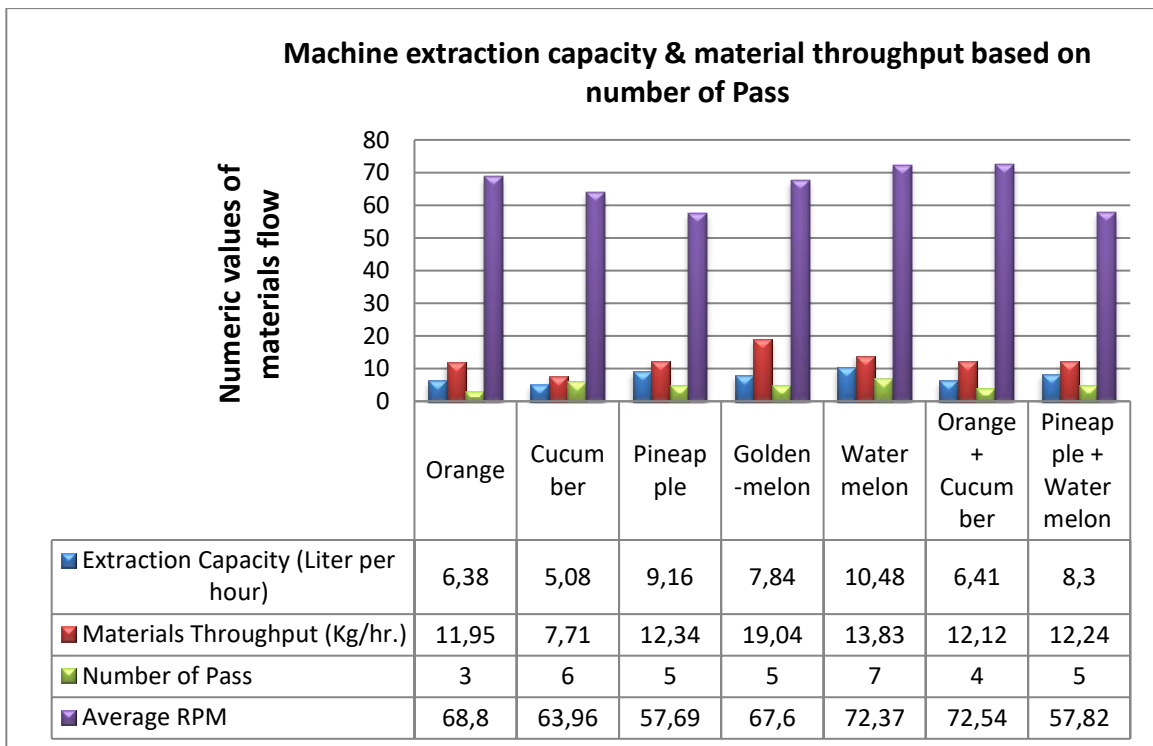
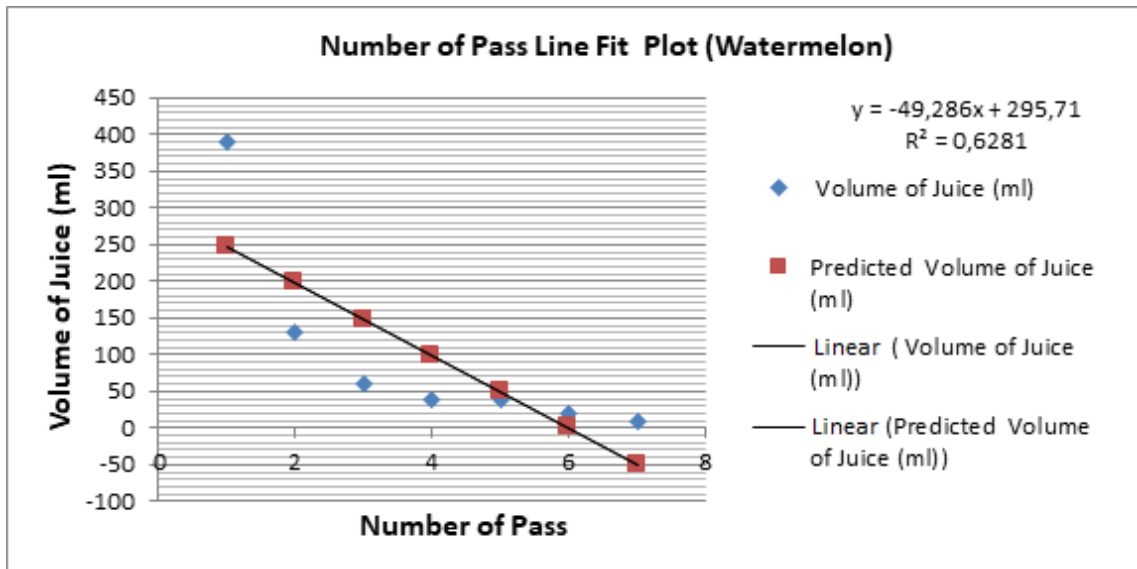


Figure 5. Influence of number of pass on extraction capacity & materials throughput.

Figure 5 is the charts of materials' throughput of the juicer at varying number of passes. From the chart, golden melon has the highest materials throughput ( $19.0 \text{ kg h}^{-1}$ ) followed by watermelon ( $13.83 \text{ kg h}^{-1}$ ). It can be inferred that less fibrous fruits give more material throughput as pulp or other waste product.



**Figure 6.** Relationship between number of pass and volume of juice extracted in one of the evaluation exercises (Watermelon).

Bivariate linear regression was the statistical model used to understand the relationship between extraction capacity in volume and number of passes for watermelon fruit in Figure 6. The model was developed for watermelon because in the list of the fruits evaluated, it has the highest extraction capacity and highest number of passes. The statistical model of the analysis is given as  $y = -49.286x + 295.71 \pm 89.75$ . Out of the 910.24 g of water melon fruit processed, 390 ml of juice was extracted at first run – for this value, extraction capacity is 16.14 liters in one hour ( see table 3 for details). At second and third run, extra volume of 130 ml and 60 ml were respectively recovered. The volume kept reducing until 10 ml is extracted at seventh run. Total volume of juice extracted from the 910.24 g of fruit is 690 ml in 237 seconds. If the extraction process is kept at single pass or first run, it would have been difficult to recover up to 300 ml of juice. From the foregoing, it can be inferred that what watermelon extraction process cannot meet in efficiency under a single pass is compensated for in multiple passes.

Tables 5 and 6 gave the summary of the output that was used to write the model.  $\beta_0$  is 295.71 ml while  $\beta_1$  is -49.29 unit and  $\epsilon$  is 89.75 ml. Variable X in the model is the number of pass of the extraction process;  $\beta_0$  is intercept on y axis,  $\epsilon$  is the model error and variable Y is the extraction volume (in milliliter). For example, every unit increase in number of pass of a particular extraction process, extraction volume increases commensurately (as it adds up). The machine reached its highest extraction capacity of 10.48 liters in one hour at very high pass of 7 units.

**Table 5.** Summary Output.

<b>Regression Statistics</b>	
Multiple R	0.792528
R Square	0.6281
Adjusted R Square	0.55372
Standard Error ( $\epsilon$ )	89.74567
Observations	7

The results presented in table 5 shows that 7 observations were used for the model of the predictor (x) and response variable (y). The coefficient of determination, R square being 0.628 implies 62.8% of the variation in the extraction volume can be explained by the number of passes an extraction process (watermelon) experienced. The multiple R value, 0.795 reveals that there is a strong level of correlation or linear relationship between the explanatory variable and response variable. It also implies that null hypothesis defined is within acceptable limit. The standard error, 89.75 is larger than the coefficient of the predictor (number of pass) which is -49.29 units. On the average, the observed value of the predictor falls 89.75 units from the regression line.

**Table 6.** Summary Output.

	df	SS	MS	F	Significance P
Regression	1	68014.29	68014.29	8.444484	0.033557864
Residual	5	40271.43	8054.286		
Total	6	108285.7			

	Standard				
( $Y = \beta_0 + \beta_1 X_1$ )	Coefficients	Error	t Stat	P-value	Lower 95%
Intercept( $\beta_0$ )	295.7143	75.84894	3.898727	0.011424	100.7383863
No. of pass ( $\beta_1$ )	-49.2857	16.96034	-2.90594	0.033558	-92.88365078

Table 6 shows the analysis of variance (ANOVA) of the regression statistics. From the table (Table 6), it can also be inferred that the number of independent variables in the model is 1 as regression degree of freedom ( $df$ ) is 1 while total  $df$  is 6. F value in the table is 8.44 and the Significance F is 0.0336. The F value assists in testing the hypothesis that the slope of the independent variable is zero. The significance F is otherwise called the p value for the null hypothesis. It assists in confirming that the coefficient of the independent variable is zero. Since the p-value is below 0.05, it implies there is 95% confidence that the slope of the regression line is not zero. Hence, there is significant linear relationship between number of pass and extraction volume of the fruit juice (watermelon). For individual p-value in table 6, it can be inferred that the predictor (number of pass) is statistically significant – meaning the predictor is applicable for the model.



*Figure 7. Screw juicer evaluation exercise.*

Figure 7 shows the picture of the materials used during the evaluation exercise of the screw juicer. Electronic scale was used to measure fruits before extraction process and juice after extraction process. The outlet for juice is beneath extraction barrel while pulp outlet is at the peripheral of the machine. The machine has comparative advantages over manual extraction of juice as it is less stressful to operate and economical to maintain. It has an extraction capacity (average of 10 liters in 1 hour for watermelon) that can meet the daily dietary requirements (400 g per person, an equivalence of 380 ml) of more than 4 households recommended by nutritionists, if operated for 1 hour ([WHO, 2021](#) and [FAO, 2022](#)). If the machine is operated for 8 hours, it can meet the daily needs of an average of 32 households.

## CONCLUSION

Screw juicer was developed in this study for small scale processing of fruits into juice. The machine developed was made of stainless steel of 2 mm thickness to avoid food contamination, corrosion of parts and eventual machine failure while in use for extended period of time. The machine performance was evaluated using different types of fruits for process optimization. The juicer gave the highest extraction capacity of 10.48 liters in one hour when watermelon was processed. With cucumber, lowest extraction capacity was recorded (5.08 L h<sup>-1</sup>). The machine has highest extraction efficiency (79.03%) when orange fruit was processed; the lowest recorded was 48.65% for cucumber.

More effort should be made to encourage fruits and vegetable farmers at all levels in the country to increase production and create awareness on the need to consume more fruits and vegetables as recommended by WHO to meet daily dietary needs recommended by nutritionists. The habit of value addition should also be encouraged amongst farmers and processors in fruit juice industry. The product (fruit juice)

should be made more economically accessible to consumers, while generating economic benefits in line with Sustainable Development Goals.

In view of government policy on local production of arable crops to ensure food security and sufficiency, heavy investment on mass production of the machine is recommended for small scale processing of fruits into juice.

## DECLARATION OF COMPETING INTEREST

We hereby declare that we have no conflict of interests

## CREDIT AUTHORSHIP CONTRIBUTION STATEMENT

**Muyiwa Abiodun Okusanya** conceptualized this project, did investigation, design and fabrication of the machine.

**Francis Ehis Agbonglaban** contributed to the methodology, data collection/analysis performance evaluation review and editing of the write-up.

## ETHICS COMMITTEE DECISION

This article does not require any ethical committee decision.

## REFERENCES

- Adetola OA, Olajide JO and Olalusi AP (2014). Development of a screw press for palm oil extraction. *International Journal of Scientific & Engineering Research*, 5(7): 1416-1422.
- Afshin (2019). Health effects of dietary risks in 195 countries, 1990–2017: A systematic analysis for the global burden of disease study 2017. *Lancet*, 392(10159): 1789-1858.
- Belonia AT (2004). Agricultural power and energy sources. TIGIM Review Center, Institute of Agricultural Engineering Manila. Central Philippine.
- Bochanic (2022), PFAs in the US population: Per-and Polyfluoroalkyl Substances (PFAs) and your health. Agency for toxic substances and disease registry.
- Delphine M. Pott, Jose G. Vallarino and Sonia Osorio (2020). Metabolite changes during postharvest storage: effects on fruit quality traits. National Center for Biotechnology Information. <https://doi.org.10.3390/metabo10050187>
- Eyeowa AD, Adesina BS, Diabana PD and Tanimola OA (2007). Design fabrication and testing of a manual juice extractor for small scale applications. *Current Journal of Applied Science and Technology*, 22(5): 1-7.
- FAO (2021). Fruits and vegetables: Essential for healthy lives. Food and Agricultural Organization. International Year of Fruits and Vegetables (2021). [www.fao.org](http://www.fao.org)
- Fonseca SC, Oliveira FA and Brecht JK (2002). Modeling respiration rate of fresh fruits and vegetables for modified atmosphere packages: a review. *Journal of Food Engineering*, 52(2), 99-119.
- Khurmi RS and Gupta JK (2005) A textbook of machine design. 14<sup>th</sup> Edition, *Eurasia Publishing House* (PVT.) Ltd, Ram Nagar, New Delhi.
- Labo V, Patil A, Phatak A and Chadra N (2010). Free radicals, antioxidants and functional foods: Impact on human health. National Center for Biotechnology Information. <https://www.ncbi.nlm.nih.gov/pmc/articles/PMC3249911/10.4103/0973-7847.70902>
- NSPRI (2023). Nigeria Records 50% Post-Harvest Losses Annually. <https://www.nspri.gov.ng/index.php/en/more/general-news/298-pessu-nigeria-records-50-post-harvest-losses-annually>
- Pietrangelo A (2020). Can teflon cookware increase your risk of cancer? <https://www.healthline.com/health/teflon-cancer>

WHO (2019). Monitoring Health for the MDGs.

<https://apps.who.int/iris/bitstream/handle/10665/324835/9789241565707-eng.pdf>

WHO (2021). Healthy diet: Practical advice on maintaining healthy diets. World Health Organization.

<https://www.who.int/news-room/fact-sheets/detail/healthy-diet>

Yahaya SM and Mardiyya AY (2019). Review of postharvest losses of fruits and vegetables. *Biomedical: Journal of Scientific and Technical Research*, 13(4): 10192-10200.

Zach, (2020). Introduction to Multiple Linear Regression.

<https://www.statology.org/multiple-linear-regression/>

Zeratsky K (2022). Is juicing healthier than eating whole fruits or vegetables?

<https://www.mayoclinic.org/healthy-lifestyle/nutrition-and-healthy-eating/expert-answers/juicing/faq-20058020>

# TURKISH JOURNAL OF AGRICULTURAL ENGINEERING RESEARCH



TURKAGER

2023

e-ISSN:2717 - 8420

<https://dergipark.org.tr/tr/pub/turkager>

